

ELECTRON ADDITION TO ORGANIC HALIDES

by

Ian G. Smith

A thesis submitted for the degree of
Doctor of Philosophy in the Faculty of Science
at the University of Leicester

April 1980

UMI Number: U311686

All rights reserved

INFORMATION TO ALL USERS

The quality of this reproduction is dependent upon the quality of the copy submitted.

In the unlikely event that the author did not send a complete manuscript and there are missing pages, these will be noted. Also, if material had to be removed, a note will indicate the deletion.



UMI U311686

Published by ProQuest LLC 2015. Copyright in the Dissertation held by the Author.
Microform Edition © ProQuest LLC.

All rights reserved. This work is protected against
unauthorized copying under Title 17, United States Code.



ProQuest LLC
789 East Eisenhower Parkway
P.O. Box 1346
Ann Arbor, MI 48106-1346



THESIS
605132
8 . 8 . 80

x752954740

STATEMENT

Except for the work documented in Chapter 8 which was carried out in conjunction with Mr. S. P. Maj, the work described in this thesis was carried out by the author in the Department of Chemistry at the University of Leicester during the period September 1977 - March 1980. This work has not been presented for any other degree.

April 1980

Ian G. Smith

STATEMENT

This thesis may be made available for consultation, photocopying and use through other libraries.

ACKNOWLEDGEMENTS

I would like to thank Professor M. C. R. Symons for introducing me to the field of study, and for all the assistance he has given me in the implementation of the ideas documented herein.

I would also like to thank all the members of the Chemistry Department at Leicester for their assistance in matters too numerous to mention. In particular, I would like to thank Miss Vicky Orson-Wright and Mrs. Ann Crane for the typing and preparation of diagrams respectively of this thesis.

Finally, I would like to thank my parents for the purchase of my first chemistry set in 1967, and all the chemistry teachers whose combined efforts have, over the years, enabled me to be in this position today.

*"When you have excluded the impossible, whatever remains,
however improbable, must be the truth."*

Sir Arthur Conan Doyle

"Experience is the name everyone gives to their mistakes."

Oscar Wilde

The first quote is expounded quite frequently throughout the text. With regard to the second, I feel I am an experienced man.

Ian G. Smith

Dedicated to

Mum 'n' Dad

and

Helen

CONTENTS

	<u>Page</u>
<u>CHAPTER 1 - The adamantane and 2,2,3,3-tetramethylbutane (TMB) matrices</u>	
Introduction	2
Adamantane: physical properties of	3
gamma radiolysis of	6
purification of	8
incorporation of substrates into	9
TMB. Generation of cation: Introduction	11
Experimental	13
Results	14
Analysis and Discussion	14
Conclusion	20
References	21
<u>CHAPTER 2 - The β-bromo story</u>	
Introduction	24
Experimental	26
Results	27
(a) The Case For and Against species W being the β -bromo Radical	37
(b) The Case For and Against species W being the $\text{Bu}^{\cdot}/\text{Br}^-$ Adduct	39
(c) The Case For species S being the Radical $\text{Me}_2\dot{\text{C}}\text{CH}_2\text{Br}$	42
Aspects of Mechanism	45
References	49
<u>CHAPTER 3 - Further $\text{R}^{\cdot}/\text{Br}^-$ and $\text{R}^{\cdot}/\text{I}^-$ adducts</u>	
Introduction	52
Experimental	52
<u>Part 1: Proof that A_1 is negative for the adducts</u>	
Introduction	53
Results	56
Discussion	58

	<u>Page</u>
<u>Part 2: R•/Br⁻ and R•/I⁻ adducts in the adamantane-d₁₆ matrix:</u>	
Gamma radiolysis of alkyl bromides	61
Gamma radiolysis of alkyl iodides	63
Discussion: bromides	74
iodides	76
Absence of β-iodo radical Me ₂ \dot{C} CH ₂ I	78
References	82

CHAPTER 4 - R•/Cl⁻ adducts

Introduction	84
Experimental	84
Results	89
Discussion	93
Gamma radiolysis of polycrystalline Bu ^t Cl:	
Results and Discussion	101
Conclusion	106
References	107

CHAPTER 5 - Abnormal R•/X⁻ adducts (X = Cl, Br, I) and character analysis of "the adduct"

Introduction	109
Experimental	109
Results and Discussion	110
The Adduct: bromo- and chloro- adducts	126
iodo- adducts	131
References	134

CHAPTER 6 - Formation of σ* anions

Introduction	136
Bonding in σ* anions	139
Consistency of bonding in σ* anions	143
Experimental	145

	<u>Page</u>
CCl ₃ X (X = F, Cl, Br): Results and Discussion	146
Formation of σ^* anion	154
Conclusion	155
1-haloadamantane (hal = Cl, Br): Results	156
Discussion	156
References	162

CHAPTER 7 - Gamma radiolysis of methylhalosilanes

Introduction	164
Experimental	167
Results and Discussion	169
Conclusion	186
References	190

CHAPTER 8 - The thermally and photolytically induced [1,2] hydrogen atom shift

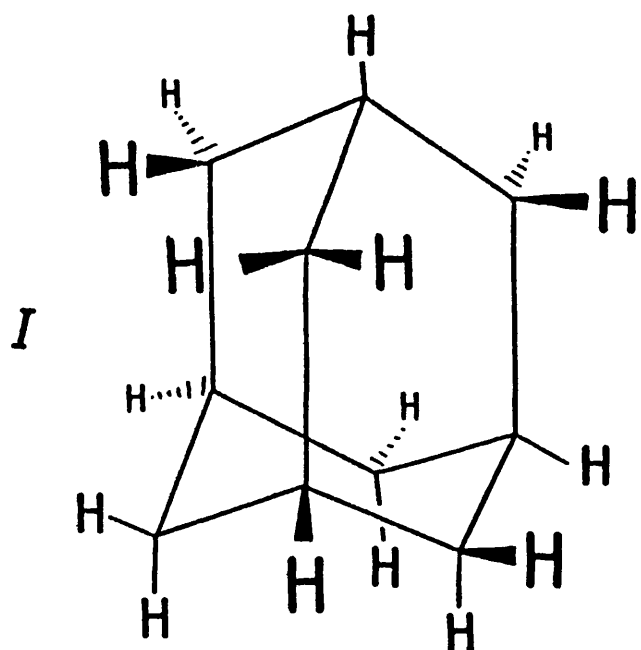
The [1,2] radical shift	192
Introduction	194
Experimental	202
Results and Discussion	203
Conclusion	219
References	221

CHAPTER 1

The adamantane and 2,2,3,3 tetramethylbutane
(TMB) matrices

INTRODUCTION

As the reader of this thesis will discover when reading through the next 220 pages, adamantane (I) has been used as a matrix for the isolation and dilution of a number of paramagnetic species, often yielding quite exemplary results. A brief review will therefore be attempted of the physical properties of adamantane, and of the products derived from its γ -radiolysis, with a view to discovering the implications they may have concerning the compound's efficiency as a matrix for the e.s.r. spectroscopist. A description of the basic methods for



$$C-C = 1.54\text{\AA} \pm 0.01\text{\AA}$$

$$C-H = 1.08\text{\AA}$$

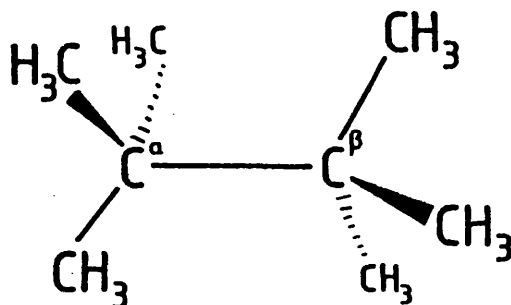
$$C-\hat{C}-C = 109.5^\circ \pm 1.5^\circ$$

Free from angle and
torsional strain

its purification and for the incorporation of substrates into its matrix will also be made.

We shall also look at another molecule with a plastic phase transition, 2,2,3,3-tetramethylbutane (T.M.B) (II), to consider its ability to act as a rotator phase matrix, and to document the detection

of an authentic saturated hydrocarbon cation.



$$C^{\alpha}-C^{\beta} = 1.58 \text{ \AA}$$

$$C-H = 1.09 \text{ \AA}$$

$$C-C = 1.54 \text{ \AA}$$

$$C-\hat{C}^{\alpha}-C = C-\hat{C}^{\beta}-C = 111^{\circ} \pm 2^{\circ}$$

ADAMANTANE

Physical properties of adamantane

Most groups have studied the spectra of damaged impurities in adamantane only at elevated temperatures (ca. >160 K), when the best resolution is likely to be obtained. However, experience has shown this can lead to mistakes in interpretation.¹ Rearrangement of species and/or disappearance of species very often takes place prior to the onset of highest resolution: therefore, conclusions could be drawn with much greater certainty if the experiments were commenced at lower temperatures. This laboratory feels strongly about the importance of looking at the spectra produced over a wide temperature range. Hence this review will rehearse the internal changes taking place in the adamantane matrix as the temperature is raised, beginning at the temperature of the liquification of nitrogen: 77 K.

Nordman and Schmitkons² concluded that, at 77 K, the low temperature

form of adamantane grows in an ordered tetrahedral $P4_21c(D_2^2d)$ crystal structure with $a = 6.60 \text{ \AA}$, $c = 8.81 \text{ \AA}$ and 2 molecules per unit cell. The molecules are rotated 9° relative to the a and b axes and are also marginally squashed in the c direction. This result is generally supported by Donohue and Goodman³ although they believe that the squashed molecule is a consequence of misinterpreted results and conclude the molecule is, in fact, undistorted. Despite the controversy over this detail, the picture is of a molecule with no rotation and packed into a lattice that allows the maximum use of space; this being best achieved by rotating the molecule by 9° and, hence, avoiding methylene group interaction (Fig. 1).

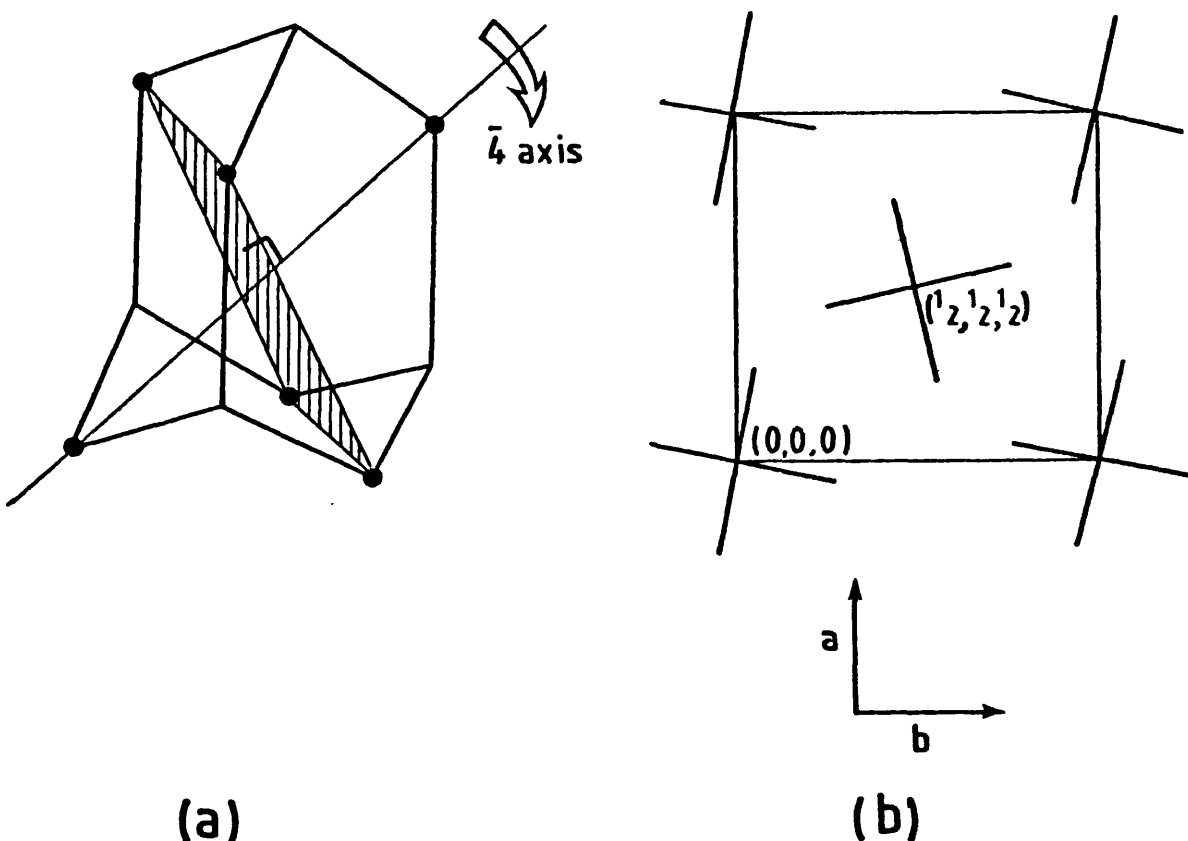


Figure 1

Showing (a) one of the three mutually perpendicular $\bar{4}$ axes of the adamantane molecule and (b) the 9° tilt of this axis in the adamantane low temperature crystal structure.

Numerous variable temperature proton n.m.r. studies have been made on adamantane.^{4,5,6,7} It appears that the molecule begins to librate extensively at ca. 125 K⁷ and continues to increase its libratory motion until ca. 170 K;⁶ whereupon the picture is of a rapidly rotating molecule but at a fixed site. Resing's relaxation results predict an activation energy for rotation of 6.5 kcal. mol⁻¹⁶ (27.2 kJ mol⁻¹).

The phase transition at 208.6 K was first detected by Westrum et al.⁸ with their heat capacity experiments showing an accompanying entropy change of 3.87 cal. deg⁻¹ mol⁻¹ (16.19 J K⁻¹ mol⁻¹). There is a simultaneous decrease in density from 1.18 g cm⁻³ to 1.08 g cm⁻³.⁹ This marked expansion of the lattice allows an increase in the rotational jump rate by lowering the rotational potential barrier.⁶ However, it does appear that this transition is by no means complete and instantaneous at this temperature, as is borne out by the difficulties encountered by Dows et al.⁹ Their infra-red study showed there was a 10° range of temperature over which a smeared transition took place. The pressure induced phase transition showed exactly the same situation.¹⁰ [This co-existence of 2 phases at the same temperature has proven to be a very important point in the analysis of certain of our experiments.]

There is some controversy regarding the crystal structure of the high temperature phase. There have been a number of X-ray studies carried out,^{2,3,11,12,13} showing that the structure is either an ordered F $\bar{4}3m$ or a disordered Fm $\bar{3}m$. However, n.m.r. studies⁶ show conclusively the rotation of the adamantane molecule at this temperature with an activation energy of 3.08 kcal. mol⁻¹ (12.89 kJ mol⁻¹). Slow electron scattering experiments^{14,15} show, in fact, the 90° rotational

jump rate has a frequency of $\sim 10^{11} \text{ s}^{-1}$. The correct structure must surely be $Fm\bar{3}m (T^2_d)^2$ with $a = 9.45 \text{ \AA}$ and 4 molecules per unit cell. Further warming to room temperature, and beyond, shows an increase in the rate of rotation.⁶ It should be noted that at no time through this sequence of events has diffusion been a significant phenomenon, the $36 \text{ kcal. mol}^{-1}$ (150 kJ mol^{-1}) activation energy¹⁶ making it negligible below 475 K.

I think it now becomes obvious why adamantane has proved to be such an efficient matrix. Rotational motion of the adamantane molecule commences at ca. 120 K⁷ and persists up to 475 K⁶ without any appreciable translational motion. Thus, if a radical is incorporated into the matrix, it too experiences this gradation in rotational freedom, but without the added liquid phase problem of diffusion which leads to the killing of radicals via radical-radical interactions. Of course, the diffusion through the lattice will be dependent on radical size. For instance, we have not, as yet, detected the methyl radical even at 77 K. However, the ethyl radical has been detected,¹⁷ and large molecules such as di-tertiary butyl nitroxide,¹⁸ hexafluorobenzene¹⁹ and tertiary butyl iodide¹⁷ have all yielded results over a wide temperature range; the tertiary butyl radical reportedly having a half-life of 2 hours at room temperature.²⁰

Gamma radiolysis of adamantane

If the formation of radicals from doped impurities are to be fully understood, it must surely be necessary to clarify the species formed from the γ -radiolysis of the pure matrix. A number of studies have been carried out on the subject through the years, producing amazingly contradictory results. However, it seems that, at the moment, the controversy is over whether a broad, featureless spectrum is the 1-

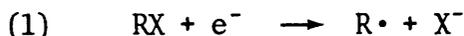
adamantyl radical or 2-adamantyl radical (or both!). All previous assignments have been explained as the result of damaged unintentional impurities.²¹⁻²⁶ An authentic 1-adamantyl radical has been isolated by Krusic et al. in a cyclopropane matrix,²⁷ all the parameters being extracted quite satisfactorily. Unfortunately, the adamantane matrix does not permit such high resolution. Hence the 448 closely spaced lines in cyclopropane would become essentially a singlet in adamantane if the linewidth was >1.8 G.²⁸

The 2-adamantyl school of thought has an e.s.r.²⁰ and an electron-nuclear double resonance (ENDOR)²⁹ study of X-irradiated adamantane to its credit; together with a very complete study by Willard et al.,³⁰ with and without doped impurities. The latter group concluded the 2-adamantyl radical is the primary radiation damage product. However, if a suitable substrate is present, a hydrogen atom exchange process can take place, resulting in the formation of the more stable 1-adamantyl radical.³¹ This is a perfectly reasonable sequence of events.

A very convincing series of experiments by Hyfantis et al.,²⁸ however, has shown that the 1-adamantyl radical is formed predominantly. This result is based on a bromine scavenging experiment where the damaged adamantane, at room temperature and under vacuum, was poured into a bromine/cyclohexane solution and the products analysed chromatographically. They found the generation of 1-bromo-adamantane and 2-bromoadamantane to be in the approximate ratio of 3:1. [They did find, however, that prolonged radiolysis enhanced the generation of the latter.]

Other important indications were uncovered by this team when looking at the products from the radiolysis of 1- and 2-bromo and 1- and 2-

chloro adamantanes.³² Employing the reaction:

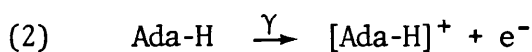


the 1-adamantyl radical should be formed from the 1-bromo and the 1-chloro derivatives; the 2-adamantyl radical from the 2-bromo and the 2-chloro derivatives. The spectrum from the 1-halo derivatives proved to be the same as that from adamantane itself. This is particularly strong evidence in favour of the 1-adamantyl radical.

Although the broad spectrum produced from adamantane makes conclusive classification of the radical impossible, it does, however, prove to be of great assistance when looking at spectra derived from added impurities, as the radical (whichever it is) makes only a small contribution to the overall spectrum.

At no time, in this laboratory or elsewhere, has the adamantane cation been detected. This is not surprising considering the species is, without doubt, very unstable. The presence of electron scavengers in the matrix has shown that adamantane can generate electrons in high yield.

Therefore, the cation thus formed must presumably break down to give a proton and either the 1-adamantyl or 2-adamantyl radical as in reactions (2) and (3).



Purification of adamantane

Past experience has shown adamantane to be a particularly excellent host, not only of intentional impurities, but also of unintentional impurities.²¹⁻²⁶ It therefore became necessary to procure a method for the purification of the compound which could be carried out prior

to any substrate incorporating experiments. The following methods have been employed by e.s.r. spectroscopists.

(a) The most widely used method is the reflux for ca. 2 hrs of activated charcoal and adamantane in either (i) methylcyclohexane, (ii) n-heptane, (iii) n-octane, (iv) n-nonane or (v) n-decane. The product is recrystallised from the filtered solution and dried.

(b) One of the characteristic properties of adamantane is the ease with which it sublimes. This has been utilised as a means of purification. A small sample of adamantane is placed in the bottom of a tube which is then connected to a vacuum line. If a suitable temperature gradient is employed the compound can be made to sublime further up the tube; the resolidified sample, hopefully, being devoid of impurities.

(c) Willard et al.³⁰ found the previous 2 methods unsuitable for their experiments. They therefore carried out a further purification by passing a solution of adamantane in cyclohexane through a 150 cm column containing activated silica gel. The recrystallised product was then dried.

(d) This laboratory experienced similar difficulties to Willard et al.³⁰ with techniques (a) and (b). However, good quality adamantane was obtained by passing a solution of ca. 3 g of adamantane in 30 cm³ of cyclohexane through two 30 cm columns containing activated silica gel. The recrystallised adamantane was dried on a vacuum line.

Incorporation of substrate into adamantane matrix

When attempting to introduce a substrate into the adamantane matrix, the simple problem to overcome is that of obtaining both compounds in either the liquid or the gas phase. There are basically

three methods employed.

(a) If the substrate is a liquid and if it is available in fairly large quantities, it may be possible to dissolve the adamantane in the substrate. The adamantane is then recrystallised and any external substrate is removed by drying in a dessicator with a suitable drying agent and/or on a vacuum line.

(b) Another method of obtaining the adamantane and the substrate in the liquid phase is by the employment of a cosolvent. Dissolve adamantane and ca. 1 mole % of the required substrate in a suitable solvent. Recrystallise and dry as above. Care should be taken, however, when choosing the solvent, or doping of the matrix with solvent molecules will predominate. A small molecular weight alkane such as n-pentane has been shown to be effective.¹⁸

(c) Scanning the literature reveals that cosublimation of the adamantane and the substrate is the most popular method. Adamantane and ca. 1 mole % of the substrate are placed in a vacuumed, sealed, quartz tube. Heating in an oil bath to ca. 180°C produces cosublimation of the mixture which solidifies farther up the tube. By carrying out this procedure a few times and progressing up the tube, a suitably doped sample can be obtained.

Having obtained the doped sample, it is placed in a quartz tube, degassed via the freeze-thaw method and the tube sealed. The tube is then placed in a Dewar flask containing liquid nitrogen and γ -irradiated.

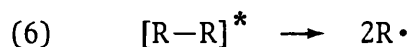
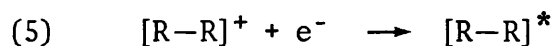
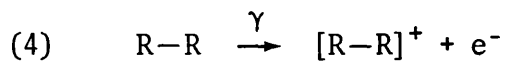
Generation of an authentic hydrocarbon cation [Me₃C-CMe₃]⁺

Introduction

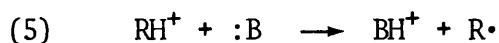
As already stated, there was no sign of the adamantane cation formed from the radiolysis of adamantane, even when the matrix was doped with efficient electron scavengers. Although the literature does reveal the existence of e.s.r. studies of saturated hydrocarbon cations, the broad singlet features formed are after the subtraction of other complex spectra,^{33,34} and yield little information on the structure of the cation involved. Thus, the problem was: can we isolate a stable, saturated, hydrocarbon cation with suitably resolved e.s.r. features?; the latter being essential for structure elucidation.

In order to maximise our chances, we considered the probable properties necessary for the stability of such a species, and for its e.s.r. spectrum to be resolved. These considerations (rehearsed below) led us to the compound 2,2,3,3-tetramethylbutane (TMB). Our interest was further aroused by the discovery that this compound has a phase transition at 152.5 K to a plastic phase (cf. adamantane), and may therefore prove to be an efficient rotator phase matrix. Hence, the reasons were two-fold for our investigations into the products to be derived from the γ -radiolysis of this compound.

Electron return is a highly efficient reaction in irradiated hydrocarbons: the resulting vibrationally and/or electronically excited intermediate decaying to give a considerable yield of alkyl radicals [reactions (4)-(6)].



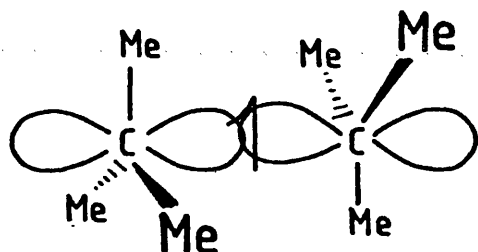
Obviously it is necessary to eliminate this back reaction if we are to generate a sufficient concentration of cation. We therefore employed tetrachloromethane (CCl₄), tetrabromomethane (CBr₄), tetraiodomethane (CI₄) and trichlorofluoromethane (CCl₃F) as electron scavengers. A further difficulty likely to be encountered in the isolation of a cation is the ease with which it may react with any proton accepting species as in reaction (5). We therefore excluded the use of any compound likely to behave in such a manner.



Assuming these steps can produce a cation, we also need to ensure the cation will exhibit a suitably resolved spectrum. Delocalisation of spin into a number of C-C bonds is highly undesirable, so a molecule with either a unique C-C bond or, preferably, with only 1 C-C bond is required. Another culprit for bad resolution of spectra is the existence of protons in different environments exhibiting different coupling constants. It is therefore necessary to choose a molecule with as many of its protons equivalent as possible; 2,2,3,3-tetramethylbutane fits these considerations. Our experiments were therefore the γ -radiolysis of TMB doped with CCl₄, CBr₄, CI₄ and CCl₃F, with the expectation of the ejected electron originating from the unique C-C bond in TMB to give [Me₃C \uparrow CMe₃]⁺.

Although still a source of controversy, we firmly believe the Me₃C \cdot radical to be essentially planar,³⁵ as of course is the $\overset{+}{\text{C}}\text{Me}_3$ carbonium ion. We therefore envisaged our cation (if formed) having its 2 -CMe₃ groups in a near planar arrangement, with the single electron bond perpendicular to this plane, as in III.

Theoretical considerations on B₂H₆⁻ predict the same configuration.³⁶ Thus, we were looking for a species with 19 equally spaced lines of



III

ca. 11 G (half the 22 G for the tertiary butyl radical) in approximately binomial intensities.

EXPERIMENTAL

TMB (Aldrich), CCl_4 (Fisons), CCl_3F (Stohler Isotopes), CBr_4 (Aldrich) and Cl_4 (K & K Labs) were used as supplied. Saturated solutions of TMB in CCl_4 and TMB in CCl_3F were pipetted into 4 mm O.D. quartz tubes and degassed via the freeze-thaw method. 5% Mol fraction solutions of CBr_4 in TMB and Cl_4 in TMB were prepared by warming the appropriate mixture to ca. 105°C (melting point TMB = $99\text{-}101^\circ\text{C}$) in 4 mm O.D. quartz tubes. Samples were exposed to ^{60}Co γ -rays at 77 K in a Vickrad cell at a nominal dose rate of 1.7 Mrad h^{-1} for periods of up to 2h.

E.s.r. spectra at all temperatures were recorded using a Varian E.109 spectrometer. Spectra at temperatures greater than 77 K were obtained using a variable temperature system.

RESULTS

The radiolysis of TMB has been carried out elsewhere³⁷ and the products analysed accordingly. As expected, a high yield of various alkyl radicals were generated via reaction (6), namely the $\text{Me}_2\dot{\text{C}}\text{Me}_3$, $\text{Me}_3\dot{\text{C}}$ and $\text{H}_2\dot{\text{C}}\text{C}(\text{Me}_2)\text{Me}_3$ radicals. Although broad and badly defined at 77 K (Fig. 2a), these radicals show excellent resolution on annealing to ca. 160 K (Fig. 2b). Radiolysis of the doped TMB gave a totally different spectrum at 77 K (Fig. 2c). Minor annealing reversibly broadened out all features while simultaneously uncovering the spectrum of the 3 alkyl radicals. The important point being, however, that their concentrations were drastically reduced compared with the same experiment without the electron scavenger. Prompt cooling back to 77 K reproduced Fig. 2c. If allowed to warm to ca. 160 K before cooling, Fig. 2a is reproduced at much lower intensity. The species formed in Fig. 2c at 77 K was independent of electron scavenger.

ANALYSIS AND DISCUSSION

We feel the species in question is probably the $[\text{Me}_3\text{C}\cdot\text{CMe}_3]^+$ cation. As can be seen, the spectrum consists of a septet of ca. 32 G with each feature consisting of at least 11, perhaps 13 or 15, hyperfine splittings of ca. 4.0 G. Unfortunately, a certain ambiguity exists and the precise number of lines cannot be extracted with certainty. Because the species is independent of electron scavenger it must be derived from the TMB. Hence, we have a species with 6 large, equally coupled protons and 10, 12 or 14 small, equally coupled protons. In our view, the only contender is the aforementioned cation,

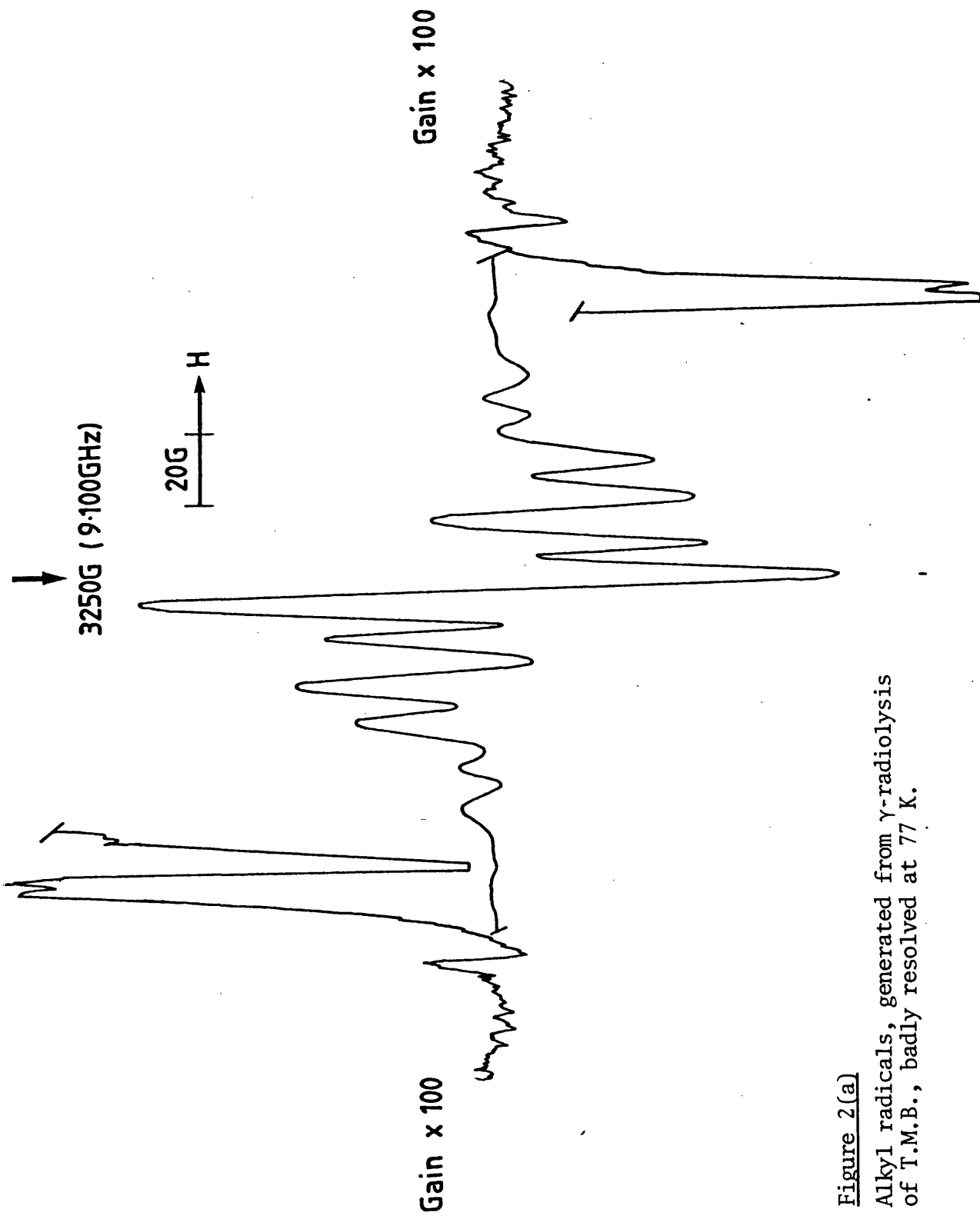


Figure 2(a)
Alkyl radicals, generated from γ -radiolysis
of T.M.B., badly resolved at 77 K.

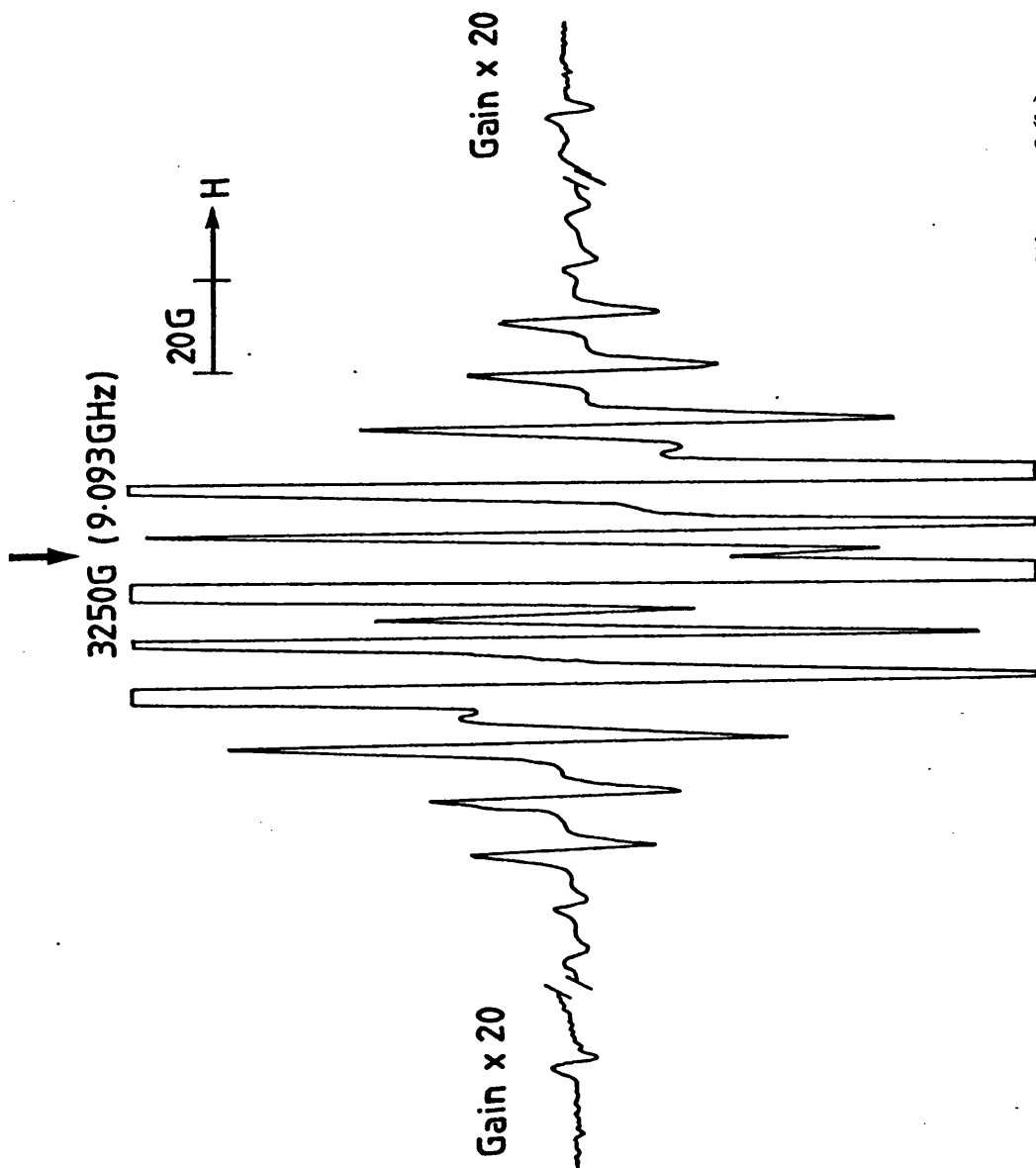


Figure 2(b)

Alkyl radicals exhibiting better resolution at ca. 160 K.

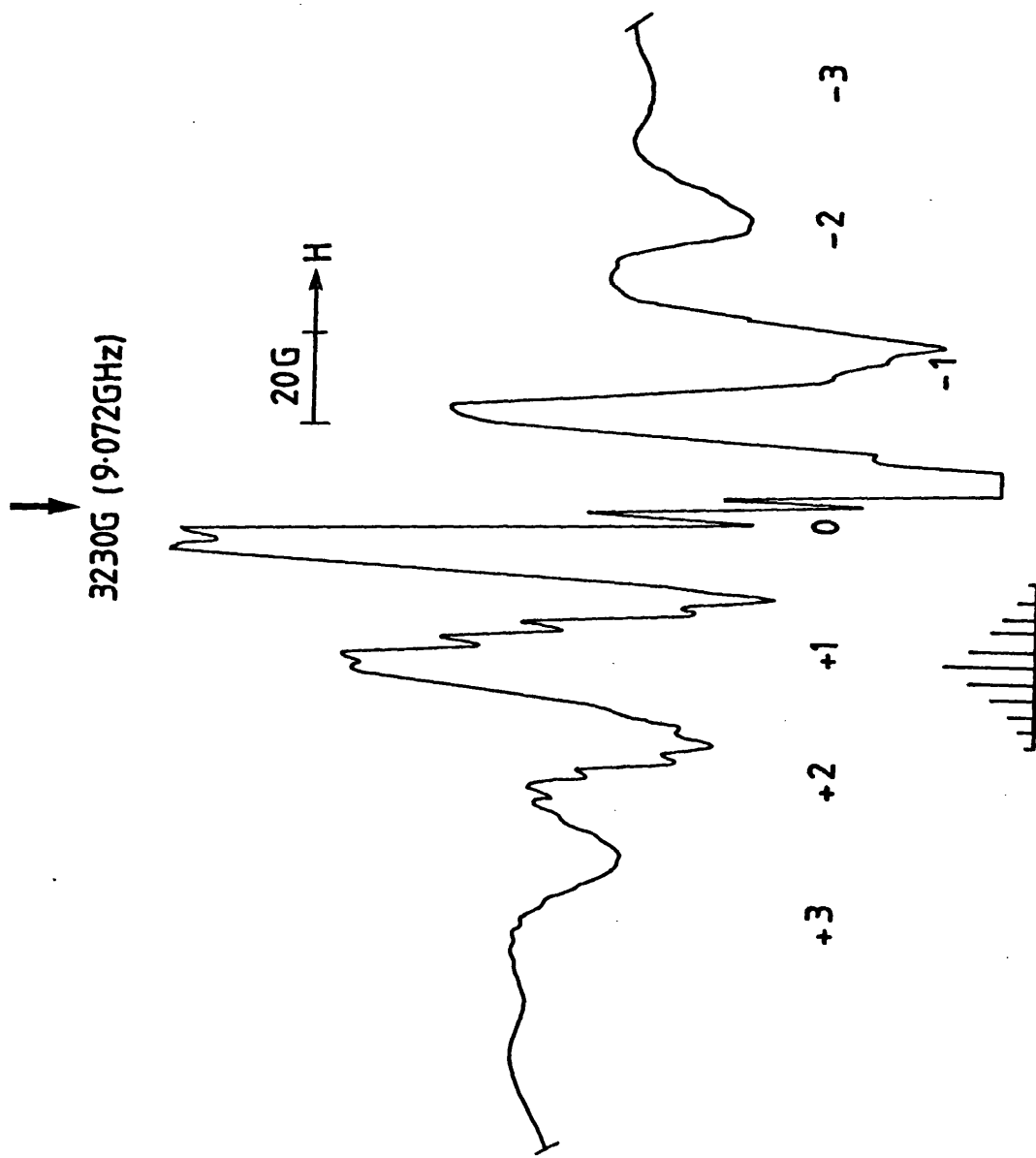


Figure 2(c)
 The $(\text{Me}_3\text{C}-\text{CMe}_3)^+$ cation from γ -radiolysis of T.M.B. doped with electron scavengers.

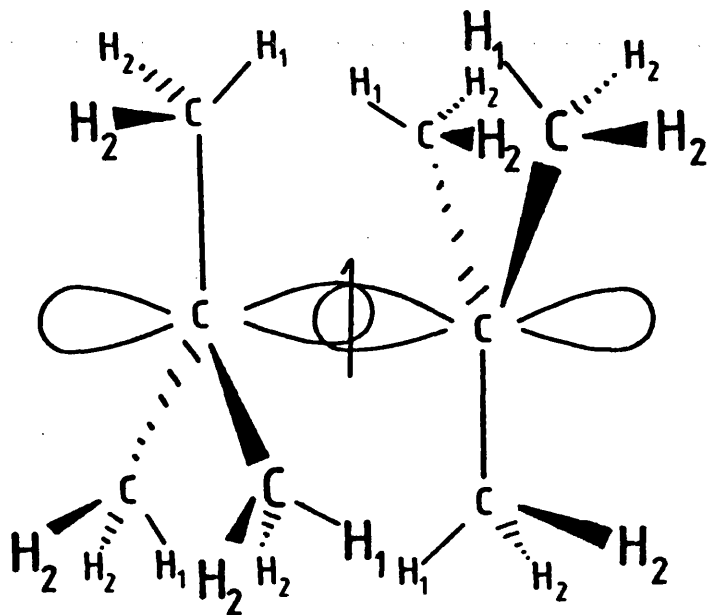
but with a restricted rotation of the methyl groups giving rise to this inequivalence of protons. [The results of a molecular motion study, using proton n.m.r. spectroscopy, by Koide³⁸ has shown just this situation for the parent molecules. Between 77 K and 113 K there exists a restricted methyl group rotation; between 113 K and 153 K the methyl and tertiary butyl groups rotate and above the phase transition at 153 K there is complete molecular rotation.] Fig. 2a shows conclusively the restricted rotation of the alkyl radicals. It is therefore not surprising that the cation also has this problem at 77 K. Unfortunately, annealing does not generate a rotating cation; decomposition into further alkyl radicals pre-empting this motion.

Averaging these coupling constants over 18 protons predicts a splitting of ca. 13.3 G, which is perfectly reasonable for structure III. If restricted methyl group rotation is responsible for the observed spectrum, greatest stability would be achieved by allowing one proton (H_1) of each methyl group to point in towards the one electron bond, simultaneously increasing electronic stability and lowering steric interaction, as in IV. This position of maximum overlap thus predicts the 6 H_1 protons should exhibit coupling constants of ca. 22 G, half the value of 45 G for a maximum overlapped β -proton for a normal alkyl radical V.

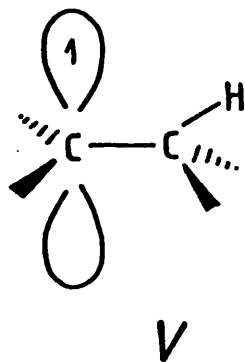
Employing the simple $\cos^2\theta$ law³⁹ for the remaining 12 (H_2) protons predicts coupling constants of ca. $22 \cos^2\theta = 5.5$ G.

The larger experimental value of 32 G for H_1 probably reflects the effect of the positive charge⁴⁰ as hyperconjugative delocalisation is more important for cations than for radicals. If these protons are, therefore, pulled closer to the one electron bond to achieve greater

IV



	theoretical	experimental
H ₁	22G	32G
H ₂	5.5G	4.0G



stabilisation, then surely the H₂ protons will be distorted away from it. Hence our decreased experimental value of 4.0 G.

CONCLUSION

Radiolysis of pure TMB does, in fact, produce cations. However, electron return is so efficient that quantitative decomposition into alkyl radicals predominates. Doping with electron scavengers reduces appreciably this back reaction, resulting in a decrease in alkyl radical concentrations. This also allows for the stability of the (Me₃C + CMe₃)⁺ cation whose parameters are observed at 77 K. The species is, however, particularly reactive and thermal energy leads to decomposition rather than molecular rotation. The envisaged structure is as in IV.

As regards using TMB as a matrix; unfortunately, it appears that the crystal structure is much more constricting than that of adamantane, as even the tertiary butyl radical is not permitted to rotate at 77 K. Also, the products of γ-radiolysis exhibit features spanning over 200 G, making the detection of any damaged impurities very difficult. I would therefore suggest that only small molecules with atoms exhibiting large coupling constants would produce beneficial results when doped into the TMB matrix.

REFERENCES

1. I. G. Smith, M. C. R. Symons, *J.C.S. Perkin II*, 1979, 1362.
2. C. E. Nordman, D. L. Schmitkons, *Acta Cryst.*, 1965, 18, 764.
3. J. Donohue, S. H. Goodman, *Acta Cryst.*, 1967, 22, 352.
4. D. W. McCall, D. C. Douglass, *J. Chem. Phys.*, 1960, 33, 777.
5. H. A. Resing, *J. Chem. Phys.*, 1965, 43, 1828.
6. H. A. Resing, *Mol. Cryst. Liq. Cryst.*, 1969, 9, 101-32.
7. J. D. Graham, J. K. Choi, *J. Chem. Phys.*, 1975, 62, 2509.
8. Shu-Sing Chang, E. F. Westrum, *J. Phys. Chem.*, 1960, 64, 1547.
9. Poe-Ju Wu, L. Hsu, D. A. Dows, *J. Chem. Phys.*, 1971, 54, 2714.
10. N. I. Liu, J. Jonas, *Chem. Phys. Letters*, 1972, 14, 555.
11. G. Giacometti, G. Illuminati, *Gazz. Chem. Ital.*, 1945, 75, 246.
12. W. Nowacki, *Helv. Chim. Acta*, 1945, 28, 1233.
13. P. A. Reynolds, *Acta Cryst.*, 1978, A34, 242.
14. R. Stockmeyer, N. Stiller, *Phys. Stat. Sol.*, 1968, 27, 269.
15. R. Stockmeyer, *Disc. Far. Soc.*, 1969, 48, 156.
16. H. A. Resing, N. T. Corke, J. N. Sherwood, *Phys. Rev. Lett.*, 1968, 20, 1227.
17. This thesis, Chapter 3.
18. J. A. Berman, R. N. Schwarz, *Mol. Cryst. Liq. Cryst.*, 1973, 28, 51-61.
19. M. B. Yim, D. E. Wood, *J.A.C.S.*, 1976, 98, 2053.
20. J. R. Ferrell, G. R. Holden, R. V. Lloyd, D. E. Wood, *Chem. Phys. Letters*, 1971, 9, 343.
21. D. R. Gee, L. Fabes, J. K. S. Wan, *Chem. Phys. Letters*, 1970, 7, 311.
22. L. Bonnazola, R. Marx, *Chem. Phys. Letters*, 1971, 8, 413.
23. W. G. Filby, K. Günther, *Chem. Phys. Letters*, 1972, 14, 440.
24. W. G. Filby, K. Günther, *Chem. Phys. Letters*, 1972, 17, 150.

25. W. G. Filby, K. Günther, Z. Naturforsch., 1972, 27, 1289.
26. R. Marx, Chem. Phys. Letters, 1972, 17, 152.
27. P. J. Krusic, T. A. Rettig, PRSchleyer, JACS, 94, 995,
28. G. J. Hyfantis, A. C. Ling, Chem. Phys. Letters, 1974, 24, 335.
29. R. V. Lloyd, M. T. Rodgers, Chem. Phys. Letters, 1972, 17, 428.
30. G. C. Dismukes, J. E. Willard, J. Phys. Chem., 1976, 80, 1435.
31. I. Tabushi, Y. Aoyama, S. Kojo, J. Hamuro, Z. Yoshida, J.A.C.S., 1972, 94, 1177;
32. G. J. Hyfantis, A. C. Ling, Can. J. Chem., 1974, 52, 1206.
33. H. Yoshida, T. Shiga, W. Schmidt, J.C.S. Faraday II, 1972, 68, 1709.
34. J. Ceulemans, Discuss. Faraday Soc., 1977, 63, 192.
35. T. A. Claxton, E. Platt, M. C. R. Symons, Mol. Phys., 1976, 32, 1321;
D. Griller, K. U. Ingold, P. J. Krusic, H. Fischer, J.A.C.S., 1978, 100, 6750.
36. T. A. Claxton, R. E. Overill, M. C. R. Symons, Mol. Phys., 1974, 27, 701.
37. H. Shiraishi, H. Kadoi, K. Hasegawa, Y. Tabata, K. Oshima, Bull. Chem. Soc. Japan, 1974, 47, 1400.
38. T. Koide, Bull. Chem. Soc. Japan, 1967, 40, 2026.
39. M. C. R. Symons, J. Chem. Soc., 1959, 277.
40. R. Hume, M. C. R. Symons, J. Chem. Soc., 1965, 1120.

CHAPTER 2

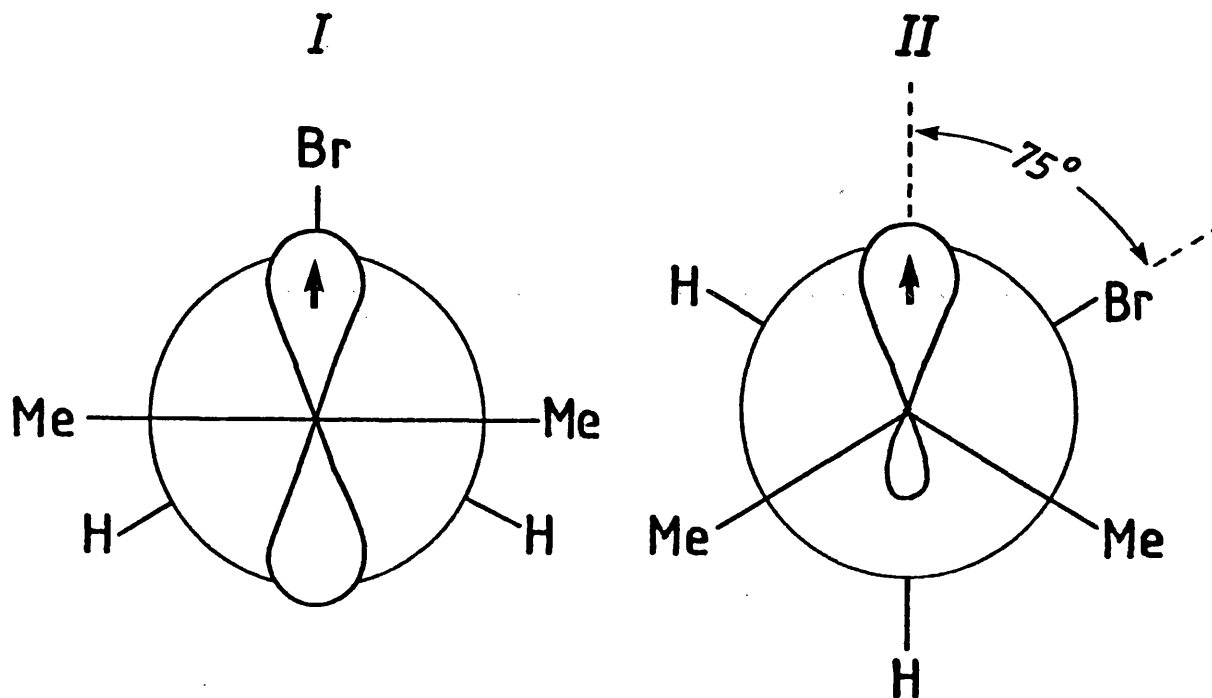
The β -bromo story

INTRODUCTION

Previous work in this laboratory¹ on the radiolysis of alkyl bromides had shown the presence of a novel species exhibiting a large hyperfine coupling to the bromine. The coupling of ca. 300 G was clearly too large for an α -bromo radical $[R_2\dot{C}-Br]$,^{2,3,4,5} it was therefore postulated that the species responsible was the β -bromo radical $[R_2\dot{C}-C\begin{smallmatrix} \swarrow Br \\ \searrow R \end{smallmatrix}]$. The large A_x coupling is explained quite satisfactorily in terms of a conformation which allowed maximum $\sigma \rightarrow \pi$ overlap (I), as is the case with the well documented β -chloro radicals.^{6,7,8} Unfortunately, only A_x and g_x could be extracted with any real certainty making complete comparison with the analogous β -chloro radicals impossible. All attempts to produce β -bromo radicals in the liquid phase or in a single crystal have also failed, so as yet the remaining parameters still elude us.

A highly characteristic spectral property of these β -bromo radicals is the isotropic appearance of the $M_I = +\frac{1}{2}$ features which often exhibit proton hyperfine couplings. In the particular case of the $Me_2\dot{C}H_2Br$ radical (hereafter designated as species S), generated from Bu^tBr , a value of 13 G for the 6 methyl protons was apparent; again in good agreement with the 17 G from the analogous β -chloro radical $Me_2\dot{C}H_2Cl$.⁶

Wood and Lloyd then published a liquid phase spectrum from the radiolysis of $isoBuBr$ in adamantane.⁹ The spectrum, exhibiting proton couplings of 21.4 G and 42.8 G and a bromine coupling of 6 G, was also interpreted in terms of the β -bromo radical $Me_2\dot{C}H_2Br$ (hereafter designated as species W) with the conformation as shown in (II). Hence, species S (formed in a Bu^tBr matrix) and species W (formed in



an adamantane matrix) are both contenders for the same radical. It was suggested⁹ that perhaps both are the β -bromo radical, exhibiting different conformations in different media. However, this seems unlikely and, in fact, we have detected both species S and species W in the same medium. We then postulated that species W could be the t-butyl radical weakly associated with its ejected bromide ion;¹⁰ an "adduct". This family of species has been detected in certain solid state systems here^{11,12} and elsewhere.^{13,14} However, this tentative assignment was dismissed by Wood and Lloyd.¹⁵

Thus, the situation was in an obvious state of controversy. The correct assignment to the β -bromo radical is also of some mechanistic significance as these species have been postulated as intermediates in a range of organic reactions.¹⁶ It was at this stage that we decided a closer scrutiny of the systems involved was called for if the problem was to be resolved.

EXPERIMENTAL

Tertiary butyl bromide (B.D.H), isobutyl bromide (B.D.H), tetramethyl silane [TMS] (B.D.H), and di-t-butyl peroxide (Koch-Light) were purified by distillation, only the middle fractions with acceptable boiling points being used. Adamantane (Aldrich) was purified as described in Chapter 1. Adamantane-d₁₆ (Merck, Sharpe & Dohme) and TMS-d₁₂ (Merck, Sharpe & Dohme) were used as supplied. The purities of the substrates and matrices were checked using n.m.r. spectroscopy prior to any experimentation.

1% Mol fraction solutions in TMS were pipetted into 4 mm O.D. quartz tubes and degassed via the freeze-thaw method. Samples in adamantane were prepared by recrystallising the adamantane from the required substrate and pressing the solid into a hard pellet. Samples were exposed to ⁶⁰Co γ-rays at 77 K in a Vickrad cell at a nominal dose rate of 1.7 Mrad h⁻¹ for periods of up to 4h.

Photolysis of TMPD* (Aldrich) in TMS and adamantane solutions was carried out by exposure at 77 K to radiation from a low pressure mercury lamp through a 253 n.m. filter. Photolysis of the peroxide mixtures was carried out in the same way.

E.s.r. spectra at all temperatures were recorded using a Varian E109 spectrometer. Spectra at 4.2 K were obtained using a liquid helium insert, while those at temperatures greater than 77 K were obtained using a variable temperature system. It was appreciated that the spectra of the Me₂ \dot{C} CH₂Br radical in a single crystal would shed a great deal of light on the problem. Unfortunately, as previously reported,²⁵ crystals of Me₃CBr shattered at temperatures lower than 233 K, and irradiation of the crystal above this temperature did not yield the required species.

*

RESULTS

The 4 systems studied were those of isoBuBr and Bu^tBr in matrices of adamantane and TMS. The results for each system are presented individually below in terms of their temperature dependent spectral changes.

1. isoBuBr in adamantane-d₁₆

Although already studied by Wood and Lloyd at ca. 200 K, we felt a complete analysis beginning at the radiolysis temperature of 77 K was called for.

The first discernible features grew in on minor annealing, the best resolution being obtained at ca. 94 K, (Fig. 1a), and were due to a species we shall for the time call species A. The features grew reversibly less well defined as the temperature was increased until at ca. 140-160 K they were replaced with those from species W. These features persisted up to ca. 206 K by which time extra features due to species B presented themselves, (Fig. 1b). Cooling back to 77 K produced an unanalyseable spectrum where all but the outer features of species W were broadened reversibly, similar to that shown in Fig. 2a. Annealing to temperatures >208 K generated unambiguous (CH₃)₃C• radicals and (CH₃)₂Ċ(CH₂D) radicals, (Fig. 1c). During the whole experiment, a badly resolved species S was present. When the same experiment was carried out with adamantane-h₁₆, neither species B nor the (CH₃)₂Ċ(CH₂D) radicals were detected.

2. isoBuBr in T.M.S.

At 77 K, Me₂CHCH₂• radicals were generated in high yield together with species C, (Fig. 1d). Annealing produced the simultaneous

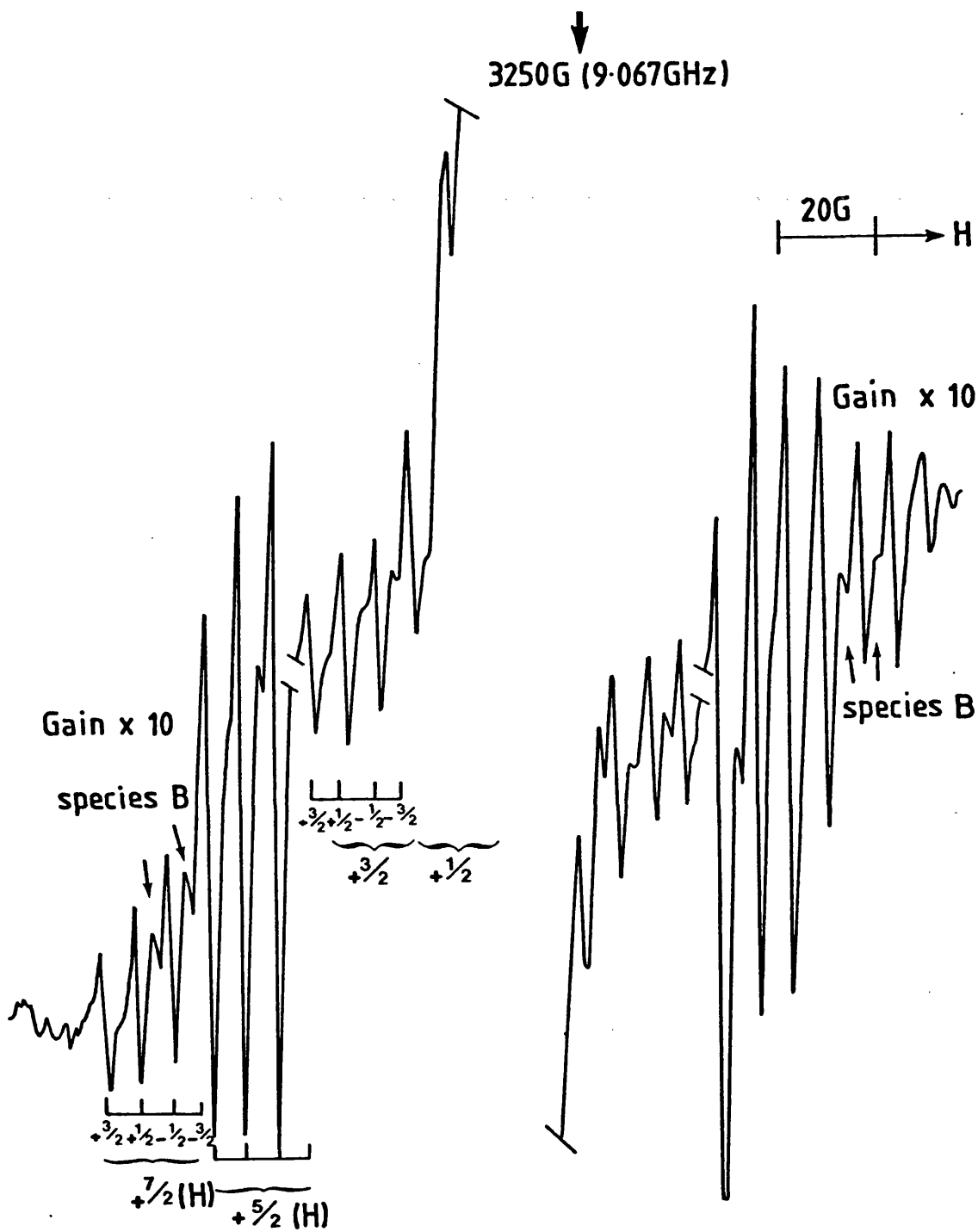


Figure 1(b)

Species (W) and species (B). The $(\text{CH}_3)_3\text{C}\cdot/\text{Br}^-$ and $(\text{CH}_3)_2\dot{\text{C}}(\text{CH}_2\text{D})/\text{Br}^-$ adducts.

↓
3230G (9.088GHz)

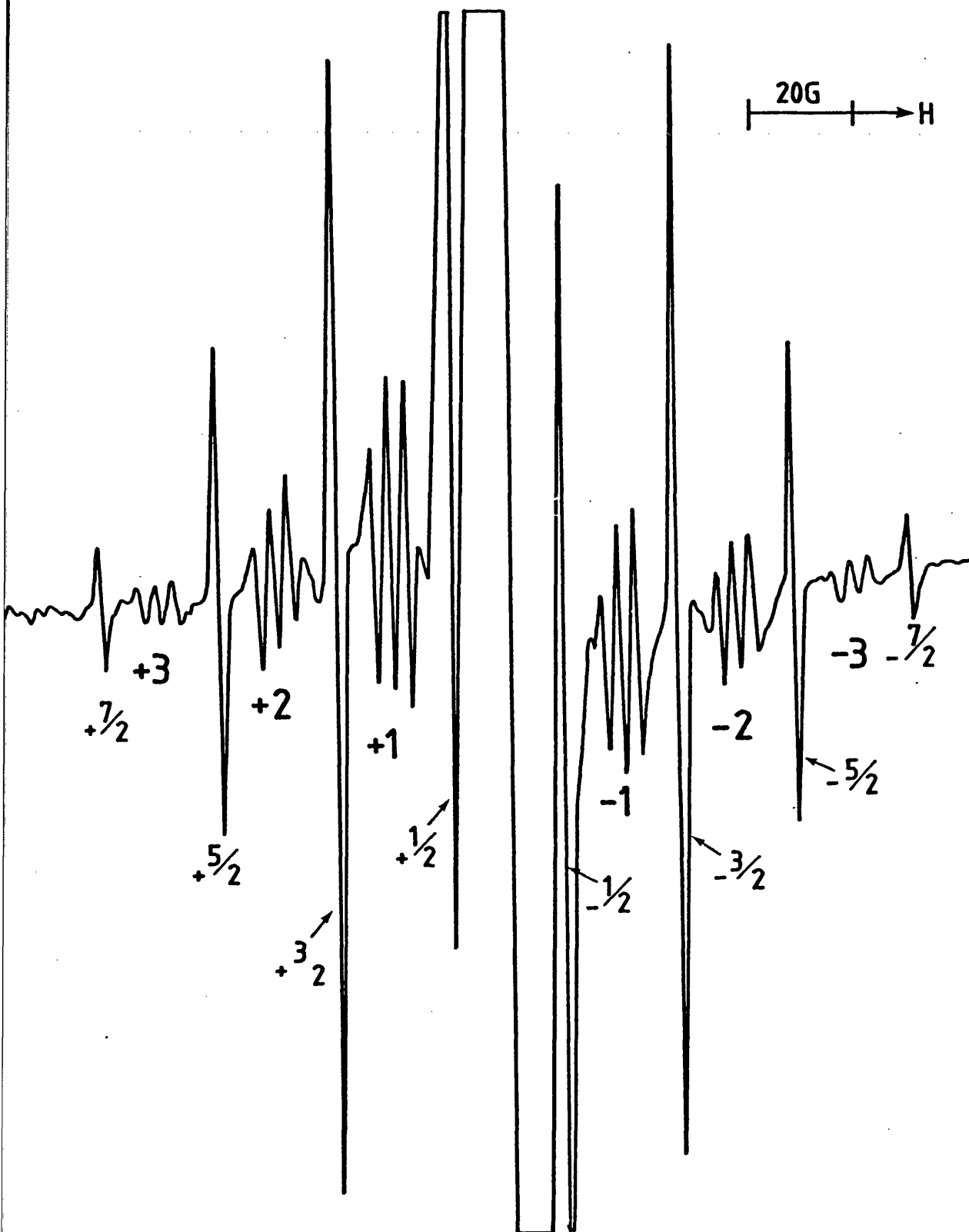


Figure 1(c)
(CH₃)₃C• and (CH₃)₂C•(CH₂D) radicals.

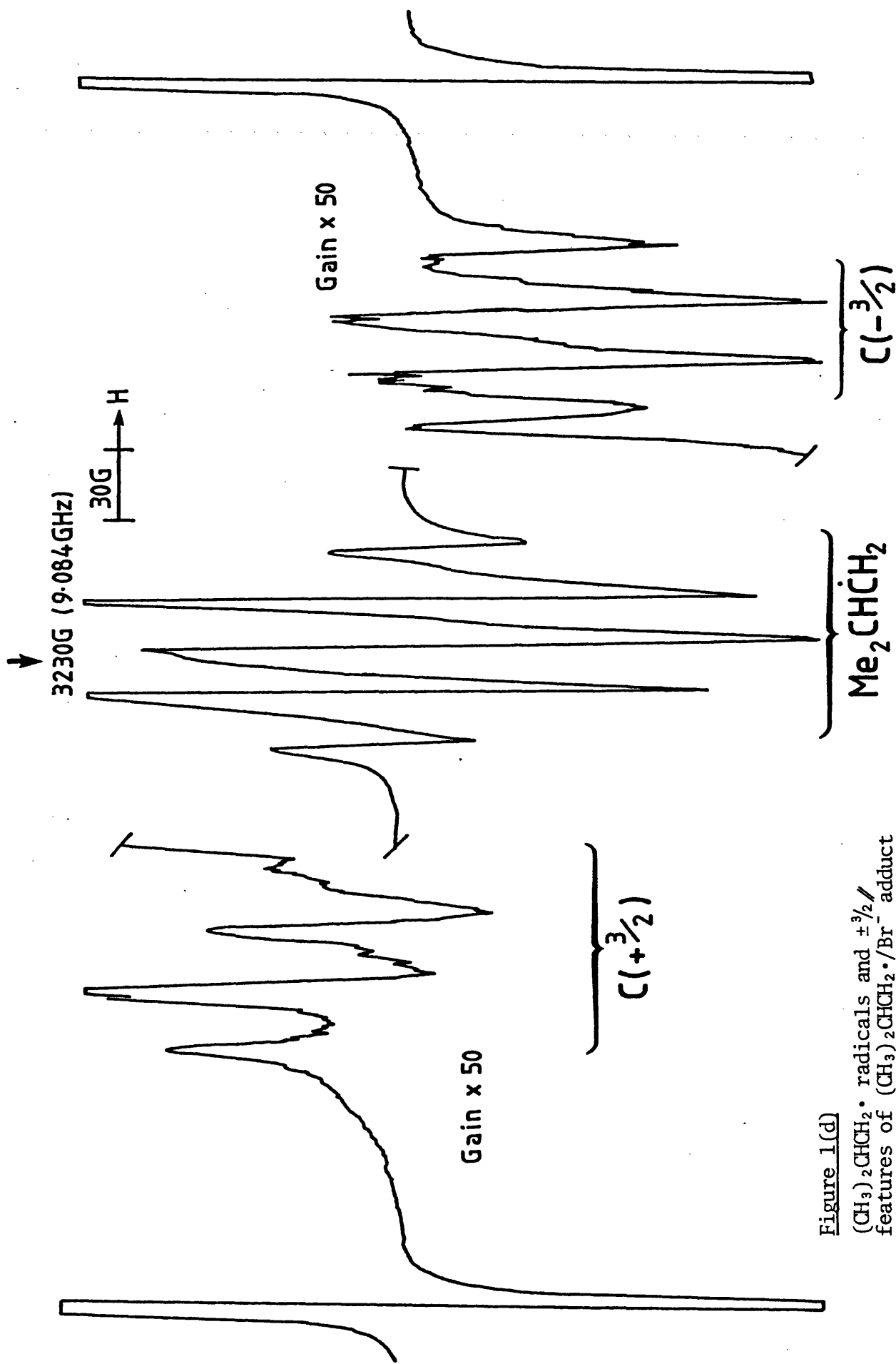


Figure 1(d)
 (CH₃)₂CHCH₂• radicals and ± $\frac{3}{2}$ features of (CH₃)₂CHCH₂•/Br⁻ adduct [species (C)].

disappearance of both species, with the replacement by $(\text{CH}_3)_3\text{C}\cdot$ radicals and a small concentration of species W. Very weak features detected in the wings were due to small yields of the α -bromo radical $\text{Me}_2\text{CH}\dot{\text{C}}\text{HBr}$ and species S. Further annealing resulted in the removal of species W, but an increase in the concentration of $(\text{CH}_3)_3\text{C}\cdot$ radicals. Only the α -bromo radical features now remained in the wings. Employing T.M.S- d_{12} as the matrix did not result in the formation of species C, neither was there any sign of $(\text{CH}_3)_3\text{C}\cdot$ or $(\text{CH}_3)_2\dot{\text{C}}(\text{CH}_2\text{D})$ radicals growing in on annealing.

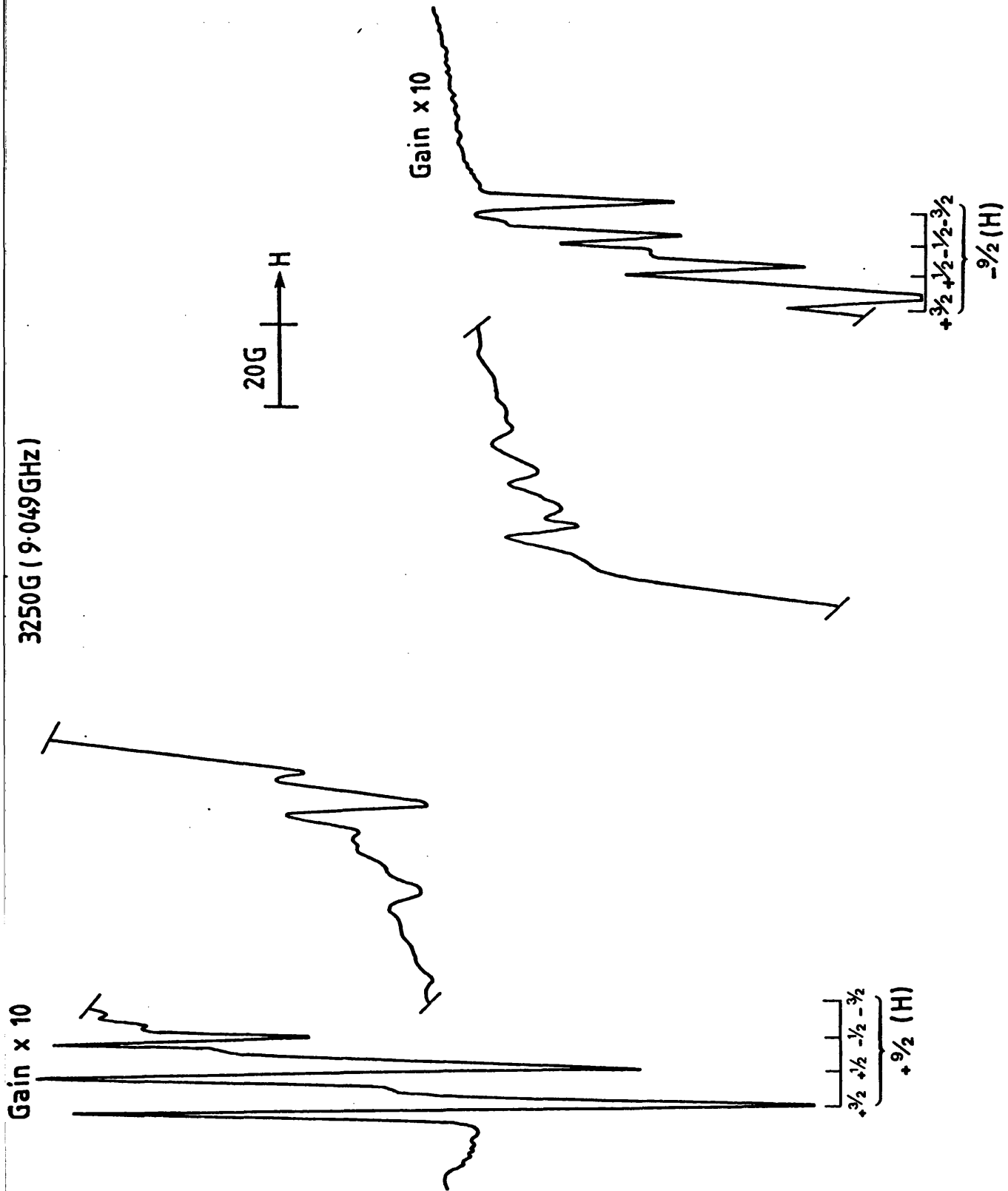
To validate the tentative assignment of species W to the $\text{Bu}^{\text{t}}\cdot/\text{Br}^-$ adduct,¹⁰ this laboratory had looked at the $\text{Bu}^{\text{t}}\text{Br}/\text{adamantane}$ system, and had in fact detected species W in large yield. However, Wood and Lloyd¹⁵ then insisted that the sole product from this particular radiolysis is the $\text{Bu}^{\text{t}}\cdot$ radical, and that any species W formed in our experiment must have been from an isoBuBr impurity in our $\text{Bu}^{\text{t}}\text{Br}$. The $\text{Bu}^{\text{t}}\text{Br}$ used in the following experiments has been analysed using n.m.r. spectroscopy. Our results show absolutely no sign of any isoBuBr impurity.

3. $\text{Bu}^{\text{t}}\text{Br}$ in adamantane- d_{16}

The spectrum as shown in Fig. 2a was produced immediately at 77 K. All changes up to ca. 208 K were reversible. The familiar spectrum of species W evolved at ca. 150 K and persisted until 208.6 K whereupon it was lost, being replaced by a high yield of $\text{Bu}^{\text{t}}\cdot$ radicals. Species S was present in a badly defined form from 77 K to temperatures greater than 208 K. There was no sign of species A, species B or $(\text{CH}_3)_2\dot{\text{C}}(\text{CH}_2\text{D})$ radicals. Adamantane- h_{16} produced the same results.

Figure 2(a)

Species (W) at 77 K. $[(\text{CH}_3)_3\text{C}\cdot/\text{Br}^- \text{ adduct}]$



4. Bu^tBr in T.M.S.

Spectra, as shown in Figs. 2b and 2c, were recorded at 77 K after storage in liquid nitrogen for ca. 24 hrs. Fig. 2b shows a well resolved species S, Fig. 2c showing a good yield of species W, superimposed on top of Bu^t• radicals. Annealing produced a minor improvement in resolution of both species S and species W, the former then becoming irreversibly broad (similar to the resolution obtained for species S in the other 3 systems), the latter decreasing in concentration with a simultaneous growth of more Bu^t• radicals.

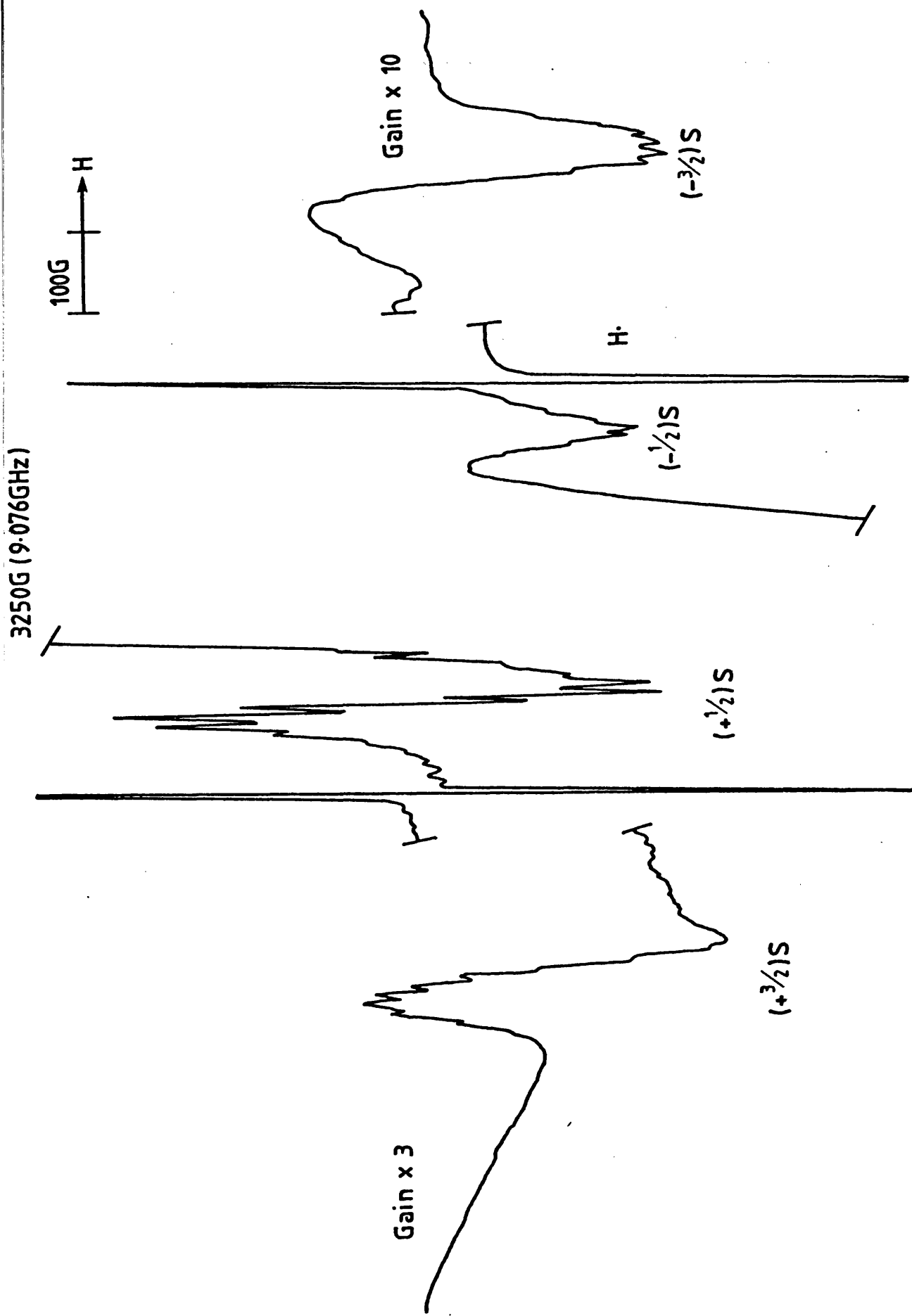
Assignment of Species A, B and C

A species likely to be formed from isoBuBr would, of course, be the Me₂CHCH₂• radical. Analysis of the isotropic spectrum in Fig. 1a shows species A is, in fact, closely related to this alkyl radical (see Fig. 1d), the spectrum being complicated somewhat by further hyperfine couplings of ca. 3.5 G. We are quite convinced species A is the Me₂CHCH₂• radical weakly associated with its ejected bromide ion, the Me₂CHCH₂•/Br⁻ adduct, with $A_{H(\alpha)} = -19.0$ G, $A_{H(\beta)} = +36.2$ G and $A(^{79}\text{Br}, ^{81}\text{Br}) = \pm 3.5$ G. The proton couplings are marginally less than those for the pure Me₂CHCH₂• radical, possibly due to a modest transfer of spin to the bromide ion, as found for the other adducts.

The isolation of the Me₂CHCH₂•/Br⁻ adduct must, therefore, add credence to this laboratory's identification of species W as the Bu^t•/Br⁻ adduct. Its reduced proton couplings of 21.4 G [22.7 G for the pure Bu^t• radical] split into quartets of ± 6.7 G by the bromide ion. Species W and species B are, of course, the successors to the Me₂CHCH₂•/Br⁻ adduct in the isoBuBr/adamantane-d₁₆ system, before they are themselves superceded by Bu^t• and (CH₃)₂Ĉ(CH₂D) radicals. We therefore not only assign species W to the Bu^t•/Br⁻ adduct but also

Figure 2(b)

Well resolved species (S) $[(\text{CH}_3)_2\dot{\text{C}}-\text{CH}_2^{\text{Br}}]$



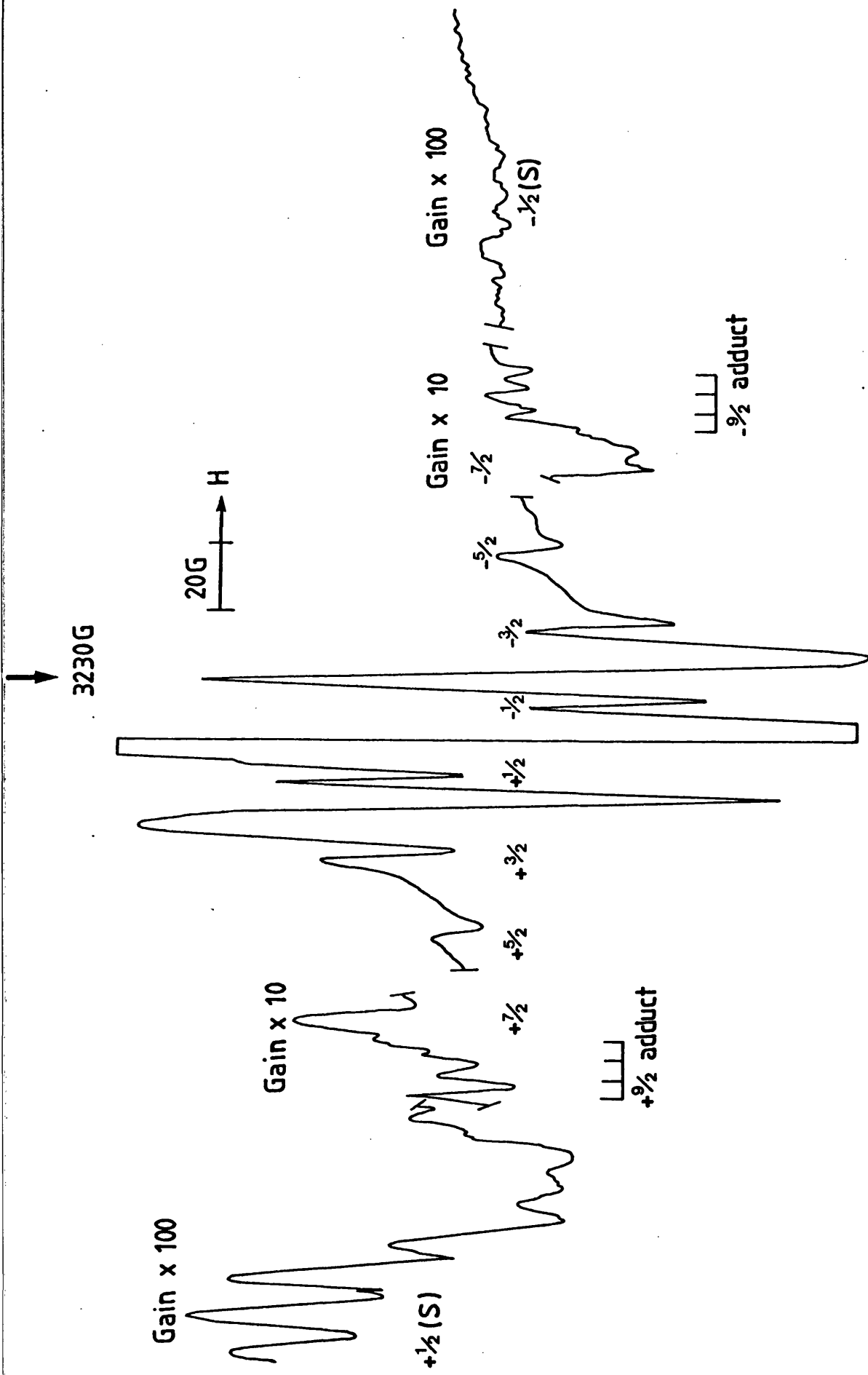


Figure 2(c) Showing $\pm 1/2$ features of species (S); features attributable to $(CH_3)_3C\cdot$ radicals and the $(CH_3)_3C\cdot/Br^-$ adduct.

species B to the $(\text{CH}_3)_2\dot{\text{C}}(\text{CH}_2\text{D})/\text{Br}^-$ adduct.

In T.M.S., $\text{Me}_2\text{CHCH}_2\cdot$ radicals are produced in high yield with no real sign of the isotropic $\text{Me}_2\text{CHCH}_2\cdot/\text{Br}^-$ adduct. However, a small concentration of the $\text{Bu}^t\cdot/\text{Br}^-$ adduct is generated on annealing, the precursor for which must be the $\text{Me}_2\text{CHCH}_2\cdot/\text{Br}^-$ adduct. We therefore postulate species C is the rigid $\text{Me}_2\text{CHCH}_2\cdot/\text{Br}^-$ adduct, the large coupling of ca. 75 G being the parallel component of the bromine A tensor. The relative intensities of the $\pm 3/2$ features suggests the g parameters are all close to 2.002, adding further credibility to our assignment.

In view of the intricacies of the claims and counter-claims involved, the following discussion will be divided into 3 sections for ease of presentation. They are:

- (a) The Case For and Against Species W being the β -bromo Radical;
- (b) The Case For and Against Species W being the $\text{Bu}^t\cdot/\text{Br}^-$ Adduct;
- (c) The Case For Species S being the β -bromo Radical.

(a) The Case For and Against Species W being the β -bromo Radical

(i) Wood and Lloyd argue that since isoBuF and isoBuCl generate unambiguous β -fluoro and β -chloro radicals respectively in adamantane, isoBuBr and isoBuI are expected to produce the analogous β -bromo and β -iodo radicals.⁹ We totally agree. However, we feel Wood and Lloyd were a little hasty in assigning the best defined species in the isoBuBr/adamantane and isoBuI/adamantane systems to the radicals in question. Species S is indeed formed from isoBuBr.

(ii) To explain the spectrum obtained, Wood and Lloyd need to postulate a coupling of 21.4 G for the 6 methyl protons and one of the β -protons, and a fortuitous coupling of exactly twice this (42.8 G) for the other β -proton. Then, to explain the incorrect line intensities

for this interpretation, a certain amount of motional broadening is suggested.^{9,15} We consider this analysis incorrect. Firstly, annealing should produce sufficient further motion to result in a non-coincidence of proton couplings. [In fact, the 10 proton components persist on anneal while the bromine coupling decreases.] Secondly, the same coincidences and motional effects are postulated for the β -iodo radical $\text{Me}_2\dot{\text{C}}\text{CH}_2\text{I}$,⁹ which seems most improbable considering the drastic change in size of halide atom.

(iii) Wood and Lloyd have claimed that Bu^tBr generates only $\text{Bu}^t\cdot$ radicals in adamantane.¹⁵ Unfortunately, they are very much mistaken and, in fact, the yield of species W is some 10 times greater than from isoBuBr , as would be expected if W was the $\text{Bu}^t\cdot/\text{Br}^-$ adduct.

(iv) The product from the radiolysis of 1-bromo-1,1-dideutero-2-methylpropane $\text{Me}_2\text{CHCD}_2\text{Br}^*$ resulted in a badly defined spectrum, analysed by Wood and Lloyd in terms of the $\text{Me}_2\dot{\text{C}}\text{-CD}_2\text{Br}$ radical with one deuteron exhibiting fortuitously twice the coupling of the other (3.28 G and 6.55 G). Our theory predicts the occurrence of the $\text{Me}_2\dot{\text{C}}\text{CHD}_2/\text{Br}^-$ and $\text{Me}_2\dot{\text{C}}\text{CD}_3/\text{Br}^-$ adducts. The major species present actually exhibits couplings to 6 equivalent protons, a bromine atom and 3 equivalent deuterons and is, of course, this latter adduct. It appears that, in this case, the intermolecular reaction with the matrix predominates over the intramolecular rearrangement (see next section).

(v) Perhaps the strongest argument against Wood and Lloyd's assignment is the requirement of the β -bromo and β -iodo radicals to adopt conformation II in preference to conformation I. The β -chloro radical

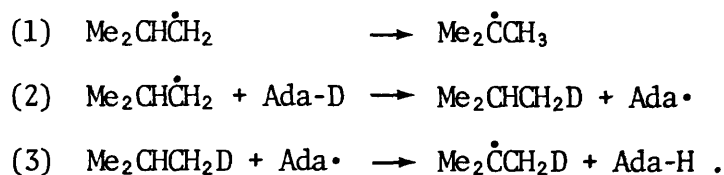
* Spectrum kindly supplied by Professor D. E. Wood.

adopts the latter^{6,7,8} and we can see no reason why the 2 heavier atoms should digress from the usual halogen conformity. In fact, steric and electronic arguments favour conformation I. Also, the postulate that the C atom at the radical site is markedly non-planar¹⁵ is extremely controversial^{17,18} and relies upon the hypothesis of the Bu^t• radical being pyramidal. We are firm believers in the effective planarity of the Bu^t• radical, for reasons discussed elsewhere,¹⁷ and therefore see no reason why the carbon at the radical site in the Me₂ĊH₂Br radical should not also be planar. This carbon atom is clearly planar in the analogous Me₂ĊH₂Cl radical (and in the Me₂ĊH₂F radical), therefore Wood and Lloyd are requiring yet another digression from the usual Cl, Br, I uniformity.

(vi) In the isoBuBr/adamantane-d₁₆ system, species W and B are replaced by Bu^t• and Me₂ĊH₂D radicals above 208 K. If W is the Me₂ĊH₂Br radical, what mechanism could account for the formation of these final radical products? Wood and Lloyd do not discuss this problem.^{9,15} Our chemical reactions make good mechanistic sense.

(b) The Case For and Against Species W being the Bu^t•/Br⁻ Adduct

(i) In adamantane-d₁₆ above 208 K, isoBuBr generates a mixture of Bu^t• and Me₂ĊH₂D radicals, while Bu^tBr generates Bu^t• radicals alone with no sign or growth of Me₂ĊH₂D radicals. Hence, monodeuteration from the matrix does not occur at the Bu^t• stage, as suggested by Wood and Lloyd,^{9,15} and only takes place with isoBuBr. To explain this phenomenon, we therefore suggest the existence of 2 competing mechanisms for the generation of these 2 alkyl radicals from isoBuBr. An intramolecular rearrangement (1), and two intermolecular reactions with the matrix (2) and (3).

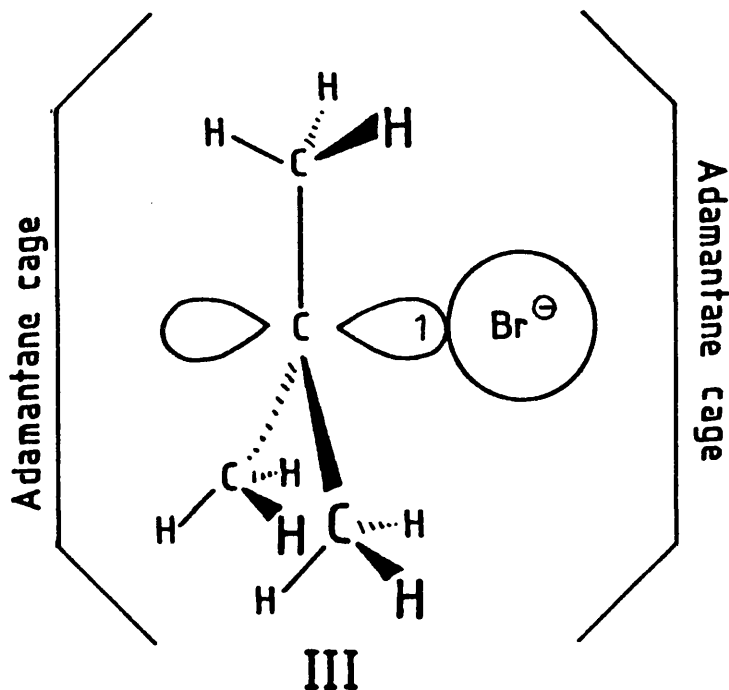


The driving force behind both these mechanisms is the formation of a tertiary radical from a less stable primary radical. If these reactions take place while the radicals are still weakly associated with their bromide ions, we would also expect the presence of the $\text{Me}_2\dot{\text{C}}\text{CH}_2\text{D}/\text{Br}^-$ adduct. As already stated, the extra features in Fig. 1b (species B) have been assigned to this adduct, the expected parameters fitting perfectly with the spectrum. At the adamantane transition temperature of 208.6 K, the adducts $\text{Me}_2\dot{\text{C}}\text{CH}_3/\text{Br}^-$ and $\text{Me}_2\dot{\text{C}}\text{CH}_2\text{D}/\text{Br}^-$ simply break down, and the radicals become disassociated from their respective bromide ions.

(ii) One of the main criticisms of this assignment is the small value of the isotropic halide coupling. Other solid state examples of adducts^{11,12,13,14} predict much larger isotropic couplings in the order of ca. 40 G, obviously much too large. However, if the perpendicular parameters for these systems are taken as negative (and the sign cannot be extracted from the spectra), then isotropic halide couplings of ca. 0 G are predicted. [Chapter 3 deals with this problem and, in fact, shows our assumption to be perfectly correct.]

(iii) Wood and Lloyd point out that the line intensities are incorrect for this assignment.^{9,15} This is indeed the case, but only for the more intense $\pm 9/2$ quartets. In fact, this phenomenon becomes increasingly obvious as the temperature is lowered, until at 77 K only these outer quartets persist, all intermediate features broadening out (Fig. 2a). To explain this narrow-broad-narrow appearance, we need to postulate a situation where the protons become inequivalent,

and yet the adduct as a whole is permitted to rotate. We therefore envisage a conformation as in III where the methyl groups are not able to rotate at low temperatures. We appreciate this particular explana-



tion for the spectral properties may be the weak point of our argument, however, the evidence in favour of our $\text{Bu}^{\cdot+}/\text{Br}^-$ adduct assignment is so strong that there must be some sort of proton asymmetry within the adduct at 77 K.

(iv) It was appreciated that a useful experiment would be the cooling down of the $\text{Bu}^{\cdot+}/\text{Br}^-$ adduct to such a temperature that would cause its rigidity, and hence enable the extraction of its solid state parameters. Unfortunately, the resulting spectrum produced at 4.2 K was not perfect, and any values extracted were far from unambiguous.

(v) Wood and Lloyd's contention that species W was not an electron gain species was based on an experiment where the $\text{isoBuBr}/\text{adamantane}$ system was doped with Me_3NBH_3 and irradiated.¹⁵ The yield of W was the same as without the additive. Our experience¹⁹ strongly suggests Me_3NBH_3 is no more efficient at scavenging positive holes than it is

electrons, therefore no difference in yield is expected. We carried out a more definitive experiment using the photolysis of tetramethylphenylenediamine as the source of electrons and we did detect species W. The yield from Bu^tBr was again greater than the yield from isoBuBr . Species S was not detected.

(c) Case For Species S being the Radical $\text{Me}_2\dot{\text{C}}\text{CH}_2\text{Br}$

There have been no other interpretations for the spectrum of species S, the only argument against the β -bromo assignment being the contention that W is, in fact, the β -bromo radical.^{9,15} We have shown W and S are not the same species exhibiting different conformations in different media, as suggested by Wood and Lloyd. We also believe we have shown that W must be the $\text{Bu}^t\cdot/\text{Br}^-$ adduct. In this section we will, therefore, rehearse the analysis of the spectrum obtained for species S, making suitable inferences and comparisons as we progress.

(i) A well-resolved species S was obtained from a 1% mole solution of Bu^tBr in tetramethylsilane (Fig. 2c). Resolution was such that 6 methyl proton couplings of ca. 13 G could be observed on each of the 4 ^{79}Br A_x components as well as the 4 ^{81}Br A_x components, permitting $A_x(^{79}\text{Br})$ and $A_x(^{81}\text{Br})$ to be extracted with precision. The ratio of these values [$A_x(^{79}\text{Br}) = 338.0$, $A_x(^{81}\text{Br}) = 362.0$] are exactly the same as the ratio of the 100% orbital populations for the respective isotopes.²⁰ Hence we have an unambiguous monobromo radical with an $A_x(^{81}\text{Br})$ parameter clearly much too large for an α -bromo radical.

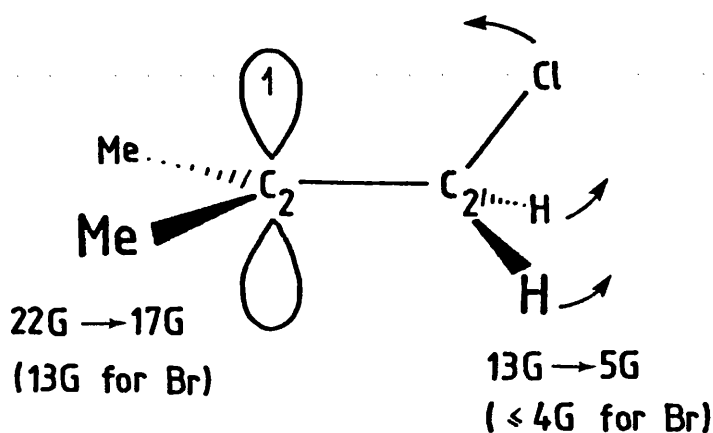
(ii) Although the complete g tensor cannot be extracted for S, g_{\parallel} can be measured at about 2.002 and g_{\perp} can be inferred, by the fact that the downfield A_x features are much more intense than the corresponding upfield features, to be >2.0023 . Thus, $g_{\text{av}} > 2.0023$. This is also the case for the β -chloro radicals.⁶ Δg (difference between g_{av} and

$g_{x,y,z}$) is clearly greater for species S than for the $\text{Me}_2\dot{\text{C}}\text{CH}_2\text{Cl}$ radical, as expected considering the large spin-orbit coupling constant of bromine.

[This would seem a suitable time to point out that all the adducts so far isolated yield $g_{\text{av}} < 2.002$,^{11,12,13,14} which is comparable to the g_{av} value for species W.]

(iii) The proton couplings of 13 G extracted from the spectrum in Fig. 2c are in good agreement with the 17 G from the analogous β -chloro radical.⁶ Also, the linewidth involved predicts the coupling constants for the 2 methylene protons to be ≤ 4 G, again quite comparable with the ca. 5 G for the β -chloro radical. Although a precise comparison between the $A(^{81}\text{Br})$ and $A(^{35}\text{Cl})$ tensors is impossible, we can however compare their respective A_x parameters. By multiplying the $A_x(^{35}\text{Cl})$ coupling constant of 45 G by the ratio of the magnetic moments for chlorine and bromine we obtain an expected $A_x(^{81}\text{Br})$ value of ca. 225 G. The experimental value of 362 G is clearly in good agreement.

What is of interest here is the apparent decrease in proton couplings yet increase in halide coupling in progressing from the chloro- to the bromo- derivative. Proton couplings of ca. 22 G for the 2 methyl groups and ca. 13 G for the methylene protons has been predicted for a purely classical conformation of the β -chloro radical $\text{Me}_2\dot{\text{C}}\text{CH}_2\text{Cl}$ (see IV),²¹ with C_1 planar and C_2 tetrahedral. Actually, these values turn out to be ca. 17 G and ca. 5 G respectively.⁶ To explain this result it was suggested that perhaps the halide atom bends in towards the radical site, while the methylene protons simultaneously bend towards the radical plane (as depicted by the arrows in IV).^{8,22} This adoption would not only stabilise the radical but would also hold the conformation rigid allowing no, or very little,

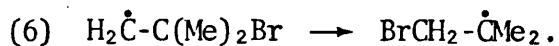
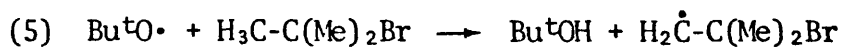
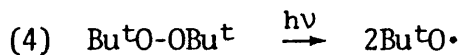


IV

rotation about the $\text{C}_1\text{-C}_2$ bond. The motional broadening results of Kochi *et al.*⁸ substantiate this prediction. If this is the explanation, we would expect this phenomenon to be extended further with the $\text{Me}_2\dot{\text{C}}\text{CH}_2\text{Br}$ radical. A decrease in the proton couplings and an increase in the halide coupling for this latter species is therefore predicted; as is indeed the case.

The trend established, we also predict the β -iodo radical to act accordingly. Unfortunately, the species has not yet been isolated.

(iv) A well-known method for the generation of $\text{H}\cdot$ abstraction products is the photolysis of a possible precursor in a matrix of di-tertiary butyl peroxide. We therefore employed Bu^tBr as the precursor and generated species S accordingly. The reaction sequence being:



The 1,2-halogen shift, accepted for the analogous chloride,⁶ taking place even at 77 K. IsoBuBr also generated species S but in poorer

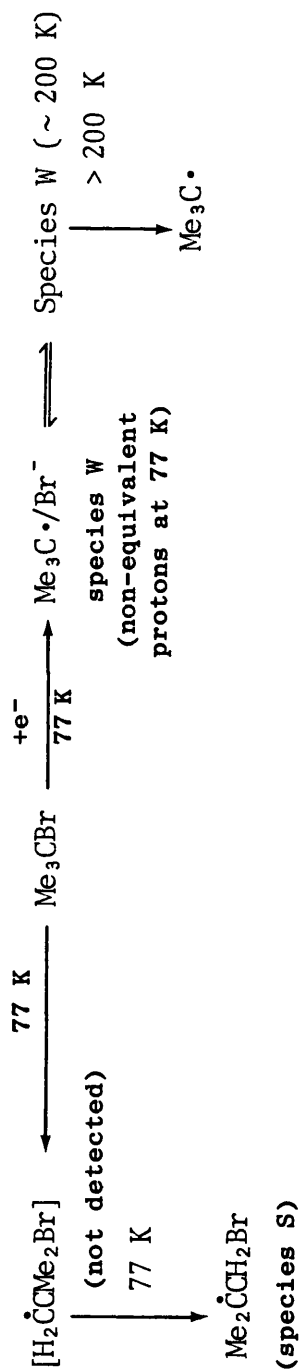
yield. There was no sign of species W. This experiment surely establishing species S as a hydrogen atom loss species.

ASPECTS OF MECHANISM

The enigma of "symmetrical vs unsymmetrical" bridging for β -halo radicals is still not conclusive, particularly where the α - and β -carbon atoms have equivalent substituents. A CIDNP study by Hargis and Shevlin²³ on the β -bromoethyl radical does seem to show the inequality of the 2 methylene groups, supporting the majority of work on these species. However, a very thorough piece of research by Skell et al.²⁴ on the 2,3-bromobutyl radical ($\text{H}_3\text{C}-\dot{\text{C}}\text{H}-\overset{\text{Br}}{\text{C}}\text{H}-\text{CH}_3$) indicates very strongly that either the radical exists in a symmetrically bridged form or the rate of 1,2-halogen migration is greater than 10^{11} s^{-1} . The former alternative does not fit in with what this and other papers indicate, yet the migration rate seems unreasonably fast.

There obviously remains a need for more work to be done on this problem.

SCHEME I - Me_3CBr in Adamantane



SCHEME II - $\text{Me}_2\text{CHCH}_2\text{Br}$ in Adamantane

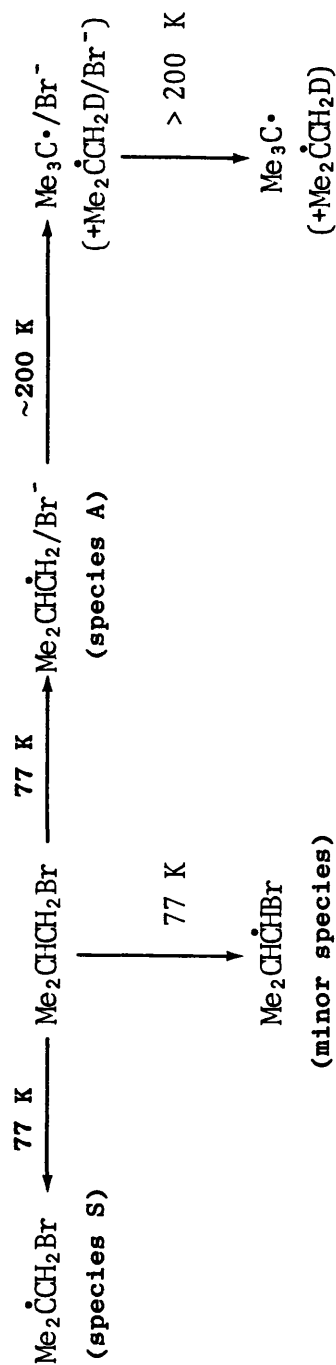


TABLE I

E.s.r. data for alkyl-radical bromide-ion adducts, together with results for species A and W.

Radical	Medium	¹ H hyperfine coupling/G ^a		⁸¹ Br hyperfine coupling/G ^a	
		//	⊥	//	⊥
Me ₃ C•/Br ⁻ (W)	adamantane ^b at 208 K	-	-	21.4	-
Me ₃ C•/Br ⁻ (W)	adamantane at 4 K	-	-	ca. 21	ca. 56, ^e ca. (-)10, ca. 12
Me•/Br ⁻ ^c	CD ₃ CN	21	21.5	21.5	58.3, (-)28.3, ±1.7
Me•/Br ⁻ ^d	CD ₃ CN	20.6	-	-	56.7, -
Me ₂ CHĊH ₂ /Br ⁻ (A)	adamantane	-	-	19.0 (αH) 36.2 (βH)	- ±4
Me ₂ CHĊH ₂ /Br ⁻ (B)	tetramethylsilane	-	-	20 (α+βH)	75 -

^a G = 10⁻⁴ T; ^b Described as Me₂ĊH₂Br in ref. 9; ^c Ref. 11;

^d Ref. 13; ^e Estimated from A₁ and A_{1so}.

TABLE II

E.s.r. data assigned to β -bromo alkyl radicals (species S), together with some results for β -chloro alkyl radicals.

Radical	Medium	^1H hyperfine coupling/G ^a // \perp iso	^{35}Cl or ^{81}Br hyperfine coupling/G // \perp iso
$\text{Me}_2\dot{\text{C}}\text{H}_2\text{Br}$ (S)	Me_3CBr ^b	13, ca. 13, ca. 13	ca. 366
$\text{Me}_2\dot{\text{C}}\text{H}_2\text{Br}$ (S)	adamantane	13, ca. 13, ca. 13	ca. 350
$\text{Me}_2\dot{\text{C}}\text{H}_2\text{Br}$ (S)	tetramethyl- silane	13, ca. 13, ca. 13	362
$\text{Et}\dot{\text{C}}\text{H}_2\text{Br}$ ^b	Bu^nBr	ca. 17 (αH) and 30 (2 βH)	ca. 280
$\text{Me}_2\dot{\text{C}}\text{H}_2\text{Cl}$	adamantane ^c	- - 21.1	- - 19.5
$\text{Me}_2\dot{\text{C}}\text{H}_2\text{Cl}$	Me_3CCl ^d	17 (2Me) and 5 (CH_2)	ca. 45

^a $G = 10^{-4}$ T.

^b Ref. 25. [x , y and z data were reported in ref. 25; we now consider that it is not possible to derive more than A_{max} (^{79}Br , ^{81}Br) from these powder spectra.]

^c Ref. 9.

^d Ref. 6.

REFERENCES

1. A. R. Lyons, M. C. R. Symons, J.A.C.S., 1971, 93, 7330.
2. S. P. Mishra, G. W. Neilson, M. C. R. Symons, J.A.C.S., 1973, 95, 605; J.C.S. Faraday II, 1974, 1165.
3. J. Hüttermann, A. Müller, Internat. J. Radiat. Biol., 1969, 4, 297.
4. H. Oloff, J. Hüttermann, M. C. R. Symons, J. Phys. Chem., 1978, 82, 621.
5. H. Oloff, J. Hüttermann, J. Magnetic Resonance, 1977, 27, 197.
6. M. C. R. Symons, J.C.S. Faraday II, 1972, 68, 1897.
7. A. J. Bowles, A. Hudson, R. A. Jackson, Chem. Phys. Letters, 1970, 5, 552.
8. K. S. Chen, I. H. Elson, J. K. Kochi, J.A.C.S., 1973, 95, 5341.
9. R. V. Lloyd, D. E. Wood, M. T. Rodgers, J.A.C.S., 1974, 96, 7130; R. V. Lloyd, D. E. Wood, J.A.C.S., 1975, 97, 5986.
10. D. Nelson, M. C. R. Symons, Tetrahedron Letters, 1975, 34, 2953.
11. S. P. Mishra, M. C. R. Symons, J.C.S. Perkin II, 1973, 391.
12. A. R. Lyons, M. C. R. Symons, S. P. Mishra, Nature, 1974, 249, 341.
13. E. D. Sprague, F. Williams, J. Chem. Phys., 1971, 54, 5425.
14. Y. Fujita, T. Katsu, M. Sato, K. Takahashi, J. Chem. Phys., 1974, 61, 4307.
15. D. E. Wood, R. V. Lloyd, Tetrahedron Letters, 1976, 5, 345.
16. P. S. Skell, K. J. Shea, "Free Radicals", ed. J. K. Kochi, Wiley, New York, 1973, Vol. 2.
17. T. A. Claxton, E. Platt, M. C. R. Symons, Mol. Phys., 1976, 32, 1321.
18. D. E. Wood, L. F. Williams, R. F. Sprecher, W. A. Latham, J.A.C.S., 1972, 94, 6241; D. E. Wood, R. F. Sprecher, Mol. Phys., 1973, 26, 1311.
19. T. A. Claxton, S. A. Fieldhouse, R. E. Overill, M. C. R. Symons, Mol. Phys., 1975, 29, 1453.
20. M. C. R. Symons, "Chemical and Biochemical Aspects of Electron Spin Resonance Spectroscopy", Van Nostrand Reinhold Company Ltd., 1979.

21. M. C. R. Symons, J. Chem. Soc., 1959, 277.
22. I. Biddles, A. Hudson, Chem. Phys. Letters, 1973, 1845.
23. J. H. Hargis, P. B. Shevlin, J.C.S. Chem. Comm., 1973, 179.
24. P. S. Skell, R. R. Pavlis, D. C. Lewis, K. J. Shea, J.A.C.S., 1973, 95, 6735.
25. A. R. Lyons, G. W. Neilson, S. P. Mishra, M. C. R. Symons, J.C.S. Faraday II, 1975, 71, 363.

CHAPTER 3

Further $R\cdot/Br^-$ and $R\cdot/I^-$ adducts

INTRODUCTION

Having isolated the $\text{isoBu}\cdot/\text{Br}^-$ and $\text{Bu}^t\cdot/\text{Br}^-$ adducts in the adamantane matrix,¹ it was decided that it would be of interest to dope the matrix with a wider range of alkyl halides, in the hope that they may yield further examples of this family of species. MeX, EtX, n-PrX, iso-PrX, iso-BuX and Bu^tX (X = Br, I) were all, therefore, individually incorporated into the adamantane matrix. Their results are discussed accordingly in the latter half of this chapter.

First, however, we shall deal with what is perhaps the weakest point in our analysis of the adducts so far detected. That is, our assumption that A_{\perp} for this family of species is negative.^{1,2} The following evidence, we believe, proves this premise to be perfectly correct.

EXPERIMENTAL

Methyl iodide- d_3 (Merck, Sharpe & Dohme), adamantane- d_{16} (Merck, Sharpe & Dohme), methyl bromide (B.D.H.), methyl iodide (M & B), ethyl bromide (Hopkin & Williams), ethyl iodide (Fisons), n-propyl bromide (Hopkin & Williams), n-propyl iodide (B.D.H.), iso-propyl bromide (Hopkin & Williams), iso-propyl iodide (Hopkin & Williams), iso-butyl iodide (B.D.H.), tert-butyl iodide (B.D.H.) and tert-butyl iodide- d_9 (Merck, Sharpe & Dohme) were all used as supplied.

Methyl iodide- d_3 beads were obtained by pipetting drops of the degassed compound directly into liquid nitrogen. Incorporation of the required alkyl halide into the adamantane- d_{16} matrix was carried out by recrystallising the adamantane from the substrate as described in

chapter 1.

Radiolyses of samples and recording of spectra were carried out as described in chapter 2.

PART 1

INTRODUCTION

The first adduct discovered by Sprague et al. was the $\text{Me}\cdot/\text{Br}^-$ adduct in a CD_3CN matrix.³ The anisotropic bromine parameters were correctly extracted with $A_{\parallel}({}^81\text{Br}) = 57 \text{ G}$ and $A_{\perp}({}^81\text{Br}) = 28 \text{ G}$. Both values were taken as positive, predicting an isotropic bromine coupling of ca. 38 G. This laboratory then, indirectly, discovered the $\text{Bu}^{\text{t}}\cdot/\text{Br}^-$ adduct in the adamantane matrix,^{2,4} where the isotropic bromine coupling was 6.7 G. Therefore, if both of these species were to be of the same family, then the perpendicular bromine coupling for the former had to be negative. As this suggestion was critical to our analysis of the structure of the adduct, and as the sign could not be extracted from the powder spectrum, it was of obvious importance to discover a means of substantiating our prediction.^{1,2}

Let us consider a simple, hypothetical, paramagnetic species with one nucleus having a spin of $\frac{1}{2}$. Its powder spectrum could be as in Fig. 1a, with the magnitude, but not the sign, of the perpendicular parameter available for extraction. At first, we considered the benefits of generating this species in a single crystal. Could the movement of features in a single crystal study supply us with the information we require? By rotating the species by 90° through its parallel and perpendicular directions, the movement of features would

produce a pattern such as that depicted in Fig. 1b. However, this pattern of movement would, unfortunately, be independent of perpendicular sign.

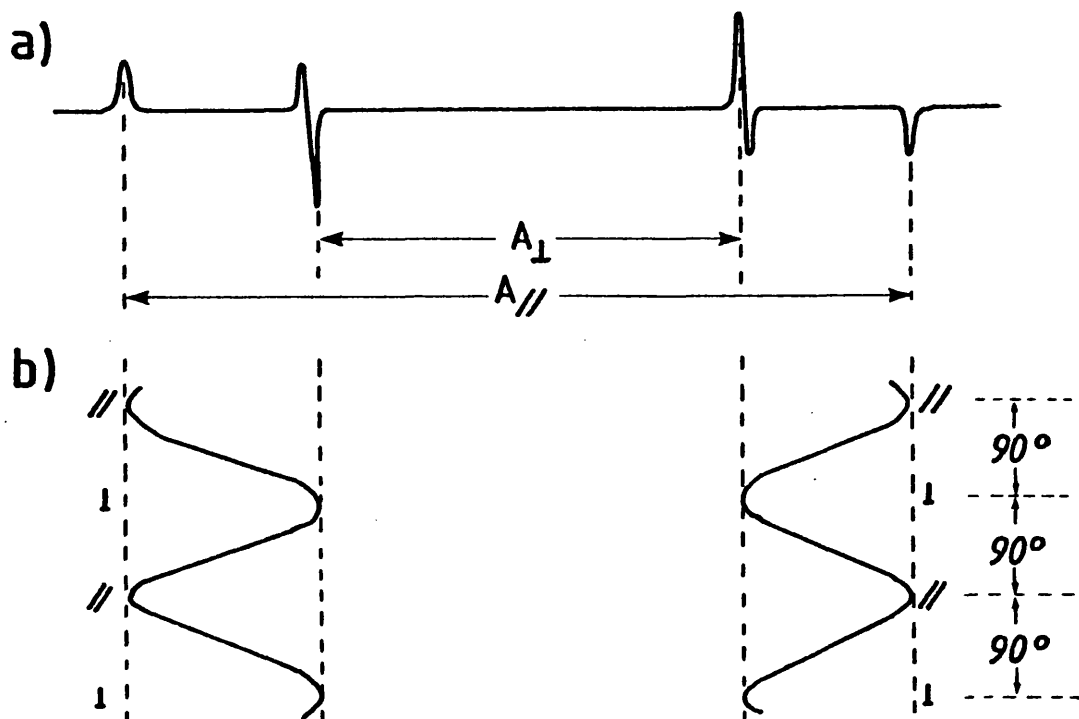


Figure 1

- (a) showing the anisotropic spectrum of a hypothetical species containing a single nucleus of spin $\frac{1}{2}$;
- (b) showing the movement of features of this hypothetical species if studied in a rotating single crystal.

We then considered what would happen to the features in its powder spectrum if this hypothetical species were allowed to rotate and, therefore, allow the spectrum to become isotropic. If A_{\perp} is positive, the parallel features would move in twice as fast as the perpendicular features would move out, resulting in a large isotropic nuclear coupling as in Fig. 2a. Yet, if A_{\perp} is negative, all features would

move in (the parallel twice as fast as the perpendicular) resulting in a very small isotropic nuclear coupling as in Fig. 2b.

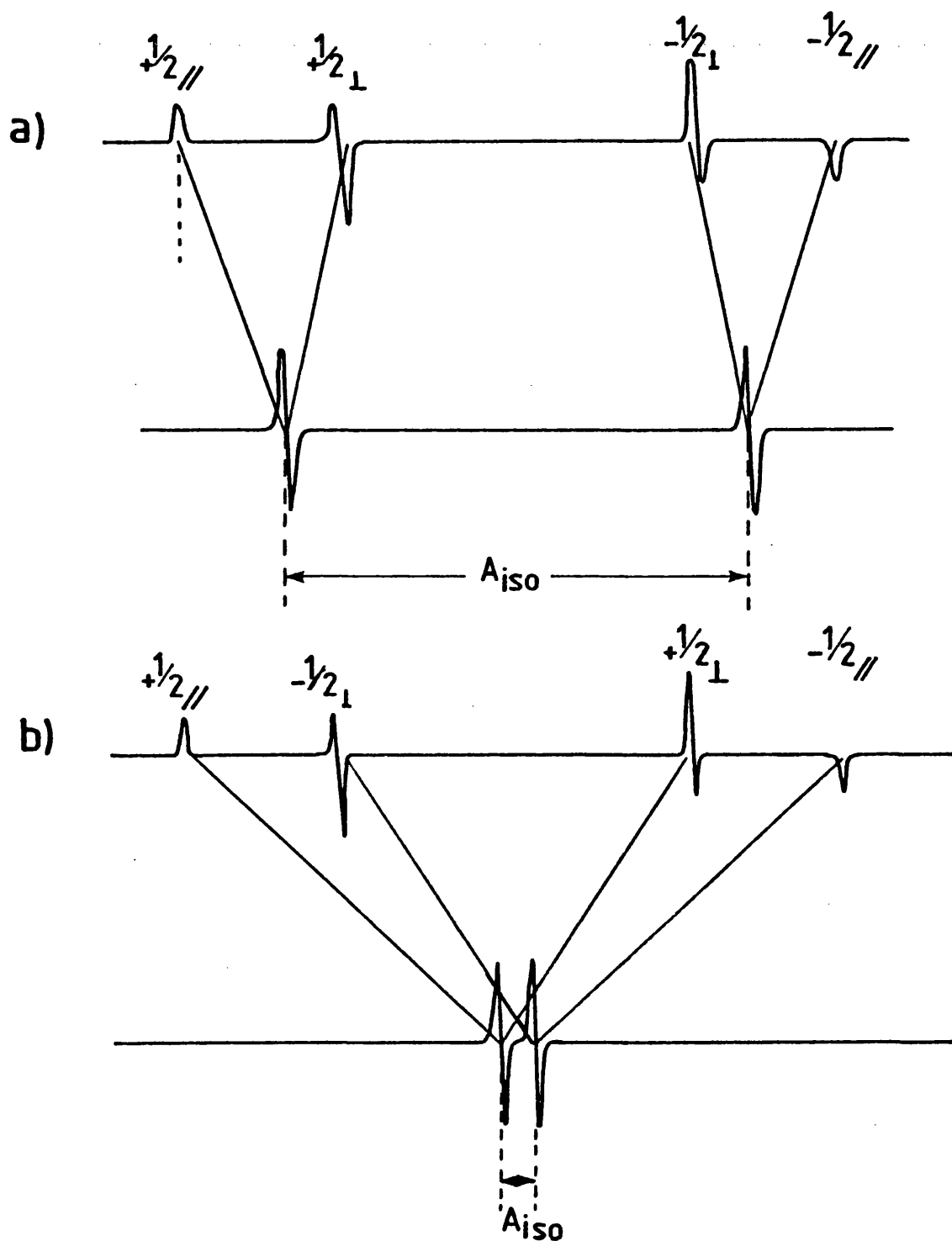


Figure 2

Showing the movement of features in the powder spectrum if the hypothetical species is permitted to rotate and/or librate. (a) if A_{\perp} is positive, (b) if A_{\perp} is negative.

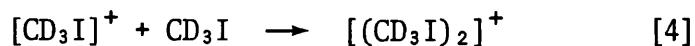
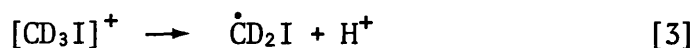
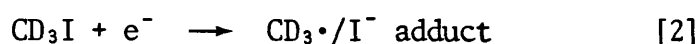
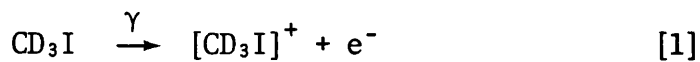
Therefore, if we can find an adduct with a solid state spectrum, which will then rotate, or at least librate, sufficiently on annealing, the pattern of movement of features should show conclusively the sign of the perpendicular parameter. The adduct supplying this phenomenon, and studied accordingly, was the $CD_3\cdot/I^-$ adduct in a CD_3I matrix.

RESULTS

$CD_3\cdot/I^-$ adduct

Fig. 3 shows the spectra produced from CD_3I beads at (a) 77 K, (b) 105 K, (c) 138 K, after exposure to γ -rays at 77 K for ca. 2 hrs. Each spectrum can be interpreted in terms of the $CD_3\cdot/I^-$ adduct; with six broad parallel features and six broad perpendicular features, all moving in with increase in temperature (the temperature dependent couplings are summarised in Table 1 and presented graphically in Fig. 4). The spectra are somewhat complicated by CH_3I , CH_2DI and CHD_2I impurities (ca. 5% as determined by mass spectrometry) however, the interference is relatively small and does not, therefore, prevent parameter extraction. Radiolysis of the pure CH_3I gave a broad, uninterpretable spectrum at 77 K and at elevated temperatures.

The reactions taking place are probably as follows:-



Continued annealing of the $CD_3I(CH_3I)$ sample induced the disappearance of the $CD_3\cdot/I^-$ ($CH_3\cdot/I^-$) adduct while simultaneously uncovering the

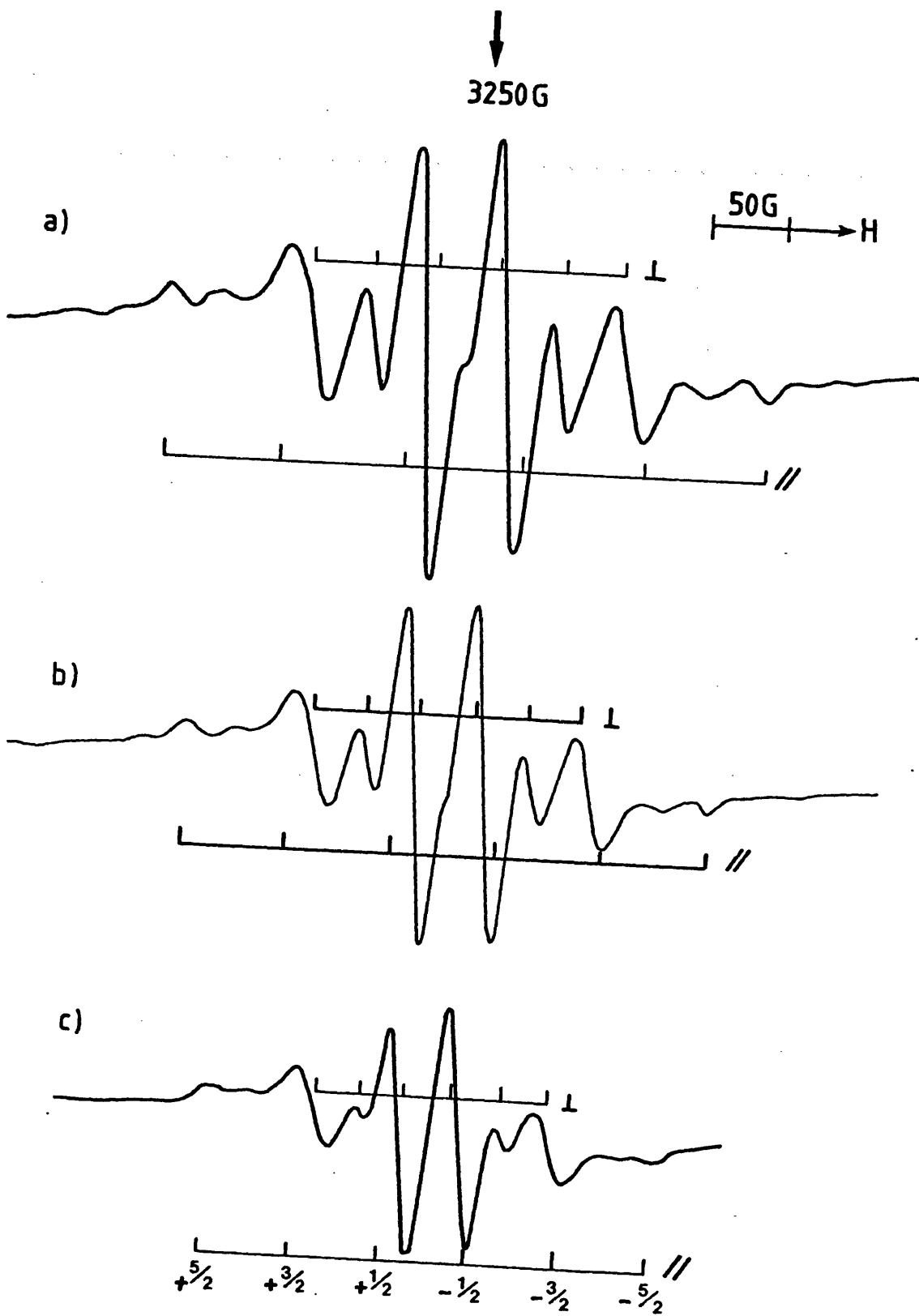


Figure 3

Showing the $\text{CD}_3\cdot/\text{I}^-$ adduct at (a) 77 K, (b) 105 K and (c) 138 K.

TABLE 1

Temperature dependent e.s.r. data for the
 $\text{CD}_3\cdot/\text{I}^-$ adduct (Gauss)

Temp/°K	Hyperfine Coupling Constants (^{127}I)		
	\parallel	\perp	iso ^a
77	80	-39	0.67
92	74	-36	0.67
99	72	-35	0.67
111	67	-33	0.33
124	64	-31	0.67
138	59	-29	0.33
all g -values close to 2.001			

^a Values calculated from parallel and perpendicular values

α -iodo $\dot{\text{C}}\text{D}_2\text{I}(\dot{\text{C}}\text{H}_2\text{I})$ radical with its diagnostic $A_{\parallel}(^{127}\text{I})$ coupling of 108 G. A further species, containing two equivalent iodine atoms and exhibiting a maximum (^{127}I) coupling of ca. 400 G, was also detected at higher gains. This latter species is almost certainly the $[(\text{CD}_3\text{I})_2]^+$ dimer cation formed from reaction [4]. Hence, all probable radiolysis products have been accounted for and, therefore, substantiates our assignment of the spectra in Fig. 3 to the $\text{CD}_3\cdot/\text{I}^-$ adduct.

DISCUSSION

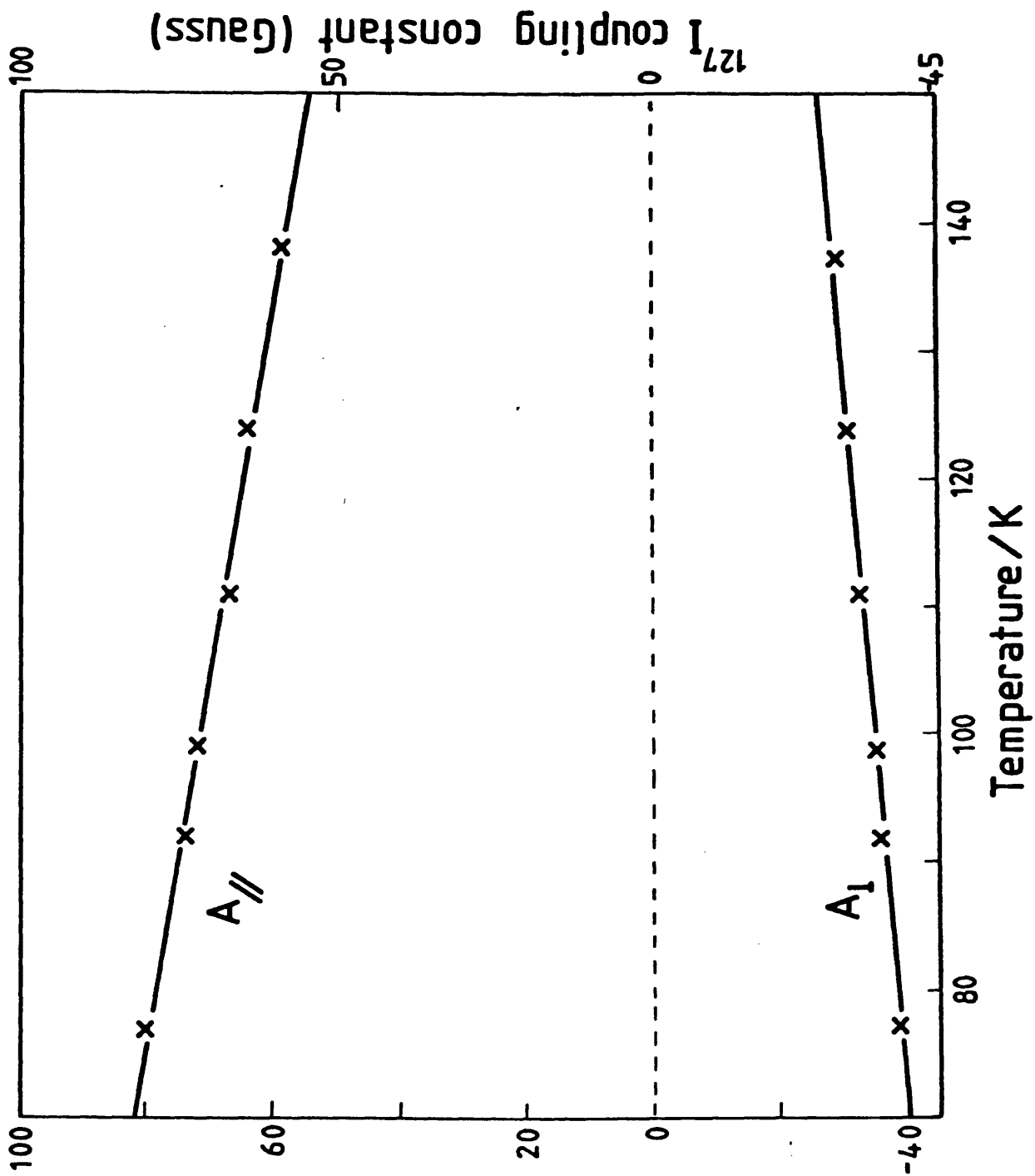
As can be seen, both the parallel and the perpendicular features for the adduct move inwards with increase in temperature, in the same manner as predicted in Fig. 2b. Taking A_{\perp} as negative predicts constant iso-

tropic iodine couplings of <1 G, in excellent agreement with the isotropic halide couplings for the adducts in the adamantane- d_{16} matrix (Table 2). These results show conclusively the negative value of the perpendicular parameters for the solid state adducts so far isolated.

The implication, therefore, is that the electron is in almost a pure 'p' orbital on the halide ion and, judging by the exceedingly low value of the isotropic coupling, any apparent 's' character is probably due to spin polarisation. This point will be discussed more fully in chapter 5 where a more complete "character analysis" of the adduct will take place.

Figure 4

Temperature dependent ^{127}I coupling constants for the $\text{CD}_3\cdot/\text{I}^-$ adduct.



PART 2

RESULTS

Gamma radiolysis of alkyl bromides in adamantane-d₁₆

Bu^tBr and isoBuBr

These results have been fully discussed in Chapter 2.

isoPrBr and nPrBr

Our results show a completely analogous situation to the reactions of Bu^tBr and isoBuBr. At 77 K, nPrBr gives a broad spectrum spanning ca. 200 G made up of contributions from predominately 2 species. Annealing to ca. 95 K brings about an irreversible growth in one of these species which becomes best resolved at 187 K (Fig. 5). The 2 species are without doubt the nPr•/Br⁻ and isoPr•/Br⁻ adducts, the former growing into the latter which becomes highly resolved. Annealing to higher temperatures does not however generate isoPr• radicals; uninterpreted complications of the spectrum instead taking place. There was no sign of the Me \dot{C} (H)CH₂D/Br⁻ adduct at 187 K or the Me \dot{C} (H)CH₂D free radical on further annealing.

isoPrBr gave the isoPr•/Br⁻ adduct at 77 K, becoming best resolved once more at 187 K. Further annealing did not produce isoPr• radicals. The concentration of adduct at 187 K was ca. 4 times greater than that generated from nPrBr.

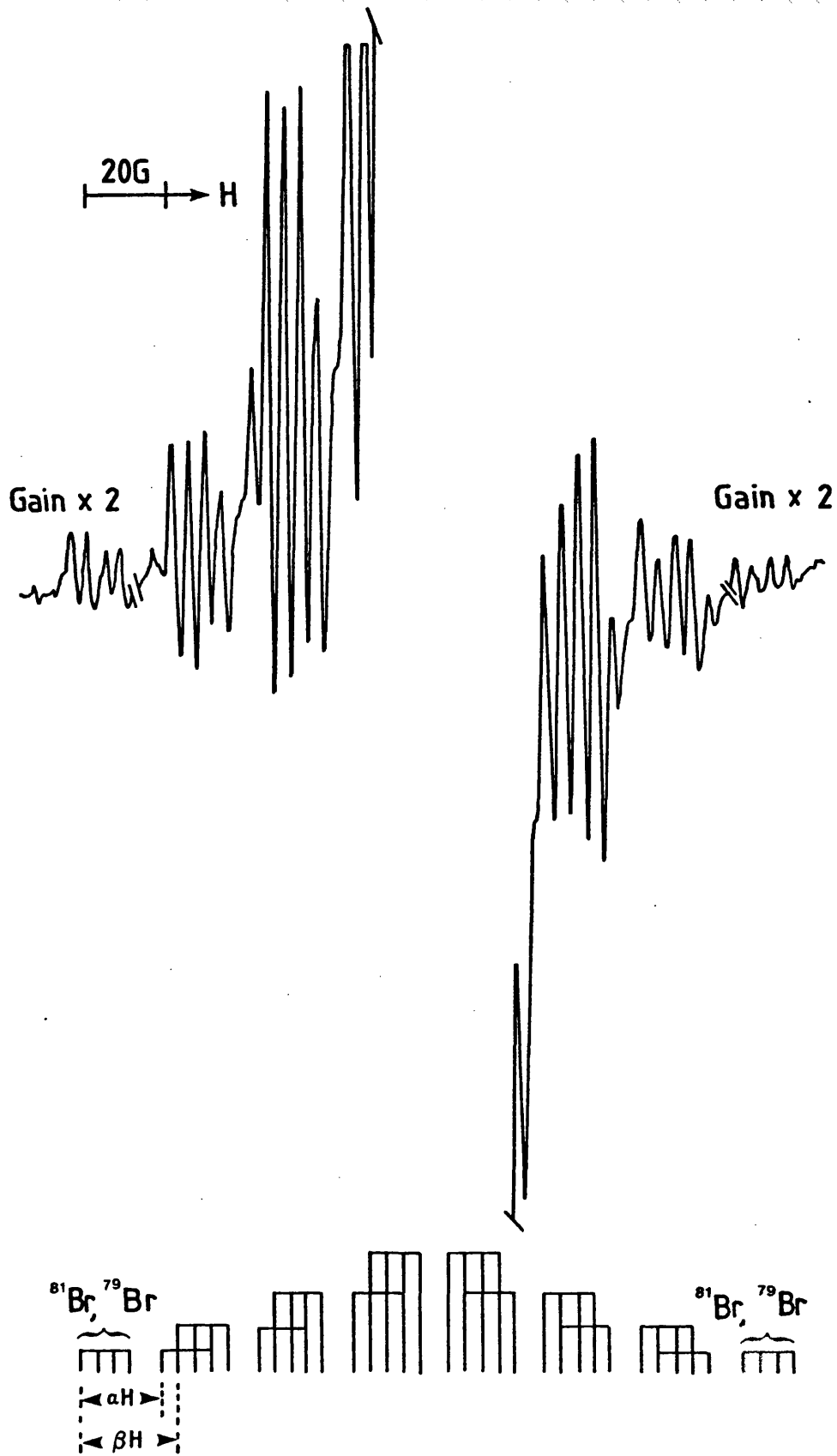
EtBr

A very low yield of Et• radicals are generated at 77 K, with another species exhibiting broad features scanning ca. 125 G. Annealing induced the disappearance of all features by ca. 165 K; a weak, complicated spectrum emerging at ca. 200 K. On the evidence of the other alkyl bromides, the Et• radical and Et•/Br⁻ adduct should be generated.

↓
3230G

Figure 5

The $(\text{CH}_3)_2\dot{\text{C}}\text{H}/\text{Br}^-$ adduct at 187 K.



The former is clearly detectable, the latter is assigned to the broad 125 G species. Unfortunately, bad resolution does not permit the extraction of authentic parameters.

MeBr

Radiolysis produced no results whatsoever at 77 K or at elevated temperatures. It is assumed that this is because the Me• radical so generated is so small that it cannot be trapped in the adamantane matrix. Hence, it migrates through the completely rigid matrix even at the low temperature of 77 K.

Gamma radiolysis of alkyl iodides in adamantane-d₁₆

Bu^tI

Figs. 6a and 6b show the spectra produced from h₉-Bu^tI and d₉-Bu^tI respectively in adamantane-d₁₆ at 77 K. The spectra consist of two iodine coupled species: species A exhibiting a maximum iodine coupling of 90 G; species B badly resolved with its spectrum uninterpretable at this temperature but spanning ca. 220 G. A variable temperature study between 77 K and 220 K (the results are summarised in Table 3 and presented graphically in Fig. 7) shows the gradual increase in resolution of species B until it finally produces the spectrum in Fig. 6c at 215 K, with $A_{\text{iso}}(^{127}\text{I}) = \pm 7 \text{ G}$ and $A_{\text{iso}}(^1\text{H}) = 21.9 \text{ G}$. Meantime, all features of species A have moved in and an $A_{\parallel}(^{127}\text{I})$ of +60 G, an $A_{\perp}(^{127}\text{I})$ of -27 G and an $A(^1\text{H})$ of +22.5 G can be extracted (Figs. 6c and 6d). Cooling back to 77 K reproduces the spectra in Figs. 6a and 6b except for the increased resolution of species A and the appearance of a small concentration of Bu^t• radicals. Repeating the anneal to beyond 215 K followed by cooling back to 77 K produces a gradual decrease in the concentration of species A and species B with a con-

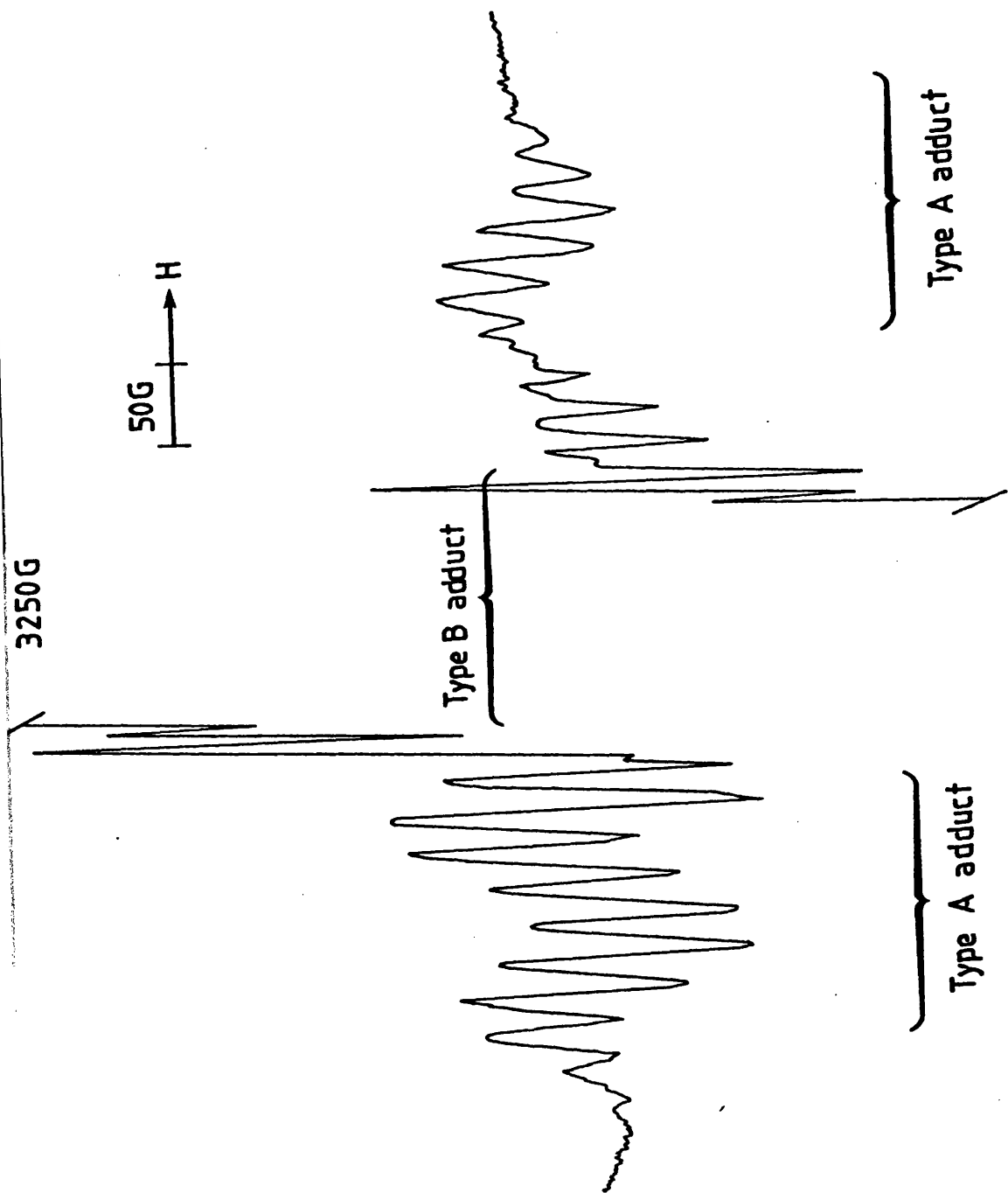


Figure 6(a)
The Type A and Type B $(\text{CH}_3)_3\text{C}\cdot/\text{I}^-$ adducts at 77 K.

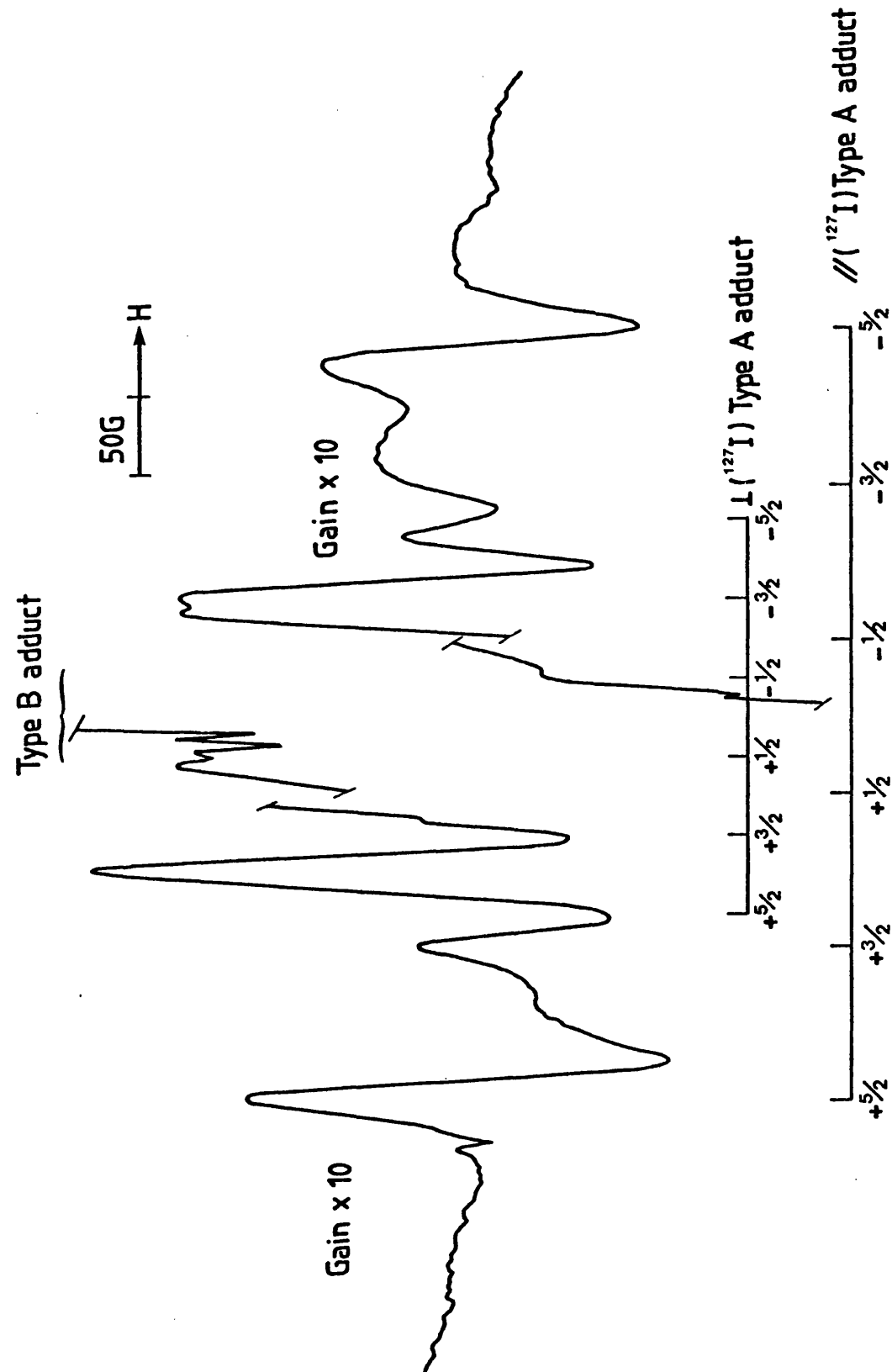


Figure 6(b)

The Type A and Type B $(\text{CD}_3)_3\text{C}\cdot/\text{I}^-$ adducts at 77 K.

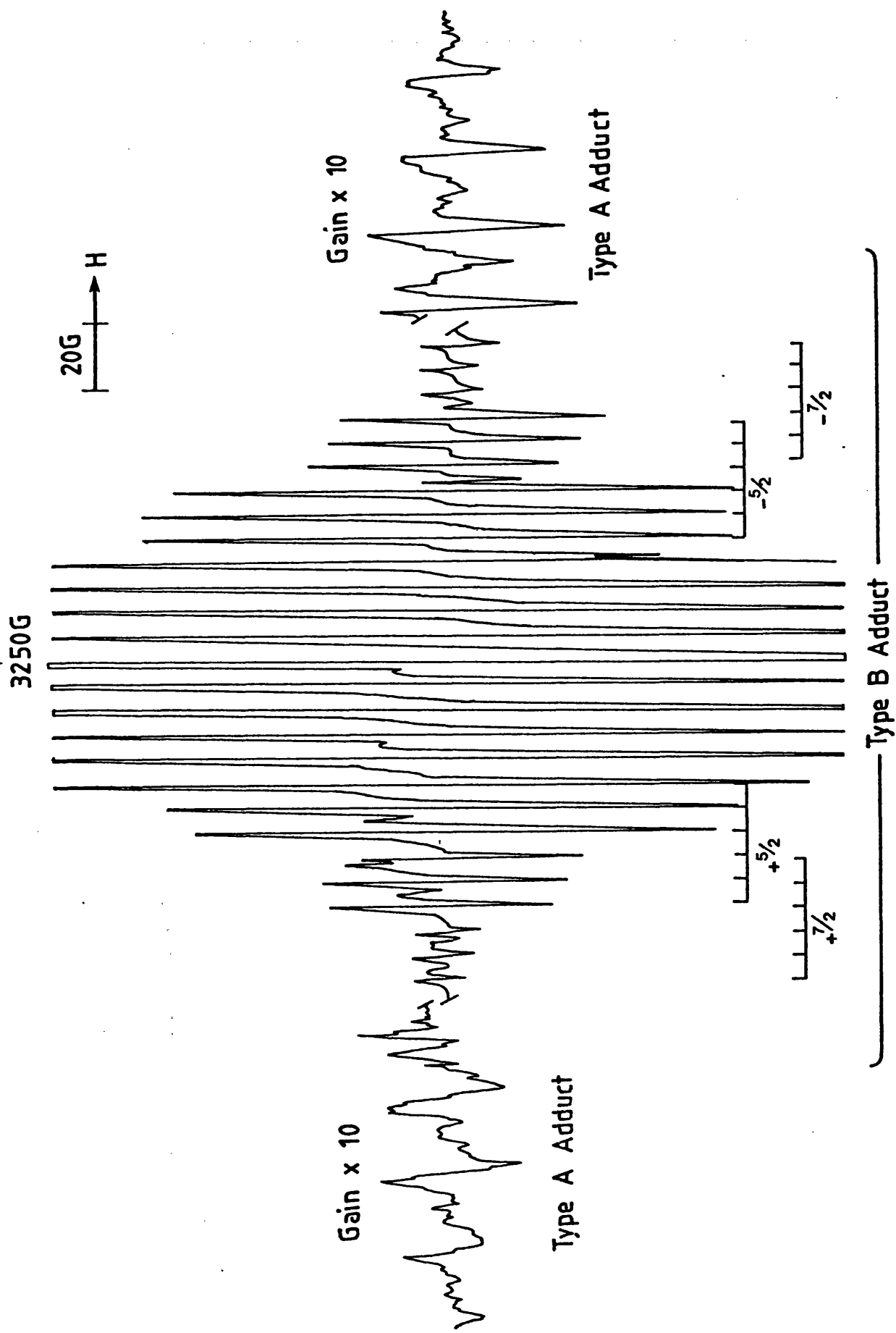


Figure 6(c) - The Type A and Type B $(\text{CH}_3)_3\text{C}\cdot/\text{I}\cdot$ adducts at 215 K.

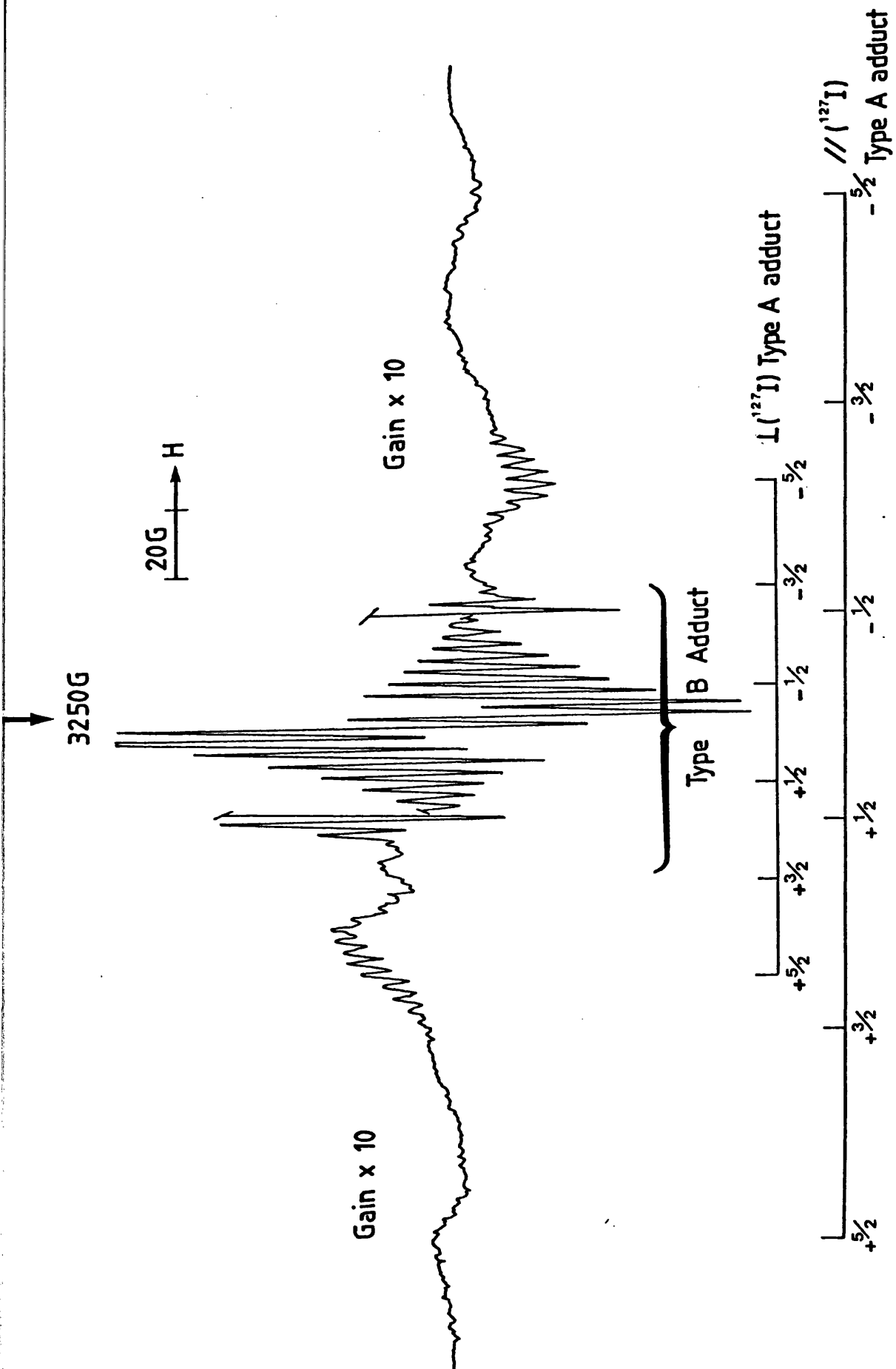


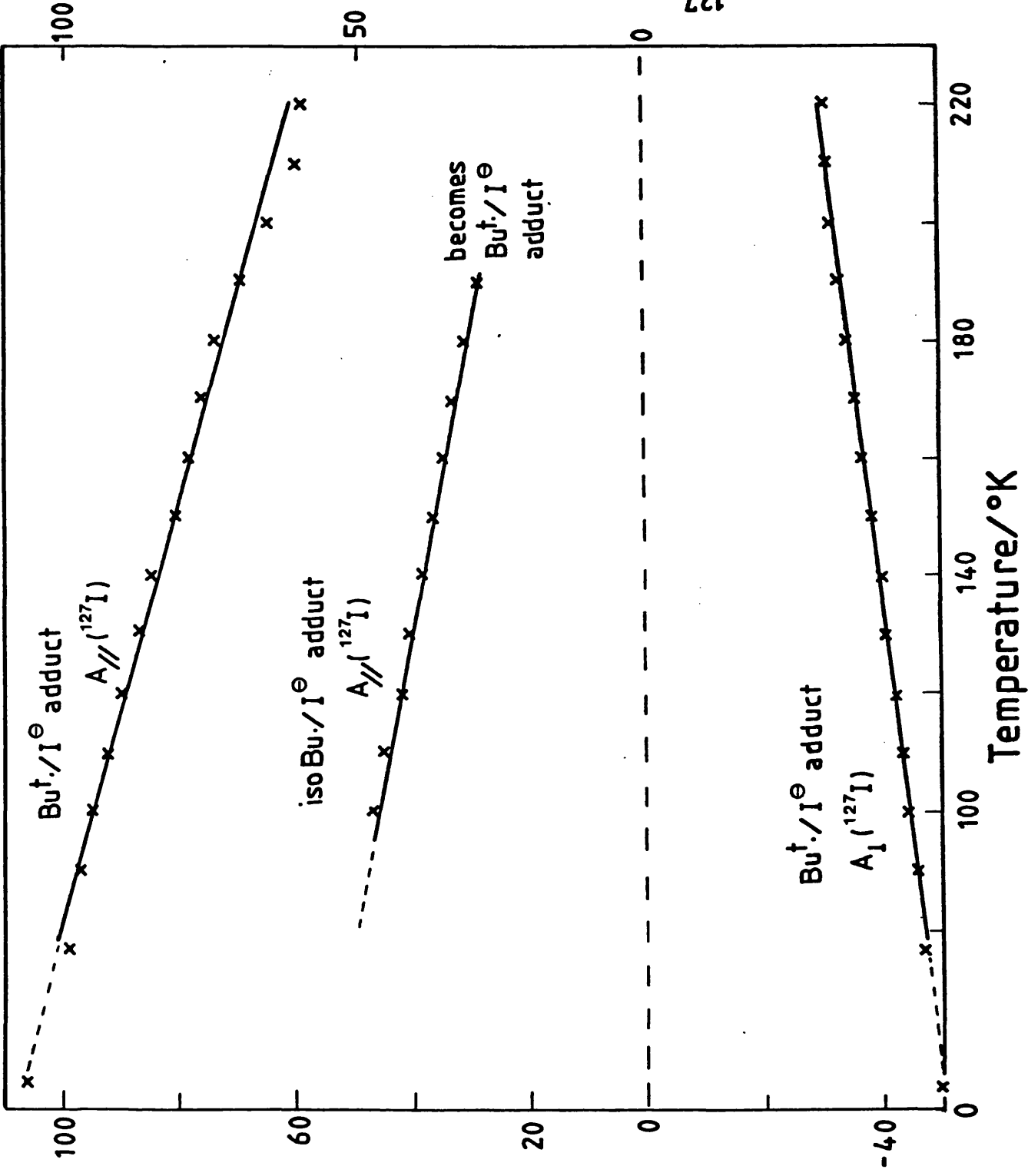
Figure 6(d)

The Type A and Type B $(\text{CD}_3)_3\text{C}\cdot/\text{I}\cdot$ adducts at 215 K.

Figure 7

Temperature dependent ^{127}I hyperfine coupling constants for $\text{Bu}^\cdot/\text{I}^-$ and $\text{isoBu}^\cdot/\text{I}^-$ adducts in the adamantane- d_{16} matrix.

^{127}I coupling constant (Gauss)



comitant increase in $\text{Bu}^{\text{t}\cdot}$ radical concentration. There was no sign of $\text{Me}_2\dot{\text{C}}\text{CH}_2\text{D}$ radicals. At temperatures greater than 220 K, a complicated spectrum not dominated by $\text{Bu}^{\text{t}\cdot}$ radicals is produced.

Species B is the unrestrained $\text{Bu}^{\text{t}\cdot}/\text{I}^-$ adduct which becomes isotropic at 215 K. This is the species studied by Wood and Lloyd⁴ (wrongly concluded to be the β -iodo radical $\text{Me}_2\dot{\text{C}}-\text{CH}_2-\text{I}$) from their work on the radiolysis of isoBuI in the adamantane- d_{16} matrix. Its parameters are in excellent agreement with the isotropic bromine couplings for the bromo adducts so far detected (Table 2). Species A is also the $\text{Bu}^{\text{t}\cdot}/\text{I}^-$ adduct, only this sample is in a different, more restricted site in the adamantane matrix, and is hence, almost completely rigid at 77 K. It is not permitted to fully rotate even at 215 K.

There was no sign, at any time during this variable temperature study, of the β -iodo radical (cf. species S from the radiolysis of $\text{Bu}^{\text{t}}\text{Br}$ in chapter 2). The possible reasons will be discussed later.

isoBuI

The same situation exists here as for $\text{Bu}^{\text{t}}\text{I}$. Again, the $\text{isoBu}\cdot/\text{I}^-$ adduct is present in two different sites. The inner adduct (Type B) becomes reversibly much better resolved on annealing, its parallel parameters are summarised in Table 3. The outer adduct (Type A) is unfortunately so weak as to make precise extraction of the temperature dependent parameters impossible. At 190 K, an irreversible rearrangement takes place (cf. isoBuBr in adamantane- d_{16} at ca. 150 K) resulting in the formation of the $\text{Bu}^{\text{t}\cdot}/\text{I}^-$ adducts, again in two different sites. Cooling back to 77 K reproduces the spectrum in Fig. 6a in approximately $\frac{1}{10}$ th the concentration as that produced from $\text{Bu}^{\text{t}}\text{I}$, and with the very definite presence of $\text{Bu}^{\text{t}\cdot}$ and $\text{Me}_2\dot{\text{C}}\text{CH}_2\text{D}$ radicals. Continued minor annealing, followed by cooling to 77 K, enhances the spectral contribu-

tion from these two free radicals (Fig. 8). Annealing to 215 K produces the isotropic spectrum attributable to the $\text{Bu}^{\cdot}/\text{I}^-$ and $\text{Me}_2\dot{\text{C}}\text{CH}_2\text{D}/\text{I}^-$ adducts. Further annealing results in an irreversible complication of the spectrum, not dominated by Bu^{\cdot} or $\text{Me}_2\dot{\text{C}}\text{CH}_2\text{D}$ radicals.

isoPrI

Fig. 9a shows the spectrum generated at 77 K. The Type A adduct exhibits an $A_{\parallel}({}^{127}\text{I})$ coupling of 60 G and proton couplings of 20-25 G. The Type B adduct has a spectrum spanning ca. 220 G but is unresolved at this temperature. Annealing produces a reversible decrease in the iodine coupling of the Type A adduct until it irreversibly disappears at ca. 150 K. Continued annealing increases the resolution of the Type B adduct until 215 K, whereupon the resolved spectrum, as in Fig. 9b, is produced with $A_{\text{iso}}({}^{127}\text{I}) = \pm 3.3$ G, $A_{\text{iso}}(\alpha\text{H}) = -19.5$ G and $A_{\text{iso}}(\beta\text{H}) = +23.5$ G. This adduct disappears on further annealing, leaving no sign, unfortunately of the isoPr \cdot radical.

nPrI

A very broad spectrum is generated at 77 K. The Type A isoPr \cdot / I^- adduct is present in fairly good yield but is the only assignment that can be made with certainty. Annealing induces the disappearance of the Type A isoPr \cdot / I^- adduct at ca. 150 K, with a weak concentration of the Type B isoPr \cdot / I^- adduct resolving itself at 215 K. There was no sign of any alkyl radicals at any temperature.

EtI

Et \cdot radicals are generated in very small yield at 77 K, with a broad, weak, uninterpretable underlying spectrum spanning ca. 130 G.

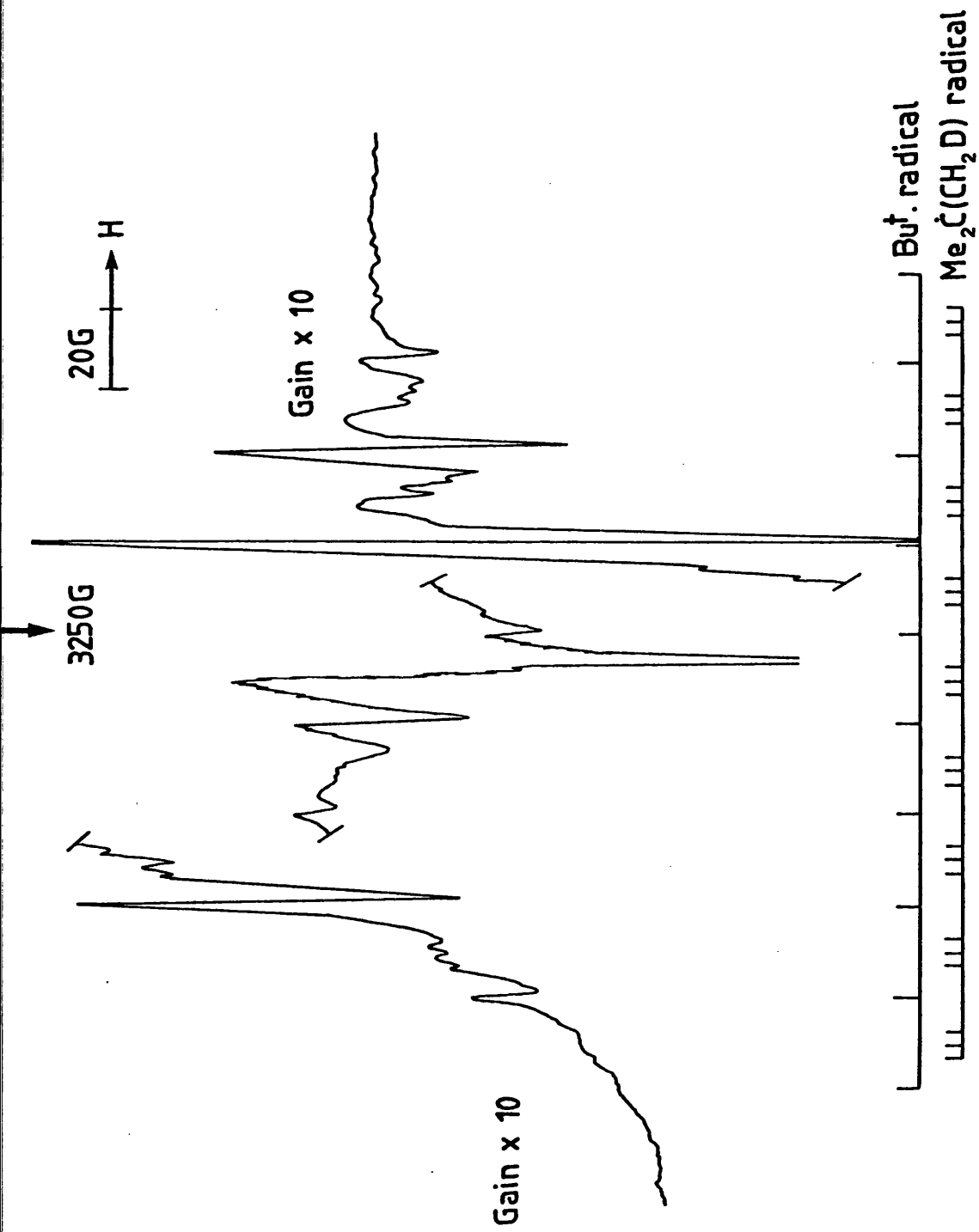
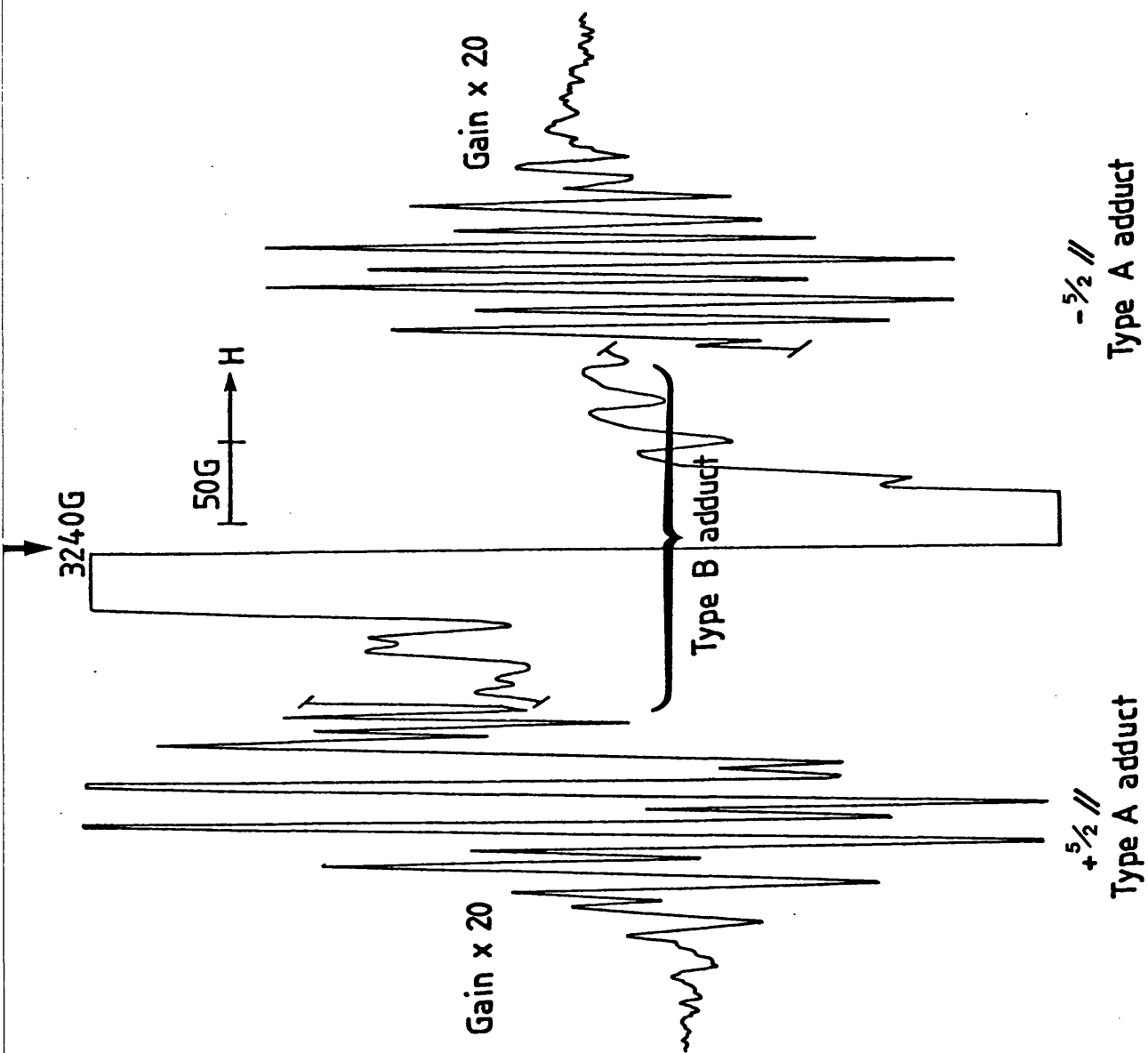


Figure 8
 $(\text{CH}_3)_3\text{C}\cdot$ and $(\text{CH}_3)_2\dot{\text{C}}(\text{CH}_2\text{D})$ radicals, generated from the $(\text{CH}_3)_2\text{CHCH}_2\cdot/\text{I}^-$ adduct.

Figure 9(a)

The Type A and Type B $(\text{CH}_3)_2\dot{\text{C}}\text{H}/\text{I}^-$ adducts.



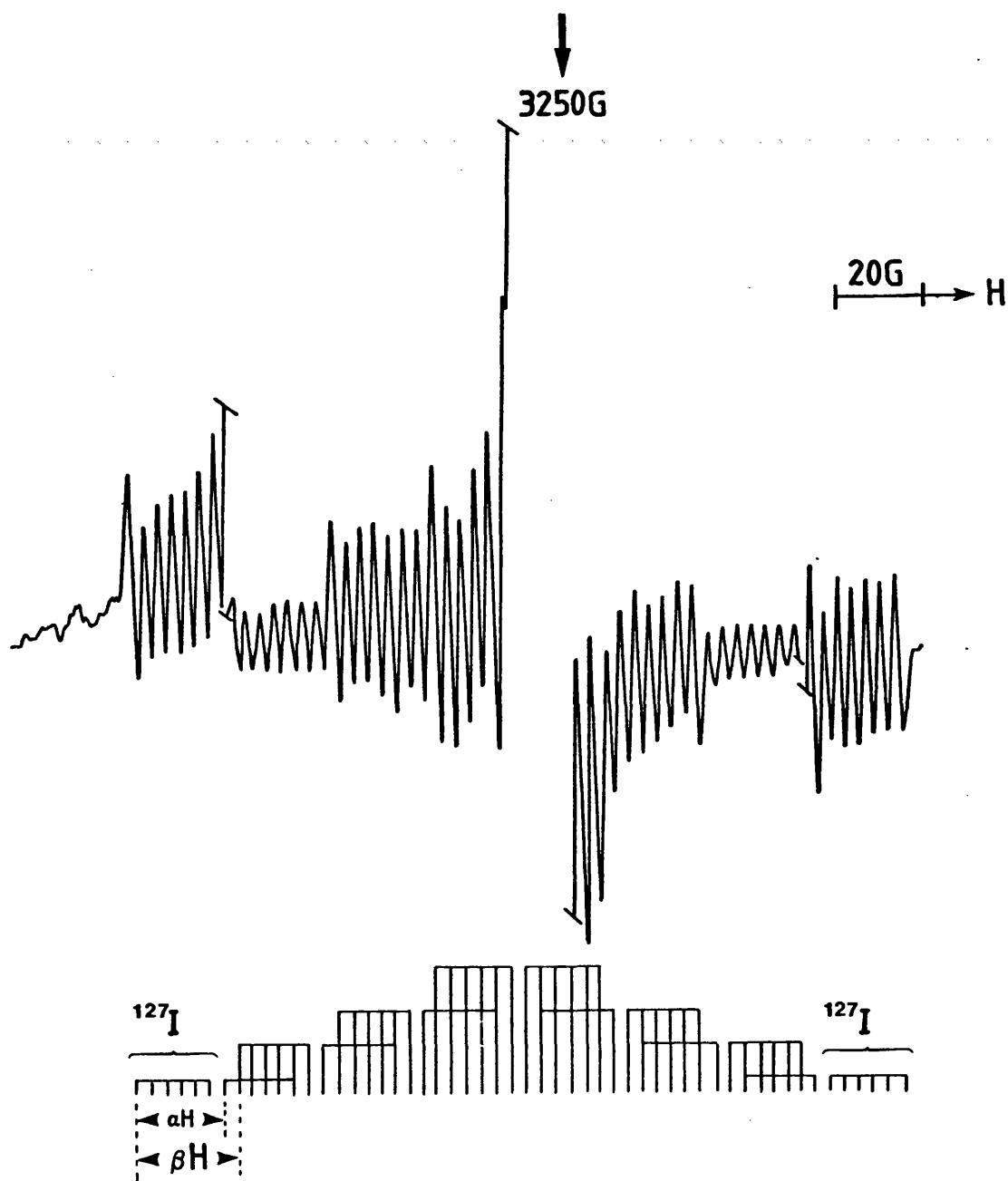


Figure 9(b)

The Type B $(\text{CH}_3)_2\dot{\text{C}}\text{H}/\text{I}^-$ adduct at 215 K.

Annealing induced the disappearance of all features. Again, the Et•/I⁻ adduct should be generated, we therefore assign it to the species exhibiting the broad spectrum. Parameters for the adduct could not be extracted.

MeI

No results were obtained, probably for the same reasons as suggested for MeBr.

Of the Type A iodide ion adducts generated by rearrangement (isoBu•/I⁻ → Bu^t•/I⁻ and nPr•/I⁻ → isoPr•/I⁻) there was no sign of the monodeuterated analogues. This is in contrast with the Type A isoBu•/Br⁻ adduct → Type A Bu^t•/Br⁻ adduct and Type B isoBu•/I⁻ adduct → Type B Bu^t•/I⁻ adduct rearrangements which, in adamantane-d₁₆, results in the generation of a certain amount of the monodeuterated adducts.

DISCUSSION

Bromides

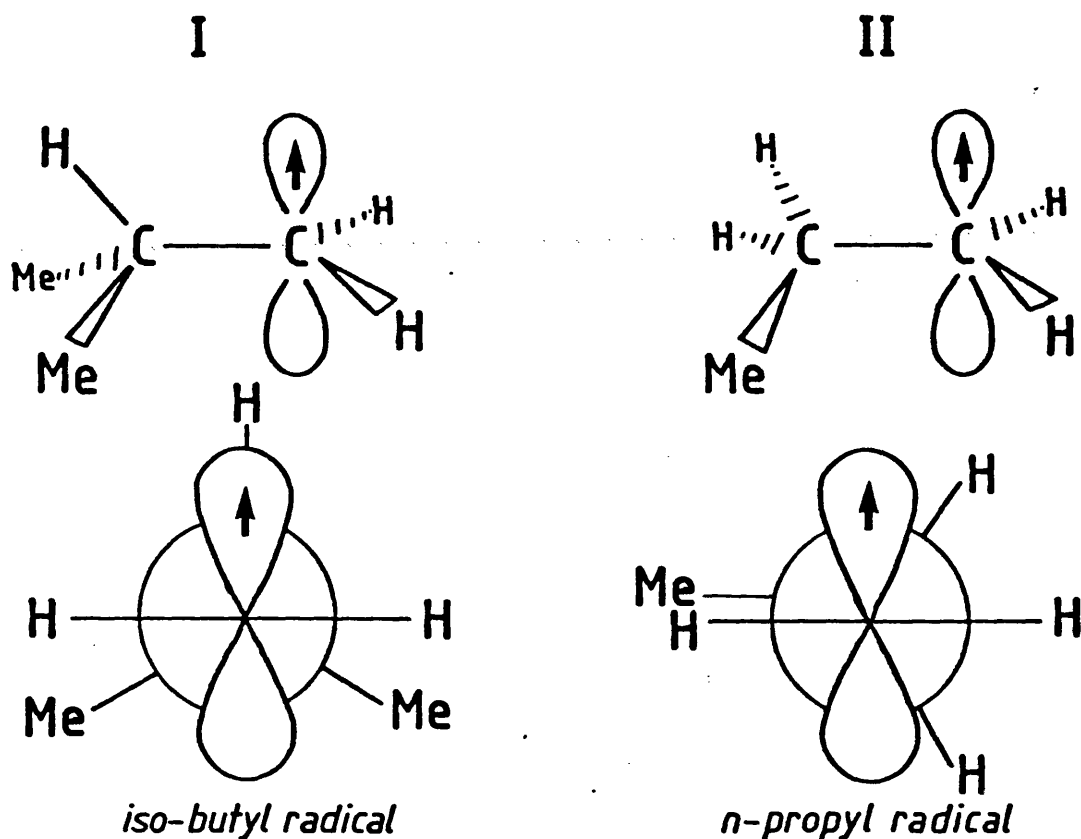
In chapter 2, we suggested a two path sequence for the rearrangement of the isoBu•/Br⁻ adduct to the Bu^t•/Br⁻ adduct. A 1,2 intramolecular H• shift (reaction [5]) and an intermolecular H• exchange with a neighbouring adamantane molecule (reactions [6] and [7]).



The results for the $n\text{Pr}\cdot/\text{Br}^-$ adduct \rightarrow $\text{isoPr}\cdot/\text{Br}^-$ adduct rearrangement seem to suggest that, for this particular case, the intramolecular $\text{H}\cdot$ shift is the primary rearrangement mechanism. Not only because of the apparent absence of the $\text{Me}\dot{\text{C}}(\text{H})\text{CH}_2\text{D}$ radical (adducted or not), but also because of the relative efficiency of conversion from $n\text{Pr}\cdot/\text{Br}^-$ adduct to $\text{isoPr}\cdot/\text{Br}^-$ adduct. Here, the concentration of $\text{Me}_2\dot{\text{C}}\text{H}/\text{Br}^-$ adduct from $n\text{PrBr}$ is ca. $1/4$ of the concentration produced from isoPrBr , whereas the concentration of $\text{Bu}^{\text{t}}\cdot/\text{Br}^-$ adduct from isoBuBr is only ca. $1/10$ of the concentration produced from $\text{Bu}^{\text{t}}\text{Br}$.

Comparing the two rearrangements, one would expect the $\text{isoBu}\cdot/\text{Br}^-$ adduct \rightarrow $\text{Bu}^{\text{t}}\cdot/\text{Br}^-$ adduct to be faster than the analogous $n\text{Pr}\cdot/\text{Br}^-$ adduct \rightarrow $\text{isoPr}\cdot/\text{Br}^-$ adduct. The driving force for the former is greater because we have a primary \rightarrow tertiary radical rearrangement as opposed to a primary \rightarrow secondary. This prediction is further enhanced on consideration of the probable conformations of the radicals involved; I and II.

The hydrogen atom is perfectly placed for a 1,2 shift in I. However, it is the $n\text{Pr}\cdot/\text{Br}^-$ adduct \rightarrow $\text{isoPr}\cdot/\text{Br}^-$ adduct rearrangement that is the fastest, i.e. takes place at the lowest temperature, suggesting these rearrangements are not therefore dependent on the properties just outlined. I would therefore suggest that the radical rearrangements in the adamantane matrix are dependent on molecular libration, i.e. molecular size. For the $\text{isoBu}\cdot$ radical \rightarrow $\text{Bu}^{\text{t}}\cdot$ radical rearrangement I propose the reaction will be dependent on $\text{isoBu}\cdot$ radical and adamantane molecule libration which both take place simultaneously. This results in the generation of a mixture of products; namely the $\text{Bu}^{\text{t}}\cdot$ and $\text{Me}_2\dot{\text{C}}\text{CH}_2\text{D}$ radicals. However, for the $n\text{Pr}\cdot$ radical \rightarrow $\text{isoPr}\cdot$ radical rearrangement, radical libration takes place prior to adamantane



molecule libration because of its smaller size, resulting in a relatively more efficient conversion with no contribution from the intermolecular rearrangement with the adamantane molecule. The reaction is possibly also enhanced by the availability of two hydrogen atoms for migration as opposed to the one for the isoBu \cdot radical.

Whatever the explanation, the fact that the expected relative efficiencies of rearrangement are not produced is very interesting and warrants, perhaps, the need for more research on the subject. A better understanding of the mechanisms involved could, therefore, prompt the suggestion that maybe these types of systems could eventually be used on a synthetic basis.

Iodides

The Type B adducts generated from Bu^tI, isoBuI, isoPrI and nPrI are,

without doubt, authentic adducts, their parameters being in perfect agreement with those derived from the bromo analogues. We must admit, however, that we were at first a little sceptical concerning our hypothesis on the existence of the adducts in two different sites in the adamantane matrix. As far as we knew, this was a completely novel concept. The species designated as the Type A adduct cannot be an α -⁵ or β -iodo species, not only because of the proton couplings (the $\pm \frac{1}{2}$ features of the Type A adduct from Bu^tI clearly showing 8, 10 or 12 equivalent proton couplings of ca. 22 G) but also because of its low g -values. These values are in excellent agreement with the g -values for the solid state adduct spectra so far discovered.^{3,6} The only possible contender is the σ^* species $\left(\begin{array}{c} \diagup \\ \diagdown \end{array} \text{C} \overset{\cdot}{-} \text{I} \right)^-$. However, it is our contention that for this species to be formed, the CR₃ group must remain in a pyramidal structure (chapter 6 deals with this prediction). If this is the case, then the proton couplings would be a great deal smaller than the ca. 22 G obtained. The iodine couplings of ca. 90 G are also much smaller than that of ca. 400 G obtained for other σ^* iodo species.⁷ Hence, not only does the process of elimination lead us to the adduct but, more importantly, its iodine and proton couplings as well as its g -values are all in excellent agreement with those of the other documented solid state adducts.⁶

Therefore, how can we have two different sites in the same adamantane matrix at the same temperature? At this point, analysis of the literature revealed certain interesting facts. First, an infra-red study by Dows et al.⁸ on pure adamantane showed the co-existence of the two phases of adamantane in a 10° temperature range around the phase transition temperature of 208.62 K. Also, judging by their difficulties encountered in obtaining reproducible results, even

greater disorder exists if the sample is not passed through a normalising procedure.

Second, it appears Berman et al.⁹ have already postulated this two site situation while studying the ditertiarybutylnitroxide (DTBN) molecule in adamantane. Their spectrum recorded at ca. 123 K showed the species in a restricted and a rotating site.

Given the conclusions of these two references, and the unavoidable deductions to be drawn from the spectral properties of the species in question, we feel there can be no doubt that the R•/I⁻ adducts can exist in two different sites in the adamantane matrix. One is essentially unrestricted at 77 K, the Type B adduct, and the other is held almost completely rigid at 77 K, the Type A adduct.

Of all the species studied in the adamantane matrix, only the DTBN⁹ and RI molecules have shown this two site phenomenon, with both molecules being of approximately equal size. We suggest therefore that these molecules are on the threshold of impurity size, such that when they are surrounded by recrystallising adamantane molecules, they tend to occupy one or two adamantane molecule sites depending on factors such as orientation, etc. The alkyl bromides do not experience this problem because of the smaller size of the halogen. The single vacancy sites are therefore filled with the Type A R•/I⁻ adducts (the same sites in which the R•/Br⁻ adducts are contained) while the Type B R•/I⁻ adducts are those which occupy the double vacancy sites, their extra freedom allowing for relatively unrestricted rotation.

Absence of β -iodo radical, $\text{Me}_2\dot{\text{C}}\text{CH}_2\text{I}$

If the Bu^t•/Br⁻ adduct and the β -bromo radical $\text{Me}_2\dot{\text{C}}\text{CH}_2\text{Br}$ (species S in chapter 2) are generated from the radiolysis of Bu^tBr in adamantane, then surely the Bu^t•/I⁻ adduct and the β -iodo radical $\text{Me}_2\dot{\text{C}}\text{CH}_2\text{I}$ should

be generated from the analogous experiment using Bu^tI. The adduct is of course detected, however, there appears to be a complete absence of any feature likely to be attributable to the β-iodo radical. This could be because its spectrum is broad and therefore undetectable in this matrix, however, the species has even eluded us in the TMS matrix (from the radiolysis of a 1 Mol % solution of Bu^tI in TMS) in which the β-bromo radical showed well defined bromine A_x features. We have concluded that the β-iodo radical is much less stable than the corresponding β-bromo and β-chloro radicals, probably breaking up to give the alkene and an iodine atom (reaction [8]).



We predict, therefore, that the radiolysis needs to be carried out at a temperature below 77 K if the isolation of the species is to be achieved.

TABLE 2

E.s.r. data for alkyl radical/halide ion adducts in adamantane-d₁₆ matrix

Alkyl radical/halide ion adduct	¹ H hyperfine coupling (Gauss)			hyperfine coupling to ⁸¹ Br, ¹²⁷ I (Gauss)			Temp	Type of adduct
	//	⊥	iso	//	⊥	iso		
(CH ₃) ₃ C•/Br ⁻	-	-	+21.4	-	-	±6.7	208 K	Type A
(CH ₃) ₂ CHCH ₂ /Br ⁻	-	-	-19.0 (αH) +36.2 (βH)	-	-	±4.0	94 K	Type A
(CH ₃) ₂ ĊH/Br ⁻	-	-	-20.5 (αH) +24.3 (βH)	-	-	±4.0	187 K	Type A
(CH ₃) ₃ C•/I ⁻	22.5	-	-	99	-47	+1.6	77 K	Type A
(CH ₃) ₃ C•/I ⁻	-	-	+21.9	-	-	±7.0	215 K	Type B
(CH ₃) ₂ CHCH ₂ /I ⁻	ca. 21 (αH) ca. 30 (βH)	-	-	ca. 86	-	-	77 K	Type A
(CH ₃) ₂ CHCH ₂ /I ⁻	20.5 (αH) 34 (βH)	-	-	33.6	-	-	170 K	Type B
(CH ₃) ₂ ĊH/I ⁻	ca. 24 (βH)	-	-	60	-	-	77 K	Type A
(CH ₃) ₂ ĊH/I ⁻	-	-	-19.5 (αH) +23.5 (βH)	-	-	±3.3	215 K	Type B

all g-values close to 2.001

TABLE 3

E.s.r. temperature dependent ^{127}I hyperfine coupling constants
for the $\text{Bu}^{\cdot}/\text{I}^-$ and $\text{isoBu}^{\cdot}/\text{I}^-$ adducts in the
adamantane- d_{16} matrix (Gauss)

Temp ($^{\circ}\text{K}$)	$\text{Bu}^{\cdot}/\text{I}^-$			$\text{isoBu}^{\cdot}/\text{I}^-$
	//	\perp	iso	//
4.2	106	50	ca. 1 + 2	↓ features too broad for parameter extraction ↓ 47 ↓ 45 ↓ 42.5 ↓ 40.5 ↓ 38.5 ↓ 37 ↓ 35 ↓ 33.5 ↓ 31.5 ↓ 29 ↓ rearrangement to $\text{Bu}^{\cdot}/\text{I}^-$ ↓
77	99	47		
90	97	45.5		
100	95	44		
110	92.5	43		
120	90	42		
130	87	40.5		
140	85	39.5		
150	81	38		
160	78.5	36.5		
170	76.5	35.5		
180	74	34		
190	69.5	32.5		
200	65	31.5		
210	61	31		
220	59	30.5		

REFERENCES

1. This thesis, Chapter 2;
I. G. Smith, M. C. R. Symons, J.C.S. Perkin II, 1362, (1979).
2. D. Nelson, M. C. R. Symons, Tetrahedron Letters, 34, 2953 (1975).
3. E. D. Sprague, F. Williams, J. Chem. Phys., 54, 5425, (1971).
4. R. V. Lloyd, D. E. Wood, M. T. Rodgers, J.A.C.S., 96, 7130, (1974);
R. V. Lloyd, D. E. Wood, J.A.C.S., 97, 5986, (1975).
5. J. Hüttermann, G. W. Neilson, M. C. R. Symons, Mol. Phys., 32, 269, (1976).
6. S. P. Mishra, M. C. R. Symons, J. Chem. Soc. Perkin II, 391, (1973);
A. R. Lyons, M. C. R. Symons, S. P. Mishra, Nature, 249, 341, (1974).
7. A. Hasegawa, M. Shiotani, F. Williams, Faraday Discuss. Chem. Soc., 63, 157, (1977);
D. J. Nelson, M. C. R. Symons, Chem. Phys. Letters, 47, 436, (1977);
G. W. Neilson, M. C. R. Symons, Mol. Phys., 27, 1613, (1974).
8. Poe-Ju Wu, L. Hsu, D. A. Dows, J. Chem. Phys., 54, 2714, (1971).
9. J. A. Berman, R. N. Schwarz, Mol. Cryst., Liq. Cryst., 28, 51-61.

CHAPTER 4

R•/Cl⁻ adducts

INTRODUCTION

The reader may well have realised by now that there has, as yet, been no mention of any alkyl radical/chloride ion adduct. For reasons such as the probable complication and/or broadening of spectra by the presence of the two isotopes of chlorine (both with a spin of $\frac{3}{2}$), these species have chosen to be particularly elusive. This chapter will therefore deal with the chloride ion adducts eventually detected. Further discussion on the character of "the adduct" will also be held in this chapter, in light of the information acquired from the forthcoming experiments.

Using the parameters for the bromo- and iodo- adducts, we can predict the expected parameters for the chloro-analogues by consideration of their relative maximum orbital populations. Hence, the anisotropic parameters for the $\text{Me}\cdot/\text{Br}^{-1}$ and $\text{Me}\cdot/\text{I}^{-2}$ adducts in CD_3CN (Figs. 1 and 2 respectively) predict an $A_{\parallel}({}^{35}\text{Cl})$ of 10-20 G and an $A_{\perp}({}^{35}\text{Cl})$ of 6-12 G. Similarly, the isotropic parameters for the $\text{Bu}^{\text{t}}\cdot/\text{Br}^{-3,4}$ and $\text{Bu}^{\text{t}}\cdot/\text{I}^{-4}$ adducts in adamantane- d_{16} predict an $A_{\text{iso}}({}^{35}\text{Cl})$ of ca. 1.5 G. We herein describe the generation of the $\text{Me}\cdot/\text{Cl}^{-}$ adduct in a CD_3CN matrix, and the generation of the $\text{Bu}^{\text{t}}\cdot/\text{Cl}^{-}$ adduct in an adamantane- d_{16} matrix, in a TMS matrix and in a $\text{Bu}^{\text{t}}\text{Cl}$ matrix.

EXPERIMENTAL

Methyl chloride (B.D.H.), acetonitrile- d_3 (N.M.R.), tetramethylsilane (B.D.H.), tert-butyl chloride (B.D.H.), and adamantane- d_{16} (Merck, Sharpe & Dohme) were all used as supplied.

Figure 1(a)

The $\text{CH}_3\cdot/\text{Br}^-$ adduct in the CD_3CN matrix.

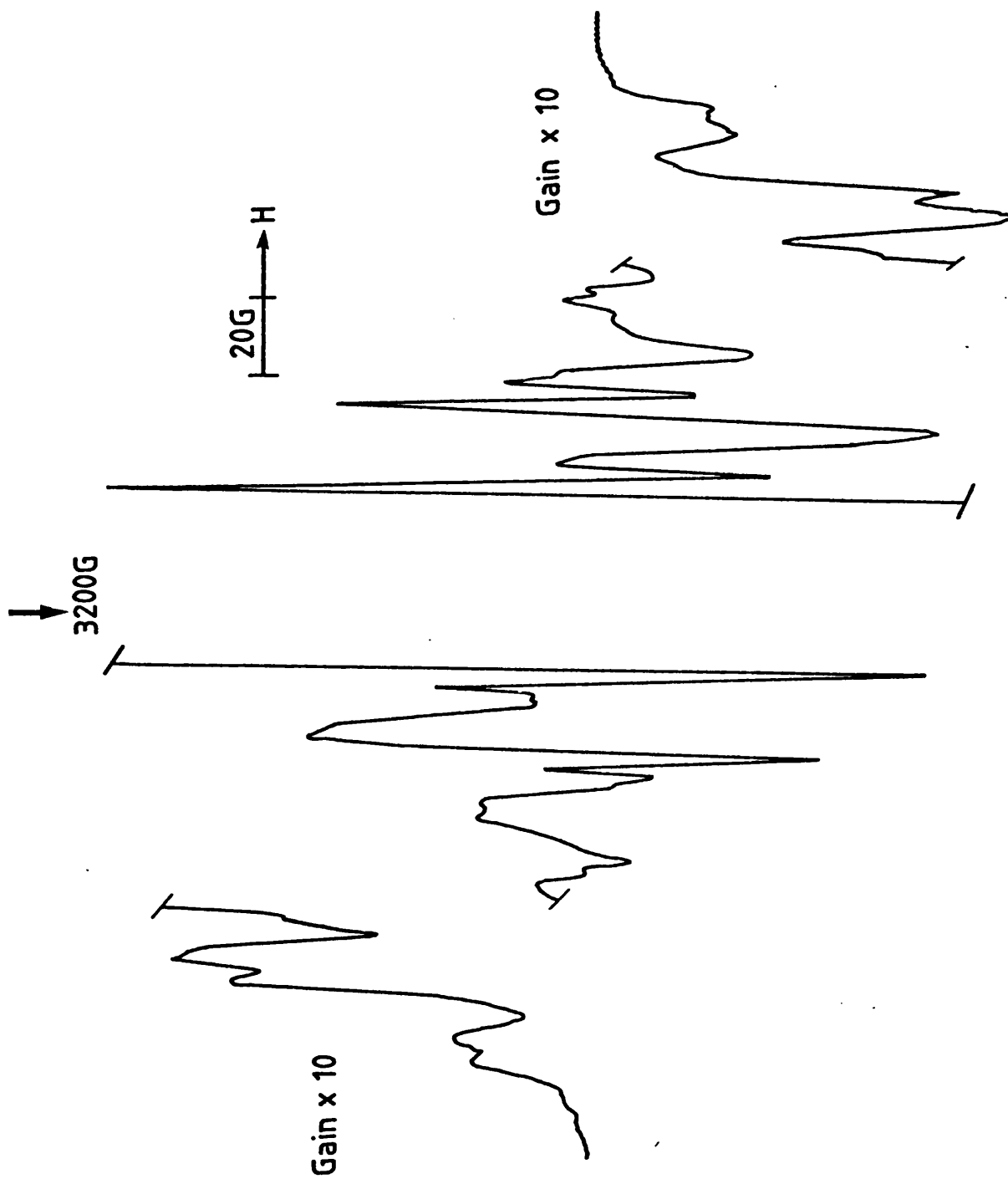


Figure 1(b)

The $\text{CD}_3\cdot/\text{Br}^-$ adduct in the CD_3CN matrix.

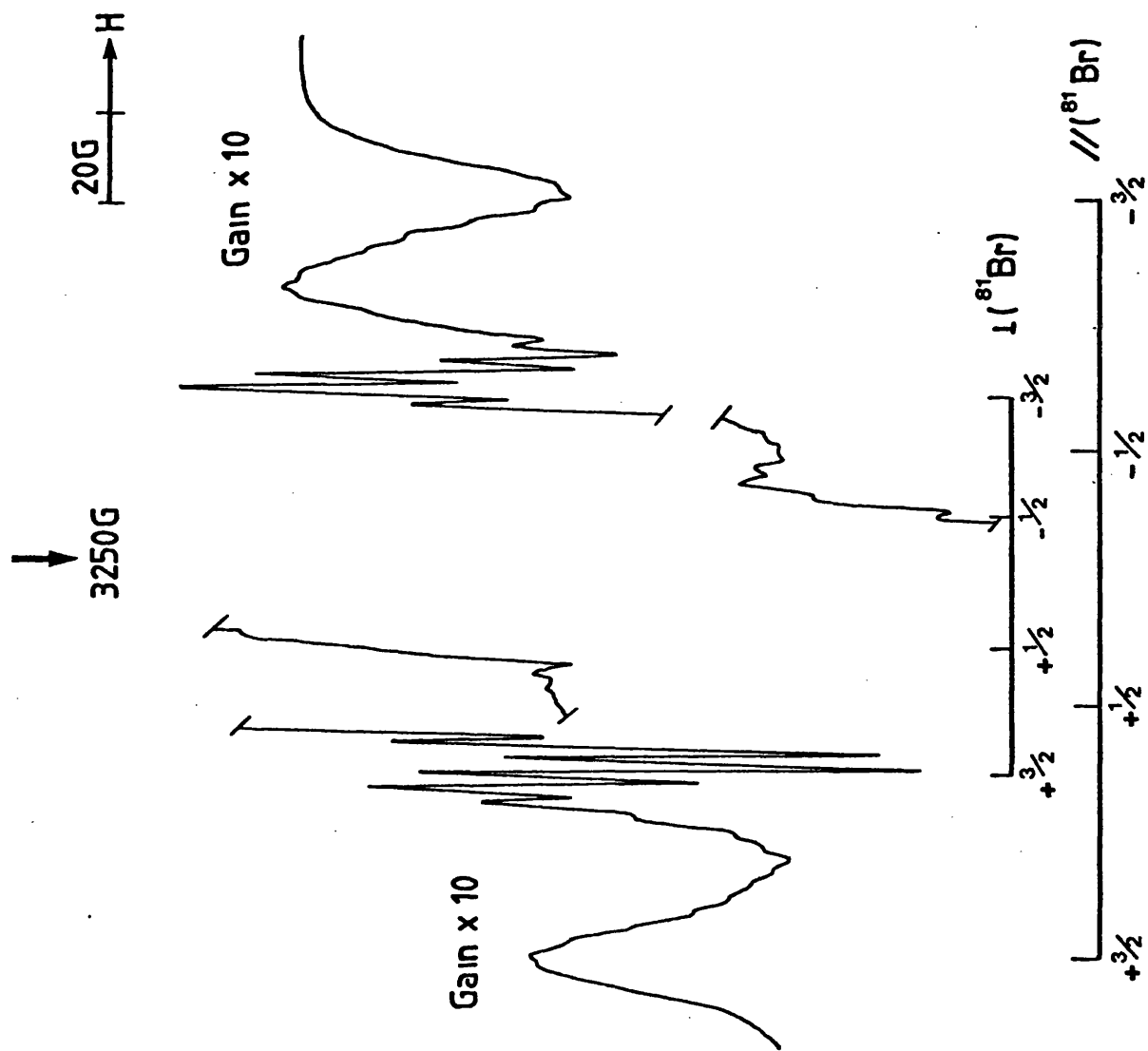


Figure 2(a)

The $\text{CH}_3\cdot/\text{I}^-$ adduct in the CD_3CN matrix.

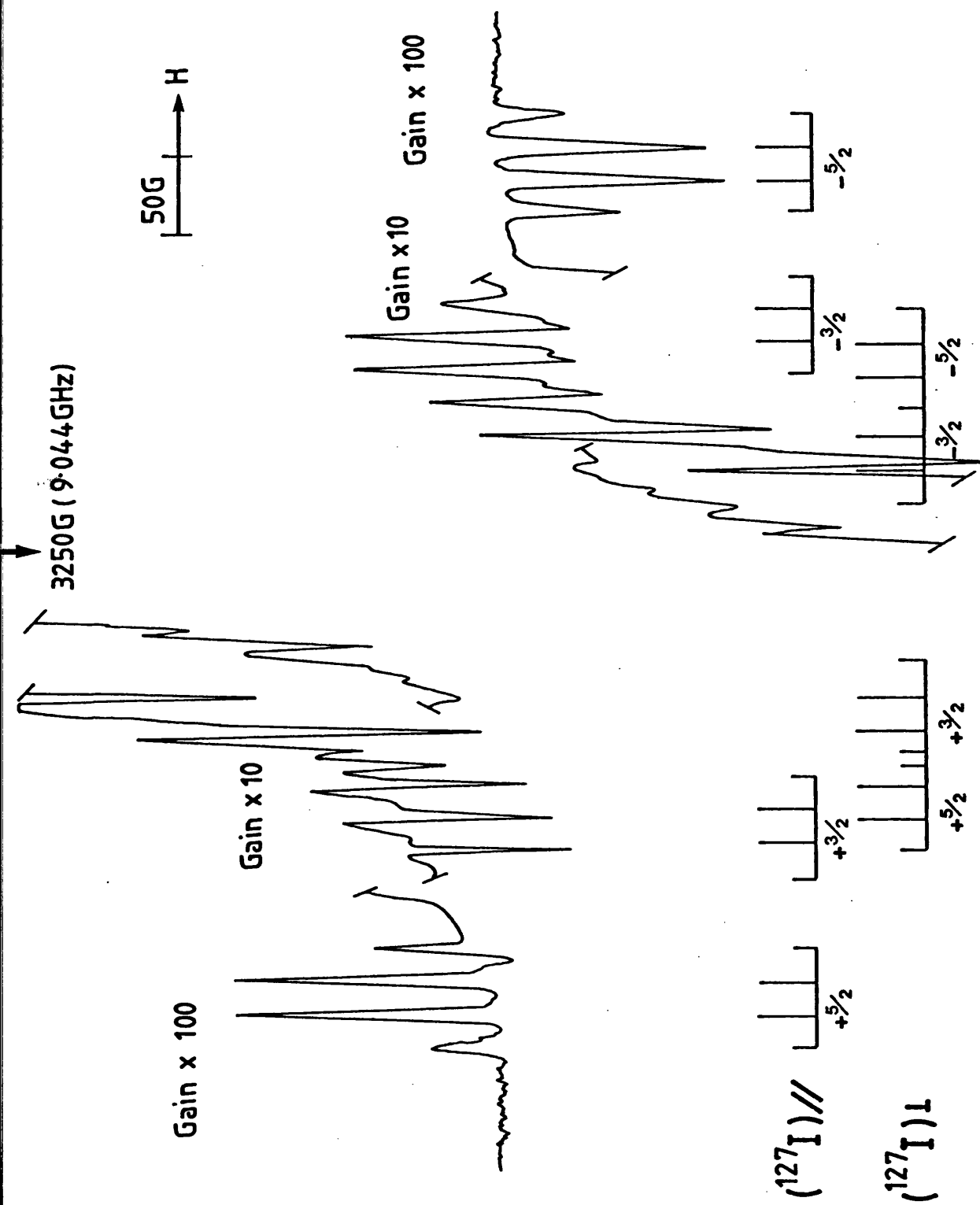
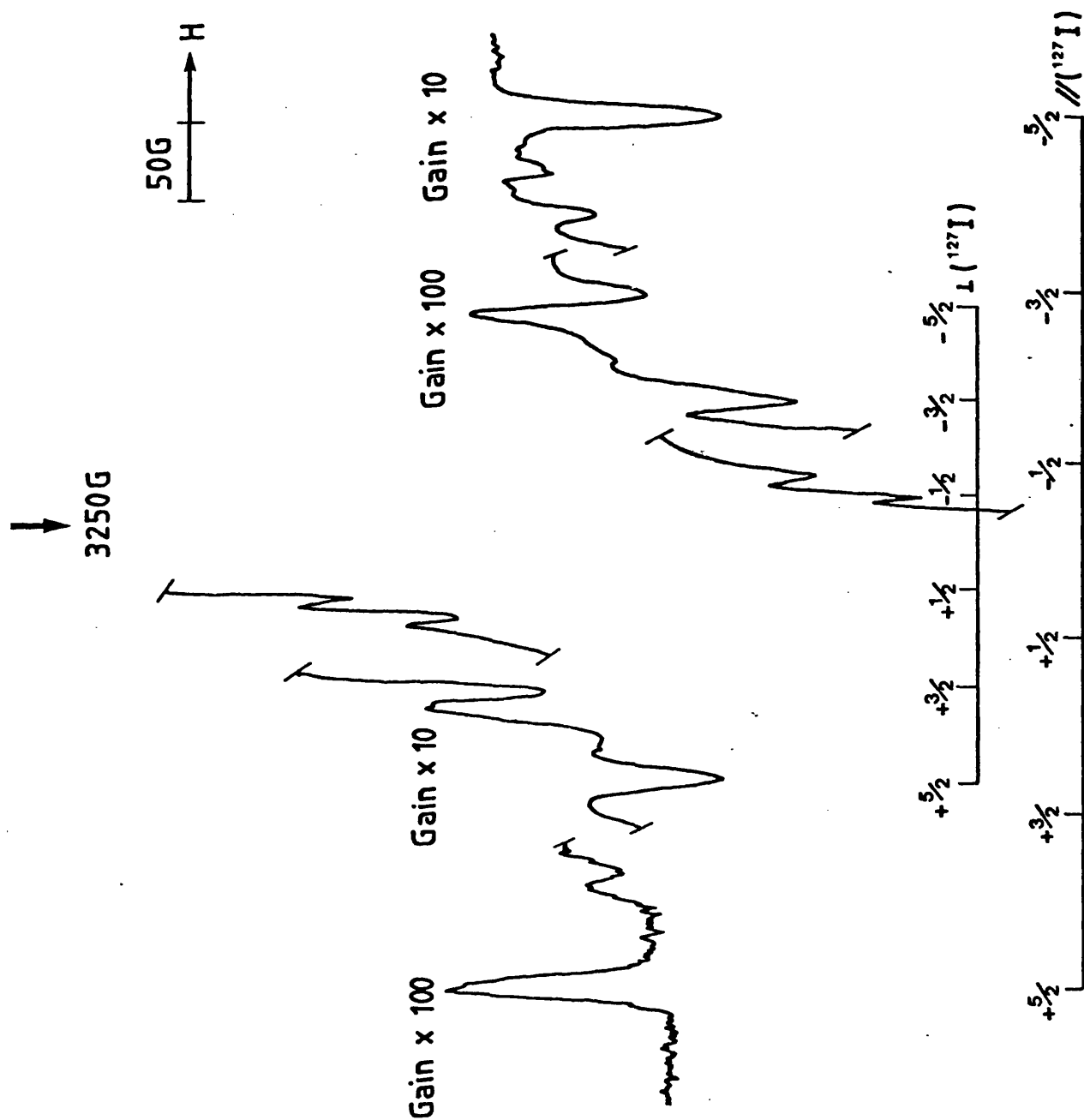


Figure 2(b)

The $\text{CD}_3\cdot/\text{I}^-$ adduct in the CD_3CN matrix.



All solutions were degassed via the freeze-thaw method prior to experimentation. Tert-butyl chloride was incorporated into the adamantane-d₁₆ matrix by recrystallising the adamantane from the substrate, as described in Chapter 1.

Radiolyses of samples and recording of spectra were carried out as described in Chapter 2.

RESULTS

MeCl/CD₃CN

Figs. 3a and 3b show the spectra produced from a 5 Mol % solution of methyl chloride in acetonitrile-d₃ at 4 K and 80 K respectively after γ -irradiation at 77 K. Annealing to 155 K brought about an irreversible growth in Me \cdot radicals whose spectrum was maintained on recooling back to 80 K, replacing the spectrum shown in Fig. 3b.

We have the rigid Me \cdot /Cl⁻ adduct at 4 K with $A_{\parallel}(^{35}\text{Cl}) = \underline{\text{ca.}}$ 9 G, $A_{\perp}(^{35}\text{Cl}) = -4$ G and $A(^1\text{H}) = -21.6$ G. Annealing to 80 K produces a reduction in the halide parameters [$A_{\parallel}(^{35}\text{Cl}) = \underline{\text{ca.}}$ 7 G and $A_{\perp}(^{35}\text{Cl}) = -3$ G] and a slight increase in the proton coupling [$A(^1\text{H}) = -22$ G]. Further annealing produces still a greater reduction in the halide parameters, with a very small increase in the proton couplings, until, at ca. 155 K, the Me \cdot /Cl⁻ adduct dissociates and only the free methyl radicals are detected.

Bu^tCl/TMS

Figs. 4a and 4b show the spectra produced from a 1 Mol % solution of tert-butyl chloride in TMS at 77 K and 111 K respectively after γ -irradiation at 77 K. As was found for the Bu^t \cdot /Br⁻ adduct in both the adamantane-d₁₆^{3,4} and the TMS matrices, there exists some sort of

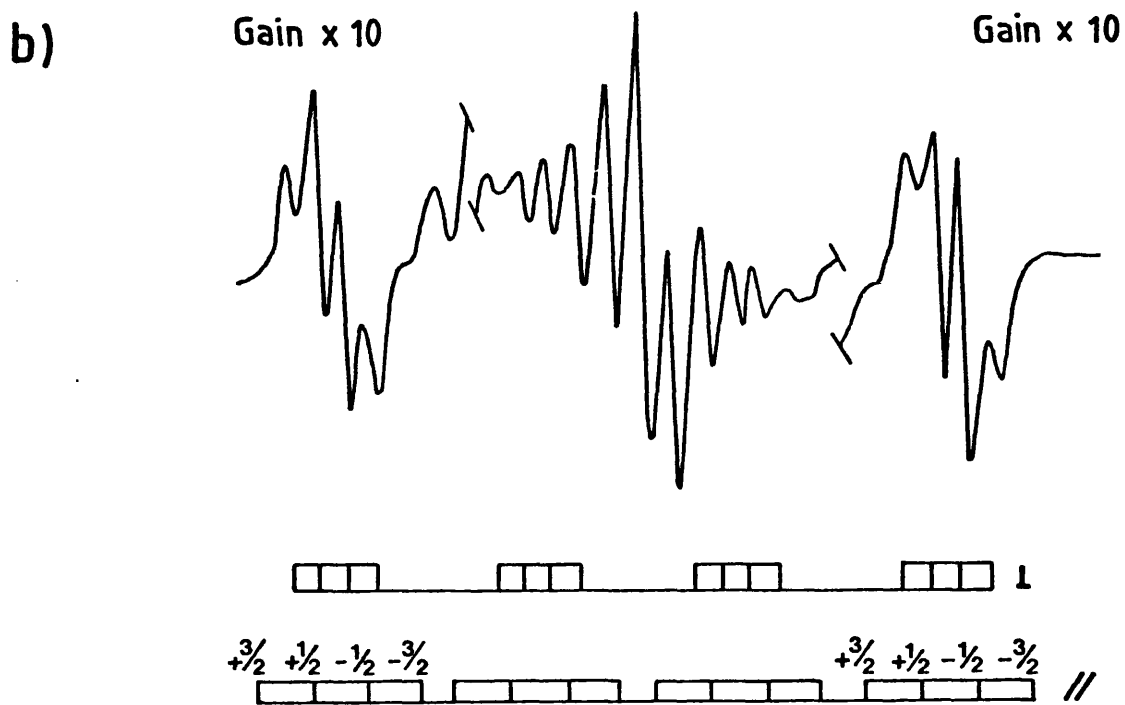
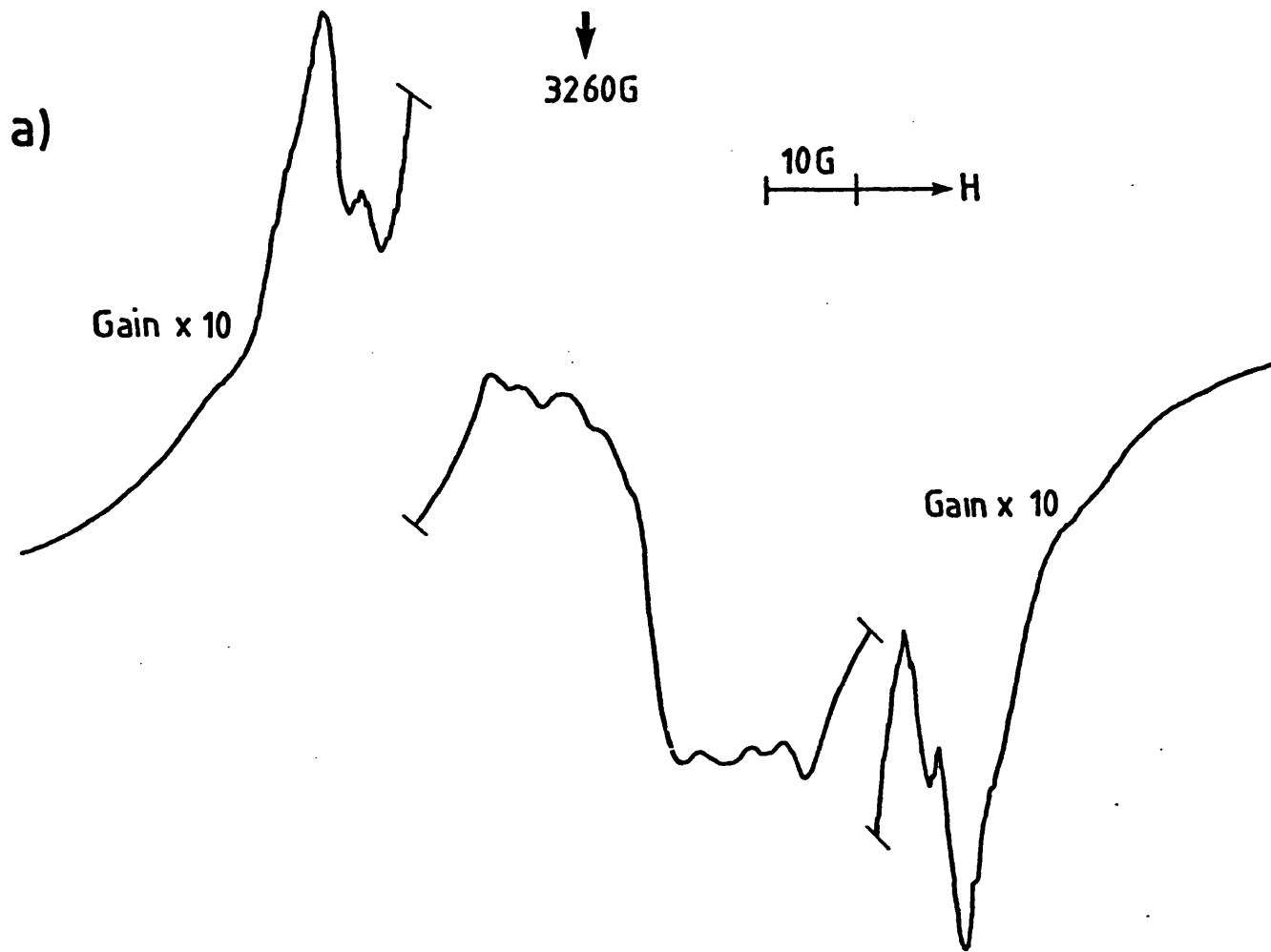


Figure 3

The $\text{CH}_3\cdot/\text{Cl}^-$ adduct in the CD_3CN matrix at (a) 4 K, (b) 80 K.

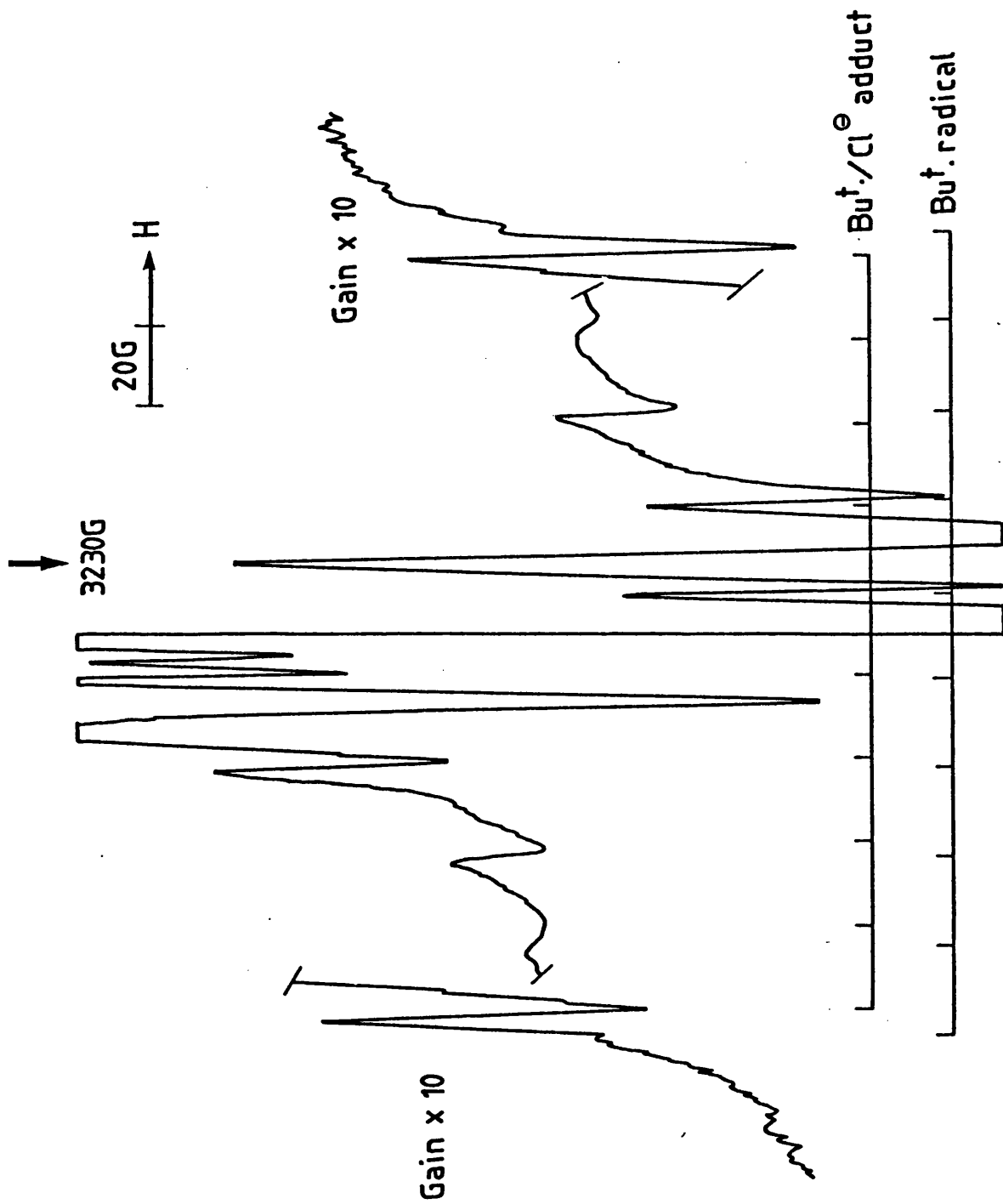
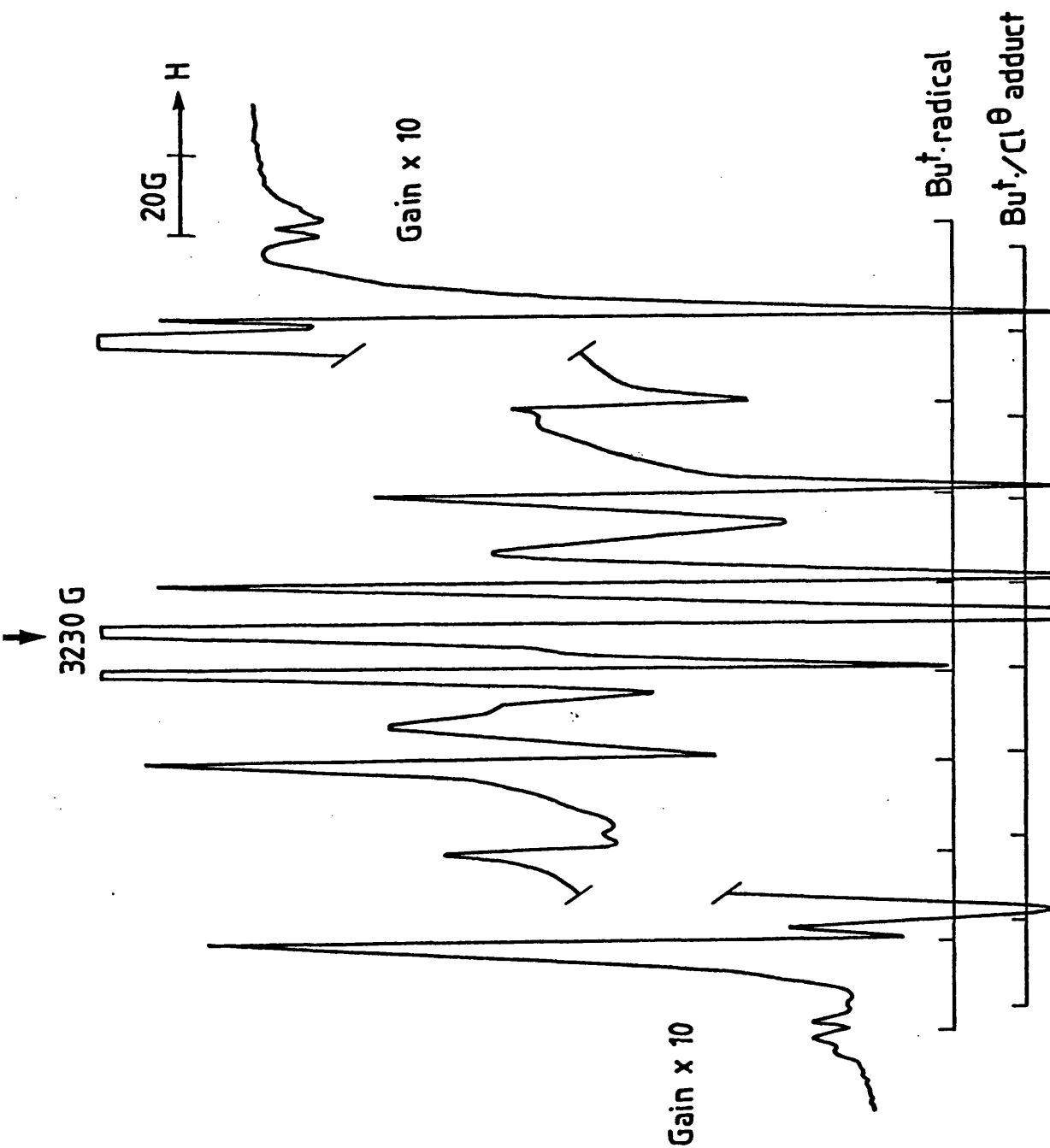


Figure 4(a)

The $(\text{CH}_3)_3\text{C}\cdot/\text{Cl}^-$ adduct in the TMS matrix at 77 K.

Figure 4(b)

The $(\text{CH}_3)_3\text{C}\cdot/\text{Cl}^-$ adduct in the TMS matrix at 111 K.



inequivalence of protons at 77 K for the $\text{Bu}^{\cdot}/\text{Cl}^-$ adduct, giving rise once more to the narrow---broad---narrow appearance of its spectrum. Hence, only the \pm^9_2 features are discernible in Fig. 4a, the spectrum due to Bu^{\cdot} radicals appearing to predominate. However, annealing to ca. 111 K (Fig. 4b) produces a much better resolved $\text{Bu}^{\cdot}/\text{Cl}^-$ adduct with $A_{\text{iso}}(^{35}\text{Cl}) = <1$ G and $A(^1\text{H}) = 21.1$ G. With further annealing, the adduct decays irreversibly to the Bu^{\cdot} radical. Cooling back to 77 K shows the absence of any feature likely to belong to the adduct, yet a 10-fold increase in the Bu^{\cdot} radical concentration.

$\text{Bu}^{\cdot}\text{Cl}/\text{adamantane-d}_{16}$

This medium is not as effective as TMS at isolating the $\text{Bu}^{\cdot}/\text{Cl}^-$ adduct. However, the same narrow---broad---narrow phenomenon exists here as in the TMS matrix at 77 K (Fig. 5a). Unfortunately, minor annealing not only results in a decay in the adduct concentration, but also in the appearance of a very well resolved β -chloro radical, $\text{Me}_2\dot{\text{C}}\text{CH}_2\text{Cl}$ (as studied by Wood and Lloyd⁵). Cooling back to 77 K broadens out all β -chloro radical features, produces an increase in Bu^{\cdot} radical concentration and a reduction in $\text{Bu}^{\cdot}/\text{Cl}^-$ adduct concentration (Fig. 5b).

DISCUSSION

Tables 1, 2 and 3 summarise the results obtained for the $\text{Me}^{\cdot}/\text{X}^-$ adducts in the CD_3CN matrix, and for the $\text{Bu}^{\cdot}/\text{X}^-$ adducts in the TMS and the adamantane- d_{16} matrices respectively ($\text{X} = \text{Cl}, \text{Br}, \text{I}$).

The CD_3CN results show an immediate trend of parameters. As the size of the halide ion increases, the percentage 'p' orbital population on the halide ion increases, while the proton coupling for the methyl

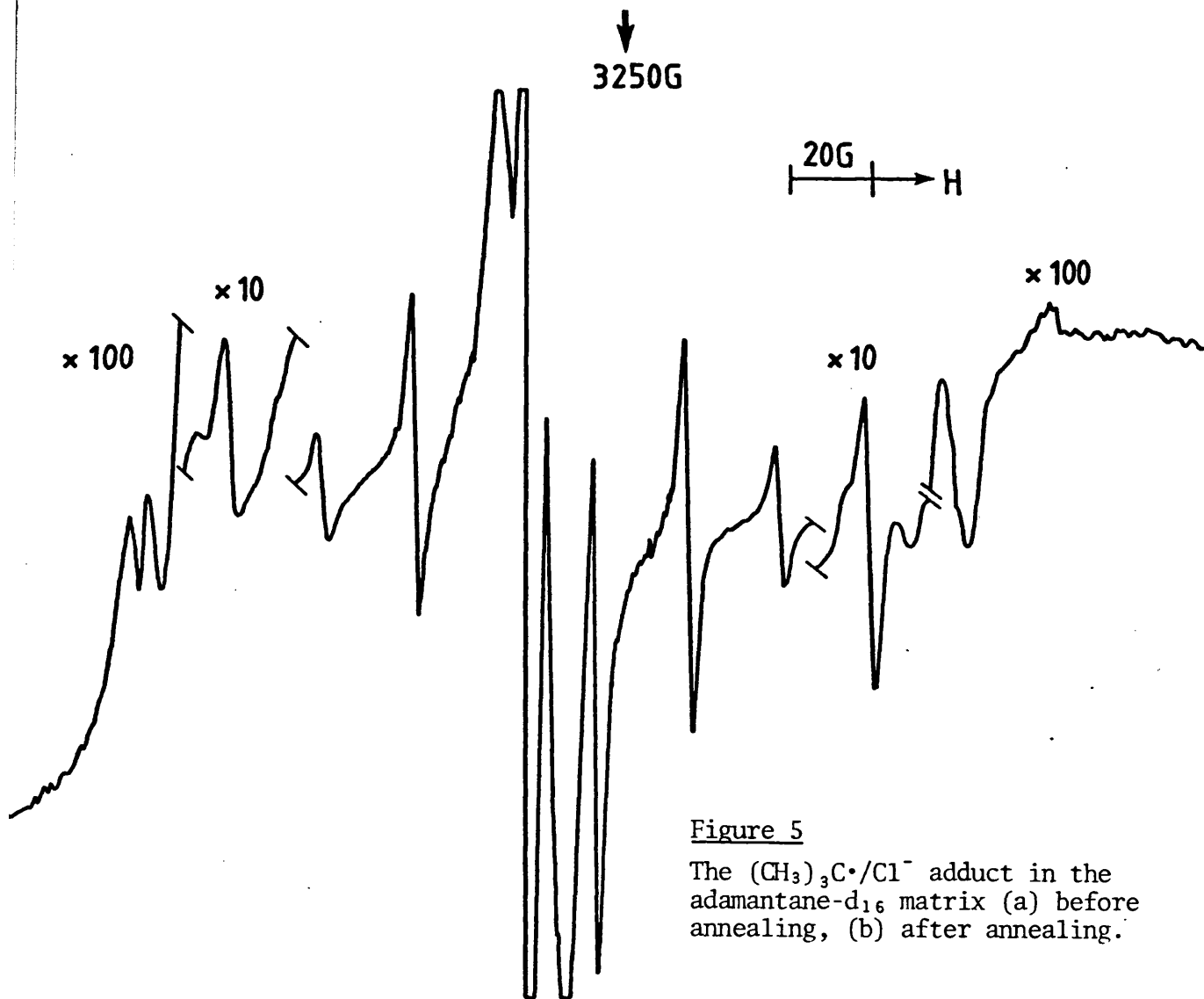


Figure 5

The $(\text{CH}_3)_3\text{C}\cdot/\text{Cl}^-$ adduct in the adamantane- d_{16} matrix (a) before annealing, (b) after annealing.

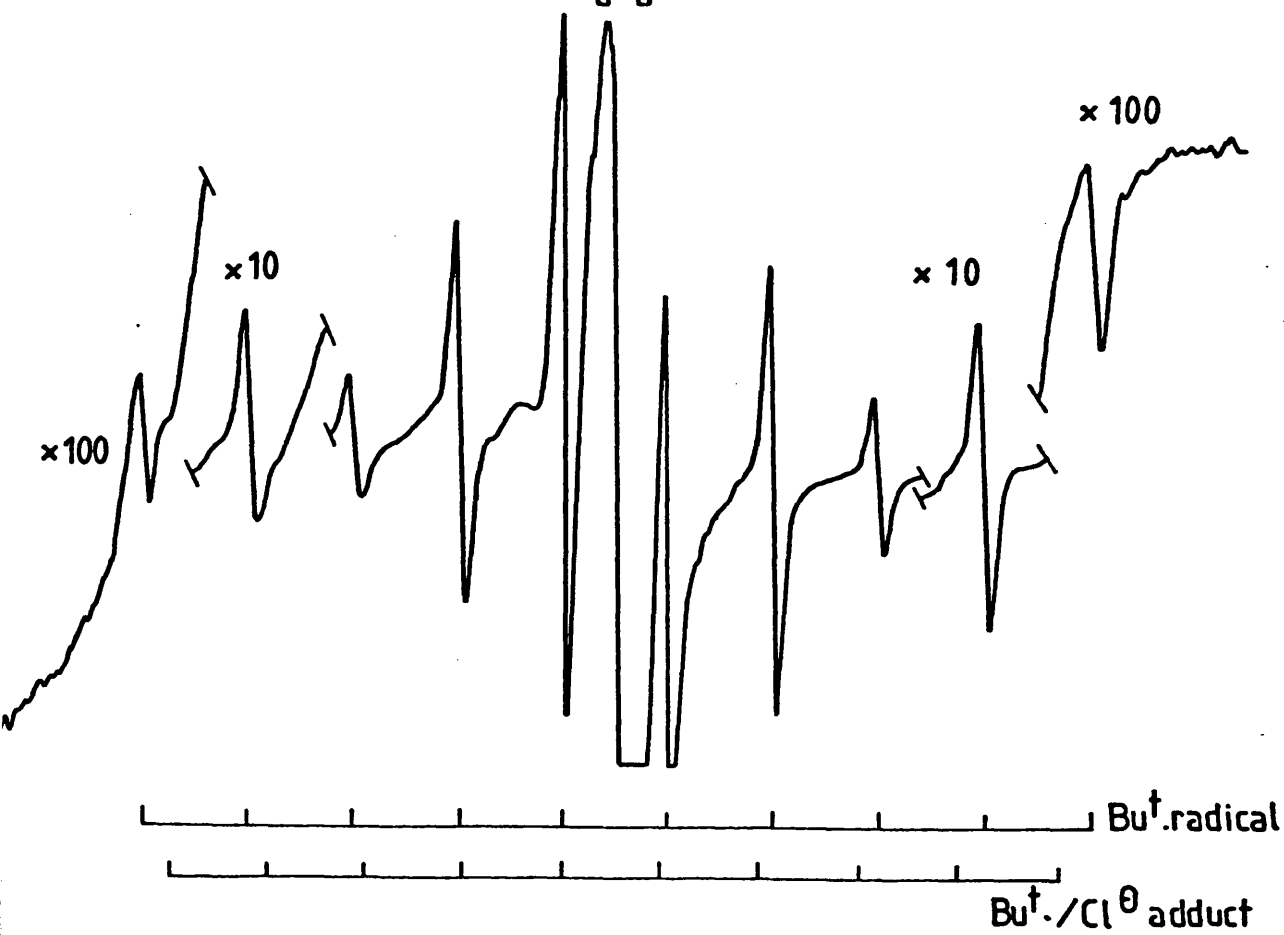


TABLE 1

E.s.r. data for the Me•/X⁻ adducts in the CD₃CN matrix (X = Cl, Br, I)

adduct	temp (°K)	³⁵ Cl, ⁸¹ Br, ¹²⁷ I couplings ^a (Gauss)		% 'p' orbital population ^b	A(¹ H) for Me• radical (Gauss)	% drop in A(¹ H) (Me• = -23 G)	% drop in A(¹³ C)
		⊥	iso				
Me•/Cl ⁻	77	ca. 7	+0.3	7.0	-22	4.4	-
Me•/Br ⁻	77	57	+0.3	11.5	-21	8.7	-
Me•/I ⁻	77	108	-4.0	24.0	-20.6	10.5	ca. 10 ^c

all g-values close to 2.001

^a Values taken from spectra in Figs. 1, 2 and 3.

^b 2B° values: ³⁵Cl = 100.68 G; ⁸¹Br = 493 G; ¹²⁷I = 453 G; ref. 6.

^c Ref. 2.

TABLE 2

E.s.r. data for the $\text{Bu}^{\cdot}/\text{X}^-$ adducts in the TMS matrix (X = Cl, Br, I)

adduct	temp (°K)	^{35}Cl , ^{81}Br , ^{127}I isotropic couplings (Gauss)	$A(^1\text{H})$ for Bu^{\cdot} radical (Gauss)
$\text{Bu}^{\cdot}/\text{Cl}^-$	77	< 1	21.1
$\text{Bu}^{\cdot}/\text{Br}^-$	77	5.6	21.2
$\text{Bu}^{\cdot}/\text{I}^-$	77	ca. 6.0	ca. 21
all <u>g</u> -values close to 2.001			

TABLE 3

E.s.r. data for the $\text{Bu}^{\cdot}/\text{X}^-$ adducts in the adamantane- d_{16} matrix (X = Cl, Br, I)

adduct	temp (°K)	^{35}Cl , ^{81}Br , ^{127}I isotropic couplings (Gauss)	$A(^1\text{H})$ for Bu^{\cdot} radical (Gauss)	dissociation temp $\text{Bu}^{\cdot}/\text{X}^- \rightarrow \text{Bu}^{\cdot} + \text{X}^-$
$\text{Bu}^{\cdot}/\text{Cl}^-$	77	< 1	21.1	< 180
$\text{Bu}^{\cdot}/\text{Br}^-$	206	6.7	21.4	208.6 ^a
$\text{Bu}^{\cdot}/\text{I}^-$	215	7.0	21.9	> 225
all g-values close to 2.001				

^a Temperature of the phase transition of adamantane.

radical decreases. Can this trend tell us anything of the character of "the adduct"?

The potential energy curves in Fig. 6a and 6b represent the alternative concepts envisaged for the adduct. Either it is a species with a definite, but weak, carbon-halogen bond and therefore has a potential minimum on its P.E. curve, Model α , or, it is simply two distinct species, the alkyl radical and halide ion, with no formal bonding between them and their interaction due simply to their close proximity in the same matrix cavity. The halide ion coupling in this case is, therefore, a reflection of a certain amount of charge transfer from the negative halide ion into the p_z orbital of the carbon atom. This latter model, Model β , would not of course require a minimum on its P.E. curve.

If Model α is a true representation of the alkyl radical/halide ion adduct, then approximately equal 'p' orbital populations would be expected for each halide ion as well as approximately equal proton couplings for their respective methyl radical. This is clearly not the case. As the size of halide ion increases, there appears to be a concomitant decrease in proton couplings. This implies either a bending of the methyl radical at the radical site or a small "transfer of spin" from the carbon p_z orbital onto the halide ion. The bending is improbable. The transfer of spin suggestion is validated not only by the observed increase in percentage 'p' orbital population as the size of halide ion is increased, but also by the work carried out by Takahashi *et al.*² They looked at a number of "abnormal methyl radicals" including the $\text{Me}\cdot/\text{I}^-$ adduct in the CD_3CN matrix and their ^{13}C results for the methyl radical showed "appreciable decreases compared with that of the normal radical". In fact, the ^{13}C isotropic coupling

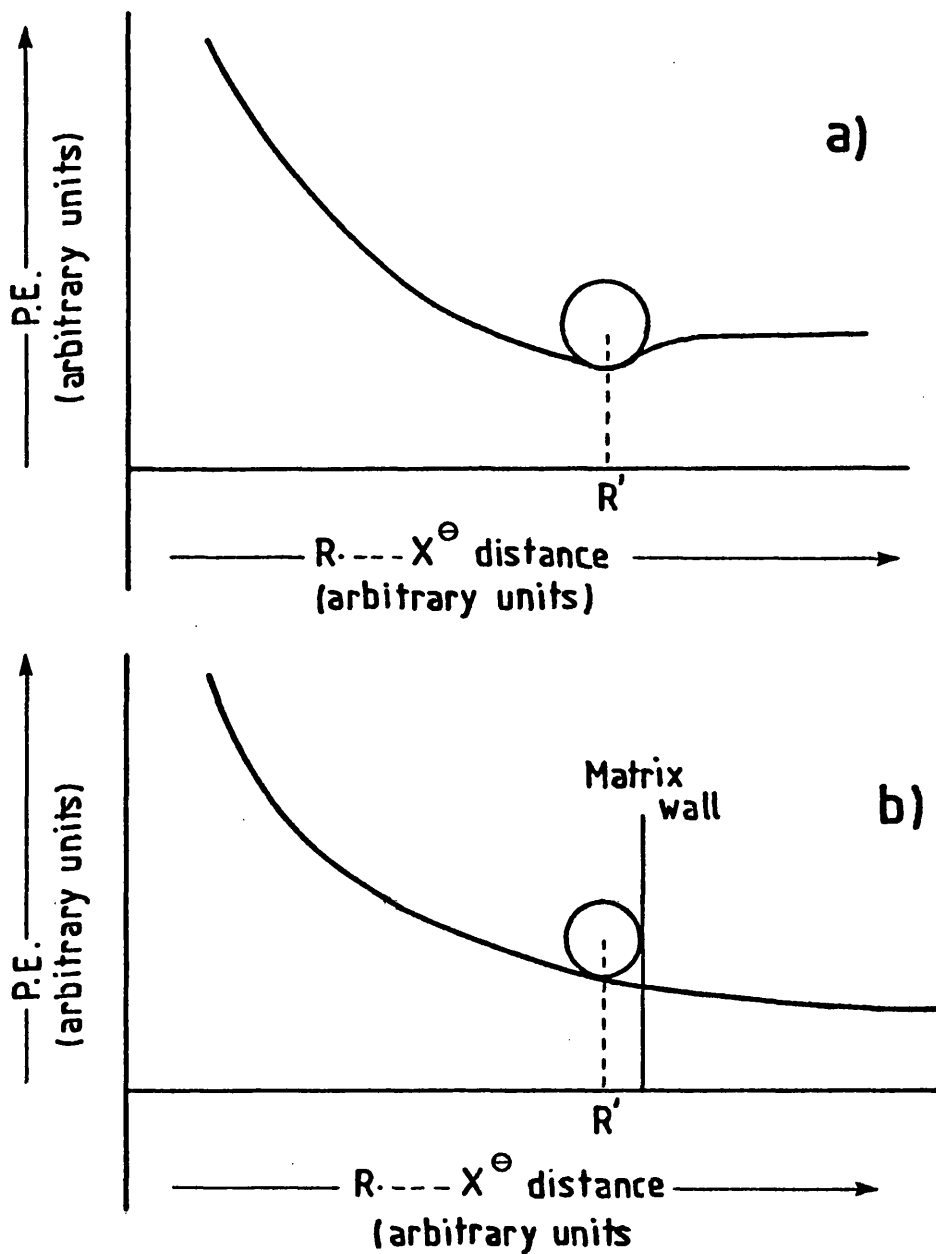


Figure 6 - (a) Model α : a potential minimum for R^\bullet/X^- adduct at distance R' .
 (b) Model β : R^\bullet/X^- adduct distance (R') determined by matrix wall.

showed an approximate 10% drop in spin density, in excellent agreement with the 10.5% drop in the $A(^1\text{H})$ coupling for the same adduct (see Table 1). Thus, what we appear to have is a very definite transfer of spin from the methyl radical onto the halide ion, the amount of spin dependent on the size of the halide ion involved. This ties in perfectly with Model β . As the size of halide ion increases, a decrease in the $\text{R}\cdot\text{---}\text{X}^-$ distance has to occur as the volume of the matrix cavity will of course remain constant. This results in increased spin transfer, i.e. a smaller $A(^{13}\text{C})$ and $A(^1\text{H})$ coupling for the methyl radical, and a larger spin density on the halide ion.

Of course, the percentage drop in the $A(^1\text{H})$ couplings should be the same as the percentage 'p' orbital population on the respective halide ion. Although these values are perfectly comparable within experimental limits for the $\text{Me}\cdot/\text{Cl}^-$ and $\text{Me}\cdot/\text{Br}^-$ adducts, there is, however, a considerable disparity for the $\text{Me}\cdot/\text{I}^-$ adduct. This apparent extra population of the iodide ion 'p' orbital is not fully understood and we can only suggest that there is a considerable contribution from processes such as spin-polarisation and/or dipolar interactions. However, for the moment this disparity will be overlooked, to be discussed in greater detail in Chapter 5 where further examples of iodide ion adduct misbehaviour are documented and discussed.

A similar analysis of the isotropic parameters for the $\text{Bu}^t\cdot/\text{X}^-$ adduct in TMS and adamantane- d_{16} was attempted, however, the trend is not as unambiguous particularly as the parameters are extracted at varying temperatures. The decrease in "dissociation temperature" in the adamantane matrix with decrease in size of halide ion is, however, consistent with our model, as it implies the dissociation is dependent upon ease of halide ion migration.

It should be noted that we believe adducts to be formed as a primary radiation damage product in a number of alkyl halide systems; the spectra are, unfortunately, often broad and very complicated. In many of these systems, annealing will generate the pure alkyl radical⁷ whose spectrum itself can be very complicated when the alkyl radical contains inequivalent protons with anisotropic parameters. It therefore becomes obvious why we have concentrated our efforts on adducts whose alkyl group exhibit a high degree of symmetry, as is the case with the methyl and tert-butyl radicals.

Chapter 5 will also deal with these less obvious adducts, as well as summing up the character of the adduct.

Gamma radiolysis of polycrystalline Bu^tCl

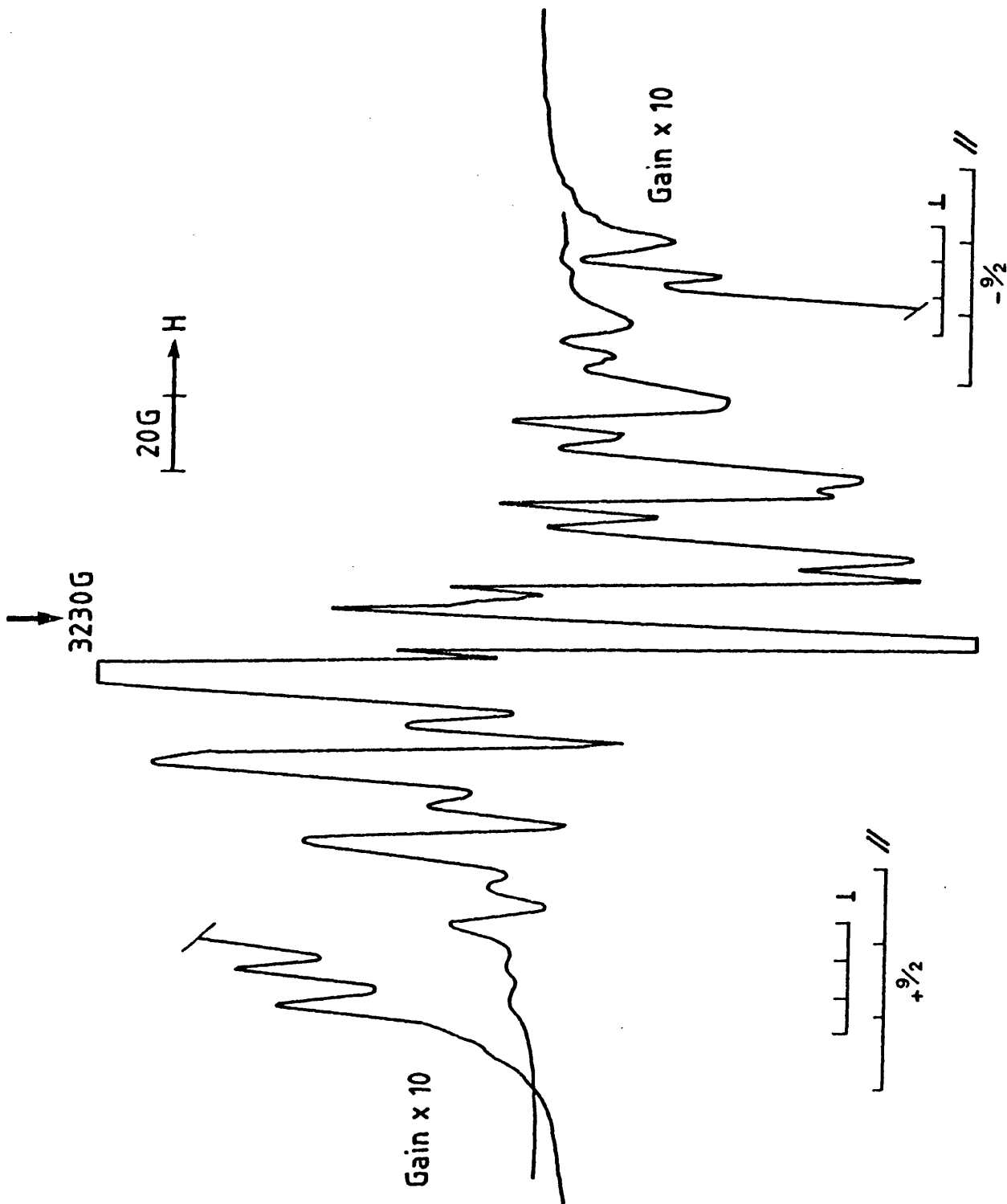
A very interesting series of spectra were generated from the γ -radiolysis of the pure polycrystalline Bu^tCl. The results are once again interpreted in terms of the Bu^t•/Cl⁻ adduct. Unfortunately, as the Bu^t•/Br⁻ and Bu^t•/I⁻ adducts cannot be generated in the same environment (the Bu^tCl matrix), and therefore precluding comparison of the halide ion parameters, this particular example has been discussed in isolation from the other experiments.

RESULTS AND DISCUSSION

Fig. 7a shows the spectrum produced at 77 K. Variation in microwave power indicates that it is probably due to one species only with a minor contribution from Bu^t• radicals. Doping with electron scavengers showed the species to be an electron gain species. The spectrum is interpreted in terms of the rigid Bu^t•/Cl⁻ adduct, with $A(^1\text{H}) = +21.7$ G, $A_{\parallel}(^35\text{Cl}) = \underline{\text{ca.}} +20$ G and $A_{\perp}(^35\text{Cl}) = -10$ G. Annealing to 131 K

Figure 7(a)

The rigid $(\text{CH}_3)_3\text{C}\cdot/\text{Cl}^-$ adduct at 77 K.



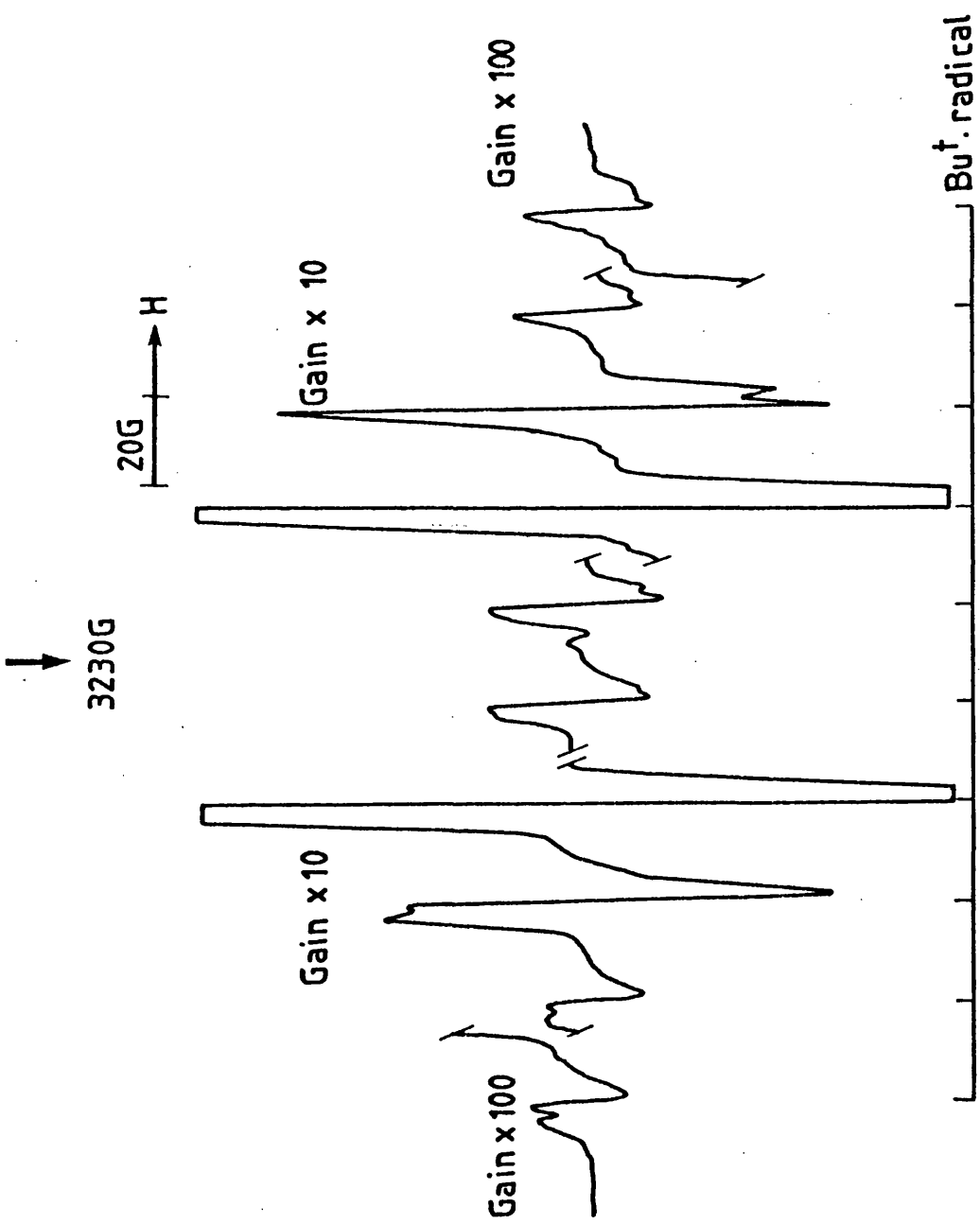
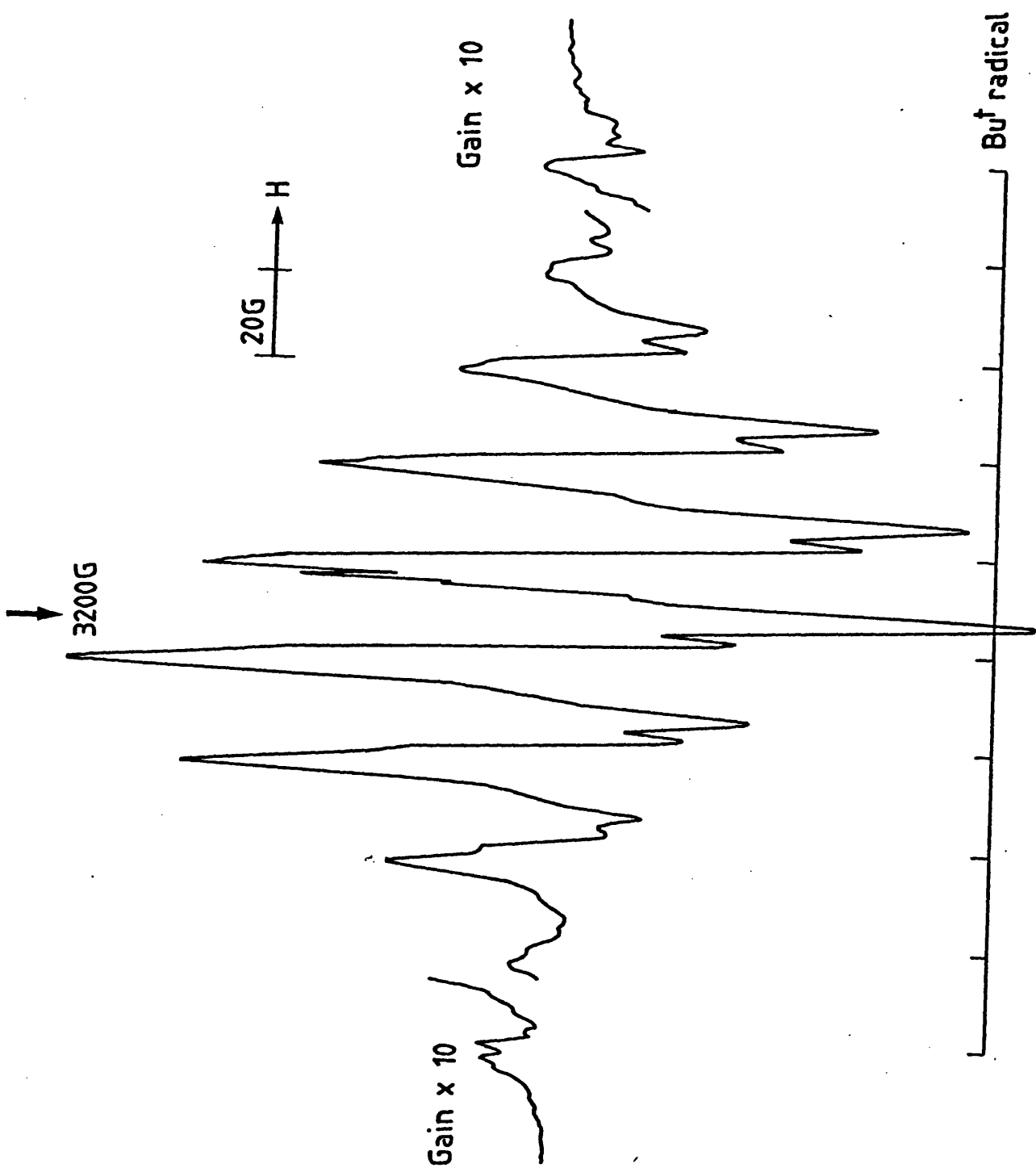


Figure 7(b)
 The $(\text{CH}_3)_3\text{C}\cdot/\text{Cl}^-$ adduct librating considerably at 131 K.

Figure 7(c)

The restricted yet 'relaxed' $(\text{CH}_3)_3\text{C}\cdot/\text{Cl}^-$ adduct at 77 K.



then produced the spectrum in Fig. 7**b** which, on cooling back to 77 K, did not reproduce the spectrum in Fig. 7**a** but rather that in Fig. 7**c**. Repeated annealing and cooling experiments showed the spectra of Figs. 7**b** and 7**c** to be completely reversible. Both these spectra contain $\text{Bu}^{\text{t}\cdot}$ radicals, the other species consisting of a 22 G dectet of linewidth ca. 14 G at 77 K, and a 22 G dectet of linewidth ca. 6 G at 131 K. This species is without doubt the restricted, but not rigid, $\text{Bu}^{\text{t}\cdot}/\text{Cl}^-$ adduct. At temperatures greater than 155 K, the adduct disappears and further $\text{Bu}^{\text{t}\cdot}$ radicals are generated.

At first glance, the spectrum in Fig. 7**b** looks simply like a rigid $\text{Bu}^{\text{t}\cdot}$ radical. However, closer scrutiny reveals that the "perpendicular" features are in the predicted positions for the isotropic $\text{Bu}^{\text{t}\cdot}$ radical features which are clearly present at 77 K (Fig. 7**c**). Also, the couplings for the "parallel" features are found to be inconsistent as one progresses across the spectrum, i.e. if the $+9/2$ feature $\rightarrow +7/2$ feature coupling is taken as 22.5 G, we achieve a $+1/2$ feature $\rightarrow -1/2$ feature coupling of ca. 31 G. A clearly impossible situation for true parallel features. What we have, as stated, is a broad, nearly isotropic dectet of ca. 22 G superimposed on the isotropic spectrum of the $\text{Bu}^{\text{t}\cdot}$ radical.

The rigid adduct first formed at 77 K is obviously greatly restricted as the $\text{Bu}^{\text{t}\cdot}$ radical and Cl^- ion have to occupy the same size site in the lattice as the original undamaged $\text{Bu}^{\text{t}}\text{Cl}$ molecule. Annealing of the sample permits a softening of the matrix and allows the two species to relax into a less restricting environment. This results in an adduct with broad features due predominantly to a small and unresolved halide ion coupling. The temperature dependence of this coupling either represents an increased rotation of the adduct with its concomitant decrease of undefined parallel and perpendicular

parameters, or a mutual repulsion of the halide ion and $\text{Bu}^{\text{t}\cdot}$ radical. Whichever the interpretation, the unambiguous and important point here is the existence of an adduct which can exhibit at least two different $\text{R}\cdot\text{---Cl}^-$ distances, and therefore consolidates our view of the adduct as simply the co-existence of the two species in the same matrix cavity. Further annealing produces an increased softening of the matrix and thus permits the two species to migrate a sufficient distance as to preclude all interactions.

CONCLUSION

We have now isolated and detected quite unambiguous alkyl radical/chloride ion adducts in a series of matrices, their parameters similar to those for the bromo- and iodo- analogues. Although by no means conclusive, our comparative study of the results for the $\text{Me}\cdot/\text{X}^-$ adducts ($\text{X} = \text{Cl}, \text{Br}, \text{I}$) in the CD_3CN matrix and for the $\text{Bu}^{\text{t}\cdot}/\text{Cl}^-$ adduct in a $\text{Bu}^{\text{t}}\text{Cl}$ matrix suggest there is no formal bonding between the alkyl radical and its ejected halide ion. The adduct can be considered as a weak charge-transfer species, with the degree of transfer largely dependent upon the $\text{R}\cdot\text{---X}^-$ distance.

REFERENCES

1. S. P. Mishra, M. C. R. Symons, J. Chem. Soc. Perkin II, 391, (1973).
2. Y. Fujita, T. Katsu, M. Sato, K. Takahashi, J. Chem. Phys., 61, 4307, (1974).
3. I. G. Smith, M. C. R. Symons, J.C.S. Perkin II, 1362, (1979).
4. This thesis, Chapter 3.
5. R. V. Lloyd, D. E. Wood, M. T. Rodgers, J.A.C.S., 96, 7130, (1974);
R. V. Lloyd, D. E. Wood, J.A.C.S., 97, 5986, (1975).
6. M. C. R. Symons "Chemical and Biochemical Aspects of Electron Spin Resonance Spectroscopy", Van Nostrand Reinhold Company Ltd., 1979.
7. P. B. Ayscough, C. Thompson, Trans. Faraday Soc., 58, 1477, (1962).

CHAPTER 5

Abnormal $R\cdot/X^-$ adducts ($X = Cl, Br, I$)
and a character analysis of "the adduct"

INTRODUCTION

The vast majority of adducts so far discussed have been produced in matrices such as adamantane, tetramethylsilane (TMS), and acetonitrile- d_3 (CD_3CN), all of which have enabled the generation of well resolved spectra suitable for the extraction of parameters. However, as mentioned in the previous chapter, adducts have been formed as the primary radiation damage product in many of our systems, where either complete parameter extraction is impossible or, as in the particular case of the radiolysis of the pure polycrystalline alkyl iodides,^{1,2,3} a totally inconsistent series of iodide ion parameters are obtained. This chapter will therefore cite a few of these examples and, I hope, demonstrate to the reader the unpredictability of the halide ion hyperfine coupling for adducts.

Lastly, as an epilogue to the last four chapters, the nature and character of the adduct will be attempted, particularly with a view to the "abnormal" adduct parameters documented in this chapter.

EXPERIMENTAL

Ethyl bromide (Hopkins & Williams), tert-butyl bromide (B.D.H.), tetramethylsilane (B.D.H.), ethyl iodide (Fisons), iso-propyl iodide (Hopkins & Williams) and ethyl iodide- d_5 (Merck, Sharpe & Dohme) were all used as supplied. All solutions were degassed via the freeze-thaw method prior to experimentation. Radiolyses of samples and recording of spectra were carried out as described in Chapter 2.

RESULTS AND DISCUSSION

EtBr/TMS

The range of alkyl halides (MeX, EtX, nPrX, isoPrX, isoBuX, Bu^tX) were all introduced individually into the TMS matrix, this particular example representing the general sequence of events. Figs. 1a and 1b show the spectra generated at 77 K before and after annealing respectively. While analysis of the former spectrum at first suggests a rigid Et• radical, the latter spectrum clearly demonstrates that the Et• radical can, in fact, tumble at 77 K. The spectrum in Fig. 1a is almost certainly a mixture of the Et•/Br⁻ adduct and Et• radical, with the adduct features badly defined.

Polycrystalline Bu^tBr

Figs. 2a and 2b show the spectra generated from the γ -radiolysis of pure Bu^tBr before and after annealing respectively. Once again, a totally unresolved adduct is the predominant species in the former ($g_{av} < \text{free spin}$) which generates unambiguous, resolved Bu^t• radicals on annealing.

Polycrystalline isoPrI

The spectrum in Fig. 3 was generated from the γ -radiolysis of polycrystalline isoPrI at 77 K. Unfortunately, the perpendicular parameters cannot be extracted but we have an $A_{\parallel}(^{127}\text{I})$ of 60 G and an $A(^1\text{H}) \alpha + \beta$ of 25 G for the isoPr•/I⁻ adduct. Annealing produces first the inward movement of all features and, second, the decrease in concentration of adduct with a simultaneous increase in concentration of isoPr• radicals.

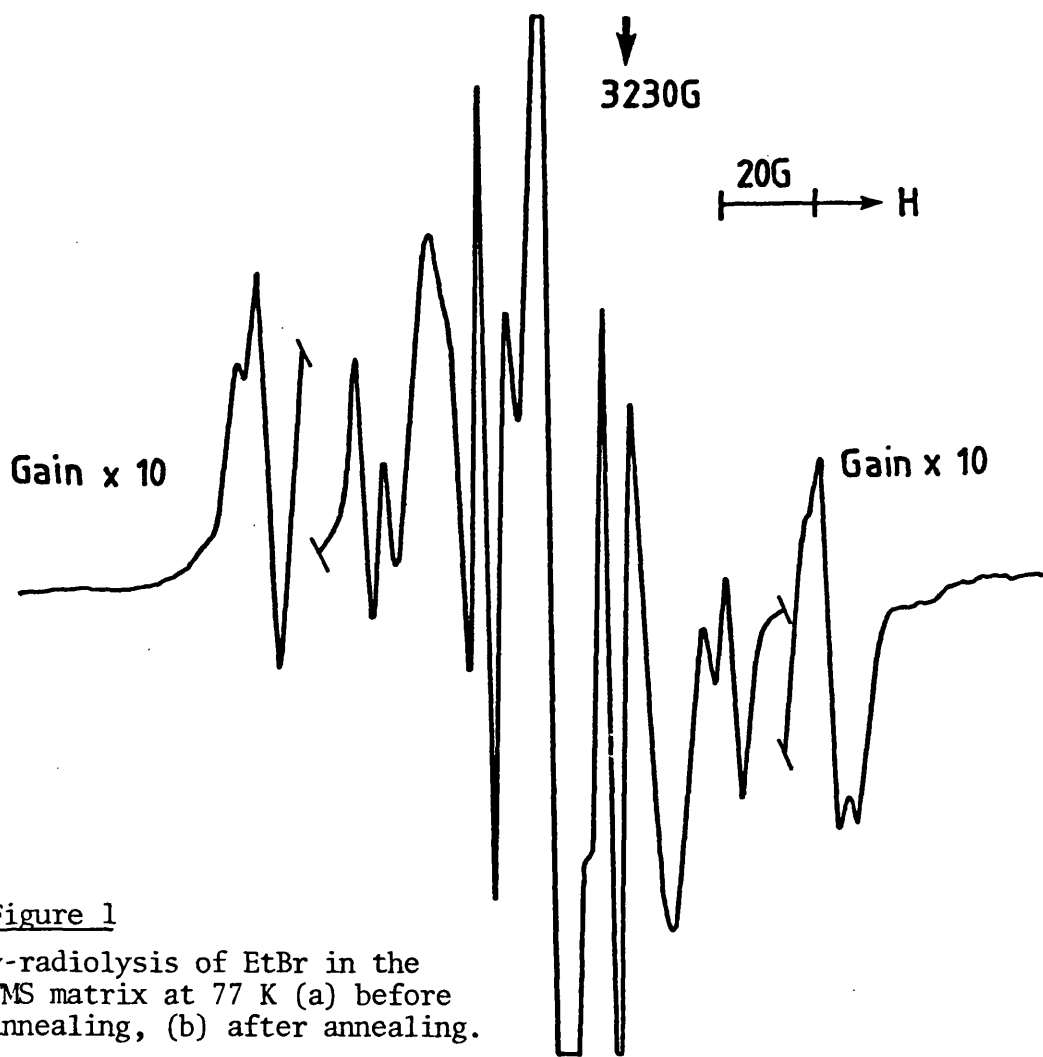
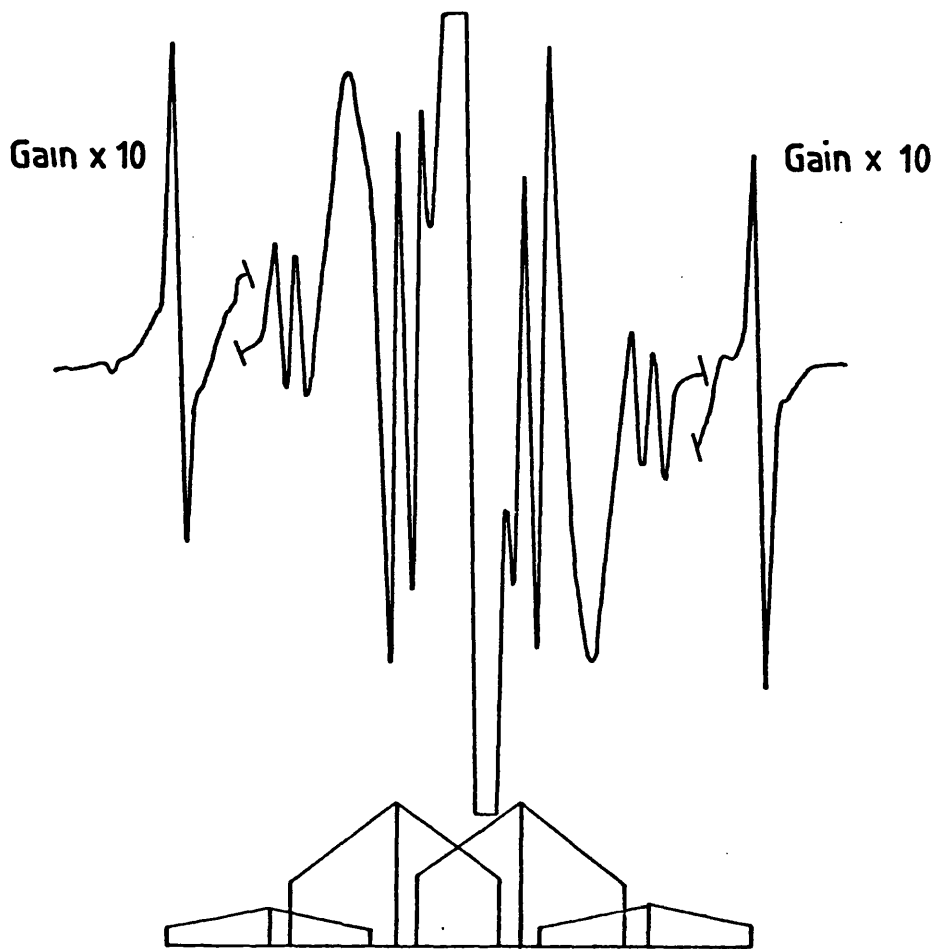


Figure 1

γ -radiolysis of EtBr in the TMS matrix at 77 K (a) before annealing, (b) after annealing.



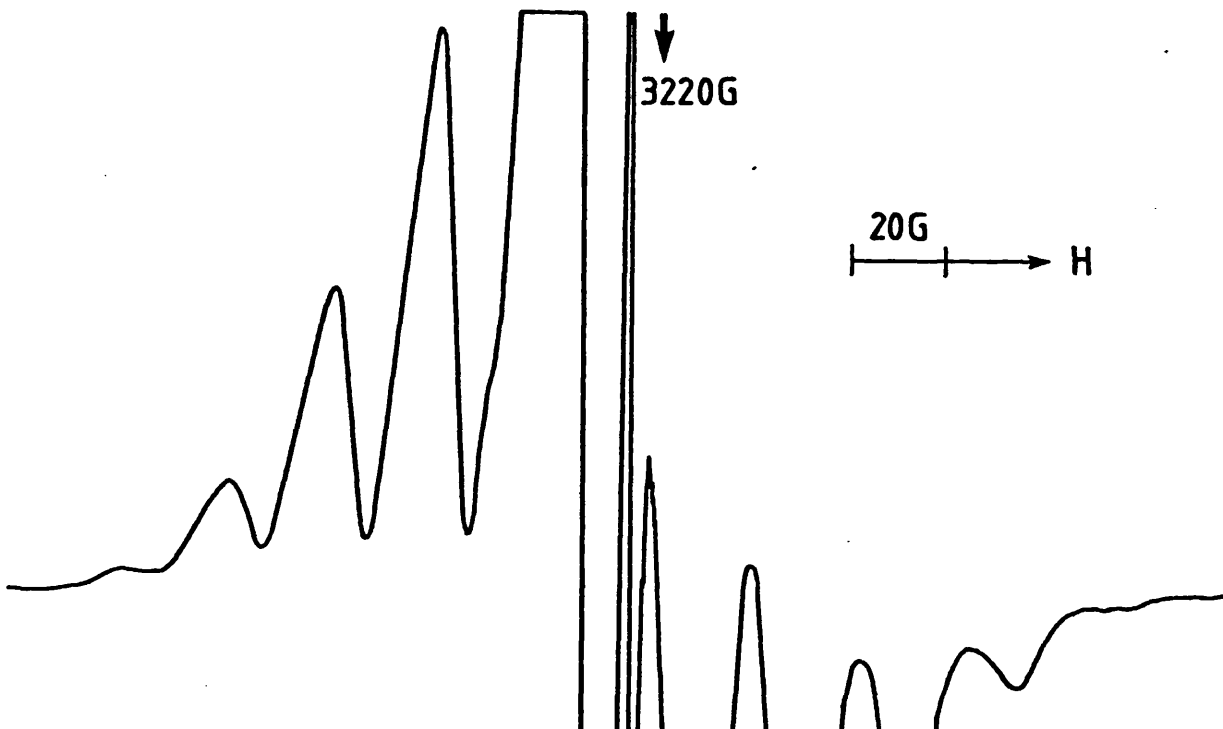
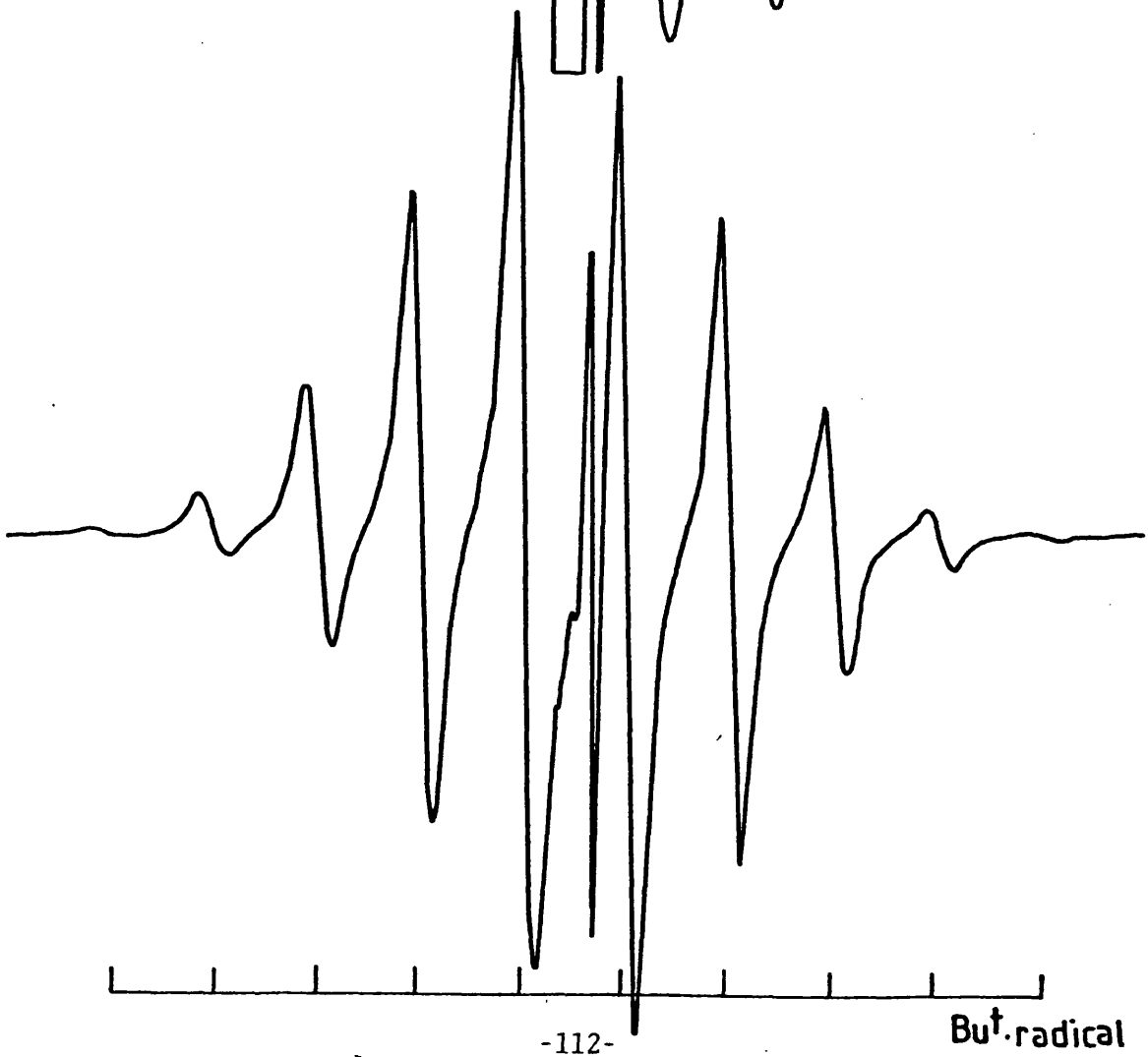


Figure 2
 γ -radiolysis of pure Bu^tBr
 at 77 K (a) before annealing,
 (b) after annealing.



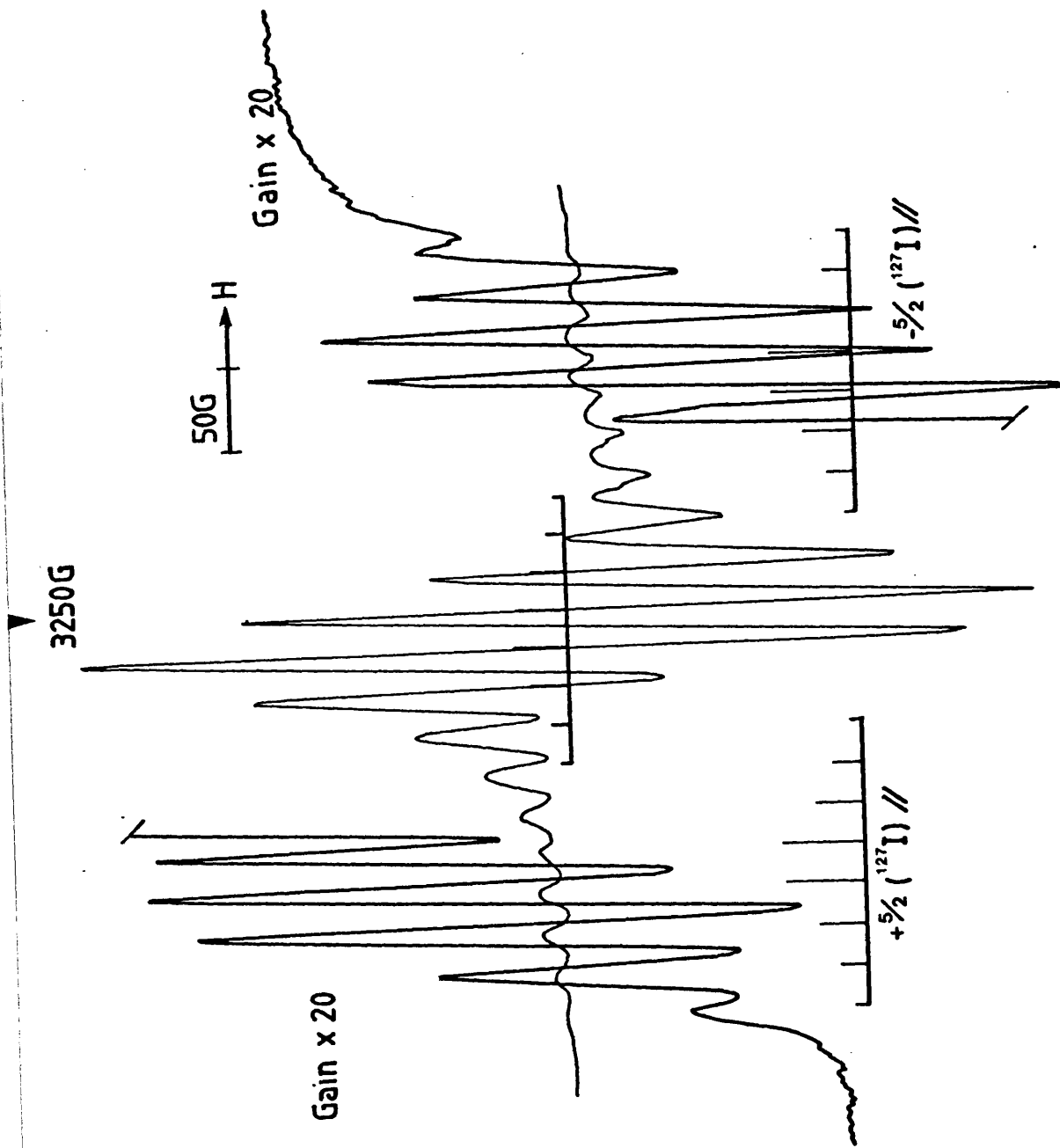


Figure 3
 The rigid $(\text{CH}_3)_2\dot{\text{C}}\text{H}/\text{I}^-$ adduct.

Polycrystalline EtI

Figs. 4a and 4b show the spectra at 77 K generated from the γ -radiolysis at 77 K of polycrystalline $\text{CH}_3\text{CH}_2\text{I}$ and $\text{CD}_3\text{CD}_2\text{I}$ respectively. Although the maximum iodine coupling of ca. 175 G is larger than has been experienced for other examples, we were perfectly prepared to analyse the species in terms of the $\text{Et}\cdot/\text{I}^-$ adduct. Annealing to ca. 150 K produced a minor inward movement of all features with a simultaneous enhancement of resolution, as in Fig. 4c for the $\text{CH}_3\text{CH}_2\cdot/\text{I}^-$ adduct. Further annealing generated a decrease in adduct concentration and an increase in $\text{Et}\cdot$ radical concentration.

Polycrystalline and glassy n-alkyl iodides

Willard et al. had carried out a series of studies on the species responsible for the above spectra, and indeed on similar spectra generated from the γ -radiolysis of a whole range of polycrystalline and glassy n-alkyl iodides from $\text{C}_2\text{H}_5\text{I}$ to $\text{C}_8\text{H}_{17}\text{I}$.^{1,2,3} His results, summarised in Table 1, show that n- $\text{C}_2\text{H}_5\text{I}$, n- $\text{C}_4\text{H}_9\text{I}$, n- $\text{C}_6\text{H}_{13}\text{I}$ and n- $\text{C}_8\text{H}_{17}\text{I}$ all yield "wide-scan spectra" when γ -irradiated in their polycrystalline states. A great many observations were made in the course of these studies as to the identity of this family of species and as to the reasons for their formation in only certain systems. Yet, for all the suggestions put forward, there was no single, strong contender. I now believe that we have the answer to these problems, and I shall, therefore, list the observations made by Willard et al. and by ourselves, proposing suitable explanations for their occurrence in terms of the $\text{R}\cdot/\text{I}^-$ adduct. As I progress through this list, I feel sure the reader will become as convinced as I am (particularly with the experience he has gained in the last three chapters) as to the true identity of the family of species responsible for these "wide-scan

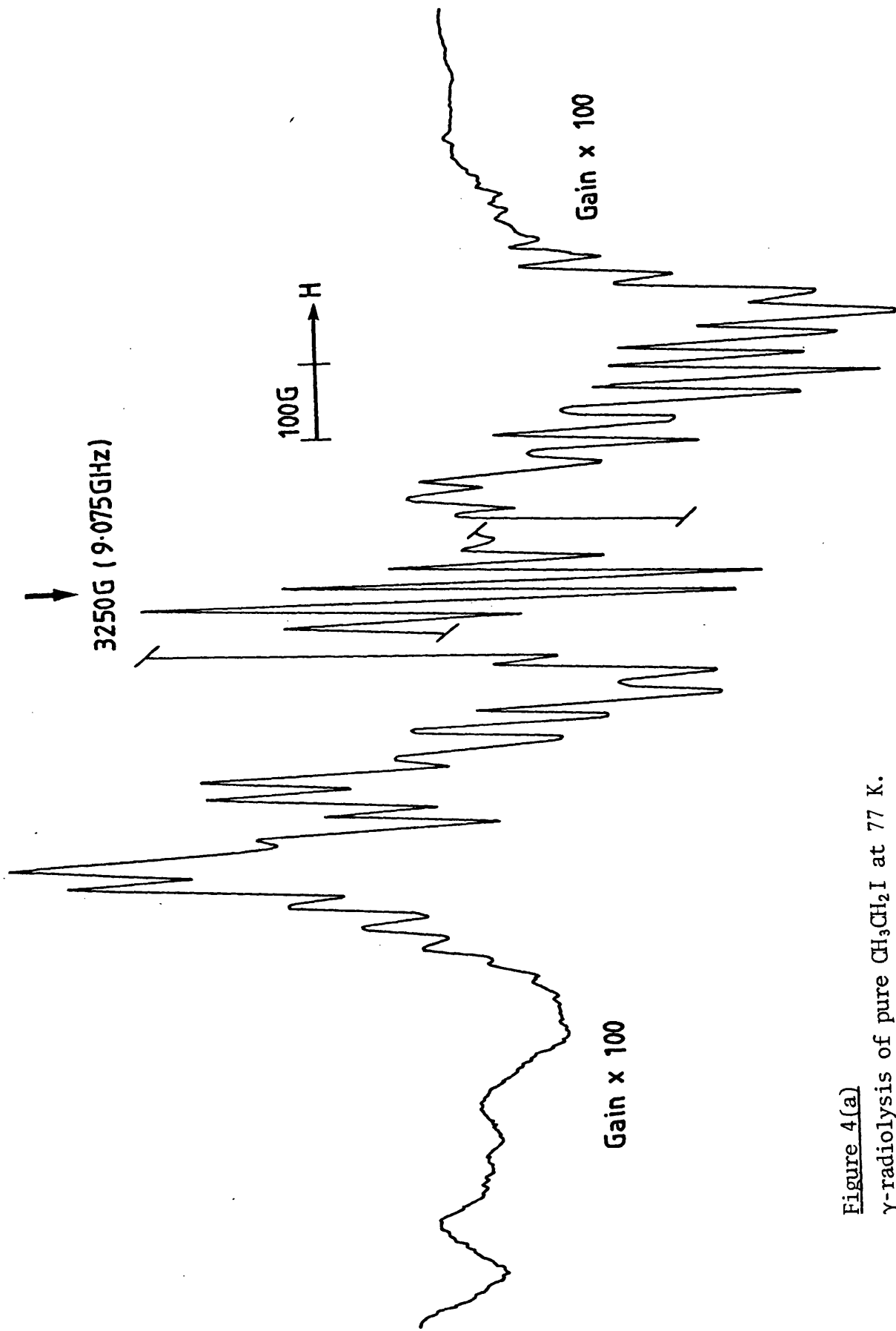


Figure 4(a)
 γ -radiolysis of pure $\text{CH}_3\text{CH}_2\text{I}$ at 77 K.

Figure 4(b)

γ -radiolysis of pure $\text{CD}_3\text{CD}_2\text{I}$ at 77 K.

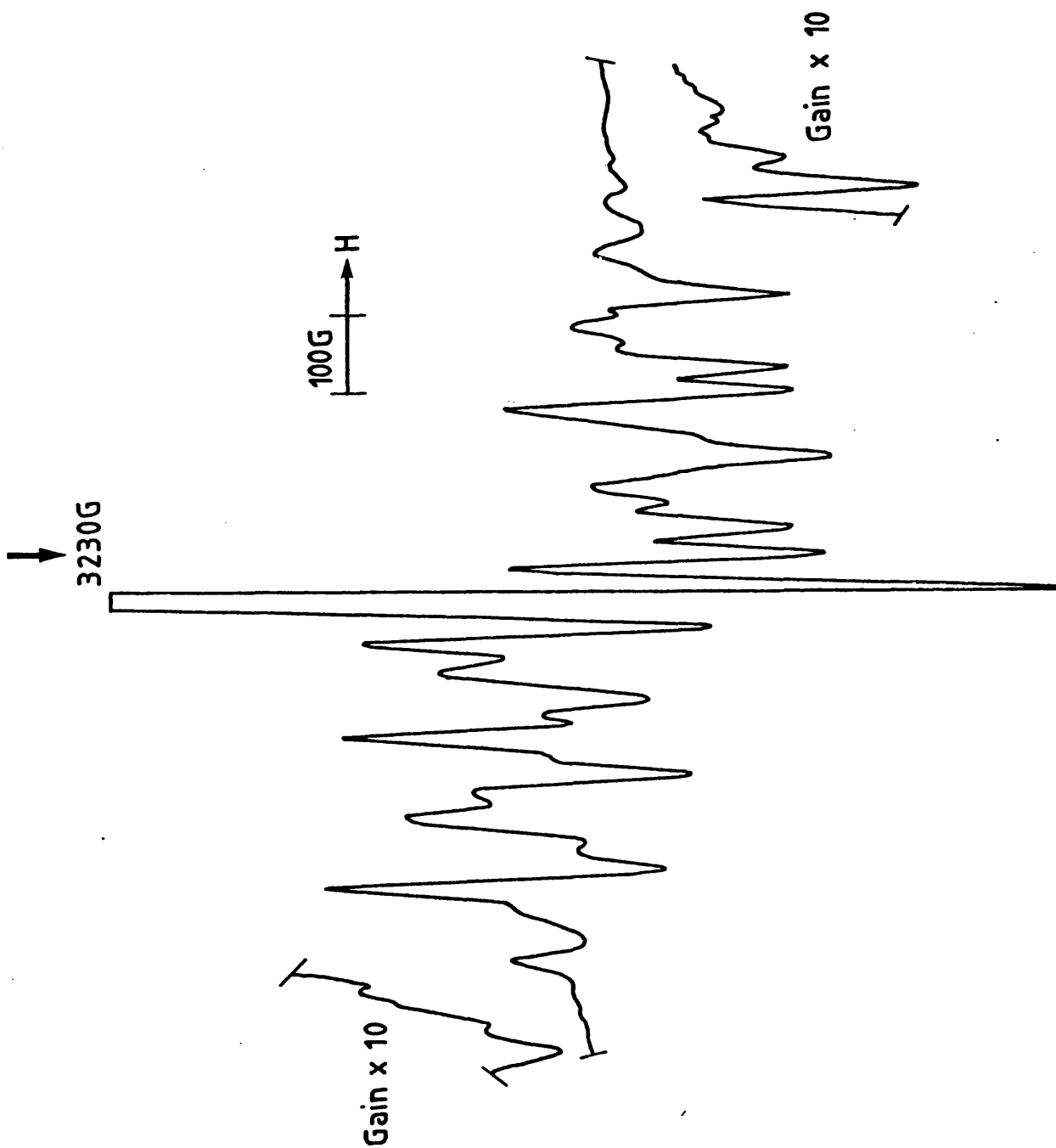


Figure 4(c)

γ -radiolysis of $\text{CH}_3\text{CH}_2\text{I}$, annealed to ca. 150 K.

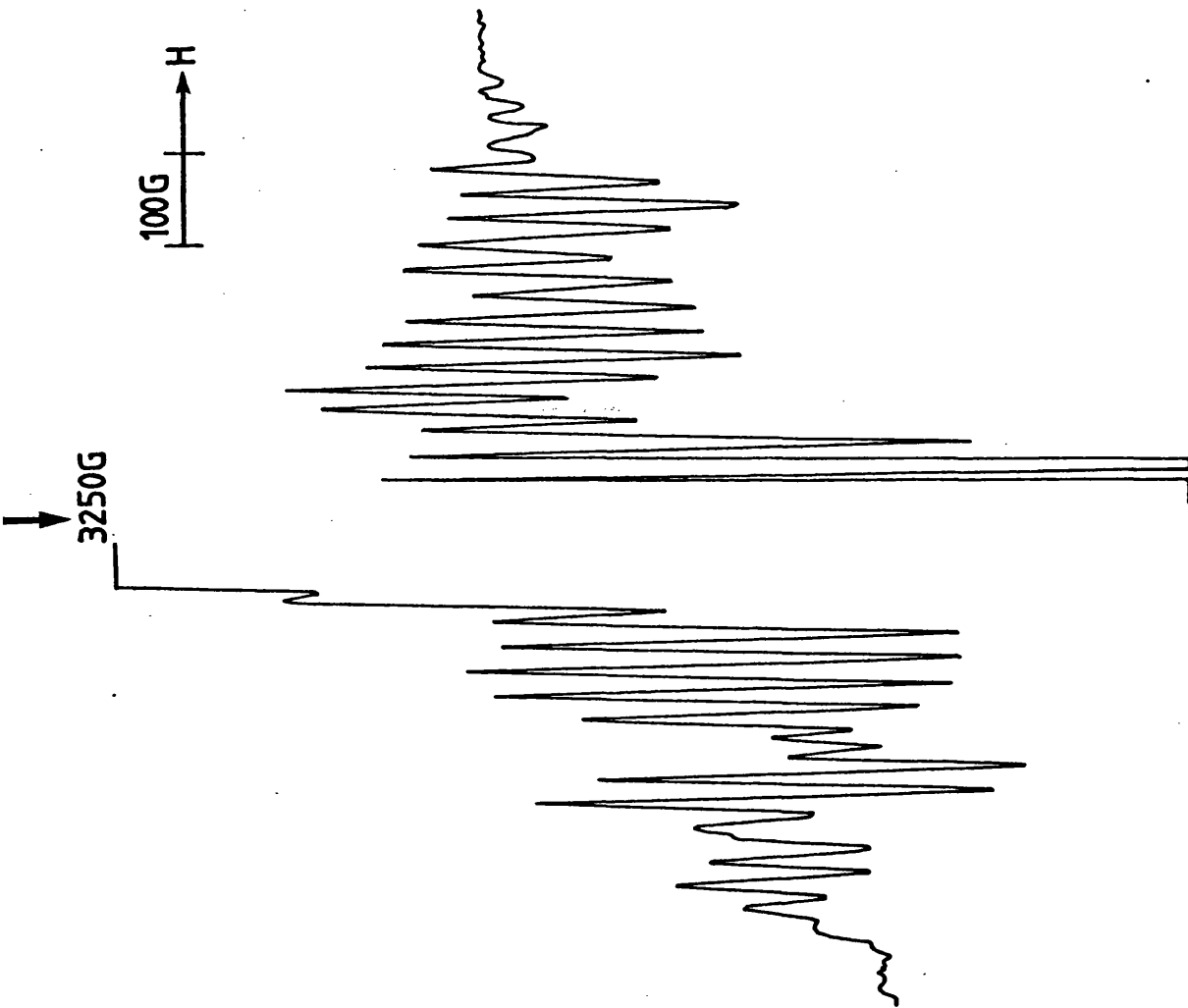


TABLE I

Comparison of E.S.R. spectra of γ -irradiated glassy and polycrystalline alkyl iodides^a

compound	state	number of lines	total spread (Gauss)	approximate intensity ratio	approximate temperature of anneal	m.p.	radical
C ₂ H ₅ I	Glass	6	160	1	100	165	C ₂ H ₅ •
i-C ₃ H ₇ I ^b	Cryst	30	1000	0.005	158	^c	?
n-C ₃ H ₇ I	Cryst	19	500	0.02	145	182	?
n-C ₃ H ₇ I	Glass	6	160	0.2	108	172	n-C ₃ H ₇ •
n-C ₄ H ₉ I	Cryst	7	160	0.2	172	172	n-C ₃ H ₇ •
n-C ₄ H ₉ I	Glass	6	160	0.5	106	170	n-C ₄ H ₉ •
n-C ₅ H ₁₁ I	Cryst	24	700	0.03	170	170	?
n-C ₅ H ₁₁ I	Glass	6	160	0.5	118	187	n-C ₅ H ₁₁ •
n-C ₅ H ₁₁ I	Cryst	6	160	0.1	187	187	n-C ₅ H ₁₁ •
n-C ₆ H ₁₃ I	Glass	6	160	0.2	123	205	n-C ₆ H ₁₃ •
n-C ₇ H ₁₅ I ^b	Cryst	15	350	0.05	205	205	?
n-C ₇ H ₁₅ I ^b	Cryst	6	160	0.2	213	225	n-C ₇ H ₁₅ •
n-C ₈ H ₁₇ I ^b	Cryst	15	350	0.05	227	227	?

^a Ref. 1.^b All attempts to obtain the glass were unsuccessful.^c Figure omitted in original table.

spectra".

Observations

(i)³ "All γ -irradiated polycrystalline n-alkyl iodides with even C numbers from C₂H₅I to C₈H₁₅I show broader, more complex e.s.r. spectra than would be produced by the alkyl radical formed by rupture of the C-I bond."

The n-alkyl iodides with an even number of C atoms produce the adduct in the polycrystalline state. Yet, in the glassy state, and in common with the n-alkyl iodides with an odd number of C atoms, the two species formed from the electron capture process (R• and I⁻) are permitted to migrate a sufficient distance away from each other as to preclude all interactions. The large iodine coupling for the adduct suggests a very small R•---I⁻ distance and hence a rigid and tightly packed lattice. The remaining lattices must be much softer if the mutual repulsion of the alkyl radical and iodide ion is permitted to predominate.

(ii)¹ The features of the large scan spectra "persist much longer at 77 K and are stable on rapid annealing almost up to the melting point".

This fits in perfectly with my vision of the "even" polycrystalline n-alkyl iodides exhibiting a much stronger and more rigid lattice structure.

(iii)¹ "On raising the temperature of the glassy samples at a rate of about 30° per hour, the spectra all disappeared at about 0.6 of the absolute melting point. The polycrystalline signals all persisted to 0.8 of the melting point and most were present until melting started."

All of the alkyl iodides seem to exhibit a much tighter crystal structure in their polycrystalline states than in their corresponding

glassy states. This is not surprising considering glasses can be considered as extremely viscous liquids and, in general, form a less dense medium than the corresponding polycrystal. Hence, even if the adduct is not formed in the polycrystalline state, the free radicals produced instead still find it very difficult to migrate through the lattice even at elevated temperatures.

(iv)¹ "The greater yield of C-I bond rupture in glassy than in polycrystalline alkyl iodides, indicated both by the e.s.r. spectra and by earlier studies on the radiolysis yields of I₂,⁴ maybe due to a greater possibility of cage escape in the glass."

Agreed.

(v)² "Momentary anneal effect: In the course of these studies, the e.s.r. spectrum of a sample of γ -irradiated polycrystalline C₂H₅I was observed at 77 K, following which the sample was placed in the Varian variable temperature device at 145-150 K for 1 minute, and then returned to 77 K for further e.s.r. examination. The treatment produced a small decay of the complex polycrystalline C₂H₅I pattern, accompanied by the appearance of a stronger central six-line, 160 G C₂H₅• radical pattern of the type observed in glassy samples. Similar behaviour for the polycrystalline i-C₃H₇I produced isoPr• radicals after minor annealing. Two features of the central six- and eight-line spectra produced by the momentary anneal of these compounds are notable. (1) There is no evidence of these signals when identical samples are slowly warmed from 77 K to the melting point. (2) The C₂H₅• radical produced in this way in polycrystalline C₂H₅I decays only slowly at temperatures up to nearly 140 K, whereas the similar signal produced by irradiation of glassy samples decays rapidly at 100 K."

This sequence of events is perfectly understandable. By giving the system just enough energy in the form of heat, the matrix allows the alkyl radical and iodide ion to mutually repel each other yet does not allow the two species to freely migrate. Hence, a decrease in adduct concentration is observed with a concomitant increase in alkyl radical concentration. The feeding of too much energy into the system not only results in the repulsion of the two species, but also in the killing of alkyl radicals via radical-radical interactions. As has been stated in (iii), radical migration through the glass is much easier than through the corresponding polycrystal.

(vi)³ "g-anisotropy does not make a major contribution to the width of the '1000 G spectrum' of polycrystalline ethyl iodide."

This conclusion is, of course, based on the fact that the Q-band spectrum of the species was virtually identical to the X-band spectrum. All solid state alkyl radical/halide ion adducts so far detected (see chapters 2, 3 and 4) have exhibited negligible g-anisotropy.

(vii)³ "The width and complexity of the spectrum (from EtI) is probably due to hyperfine splitting by iodine."

Agreed. However, even though this is true, standard, systematic techniques of interpretation still break down in that distances between features are not consistent. Even if the species responsible exhibited complete anisotropy with its orthogonal x, y and z parameters, there should be (to a first order approximation) equal distances between their respective (2I+1) features. We do not understand why this does not take place.

(viii)³ "The unpaired electrons responsible for the spectrum undergo hyperfine coupling with the β -hydrogen atoms of ethyl iodide but little

or no interaction with the α -hydrogen atoms."

This incorrect conclusion is based on the fact that the spectrum from $\text{CH}_3\text{CD}_2\text{I}$ varied very little from the original spectrum generated from $\text{CH}_3\text{CH}_2\text{I}$, whereas the spectrum from $\text{CD}_3\text{CH}_2\text{I}$ varied a great deal. The reason for this observation is that whereas the coupling to the β -hydrogen atoms is well resolved, the coupling to the α -hydrogen atoms is broad due to their greater anisotropy. Hence, greater spectral change is observed for deuteration at the β -position.

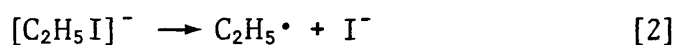
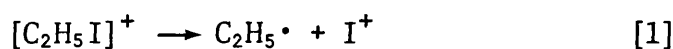
(ix)³ "The fate of the electrons in the even C number polycrystalline n-alkyl iodides must be either prompt neutralisation, formation of RI^- without dissociation, or physical trapping."

They concluded the electron had been physically trapped, and that it was able to couple with its surrounding EtI molecules, a similar conclusion having been drawn for the spectrum generated from the radiolysis of pure CD_3CN .⁵ The latter example has since been shown to be misinterpreted⁶ and is due instead to the $(\text{CD}_3\text{CN})^-$ and $[(\text{CD}_3\text{CN})_2]^-$ anions. I now strongly suggest the fate of the electron must be the formation of the RI^- anion but without complete dissociation.

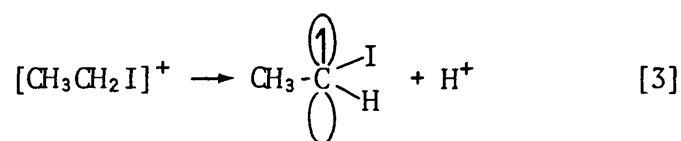
(x)³ "It is known that some alkyl halides⁷ and alkanes⁸ show systematic odd-even differences in thermodynamic properties and types of molecular packing within the crystals."

This must surely be the coup de grâce of our assignment. The variations in spectral results between the 'even' and 'odd' polycrystalline n-alkyl iodides have been explained in terms of the requirement for the two forms to adopt markedly different crystal structures. This final observation of Willard et al. has shown my prediction to be perfectly correct.

It has been suggested by Willard *et al.* that two prime contenders for the species responsible for the EtI complex polycrystalline spectrum would be either the $[\text{C}_2\text{H}_5\text{I}]^+$ electron loss species, or the $[\text{C}_2\text{H}_5\text{I}]^-$ electron gain species. This is strongly supported by the annealing results which seem to suggest the species is also the precursor of the $\text{Et}\cdot$ radical.

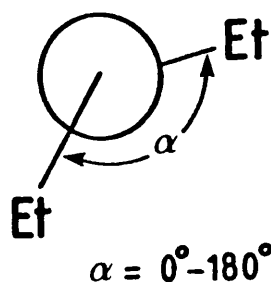
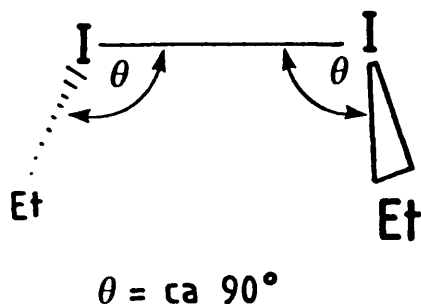


Apart from the fact that reaction [1] is most improbable, evidence from this laboratory on the γ -radiolysis of other pure polycrystalline alkyl halides has shown that these electron loss species either break down to give an α -halo radical⁹ (reaction [3]) or react with another molecule to form a dimer cation¹⁰ (reaction [4]).



If the α -iodo radical is present, it would, unfortunately, be completely obscured by the complex spectrum. However, analysis of the spectra generated over a wider scan demonstrates the most definite presence of a diiodo species exhibiting a maximum iodine hyperfine coupling of ca. 400 G. The structure of this diiodo species is such that the degeneracy of the iodine 'p' orbitals must be lifted, or else the orbital angular momentum would make such a contribution to the g-values of the species, as to probably make its e.s.r. spectrum too broad to detect. This degeneracy can be removed by the presence of two alkyl groups as in I.

I



Thus, it seems we probably have the $(\text{EtI})_2^+$ cation. This being the case, the only possible contender for the complex spectrum is the electron gain species. The addition of an electron scavenger, such as CBr_4 , showed a definite decrease in the intensity of the complex spectrum, while not affecting the concentration of the $(\text{EtI})_2^+$ dimer cation.

According to the theories of this group (see chapter 6), the electron gain species of alkyl halides should break down to give first the $\text{R}\cdot/\text{hal}^-$ adduct and then the free radical and unassociated halide ion, i.e. the $\text{Et}\cdot/\text{I}^-$ adduct should decay on annealing to give the $\text{Et}\cdot$ radical. This is, indeed, what happens.

There are two main arguments against my adduct assignment. First, as already discussed, the spectrum cannot be interpreted in terms of the $\text{Et}\cdot/\text{I}^-$ adduct even though we know the form of the spectra of other solid state iodo adducts. Second, knowledge of the adduct has shown that there is very little isotropic coupling to the halide ion (this probably arises from a spin polarisation mechanism - see the latter half of this chapter) hence, the halogen A_{\parallel} value for the adduct is virtually the same as the $2B$ value

$$A_{\parallel} = A_{\text{iso}} + 2B. \text{ if } A_{\text{iso}} \text{ is small. } A_{\parallel} \approx 2B.$$

Therefore, for the particular case of the EtI polycrystalline spectrum, we can predict a 2B value of ca. 175 G which gives a 38% 'p' orbital population on the iodide ion. Not only is this rather large for a charge transfer mechanism, but there should also be a concomitant percentage decrease in the A(¹H) hyperfine coupling for the hydrogen atoms of the Et• radical. The values are in the order of 22-24 G, a maximum percentage drop of 8%.

We therefore either have a larger A_{iso} than anticipated (clearly undesirable as this means a larger 's' character and hence implies "real" bonding as opposed to charge transfer) which reduces the value of the 2B term. Or, we have some indirect mechanism such as dipolar coupling or spin polarisation (as was invoked in chapter 4 for the Me•/I⁻ adduct in the CD CN matrix), increasing the anisotropic iodine coupling and hence contributing appreciably to A_∥.

$$A_{\parallel} = A_{iso} + 2B + \text{spin polarisation} + \text{dipolar coupling}$$

This would, of course, result in a smaller, more realistic 2B value.

Although the above possible explanations are by no means waterproof, I feel the weight of evidence in favour of the Et•/I⁻ adduct assignment is so strong that it must surely be correct.

THE ADDUCT

Chloro- and bromo- adducts

The chloro- and bromo- adducts have, in all matrices, conformed to a high degree with our model of 'the adduct' and I shall discuss these examples first. The iodo-analogues, conversely, with their large A// hyperfine couplings and their complicated spectra have, in general, chosen to be less accommodating. These will, therefore, be discussed separately.

(i) Spin polarisation of 's' orbital on the halide ion

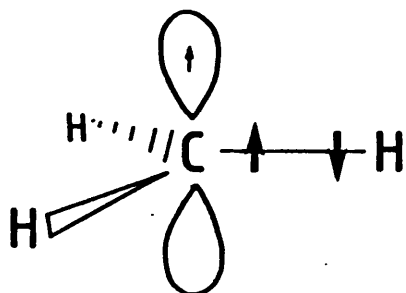
The Me•/Cl⁻ and Me•/Br⁻ adducts in the CD₃CN matrix have provided the best examples of solid state spectra in our studies. I shall use their parameters in the following discussion.¹¹

We have envisaged the adduct to be simply the presence of two species, the alkyl radical and the halide ion, in the same matrix cavity with their interaction arising from a charge transfer from the halide 'p' orbital into the 'p_z' orbital of the carbon atom at the radical site (see Fig. 7).

It is well known that an atom with an electron in a pure 'p' orbital can still exhibit a small isotropic coupling via the phenomenon of spin polarisation. For example, for the planar Me• radical, the odd electron is in a pure 'p' orbital yet there exists a ¹³C isotropic coupling of +38.5 G and a ¹H isotropic coupling of -23 G, ca. 4% 's' orbital populations in both cases. This is caused by a partial 'lining-up' of one of the electrons in the C-H bond with the electron in the 'p' orbital (Fig. 5).

In single atoms (e.g. N, O, F)¹² this effect is still observed, only

Figure 5



to a much lesser degree, such that if a single electron is in a pure 'p' orbital on an atom, the isotropic coupling for the atom will show a ca. 0.2% population of the 's' orbital.

Therefore, what isotropic (^{81}Br) hyperfine coupling do we predict for the $\text{Me}\cdot/\text{Br}^-$ adduct where we have a 11.5% 'p' orbital population?

$$\% \text{ 's' orbital population} = \frac{11.5 \times 0.2}{100} \quad A^\circ ({}^{81}\text{Br}) = 12,346 \text{ G}^{13}$$

$$\therefore ({}^{81}\text{Br}) \text{ isotropic coupling} = \frac{12,346 \times 11.5 \times 0.2}{100 \times 100} = \underline{2.84 \text{ G}}$$

Carrying out the same calculation for the $\text{Me}\cdot/\text{Cl}^-$ adduct;

$$A^\circ ({}^{35}\text{Cl}) = 2044 \text{ G}^{13} \quad \text{'p' orbital population} = 6.9\%$$

predicts (^{35}Cl) isotropic coupling of 0.28 G.

Although the $\text{Me}\cdot/\text{Br}^-$ and $\text{Me}\cdot/\text{Cl}^-$ adducts do not rotate and hence yield their respective isotropic halide couplings, the $\text{Bu}^t\cdot/\text{Br}^-$ and $\text{Bu}^t\cdot/\text{Cl}^-$ adducts in the adamantane- d_{16} and TMS matrices do.¹¹ They exhibit an $A_{\text{iso}}({}^{81}\text{Br})$ of 6.7 G and an $A_{\text{iso}}({}^{35}\text{Cl})$ of <1 G. In excellent agreement with the predicted parameters for their respective methyl adducts.

(ii) Dipolar coupling

This coupling arises from the interaction of two dipoles (dipolar) the extent of which is dependent upon the distance between them. The

two dipoles in this particular instance are the electron in the 'p_z' orbital on the carbon atom and the halide nucleus. Using a point charge approximation, and knowing the distance between the electron and the nucleus, we can predict their coupling.

For example, the C-Br bond length in the MeBr molecule is ca. 1.93 Å, so let us assume the shortest possible C --- Br⁻ distance is ca. 1.95 Å. [I agree that this is an impossibly close distance (Fig. 6) as this value is the Van der Waals radius of the bromide ion but, nevertheless, it will serve for our arguments.]

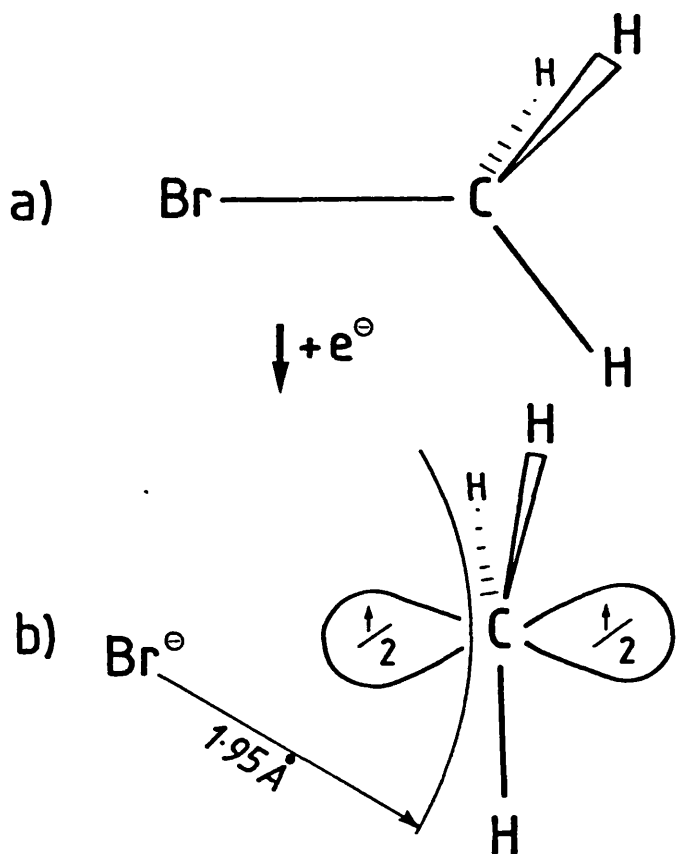


Figure 6: showing the C-Br distance in (a) the MeBr molecule, (b) the Me•/Br⁻ adduct.

It must be stressed that (b) is not a true representation of the adduct. The C-Br distance is much too short.

The point charge model says the electron spends all its time at the position of the carbon atom. This is, of course, not correct, however, it is a valid approximation for our calculation.

$$A_{//} = \frac{2 \mu_N \langle r^{-3} \rangle}{I} \left(\frac{\mu_0}{4\pi} \right)^{14}$$

μ_N = nuclear magnetic moment
 r = point charge distance
 I = nuclear spin

$$(\mu_0/4\pi) = \text{permeability of free space} \\ = 10^{-7} \text{ J.s}^2. \text{ C}^{-2} \text{ m}^{-1}$$

$$\mu_N(^{81}\text{Br}) = 2.26 \text{ nuclear magnetons (conversion factor } \rightarrow \text{J. T}^{-1} \\ = 5.05 \times 10^{-27})$$

$$I(^{81}\text{Br}) = \frac{3}{2}$$

$$r = 1.95 \text{ \AA} = 1.95 \times 10^{-10} \text{ m.}$$

$$\therefore A_{//} = \frac{2 \times 2.26 \times 5.05 \times 10^{-27} \times 10^{-7}}{1.5} \times (1.95 \times 10^{-10})^{-3} \\ = 2.05 \times 10^{-4} \text{ Tesla} \\ = \underline{2.05 \text{ G.}}$$

Hence, for an impossibly short C -- Br distance in the Me•/Br⁻ adduct, a dipolar coupling value of 2.05 G is predicted to contribute to the A_{//}(⁸¹Br) coupling. For a more realistic C --- Br distance of 2.8 Å, a dipolar coupling of 0.7 G is predicted. The unequivocal conclusion, therefore, is that any dipolar coupling to the bromine ion will be insignificant in the Me•/Br⁻ adduct.

Similar calculations for the Me•/Cl⁻ adduct predicts an A_{//}(³⁵Cl) of 0.95 G at a C-Cl distance of 1.8 Å (the Van der Waals radius of the chloride ion) and an A_{//}(³⁵Cl) of 0.3 G at a realistic C-Cl distance of 2.6 Å. Once again, insignificant contributions.

In conclusion, the R•/Cl⁻ and R•/Br⁻ adducts have been correctly envisaged as an alkyl radical and a halide ion being held close together by the constraints of a matrix, and the interaction between them being basically a charge transfer process. The amount of charge transfer (ca. 6 → 12%) is dependent upon the R• --- hal⁻ distance. The isotropic halide coupling is almost certainly due to spin polarisation of the

electrons in the halides 's' orbital and does not reflect true 's' character. Hence, there is no formal bonding between the two species (see Fig. 7). Calculations on the likely contribution to the anisotropic halide coupling via the mechanism of dipolar interaction has demonstrated its relatively insignificant effect.

Iodo-adducts

The rotating, Type B, $R\cdot/I^-$ adducts in the adamantane- d_{16} matrix¹⁵ can be compared quite favourably with the chloro- and bromo- adducts just discussed. However, there appear to be certain anomalies when considering the parameters for the solid state iodo-adducts (Table 2). Not only should the percentage decrease of the proton couplings be equivalent to the percentage 'p' orbital population on iodine (this inequivalence first pointed out in chapter 4), but there should not be more than a 15-20% spin transfer taking place even on consideration of the high electronegativity of the iodide ion. The isotropic iodine coupling is still small (the $Bu^t\cdot/I^-$, $CH_3\cdot/I^-$ and $CD_3\cdot/I^-$ adducts all enable A_{\parallel} to be extracted and hence A_{iso} to be calculated), yet, for some reason the parallel coupling is not a true reflection of the 'p' orbital population as has been the case for the chloro- and bromo-analogues. There appears to be a considerable anisotropic contribution to the iodide ion parameters, the only contender for which seemed to be the dipolar interaction just described. However, assuming the C-I distance in these adducts to be 2.10 \AA (again, very small) still only predicts an added parallel coupling of ca. 1.25 G.

We admit we do not understand the discrepancies unveiled for these alkyl radical/iodide ion adducts. The fact that the $Me\cdot/X^-$ adducts ($X = Cl, Br, I$) in the CD_3CN matrix all have to occupy the same size

site, as do the $\text{Bu}^{\text{t}\cdot}/\text{X}^-$ adducts ($\text{X} = \text{Cl}, \text{Br}, \text{I}$) in the adamantane matrix, proves there has to be greater $\text{R}\cdot$ and X^- interaction as the size of halide ion increases. I suggest this greater interaction results in the larger anisotropic iodine parameters observed, however, I cannot explain the mechanism by which they occur.

TABLE 2

Data for R•/I⁻ adducts

adduct	matrix	¹²⁷ I couplings (Gauss) // ⊥	% 'p' orbital population ^a	A(¹ H) for R•/I ⁻ (Gauss)	% drop in A(¹ H) from free radical R•
Bu•/I ⁻	ada-d ₁₆	99 -47	22%	22.5	ca. 1.0%
isoBu•/I ⁻	ada-d ₁₆	ca. 86 -	19%	ca. 21 (αH) ca. 30 (βH)	ca. 10% (max)
isoPr•/I ⁻	ada-d ₁₆	60 -	13%	- (αH) ca. 24 (βH)	ca. 3%
isoPr•/I ⁻	isoPrI	ca. 60 -	13%	ca. 25(α + β)H	-
CH ₃ •/I ⁻	CD ₃ CN	108 -60	24%	20.6	10.5%
CD ₃ •/I ⁻	CD ₃ I	80 -39	17%	-	-
C ₂ H ₅ •/I ⁻	C ₂ H ₅ I	ca. 170 -	37%	-	-
C ₄ H ₉ •/I ⁻	C ₄ H ₉ I	ca. 110 -	24%	-	-
C ₆ H ₁₃ •/I ⁻	C ₆ H ₁₃ I	ca. 40 -	9%	-	-
C ₈ H ₁₇ •/I ⁻	C ₈ H ₁₇ I	ca. 40 -	9%	-	-

^a 2B° value for ¹²⁷I = 453 G (ref. 12)

REFERENCES

1. H. W. Fenrick, S. V. Filseth, A. L. Hanson, J. E. Willard, J.A.C.S., 85, 3731, (1963).
2. H. W. Fenrick, J. E. Willard, J.A.C.S., 88, 412, (1966).
3. R. J. Eglund, P. J. Ogren, J. E. Willard, J. Phys. Chem., 75, 467, (1971).
4. E. O. Hornig, J. E. Willard, J.A.C.S., 79, 2429, (1957);
R. H. Luebbe, J. E. Willard, J.A.C.S., 81, 761, (1959).
5. M. A. Bonin, K. Tsuji, F. Williams, Nature, 218, 946, (1968);
M. A. Bonin, K. Takeda, K. Tsuji, F. Williams, Chem. Phys. Letters, 2, 363, (1968);
M. A. Bonin, K. Takeda, F. Williams, J. Chem. Phys., 50, 5423, (1969).
6. R. J. Eglund, M. C. R. Symons, J. Chem. Soc. A, 1326, (1970).
7. T. Malkin, J. Chem. Soc., 1976, (1931);
T. Malkin, Trans. Far. Soc., 29, 977, (1933);
J. D. Meyer, E. E. Reid, J.A.C.S., 55, 1574, (1933);
R. W. Crowe, C. P. Smyth, J. Phys. Chem., 72, 1098, (1950);
A. Müller, Proc. Roy. Soc., 124, 317, (1929).
8. M. G. Broadhurst, J. Res. Nat. Bur. Stand. Sect. A, 66, 241, (1962);
P. J. Ogren, Ph.D. Thesis, University of Wisconsin (1968).
9. S. P. Mishra, G. W. Neilson, M. C. R. Symons, J.C.S. Faraday II, 70, 1165, (1974).
10. S. P. Mishra, M. C. R. Symons, J.C.S. Perkin II, 1492, (1975).
11. This thesis, chapter 4.
12. M. C. R. Symons "Chemical and Biochemical Aspects of Electron Spin Resonance Spectroscopy", Van Nostrand Reinhold Company Ltd., 1979.
13. J. R. Morton, K. F. Preston, J. Magnetic Resonance, 30, 577, (1978).
14. B. A. Goodman, J. B. Raynor, Advances in Inorg. Chem., 13, 136, (1970).
15. This thesis, Chapter 3.

CHAPTER 6

Formation of σ^* anions

INTRODUCTION

Electron addition into the C-X bond of an organic halide RX (X = Cl, Br, I) can result not only in the formation of an $R\cdot/X^-$ adduct (e.g. when R is an alkyl group), but also in the formation of a $(R-\overset{\cdot}{X})^- \sigma^*$ anion^{1,2,3,4,5} (e.g. when R is the F_3C- group⁵) where the electron is in the σ^* orbital of the C-X bond. As yet, σ^* anions have not been detected from molecules giving adducts, neither have adducts been detected from the breakdown of any σ^* anion. It therefore appears that electron addition can either result in the formation of an adduct or in the formation of a σ^* anion; but not both.

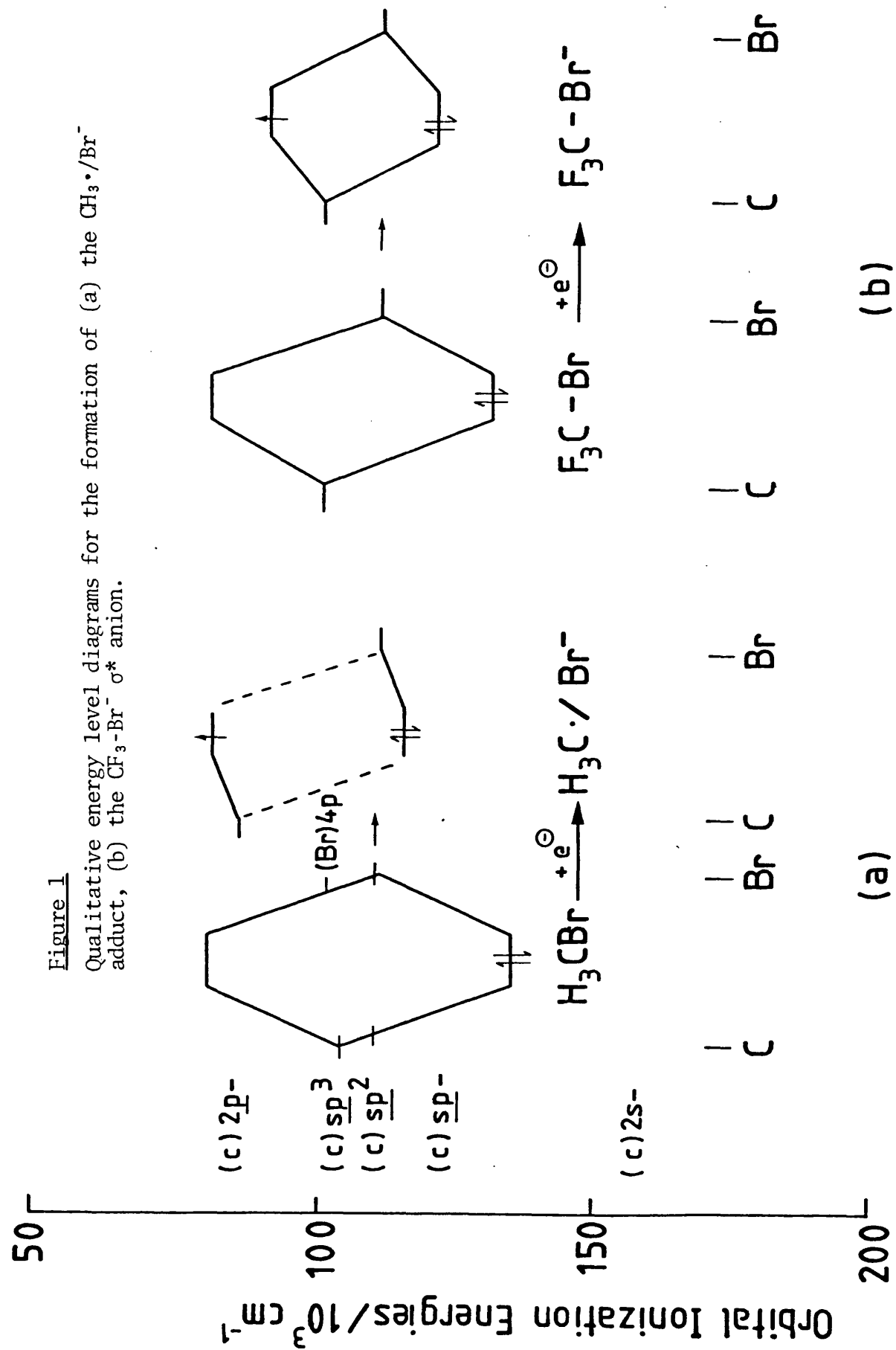
In order to explain the existence of two pathways for the same electron addition process, Symons has proposed that the formation of the adduct is dependent upon whether the carbon atom involved will change its configuration appreciably on the stretching of its C-X bond. If a change is likely to take place, then it is the adduct that is formed, e.g. the $Me\cdot/Br^-$ adduct is generated when, after electron addition into the C-Br σ^* orbital, the C-Br bond stretches and allows the H_3C- group to marginally flatten. This results in an increase in p_z character at carbon, which further weakens the C-Br bond, and hence allows the H_3C- group to become increasingly more planar. This process continues until the H_3C- group is planar and the C-Br bond is effectively broken.⁶

Although electron addition into the C-Br σ^* orbital in F_3CBr does stretch the C-Br bond, there is no real tendency for the F_3C group to flatten. Hence, there is no self perpetuating process and the species remains a σ^* anion.⁶ These two processes can be illustrated by the qualitative energy level diagrams in Figs. 1a and 1b.

Although the CF_3X^- anion does break down to give $CF_3\cdot$ radicals and

Figure 1

Qualitative energy level diagrams for the formation of (a) the $\text{CH}_3\cdot/\text{Br}^-$ adduct, (b) the $\text{CF}_3\text{-Br}^- \sigma^*$ anion.



X^- ions,⁵ no interaction between the two independent species has ever been detected (i.e. an adduct) presumably because the distance between them is too large. It has therefore been envisaged by Symons that there is a minimum in the potential energy curve such that if the $\dot{C}F_3$ radical and X^- ion were close enough to each other to permit such interaction (e.g. distance R^2 in Fig. 2) then they would be pulled into this potential well and reform the σ^* anion.⁷ This can be represented diagrammatically by the potential energy curves in Fig. 2.

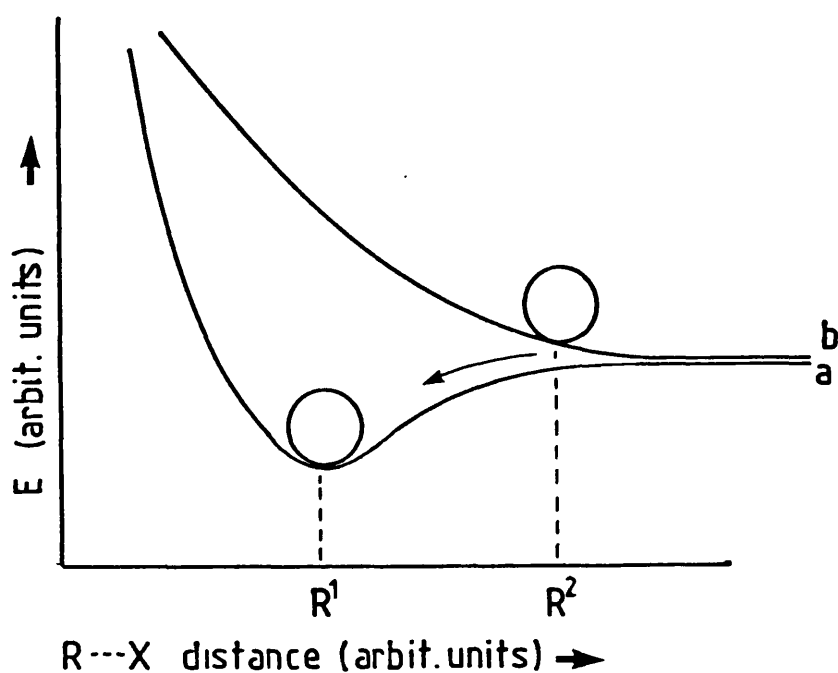


Figure 2

The potential energy curves for a the σ^* anion with a potential well at $R\text{---}X$ distance R^1 ; b the adduct with the solvent cage dictating the $R\text{---}X$ distance R^2 .

To prove the existence of this potential energy well for the CF_3X^- σ^* anion, it would be necessary to generate the $\dot{C}F_3$ radical and X^- ion independently, and let the two species approach each other. If Symons

is correct, the σ^* anion should be formed. Although the pathway of this particular thesis did not allow the execution of these experiments, I feel sure this laboratory will test this hypothesis at some time in the future.

Table 1 compiles the data on a number of σ^* anions.

Bonding in the σ^* anions

Symons had found⁸ that by plotting graphically the percentage 'p' character vs the percentage 's' character for the range of σ^* anions known, using the A° and $2B^\circ$ values of Atkins and Symons,⁹ three most definite straight lines could be drawn (see Fig. 3). One is through all the iodo- σ^* anions (a), one is through all the bromo- σ^* anions (b), and one is through all the chloro- σ^* anions (c). Morton and Preston¹⁰ have since modified the A° values for a whole range of atoms, including ^{35}Cl , ^{37}Cl , ^{79}Br , ^{81}Br , and ^{127}I , which, when combined with the $2B^\circ$ values of Atkins and Symons, has produced a modification in the position of all the points on lines a, b and c. The result is the observation that all these points now lie on a completely new straight line, d, showing quite clearly the consistency of bonding for these species. Hence, for a 100% 'p' orbital population on the halide, a percentage 's' orbital population of ca. 6% is predicted, proving the existence of a weak, but nevertheless, real bond. This conformity in bonding may also prove to be of diagnostic importance when attempting to interpret spectra. If the parameters exhibited by an unknown halo-species reflect similar 'p' orbital and 's' orbital populations, then it is possible the species could, in fact, be a σ^* halo anion.

The 6% 's' character is, of course, in marked contrast to the results for the adducts where, for a 100% 'p' orbital population, only an 's' character of ca. 0.4% is achieved. This is due solely to the spin

Figure 3

Comparing % s and % p character in a range of iodo-, bromo-, chloro- σ^* anions.

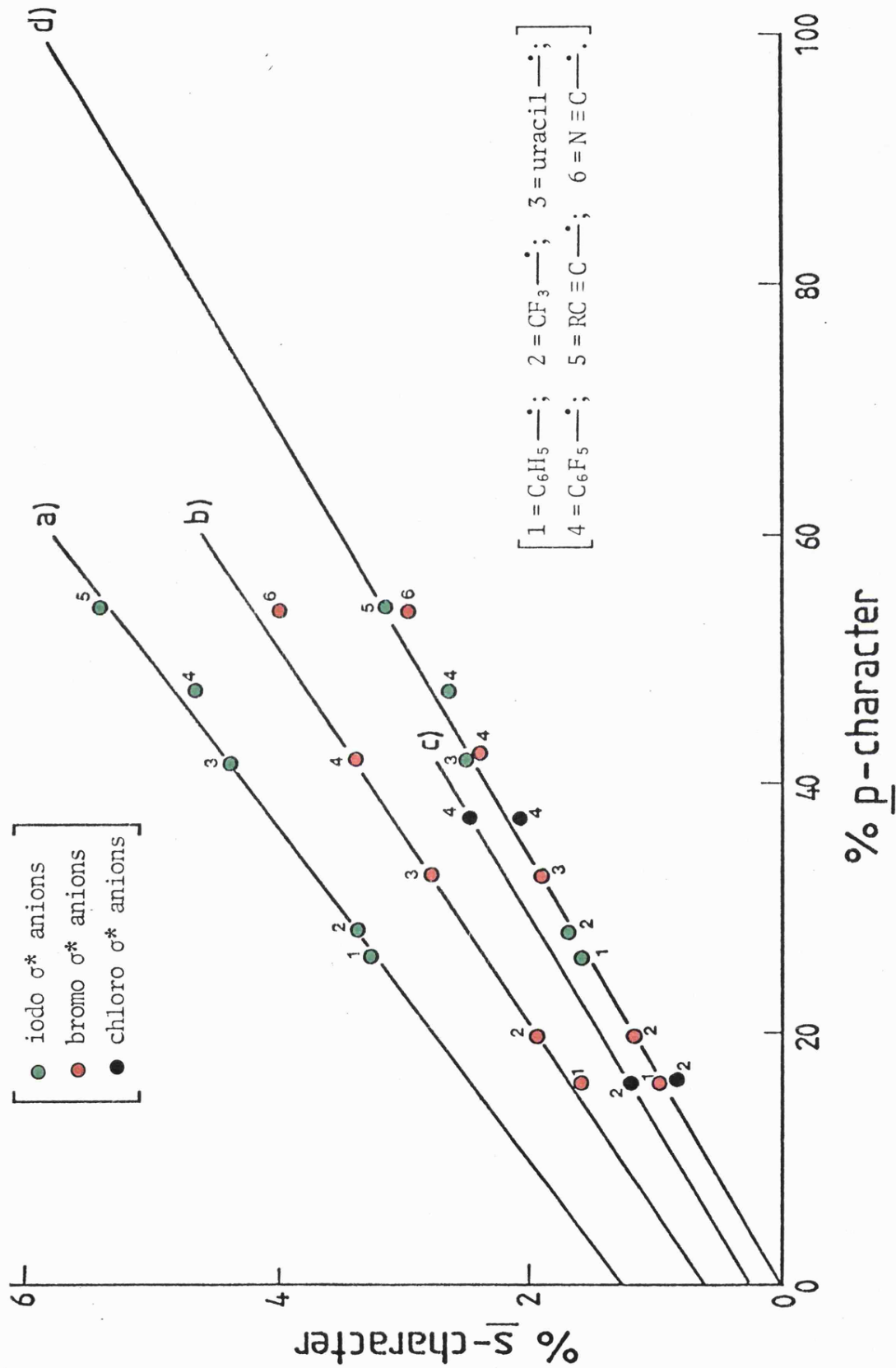


TABLE 1

E.s.r. parameters and spin densities of various bromo- and iodo- σ^* -radicals

Radical	Hyperfine tensor components in G		g-tensor		Orbital population on hal			
	A_{\parallel}	A_{\perp}	g_{\parallel}	g_{\perp}	a_p^2 (%)	f	g	
$F_3C-\overset{\cdot}{C}-Br^{-a}$	1Br	263.6	114.2	2.0036	2.0212	20	1.9	1.5
BrU^{-b}	1Br	373	143	1.997	2.030	32	2.7	1.8
$N \equiv C-\overset{\cdot}{C}-Br^{-c}$	1Br	587	180	2.00	2.07	54	3.7	2.5
$F_3C-\overset{\cdot}{C}-I^{-a}$	^{127}I	373.1	178.8	2.0002	2.0483	28.5	3.3	1.6
IU^{-d}	^{127}I	505	220	1.991	2.044	42	4.3	2.1
$PhC \equiv C-\overset{\cdot}{C}-I^{-e}$	^{127}I	639	263	1.98	2.09	55	5.3	2.6

^a Ref. 5; ^b BrU = 5-bromouracil; ^c Ref. 3; ^d IU = 5-iodouracil; ^e Ref. 4;^f Using A° values of Refs. 9 and 15; ^g Using A° values of Ref. 10.

polarisation of the electrons in the halide ions 's' orbital and is not due to any real 's' character in the C-X 'bond'.¹¹

Consistency of bonding in σ^* anions

All of the species represented in Fig. 3 are very similar in that on electron addition into the C-X bond, no appreciable change in configuration has taken place and the R-group has remained effectively rigid. Neither would there be any appreciable change in configuration on complete dissociation into $R\cdot$ and X^- . It therefore occurred to us - what would happen if the R- group were less rigid and only changed its configuration marginally on electron addition? Would the species formed become less " σ^* anion-like" and approach the appearance of an adduct?

This possibility can be represented diagrammatically by the P.E. curves in Fig. 4a where the potential well gets smaller and the C-X bond longer. This also results in an increase in percentage 'p' character of the bond (decrease in percentage 's' character) and therefore means a change in the ratio of 'p':'s'. Hence, the anion formed would not necessarily lie on line d in Fig. 3, but rather the points from the respective iodo, bromo and chloro anions would lie on a straight line intermediate of the two extremes (see Fig. 4b).

It was therefore decided to look at a further series of organic halides where the R group, on electron addition, would not retain its 'rigidity', yet neither would it change its configuration to such an extent as to allow the formation of an adduct (see Fig. 5). CCl_3X ($X = F, Cl, Br$) were the compounds duly studied in the hope that the species formed would comply with the story so far related.

It was appreciated that a further organic halide of interest to us

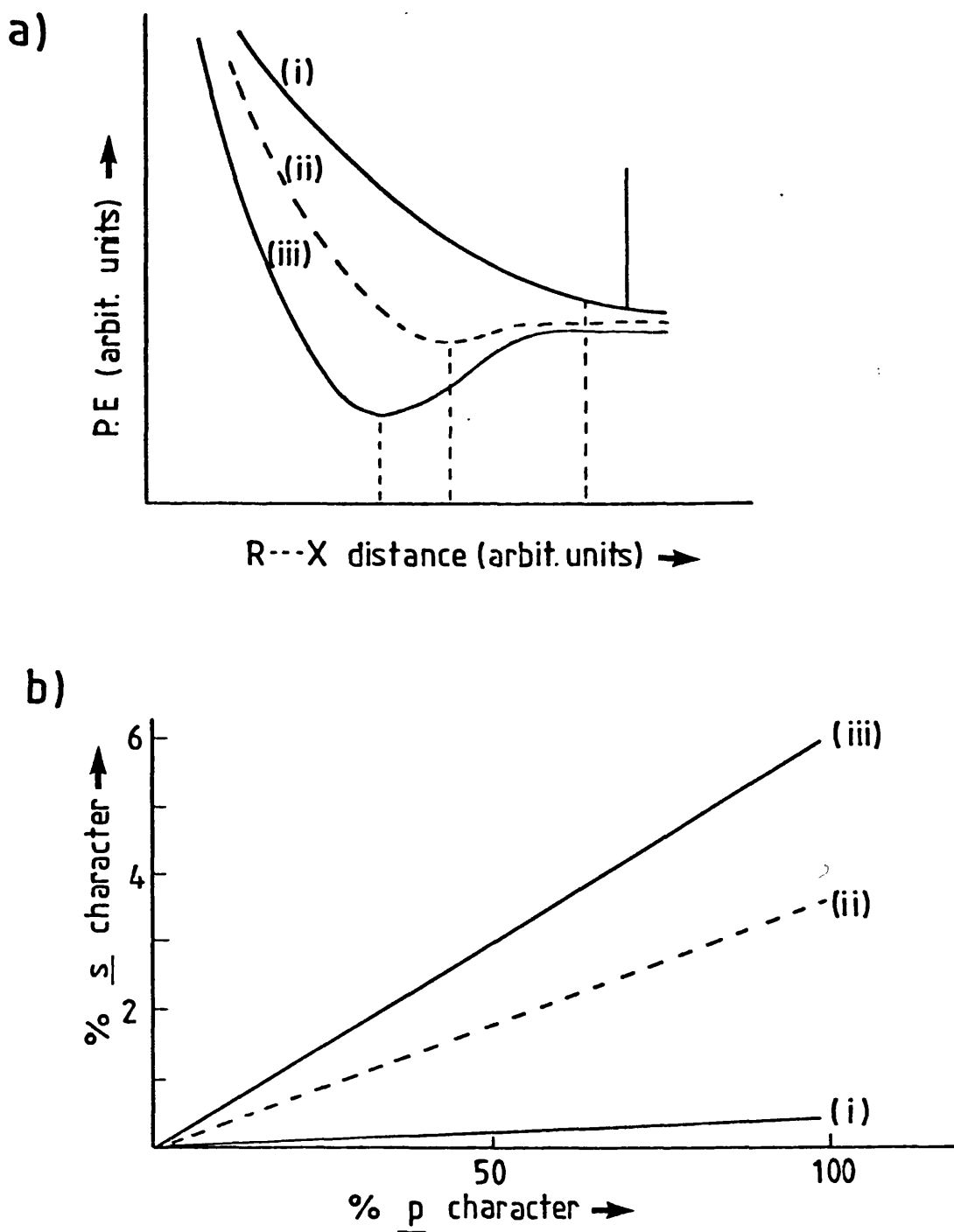


Figure 4

Showing (a) the P.E. curves, (b) the % p-character vs % s-character graph for: (i) the adduct, (ii) an intermediate [?], (iii) the σ^* anion.

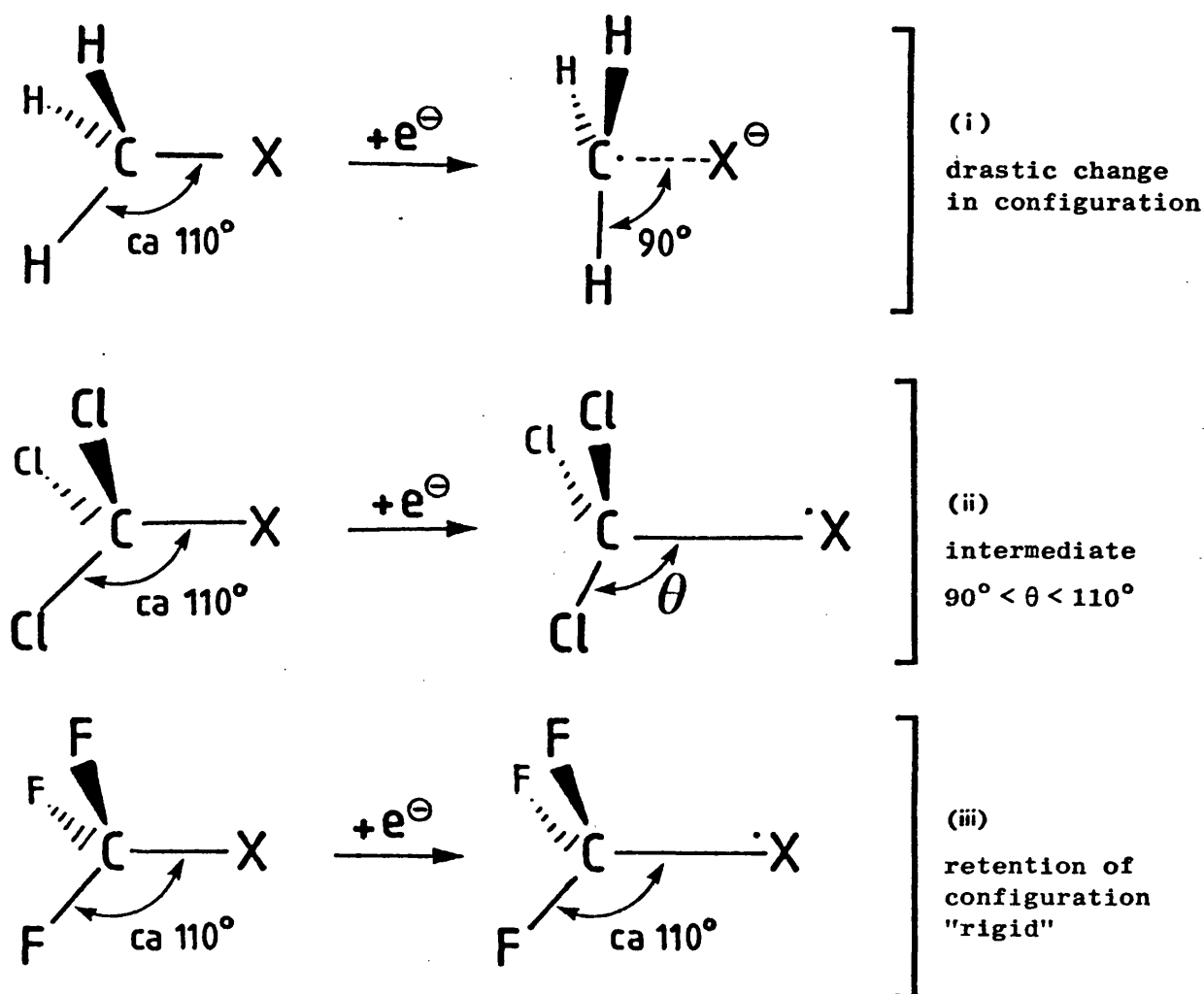
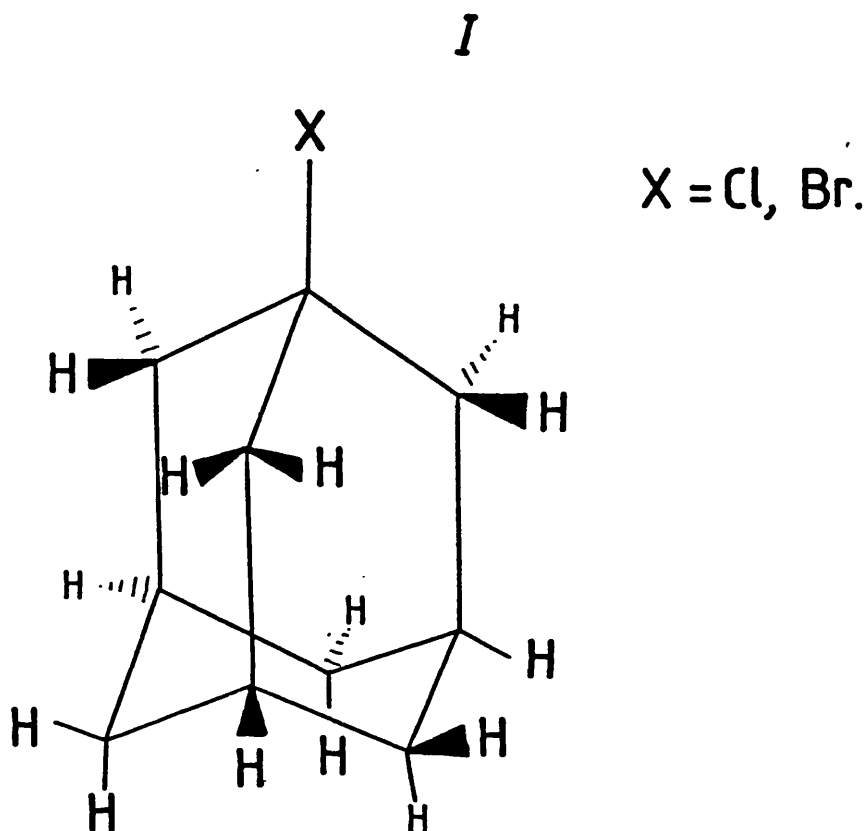


Figure 5

Showing the changes in configuration on electron addition when forming (i) the adduct, (ii) an intermediate, (iii) a σ^* anion.

is the 1-haloadamantane, I. In this particular example it is impossible for the carbon atom to become planar, as it would normally wish to do on electron addition, due to the constraints of the molecular frame.

Hence, a true σ^* anion should be formed with parameters similar to those listed in Table 1. 1-chloroadamantane and 1-bromoadamantane were the molecules studied.



EXPERIMENTAL

Preparation of 1-bromoadamantane-d₁₅¹²

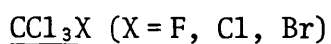
Adamantane-d₁₆ (0.3 g) was stirred at room temperature for ca. 2 hrs in bromine (3 cm³). The reaction mixture was then shaken with 100 cm³ of carbon tetrachloride and 300 cm³ of an iced, aqueous solution of sodium thiosulphate in a separating funnel. The organic layer was retained while the aqueous layer was washed twice with 50 cm³ portions of carbon tetrachloride. The three organic extracts were then combined and dried over anhydrous calcium chloride. The solvent was removed by distillation and the residue recrystallised from methanol. Colourless

crystals of 1-bromoadamantane-d₁₅ (C₁₀D₁₅Br) (m.p. 112°C) were recovered.

1-bromoadamantane-h₁₅ (Koch-Light) was recrystallised from methanol prior to any experimentation. 1-chloroadamantane (Fluka-AG), carbon tetrachloride (B.D.H.), trichlorobromomethane (Aldrich), trichlorofluoromethane (Stohler), adamantane-d₁₆ (Merck, Sharp & Dohme), tetramethylsilane (B.D.H.) and methanol-d₄ (B.D.H.) were all used as supplied.

Samples of the pure 1-haloadamantanes were pressed into hard pellets whilst the remaining solutions were placed into quartz tubes and degassed via the freeze-thaw method.

Radiolysis and recording of spectra were carried out as described in chapter 2.



RESULTS AND DISCUSSION

(i) CCl₃Br

A range of matrices were used in an attempt to isolate the electron gain species of this molecule. Unfortunately, the only products appeared to be the $\dot{\text{C}}\text{Cl}_3$ and $\dot{\text{C}}\text{Cl}_2\text{Br}$ radicals. The parameters for these species in perfect agreement with the expected parameters for a slightly pyramidal structure, II and III. Fig. 6a and 6b show the spectra generated from a 5 Mol % solution of Cl₃CBr in CD₃OD after γ -radiolysis at 77 K.

The $\dot{\text{C}}\text{Cl}_3$ radical has been fully investigated.¹³ For precisely the same structure, an ⁸¹Br parallel coupling of ca. 98 G is predicted for the $\dot{\text{C}}\text{Cl}_2\text{Br}$ radical. Our value of 120 G is in excellent agreement and

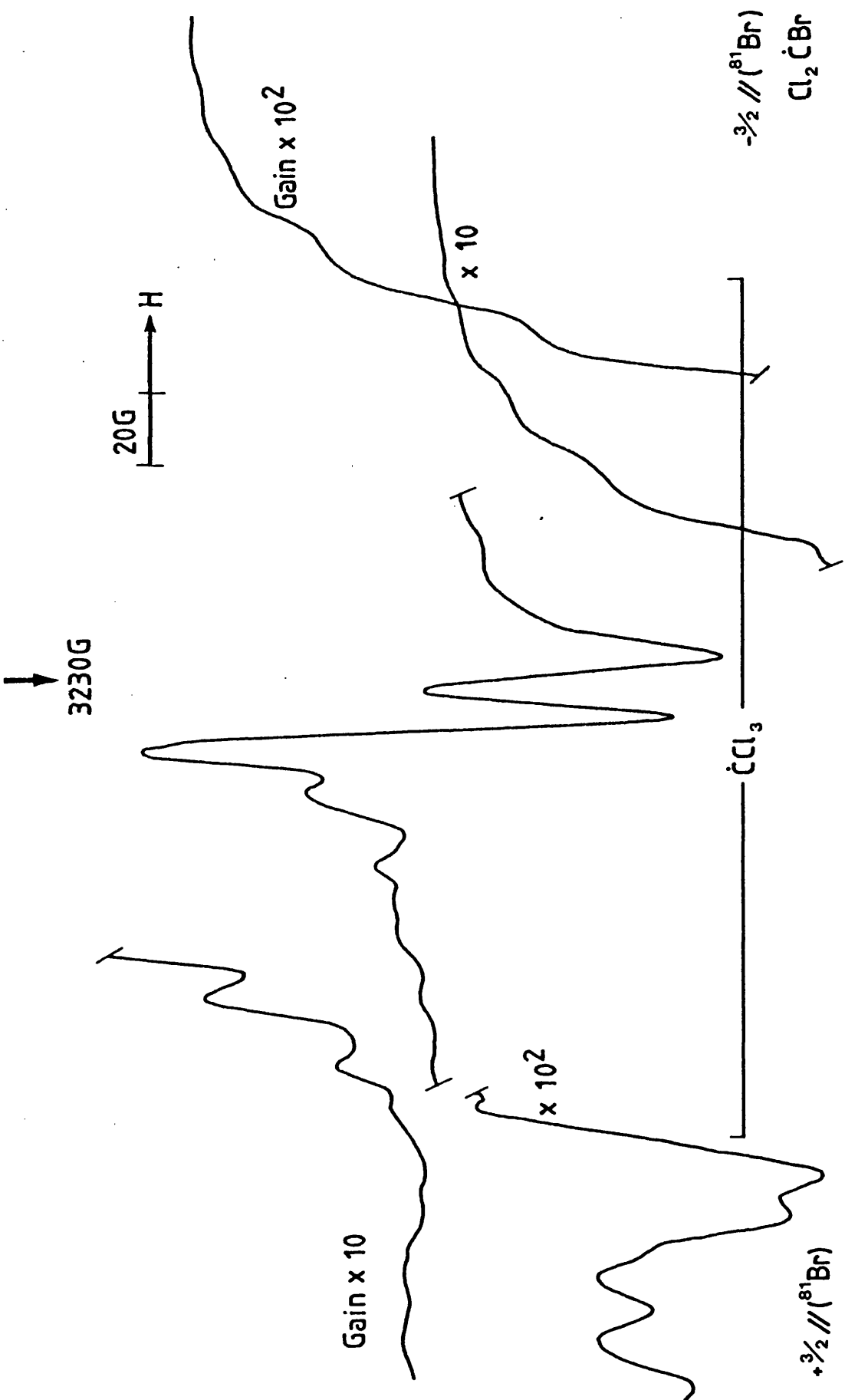


Figure 6(a)
 Showing predominantly $\text{CCl}_3\cdot$ radicals.

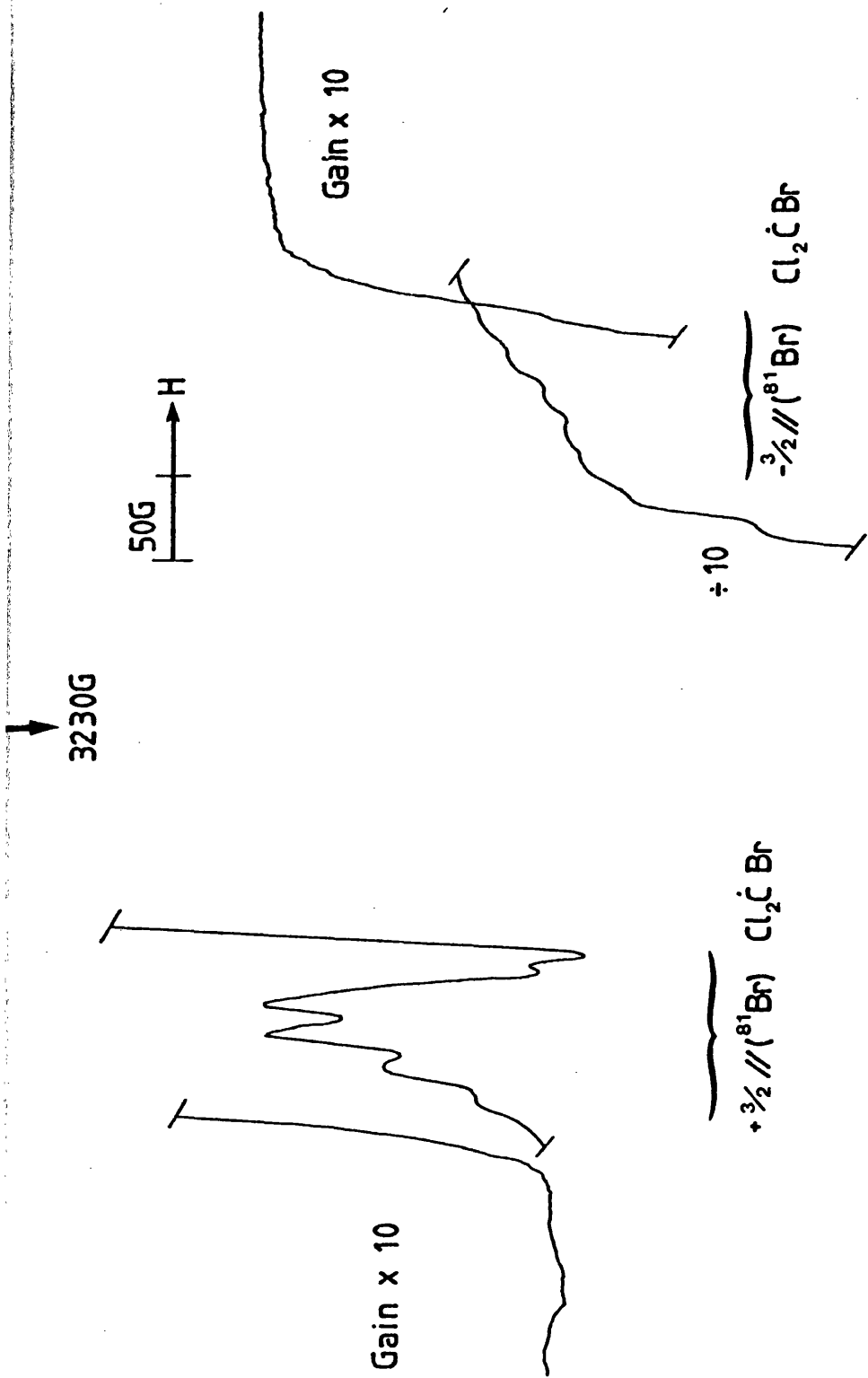
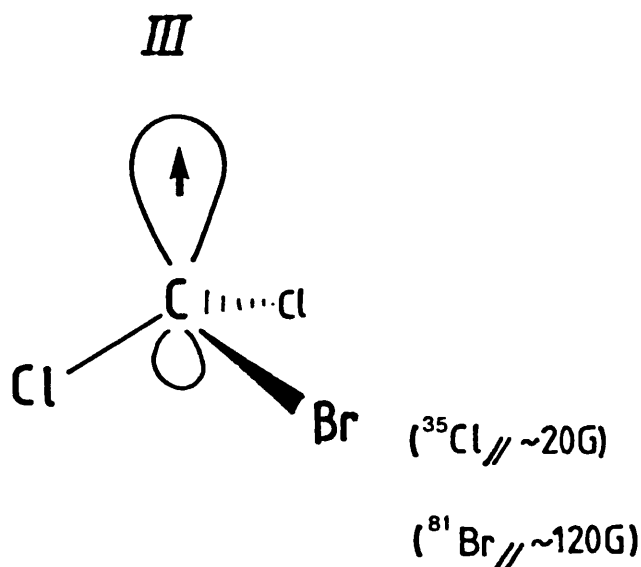
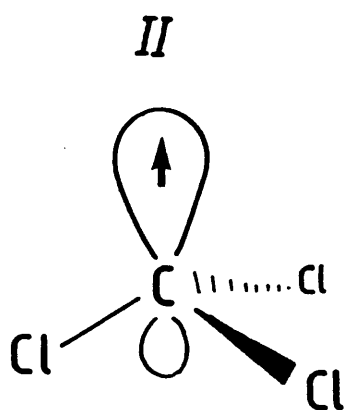


Figure 6(b)
Showing the $\pm \frac{3}{2} //$ features of $\text{Cl}_2\dot{\text{C}}\text{Br}$ radical.



	(Gauss)		
	//	⊥	iso
^{13}C	150	100	115
^{35}Cl	20	ca 0	6.25

$\sim sp^{6.7}$ configuration

implies, perhaps, a further, marginal deviation from planarity.

Conversely, it could be due simply to the increased electronegativity of the bromine atom.

(ii) CCl_4

With this particular example, there now arises the possibility of yet a further conformation of anion, with two strongly coupled chlorines (axial) and two weakly coupled chlorines (equatorial) as in IV.¹⁴ Unfortunately, only the $\dot{\text{C}}\text{Cl}_3$ radical was observed.

(iii) CCl_3F

The spectrum in Fig. 7a is attributable to the rigid $(\text{CCl}_3\text{F})^-$ anion at 77 K, generated from the γ -radiolysis of a 5 Mol % solution of trichloromonofluoromethane (CCl_3F) in CD_3OD at 77 K. The same spectrum, only less well defined, is produced after the γ -radiolysis of the

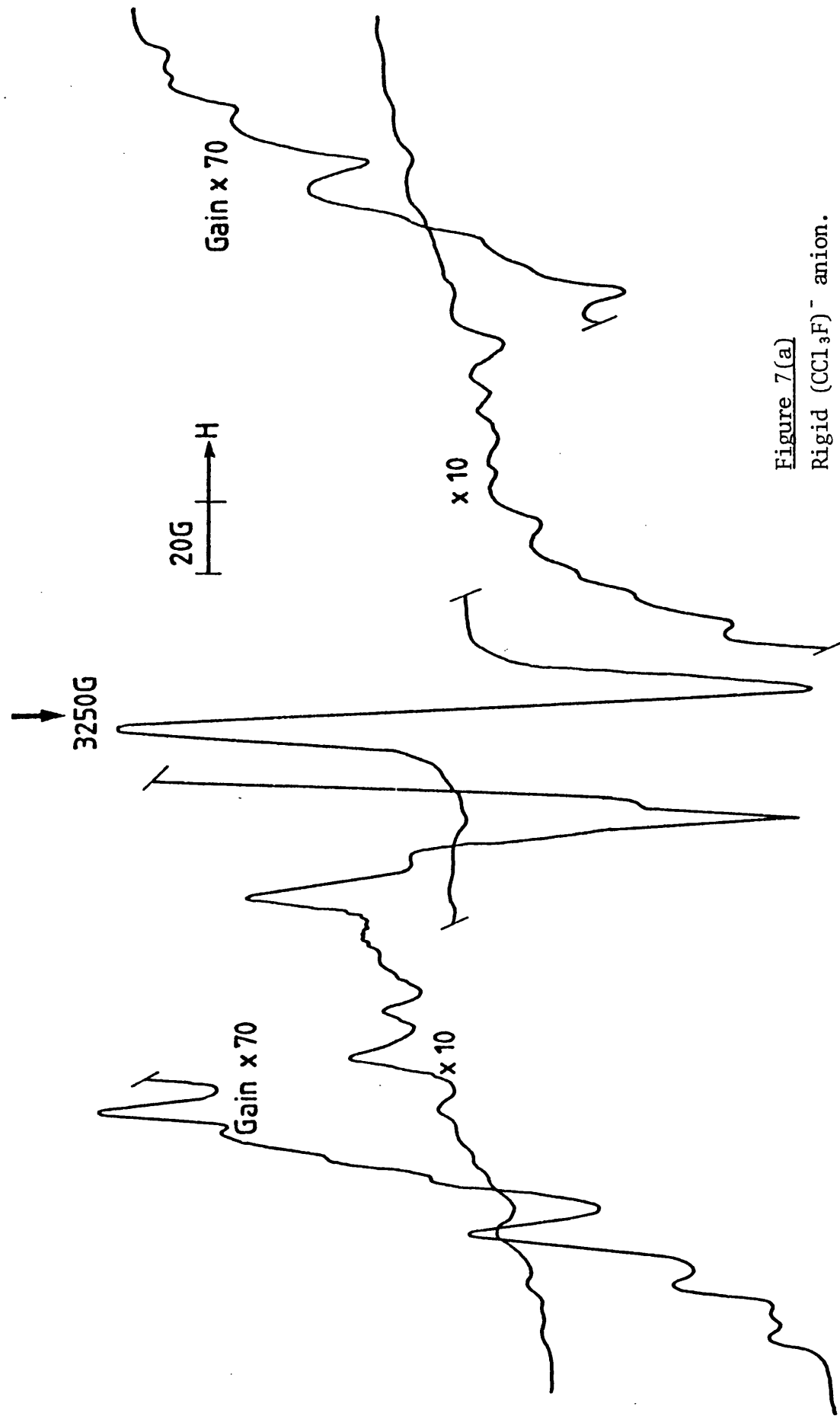


Figure 7(a)
Rigid $(\text{CCl}_3\text{F})^-$ anion.

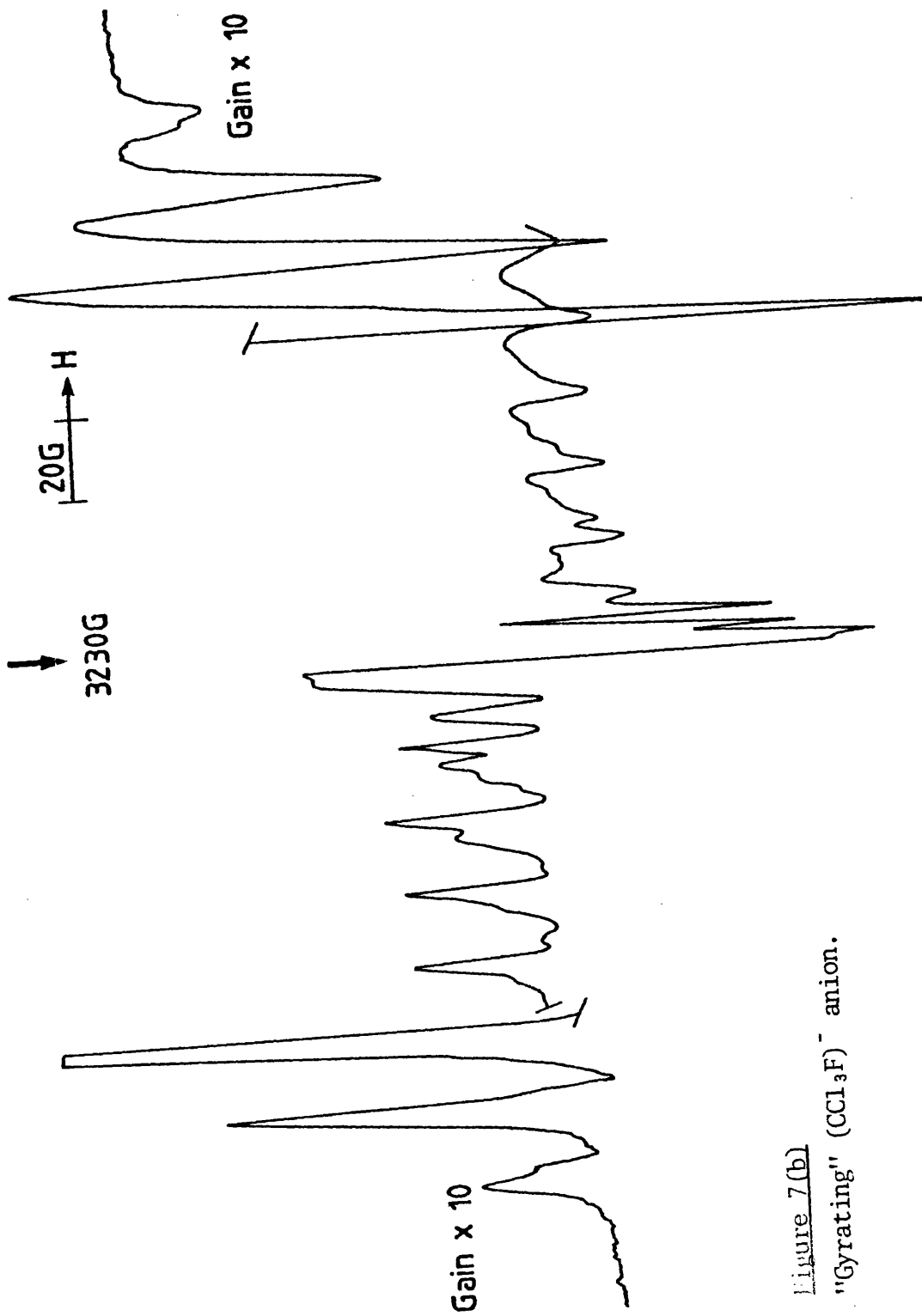
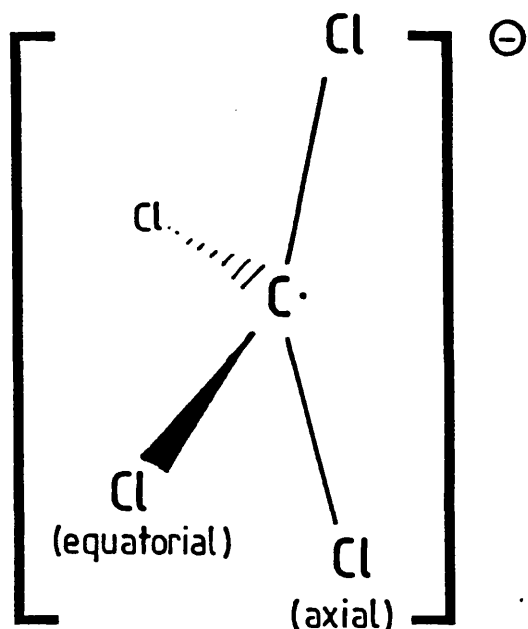


Figure 7(b)
 "Gyrating" $(\text{CCl}_3\text{F})^-$ anion.

IV



CCl_3F in its pure state and in a 1 Mol % solution in TMS. Williams *et al.* had correctly assigned the spectrum to the $(\text{CCl}_3\text{F})^-$ anion⁵ but the bad resolution achieved in the TMS matrix had not allowed them to extract its parameters. The parameters are presented in Table 2

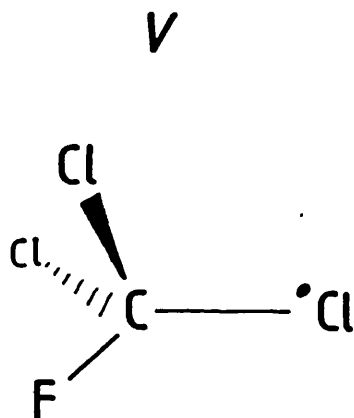
TABLE 2

E.s.r. parameters for range of fluorochloromethanes

Anion	^{19}F couplings (Gauss)			^{35}Cl couplings (Gauss)		
	//	⊥	iso	//	⊥	iso
CF_3Cl^- ^a	197 (×3)	87	124	43	17	26
CF_2Cl_2^- ^a	149 (×2)	42	78	47 27	16 16	26 20
CFCl_3^-	165	ca. 45	85	37 (×1) 15 (×2)	ca. 15 -	22

^a Values taken from Ref. 5.

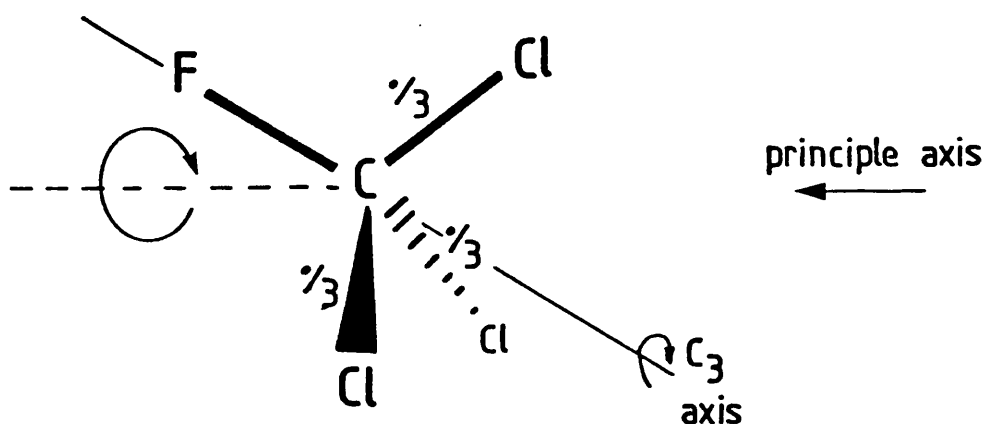
together with the results of Williams *et al.* on the $(F_3C-Cl)^-$ and $[F_2(Cl)C-Cl]^-$ anions.⁵ All three sets of parameters are in good agreement, proving the conformation of the anion is as expected, with the odd electron in the antibonding orbital of the C-Cl bond. The anion exhibits a structure with local C_{3v} symmetry at the carbon atom with the remaining chlorine and fluorine atoms placed at the trigonal sites V. Annealing of the $(CCl_3F)^-$ anion in the CCl_3F matrix to ca. 165 K



generated an interesting anisotropic spectrum (Fig. 7b) which was completely reversible with the 77 K spectrum. The spectrum can be analysed in terms of three equivalent chlorine atoms with an $A_{//}(^{35}Cl)$ coupling of 18 G and a single fluorine atom exhibiting an $A_{//}(^{19}F)$ coupling of 100 G. In our view, the only possible structural contender for this spectrum is the "gyrating" $(CCl_3F)^-$ anion as in VI.

The sharing of the odd electron between the three chlorine atoms is a perfectly reasonable suggestion, however, the low $A_{//}(^{19}F)$ hyperfine coupling of 100 G is somewhat distressing considering the principle axis should now lie along the C-F bond. We therefore need to postulate a "gyrating" movement of the C_3 axis, as depicted in VI, in order to explain this low ^{19}F coupling. This suggestion is validated by the temperature dependence of the ^{19}F coupling; ca. 10 G

VI

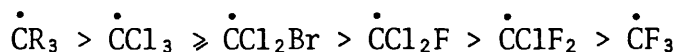


over a 30° range.

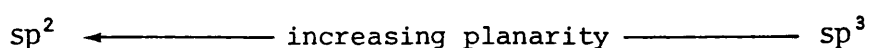
We agree that the explanation just outlined is by no means impervious to criticism. Nevertheless, the species in Fig. 7a is without doubt the rigid $(\text{CCl}_3\text{F})^-$ anion, and the spectra in Figs. 7a and 7b are completely reversible. Our "gyrating anion" suggestion therefore remains the most valid.

Formation of σ^* anion

Of the compounds studied, only the $(\text{Cl}_2\text{FC}-\dot{\text{C}}\text{Cl})^-$ anion was detected, all other molecules breaking down to give either the $\dot{\text{C}}\text{Cl}_3$ or $\dot{\text{C}}\text{Cl}_2\text{Br}$ radicals on electron addition. This strongly suggests a "limit" in σ^* anion formation. Taking the series of $\dot{\text{C}}\text{X}_3$ radicals in order of planarity,



(R = alkyl group)



only the $-\text{CCl}_2\text{F}$, $-\text{CClF}_2$ and $-\text{CF}_3$ groups allow the formation of stable

halo- σ^* anions. It would be of great interest to extract the full A tensor for our $(\text{CFCl}_3)^-$ anion as it would enable us to calculate the percentage 's' and percentage 'p' character of the bond and hence plot the point on the graph in Fig. 3. This particular anion, surely on the brink of not being formed, should then tell us whether all σ^* anions, when formed, should fall on line d. This should therefore tell us whether there is a gradation in $\sigma^* \rightarrow$ adduct as suggested in the introduction of this chapter.

It is unfortunate that even in the cases where the σ^* anion has not been detected, neither was the respective adduct. This could be a matrix effect. For example, irradiation of pure CCl_3Br produced what appeared to be broad and badly defined $\dot{\text{C}}\text{Cl}_3$ and $\dot{\text{C}}\text{Cl}_2\text{Br}$ radicals, yet they could have been the $\text{Cl}_3\text{C}\cdot/\text{Br}^-$ and $\text{BrCl}_2\text{C}\cdot/\text{Cl}^-$ adducts even though no appreciable increase in resolution was obtained on annealing. As documented in chapter 5, adducts are not always spectrally accommodating and do not always exhibit well defined parameters.

CONCLUSION

On the whole, a rather disappointing set of results with regards to their significance to the $\sigma^* \underline{\text{vs}}$ adduct story outlined in the introduction.

It should be noted, however, that the parameters for the $[\text{F}_2(\text{Cl})\text{C}-\dot{\text{C}}\text{Cl}]^-$ anion generated by Williams et al.⁵ puts the species firmly on line d in Fig. 3 with a 1.3% 's' character and 21% 'p' character. Although the documented $A_{\perp}({}^{35}\text{Cl})$ couplings of 16 G are by no means definitive, it nevertheless does tend to suggest that all σ^* anions have identical means of bonding and that there is no real gradation of $\sigma^* \rightarrow$ adduct. This suggestion is validated by the lack of

detection of the $(\text{Cl}_3\text{C}-\dot{\text{Br}})^-$ or $(\text{Cl}_2\text{BrC}-\dot{\text{Cl}})^-$ σ^* -anions.

1-haloadamantane (hal = Cl, Br)

RESULTS

Fig. 8a shows the spectrum generated from the radiolysis of pure, 1-bromoadamantane at 77 K. The spectrum is clearly attributable to a monobromo-species with an $A_x(^{81}\text{Br})$ hyperfine coupling of 371 G, and an $A_x(^{79}\text{Br})$ hyperfine coupling of 344 G split into a doublet of ca. 60 G. The radiolysis of the perdeuterated analogue brought about the collapse of this doublet (Fig. 8b) proving the splitting is due to a single hydrogen atom.

Radiolysis of the 1-chloroadamantane did not, unfortunately, generate a monochloro species nor any feature of discernible quality.

Annealing of all samples resulted in the reversible broadening of all features.

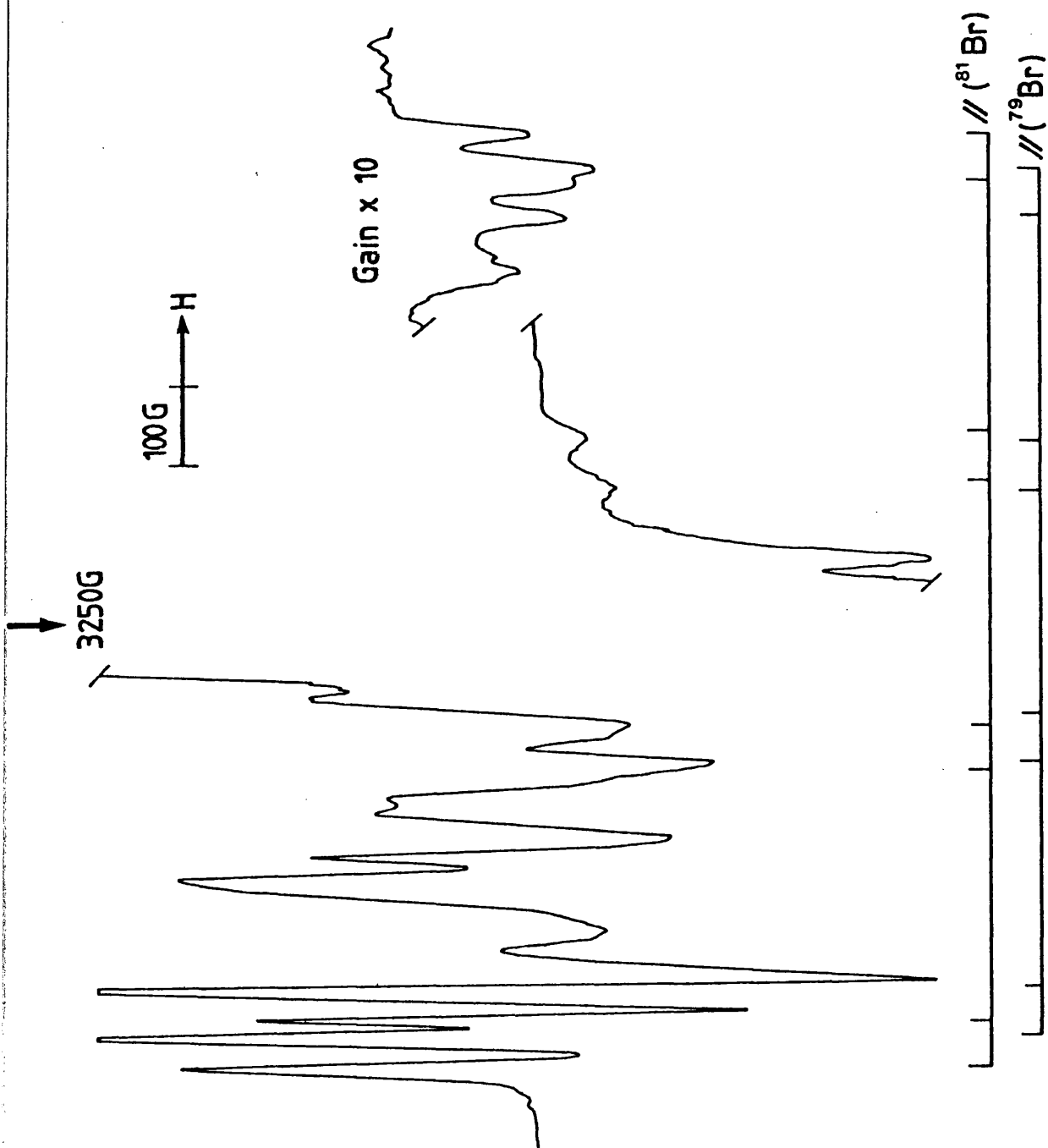
DISCUSSION

Although the $A_x(^{81}\text{Br})$ hyperfine coupling of 371 G is in excellent agreement with the bromine parameters for σ^* anions (see Table 1), there is no obvious explanation as to why there should be an added coupling of ca. 60 G (due to a single hydrogen atom) if the spectra is attributable to the $(\text{ada-Br})^- \sigma^*$ anion. A small coupling to six equivalent hydrogen atoms might have been expected (see I) but certainly not a large coupling to a single hydrogen atom.

Perhaps the β -bromo radical VII is responsible for the spectra, the species certainly contains one unique hydrogen atom. However, in our

Figure 8(a)

γ -radiolysis of 1-bromo adamantane ($C_{10}H_{15}Br$).



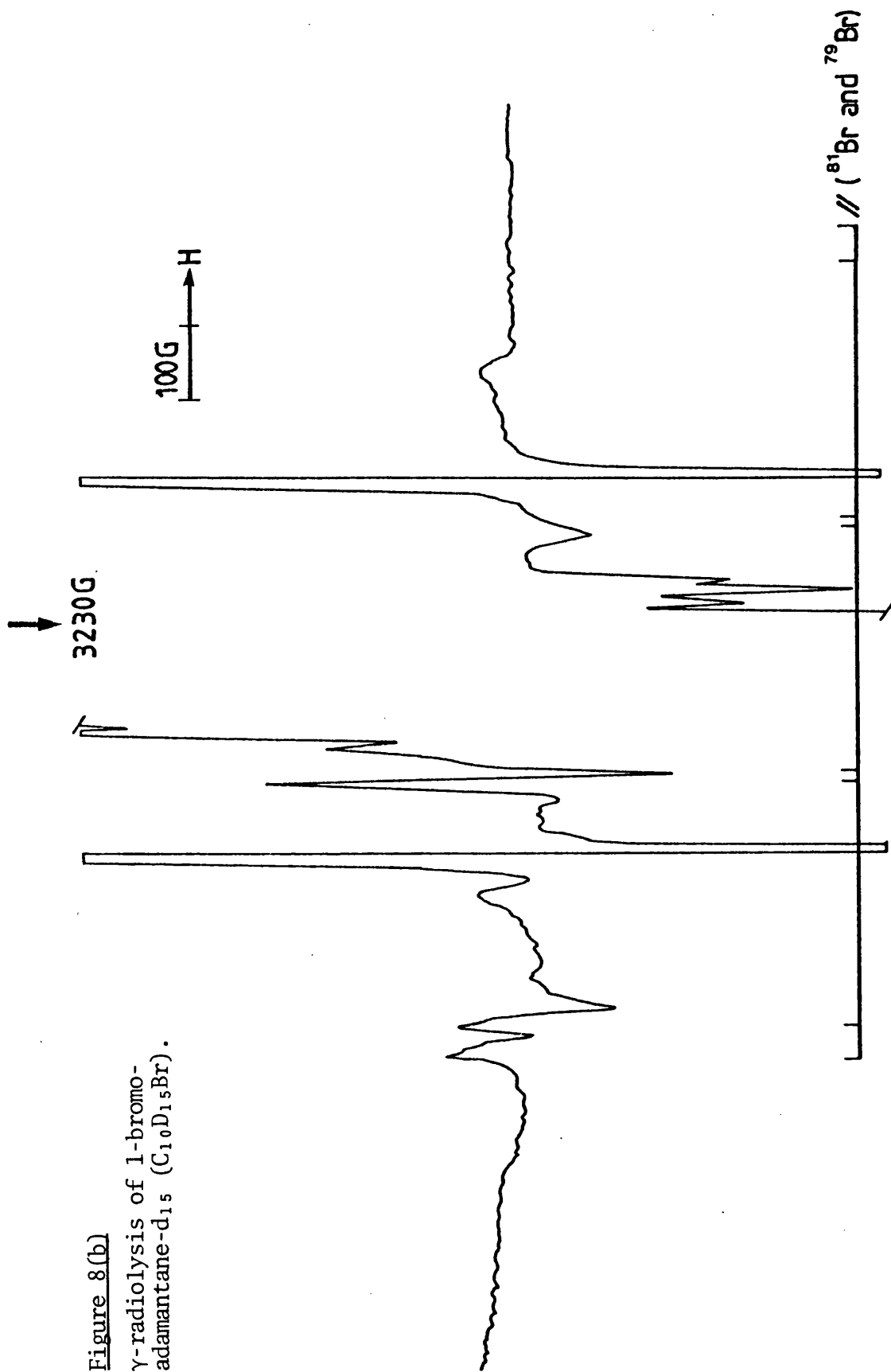
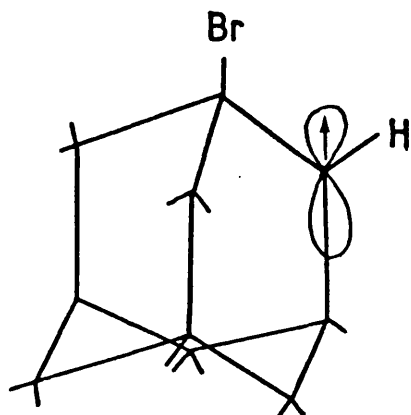


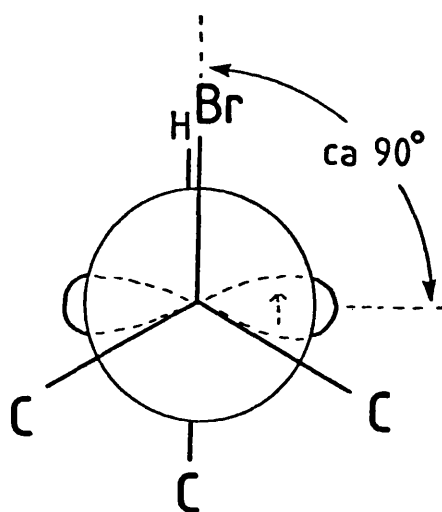
Figure 8(b)
 γ-radiolysis of 1-bromo-
 adamantane-d₁₅ (C₁₀D₁₅Br).

VII



view, the radical site would need to be planar, which would not only mean a maximum ^1H coupling of ca. -23 G (a typical α -hydrogen atom),¹⁵ but would also require the species to exhibit a structure where a large deviation from the position of maximum overlap would need to exist VIII.

VIII



This would result in a maximum bromine coupling of much less than 300 G.¹⁶ It is therefore highly unlikely that the β -bromo radical is responsible for the spectrum.

It then occurred to us that perhaps we have a hydrogen atom addition reaction to the alkyl bromide resulting in the formation of a $(\text{R}-\overset{\cdot}{\text{C}}-\text{Br}-\text{H})$ type species. There is evidence for the existence of an $(\text{Ar}-\overset{\cdot}{\text{I}}-\text{Ph})$

intermediate in the halogen abstraction reaction:¹⁷



where phenyl radicals are generated in situ at 60°C in a solution of the aryl iodide in carbon tetrachloride. It is therefore not too unrealistic to envisage, in our case, the reaction being



with the low temperature of 77 K enabling us to isolate the intermediate. To test this hypothesis we irradiated 1-bromoadamantane-h₁₅ in a matrix of adamantane-d₁₆. If our scheme is correct, we should achieve deuterium atom addition to the 1-bromoadamantane and hence, there should be a complete absence of any 60 G coupling. This proved not to be the case. A ca. 5 Mol % mixture of C₁₀H₁₅Br in C₁₀D₁₆ (produced by recrystallising from a cosolvent - n-heptane. See chapter 1) generated a weak spectrum similar to that in Fig. 8a. This could simply have been due to aggregation of bromoadamantane molecules in the adamantane-d₁₆ matrix. Unfortunately, further dilution of the substrate resulted in an insufficient yield of species and hence the experiment proved inconclusive.

It was appreciated that if the species responsible for the spectrum was either the (Ada \cdot -Br-H) intermediate or (ada \cdot -Br)⁻ σ^* anion, then it should, on further annealing, break down to give the 1-adamantyl radical and either a HBr molecule or a bromide ion respectively. We therefore attempted to monitor the growth in the generation of the 1-adamantyl radical as the sample was warmed. Alas, this too failed as the broad spectrum, presumably attributable to this radical and already formed from 'hot' reactions, also decayed at these temperatures.

In conclusion, we do not have a strong contender for the species

responsible for the spectra in Figs. 8a and 8b. Having rehearsed a few possibilities, the spectrum is still not unambiguously assigned. The fact that 1-chloroadamantane did not generate the analogous spectrum is even more perplexing.

As regards our search for the $(\text{Ada-Br})^- \sigma^*$ anion, it is unlikely that the spectrum obtained is due to this species, neither have we detected any features likely to belong to it during the course of our experiments in a variation of matrices. We do not understand why.

REFERENCES

1. G. W. Neilson, M. C. R. Symons, J.C.S. Faraday II, 1972, 68, 1582.
2. G. W. Neilson, M. C. R. Symons, Mol. Phys., 1974, 27, 1613.
3. S. P. Mishra, G. W. Neilson, M. C. R. Symons, J.C.S. Faraday II, 1974, 70, 1280.
4. D. J. Nelson, M. C. R. Symons, Chem. Phys. Letters, 1977, 47, 436.
5. A. Hasegawa, M. Shiotani, F. Williams, Faraday Discuss. Chem. Soc., 1977, 63, 157.
6. M. C. R. Symons, Radicaux Libres Organique, 1977, p.105;
M. C. R. Symons, Rad. Phys. and Chem. (Memorial Issue), in press.
7. M. C. R. Symons, J. Chem. Research (S), 1978, p.360.
8. Unpublished results.
9. P. W. Atkins, M. C. R. Symons, "Structure of Inorganic Radicals", Elsevier, 1967.
10. J. R. Morton, K. F. Preston, J. Magnetic Resonance, 1978, 30, 577.
11. See chapter 5.
12. E. Osawa, Tetrahedron Letters, 1974, 115;
H. Sletter, M. Schwarz, A. Hirschhorn, Chem. Ber., 1959, 92, 1629.
13. S. P. Mishra, M. C. R. Symons, I.J.R.P.C., 1975, 7, 617;
C. Hesse, N. Leray, J. Roncin, Mol. Phys., 1971, 22, 137;
G. Maass, A. K. Maltser, J. L. Margrave, J. Inorg. Nucl. Chem., 1973, 35, 1945;
N. E. Bibler, J. Phys. Chem., 1971, 75, 24;
N. E. Bibler, J. Phys. Chem., 1973, 77, 167;
H. R. Werner, R. F. Firestone, J. Phys. Chem., 1965, 69, 840.
14. P. Schipper, E. H. J. M. Jansen, H. M. Buck, Topics in Phos. Chem., 1977, 9, 407.
15. M. C. R. Symons, "Chemical and Biochemical Aspects of Electron Spin Resonance Spectroscopy", Van Nostrand Reinhold, 1978.
16. A. R. Lyons, M. C. R. Symons, J.A.C.S., 1971, 93, 7330.
17. W. C. Danen, D. G. Saunders, J.A.C.S., 1969, 91; 5924.

CHAPTER 7

Gamma radiolysis of methylhalosilanes

INTRODUCTION

Some years ago, Roncin *et al.* carried out a study on the products derived from the γ -radiolysis of a number of methylchlorosilanes.¹ The radiolysis of tetramethylsilane (TMS) generated a high yield of unambiguous $\text{Me}_3\text{Si}\cdot$ radicals with an $A_{\parallel}({}^{29}\text{Si})$ of 233 G, an $A_{\perp}({}^{29}\text{Si})$ of 155 G, an $A_{\text{iso}}({}^{29}\text{Si})$ of 181 G and an $A({}^1\text{H})$ (Me groups) of 6.3 G. Meantime, the spectrum from the radiolysis of the trimethylchloro derivative (Me_3SiCl) yielded badly resolved features attributable, according to Roncin, to $\text{Me}_3\text{Si}\cdot$ radicals [$A({}^{29}\text{Si}) = 129$ G, $A({}^1\text{H})$ (Me groups) = 6.2 G] and $\text{Me}_2\dot{\text{S}}\text{iCl}$ radicals [$A({}^{29}\text{Si}) = 229$ G, $A({}^1\text{H})$ (Me groups) = 5.2 G]. Furthermore, the $A({}^{29}\text{Si})$ value of 129 G in the latter analysis was concluded to "be very near to the $A({}^{29}\text{Si})$ isotropic value". Hence, the $\text{Me}_3\text{Si}\cdot$ radical was reported to exhibit an $A_{\text{iso}}({}^{29}\text{Si})$ coupling of 181 G in the TMS matrix, yet only a coupling of 129 G in the Me_3SiCl matrix. Similar disparities in ${}^{29}\text{Si}$ couplings were reportedly observed for the $\text{Me}_2\dot{\text{S}}\text{iCl}$, $\text{Me}\dot{\text{S}}\text{iCl}_2$ and $\dot{\text{S}}\text{iCl}_3$ radicals. See Table 1.

The conclusion from this work was that the $A_{\text{iso}}({}^{29}\text{Si})$ hyperfine coupling constants for the four radicals mentioned, varied by as much as 25% depending upon the matrix in which it was trapped, even though the $A({}^1\text{H})$ coupling constants for the methyl groups and chlorine atoms remained relatively unchanged. These differences were duly explained in terms of the variation in the dipole moment of the surrounding matrix molecules.

The implications of these conclusions were of importance to us as it predicted that the parameters of any given species will be greatly dependent upon the environment in which it is generated. A clearly

TABLE 1

Results obtained for methylchlorosilyl radicals¹

Radical	Matrix	A(¹ H) for Me groups (Gauss)	A _{iso} (³⁵ Cl) (Gauss)	A _{iso} (²⁹ Si) (Gauss)	μ debye dipole moment
•Si(CH ₃) ₃	Si(CH ₃) ₄	6.32	-	172.5	0
•Si(CH ₃) ₃	ClSi(CH ₃) ₃	6.2	-	129	2.09
ClSi(CH ₃) ₂	ClSi(CH ₃) ₃	5.2	-	229	2.09
ClSi(CH ₃) ₂	Cl ₂ Si(CH ₃) ₂	5.2	-	215	2.28
Cl ₂ SiCH ₃	Cl ₂ Si(CH ₃) ₂	-	10.5	295	2.28
Cl ₂ SiCH ₃	Cl ₃ SiCH ₃	-	11.4	308	1.87
Cl ₃ Si•	Cl ₃ SiCH ₃	-	12.4	416	1.87
Cl ₃ Si•	Cl ₄ Si	-	13.4	440	0

undesirable case of affairs for a laboratory team such as ourselves who attempt to generate and study the same radicals in a host of different matrices.

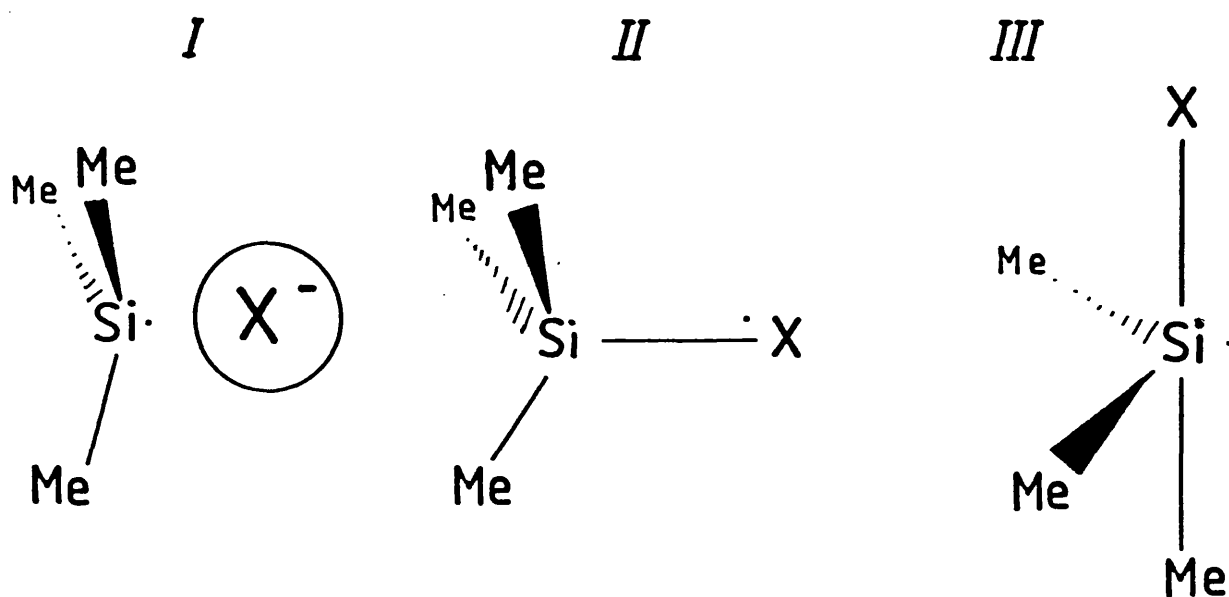
Closer scrutiny of their spectra from the Me_3SiCl sample (poor though they were) led us to the conclusion that one of the two following explanations must be responsible for the results obtained.

- (i) Either the features observed are due to the anisotropic Me_3Si radical; the $A(^{29}\text{Si})$ values of 129 G and 229 G are not too far removed from the authentic anisotropic parameters for the Me_3Si radical generated in the TMS matrix.
- (ii) Or the features are due to a completely different species. On consideration of the "adduct vs σ^* anion" arguments rehearsed in chapter 6, it occurred to us that perhaps the species responsible for the aforementioned spectrum might be the $(\text{Me}_3\text{Si}-\dot{\text{C}}\text{l})^- \sigma^*$ anion. The anisotropic ^{29}Si parameters for the $\text{Me}_3\text{Si}\cdot$ radical² show a near flat radical with the electron in an $sp^{7.8}$ orbital, hence, one would predict the formation of the σ^* anion on electron addition.

It was therefore decided to look at and compare the radiolysis products of Me_4Si (TMS), and Me_3SiX ($X = \text{Cl}, \text{Br}, \text{I}$) in a number of matrices in the hope of (a) proving the conclusions of Roncin to be incorrect even though the wealth of experience in this field here and elsewhere strongly suggests they must be; (b) isolating and detecting the $\text{Me}_3\text{Si}\cdot/\text{X}^-$ adducts (I) or the $(\text{Me}_3\text{SiX})^-$ anion (II).

During the course of our experiments, a whole range of derivatives of halosilanes^{3,5} and halogermanes^{4,5} were introduced into the TMS matrix by Hasegawa et al., the spectral results being interpreted in terms of the respective halosilyl and halogermanyl σ^* anion. Their

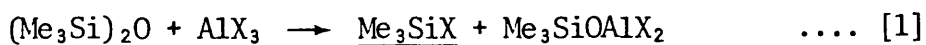
results for the halosilyl derivatives demonstrated the strong possibility of our Me_3SiX molecules, on electron addition, forming the σ^* anion not in the C_{3v} structure II but, in fact, in a trigonal bipyramidal structure, III. Hence, care had to be taken in the interpretation of any spectra produced.

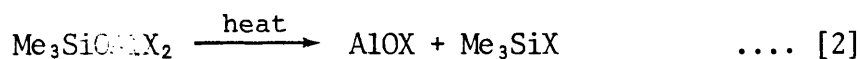


EXPERIMENTAL

Adamantane- d_{16} (Merck, Sharpe & Dohme), TMS (B.D.H.), Me_3SiCl (Aldrich), and $\text{d}_9\text{-Me}_3\text{SiCl}$ (Merck, Sharpe & Dohme) were all used as supplied.

Me_3SiX ($\text{X} = \text{Br}, \text{I}$) was synthesised utilising the following reactions:⁶

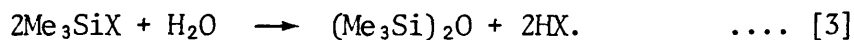




Hexamethyldisiloxane, $(\text{Me}_3\text{Si})_2\text{O}$ (Koch-Light) was carefully added to an excess of the aluminium trihalide, AlX_3 , in a round bottom flask and refluxed under dry nitrogen. The product was purified by fractional distillation using a column containing 12 theoretical plates.

Aluminium tribromide, AlBr_3 (B.D.H.) was used as supplied. Aluminium triiodide, AlI_3 , was generated in situ by refluxing powdered aluminium with iodine in dry benzene, followed by the removal of solvent by distillation. The purity of the products, Me_3SiBr (b.p. 80°C), Me_3SiI (b.p. 107°C) was checked using n.m.r. spectroscopy.

Care was taken in the handling of the trimethylhalosilanes as they are all easily hydrolysed even in moist air via reaction [3]



The incorporation of these silanes into the various matrices was therefore carried out in a dry bag whilst flushing with dry nitrogen.

Incorporation of substrates into the adamantane matrix was carried out by recrystallising the matrix from the respective substrate as described in chapter 1. 5 Mol % solutions of the respective substrate in TMS, samples of the substrates in adamantane, and all substrates in the pure state (Me_3SiCl , Me_3SiBr , Me_3SiI , TMS and $\text{d}_9\text{-Me}_3\text{SiCl}$) were all individually placed into quartz tubes, degassed via the freeze-thaw method, and the tubes sealed.

Radiolysis of samples and recording of spectra were carried out as described in chapter 2.

RESULTS AND DISCUSSION

Once again, the results from the forthcoming experiments proved to be far from conclusive in answering the questions posed in the introduction. The most interesting spectra were those generated from the radiolysis of the pure silanes, these will therefore be discussed first.

The silanes were also incorporated into the adamantane matrix. Although not achieving such exemplary results as has been obtained from the use of this matrix with other substrates,⁷ it did nevertheless prove to be of assistance with regards our quest to disprove the theories of Roncin.

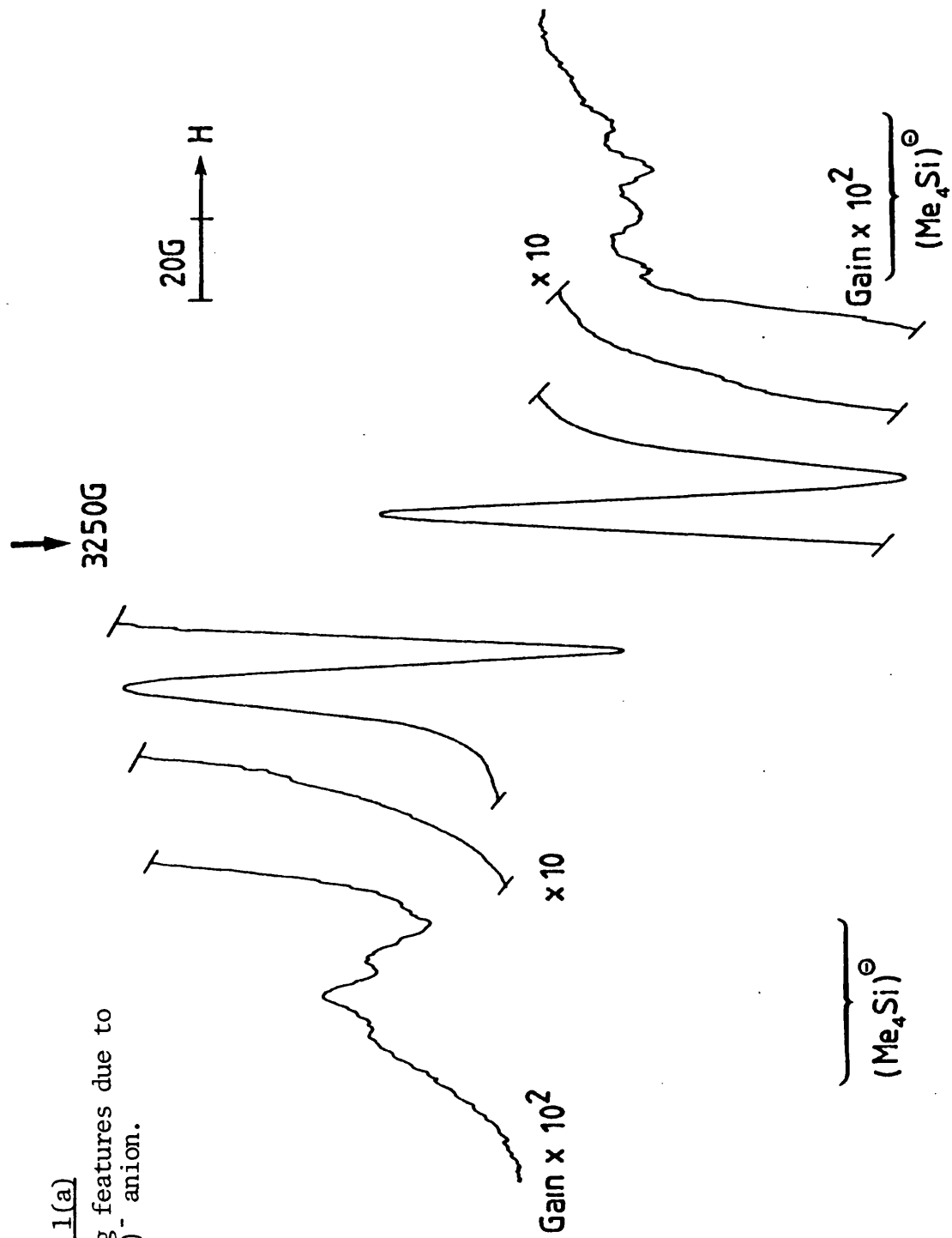
Pure tetramethylsilane; TMS (Me_4Si)

Fig. 1 shows the spectra produced from the γ -radiolysis at 77 K of pure TMS (a) at 77 K immediately after irradiation, (b) at ca. 165 K, (c) at 77 K after recooling from ca. 165 K. The species in Fig. 1a has been assigned to the $(\text{Me}_4\text{Si})^-$ anion, which decays into the $\text{Me}_3\text{Si}\cdot$ radical on annealing whose spectrum is isotropic at 165 K (Fig. 1b) and anisotropic at 77 K (Fig. 1c).

To test our hypothesis, the same experiment was carried out using perdeuterated TMS. The spectra obtained are shown in Figs. 2a, 2b and 2c at 77 K, 165 K, and 77 K respectively.

The isotropic and anisotropic parameters of the $\text{Me}_3\text{Si}\cdot$ radical are well documented.² However, what is of interest in these experiments is the fact that the radical only appears to grow in on annealing and does not appear to be present immediately after irradiation. The only possible precursor, in our opinion, is the aforementioned $(\text{Me}_4\text{Si})^-$ anion with a structure as in IV. The two axial methyl groups are

Figure 1(a)
Showing features due to
(Me₄Si)⁻ anion.



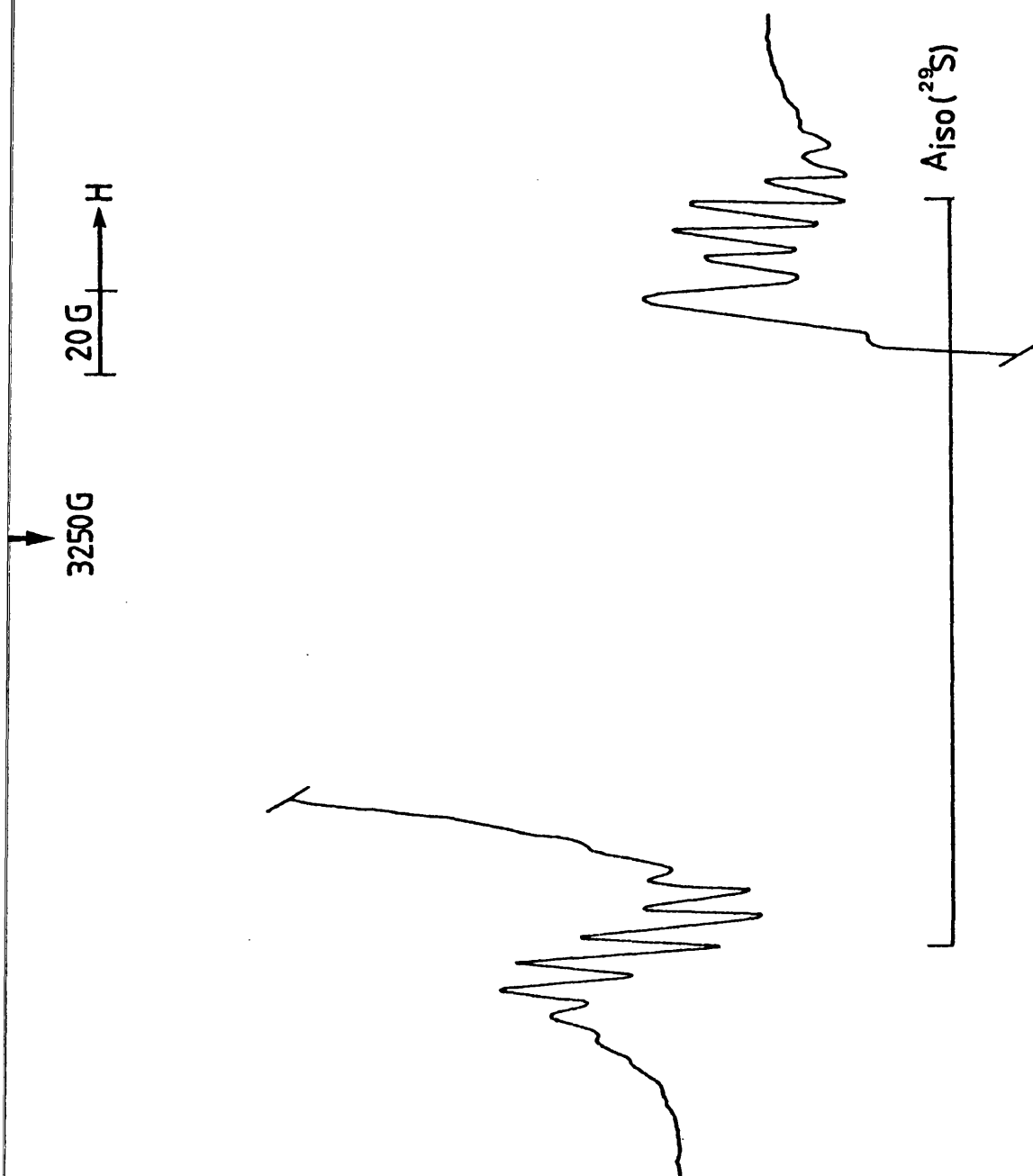
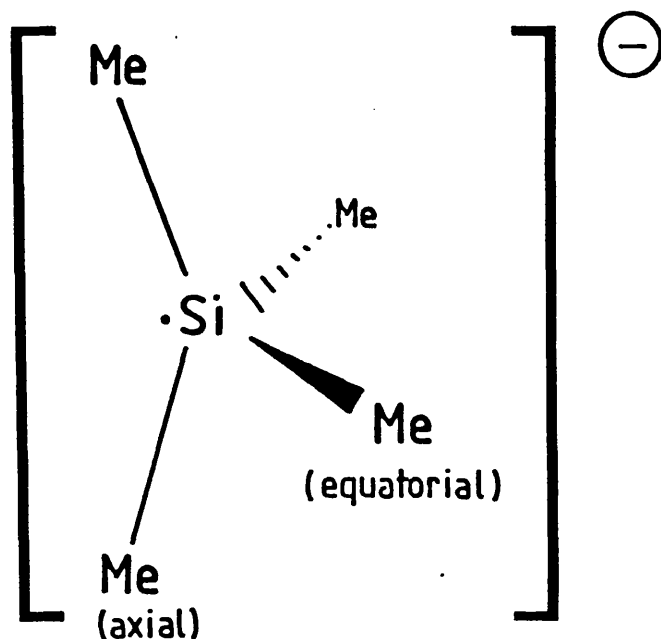


Figure 1(b)
Rotating $\text{Me}_3\text{Si}\cdot$ radical.

IV



exhibiting an $A(^1\text{H})$ hyperfine coupling of 12 G,⁸ while the coupling to the hydrogen atoms of the equatorial methyl groups remain unresolved and are lost in the linewidth of the spectrum.

The d_{12} -TMS experiment is identical in as much as the $(\text{CD}_3)_3\text{Si}\cdot$ radicals are definitely generated on annealing. Unfortunately, the sample also proved to contain a range of impurities, hence the spectra in Figs. 2a and 2c are not as clear-cut as one would like. The cost of the compound and the small quantity at our disposal did not make the attempted purification of the sample viable.

If our assignment is correct, it is in agreement with Hasegawa *et al.*^{3,5} whose results suggest a similar trigonal bipyramidal structure for the anions formed from the radiolysis of a series of halosilanes. Although our value of ca. 200 G for the $A_{\parallel}(^{29}\text{Si})$ hyperfine coupling is rather small when compared to that observed for the $(\text{SiH}_3\text{Cl})^-$ anion³ [$A_{\parallel}(^{29}\text{Si}) = 324$ G], this could be due simply to the $(\text{Me}_4\text{Si})^-$ anion

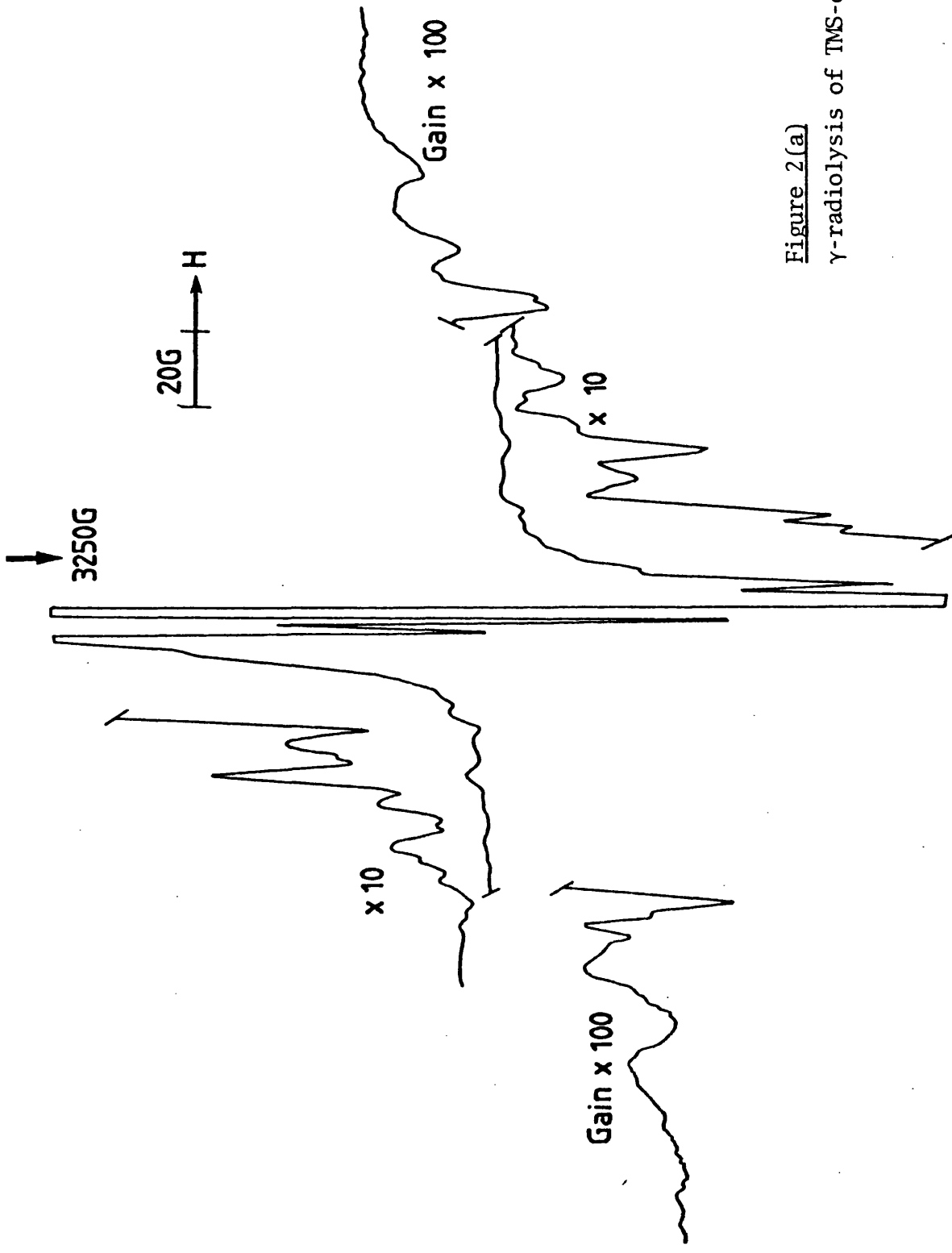


Figure 2(a)
 γ -radiolysis of TMS-d₁₂ at 77 K.

Figure 2(b)

Rotating $(\text{CD}_3)_3\text{Si}\cdot$ radicals.

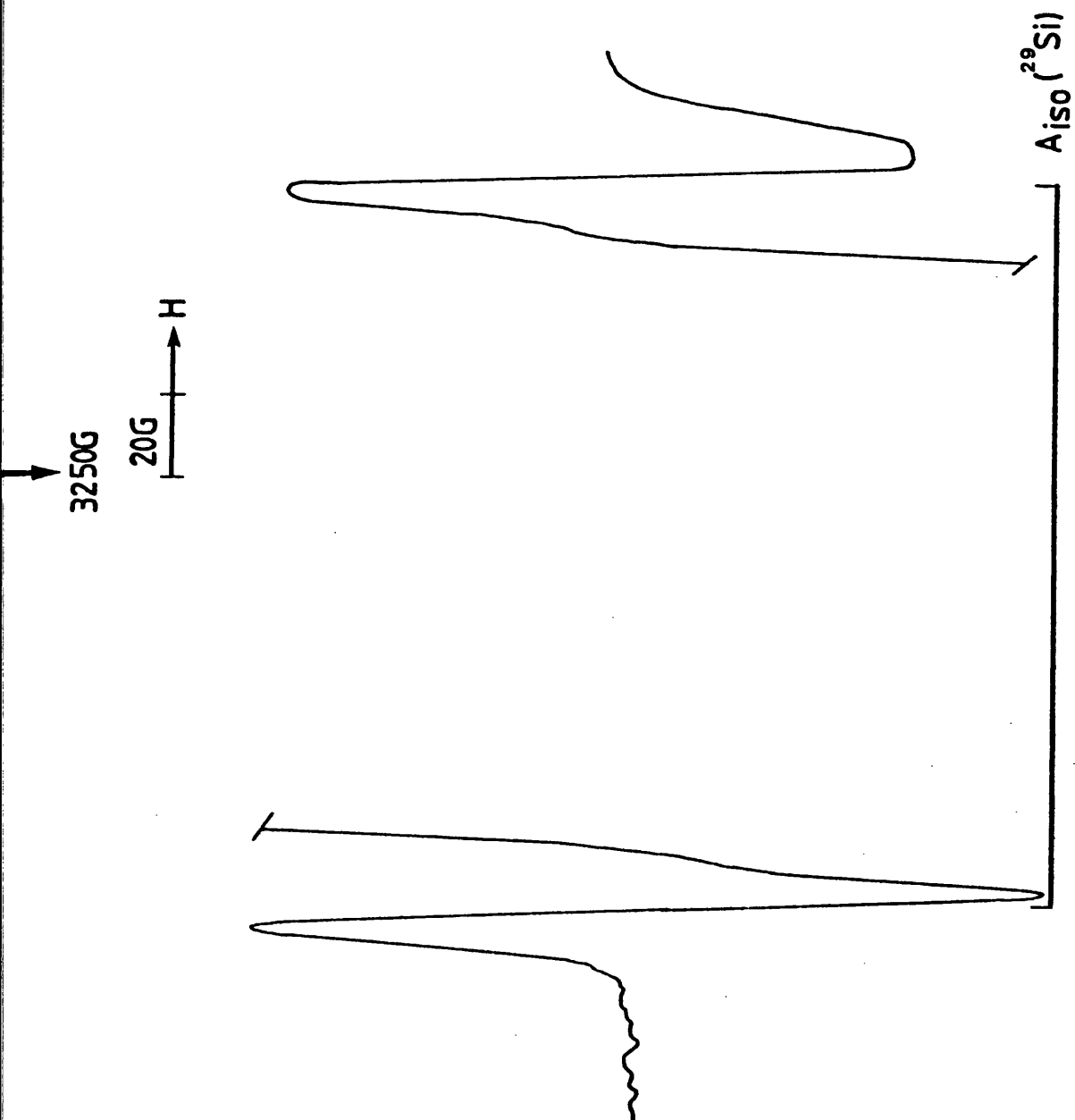
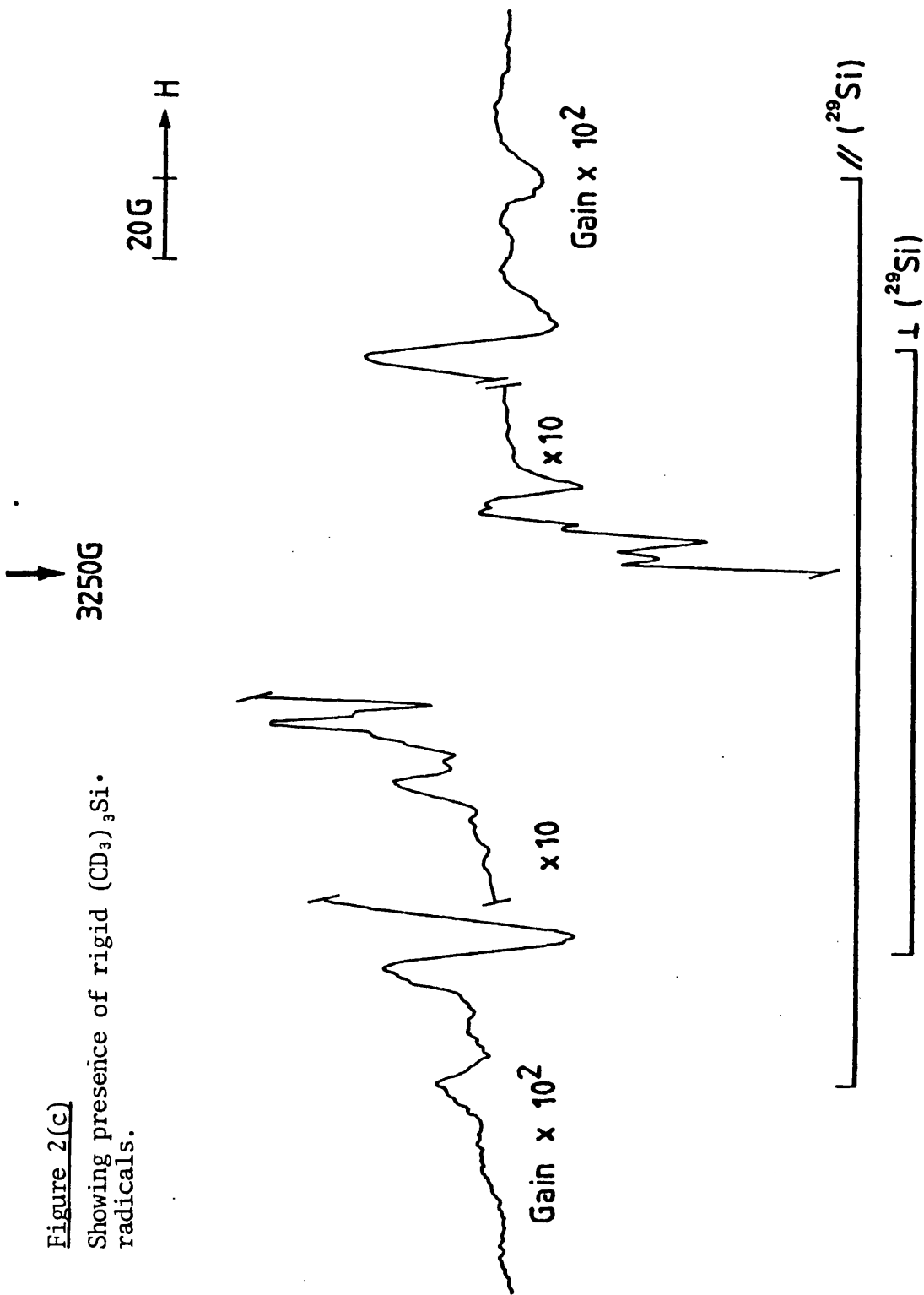


Figure 2(c)

Showing presence of rigid $(CD_3)_3Si\cdot$ radicals.



adopting a structure with a marked deviation from the "perfect" trigonal bipyramidal structure envisaged by Hasegawa. Hence, perhaps the species adopts a structure intermediate of the two extremes; it is neither a "perfect" trigonal bipyramid nor a "perfect" tetrahedron (see IV).

Pure trimethylchlorosilane (Me_3SiCl)

Figs. 3a and 3b show the spectra generated after the γ -radiolysis at 77 K of pure Me_3SiCl at ca. 120 K and ca. 190 K respectively. Roncin assigned species (A) to the $\text{Me}_3\text{Si}\cdot$ radical and species (B) to the $\text{Me}_2\dot{\text{S}}\text{iCl}$ radical.¹ The spectra generated from the analogous experiment using d_9 - Me_3SiCl are shown in Figs. 4a and 4b respectively.

The only conclusive result from this experiment was that Roncin was perfectly correct in assigning species (B) to the $\text{Me}_2\dot{\text{S}}\text{iCl}$ radical. It is now apparent that the radical has an $A_{\text{iso}}(^{29}\text{Si})$ hyperfine coupling of 244 G, an $A_{\text{iso}}(^{35}\text{Cl})$ hyperfine coupling of 9 G and each of its six equivalent hydrogen atoms exhibit an $A(^1\text{H})$ coupling of ca. 6.0 G (see V). The increased (^{29}Si) isotropic coupling shows, as would be expected, that the species is more pyramidal than the $\text{Me}_3\text{Si}\cdot$ radical.

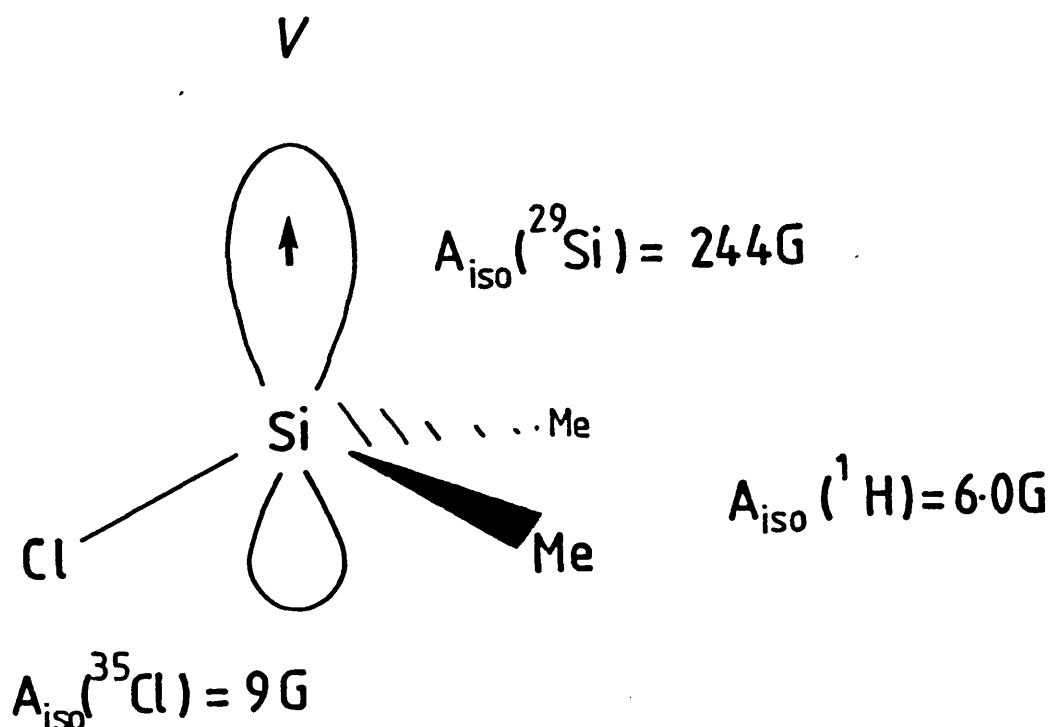
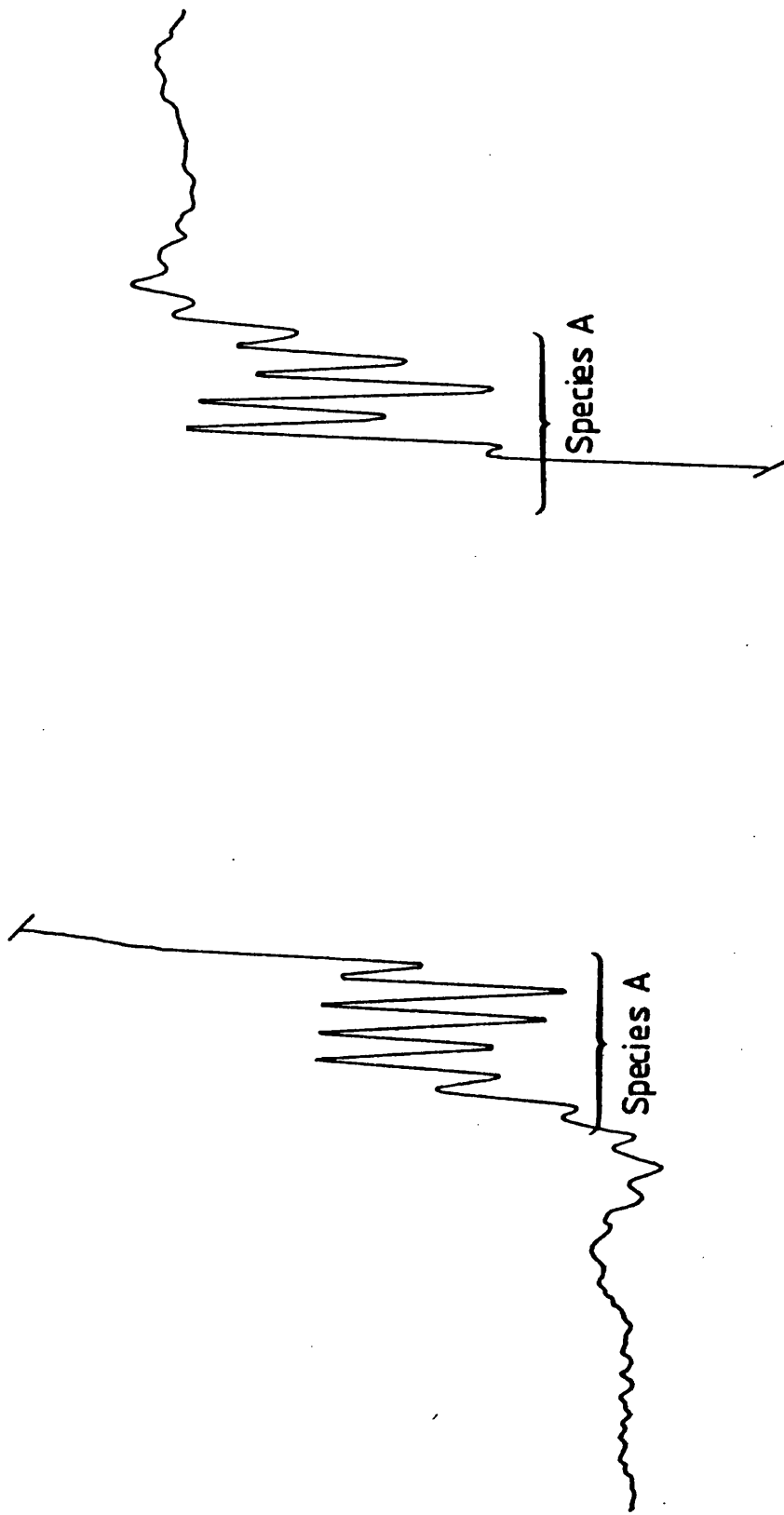


Figure 3(a)

γ -radiolysis of Me_3SiCl at ca. 120 K.



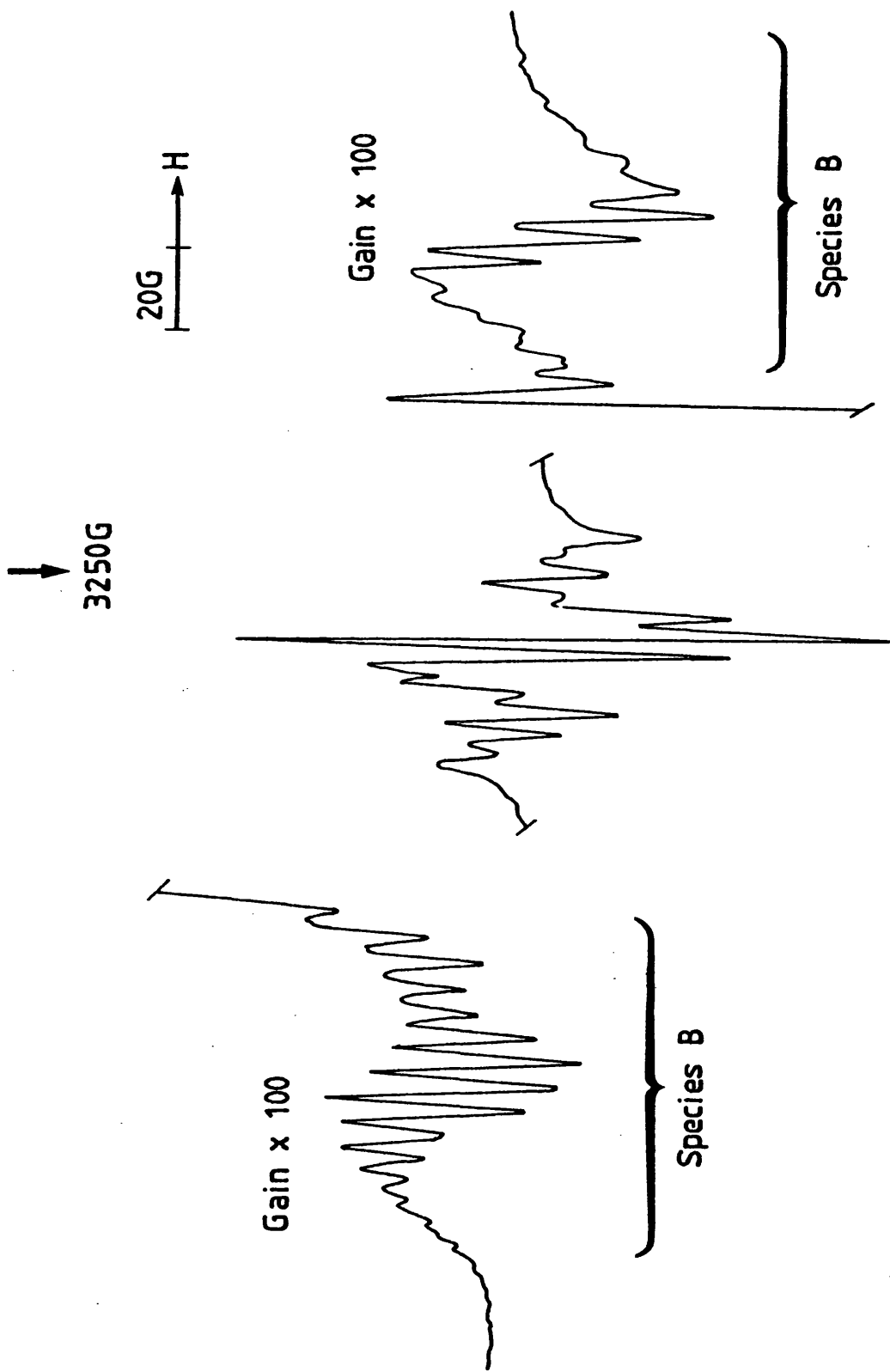


Figure 3(b)

At 190 K.

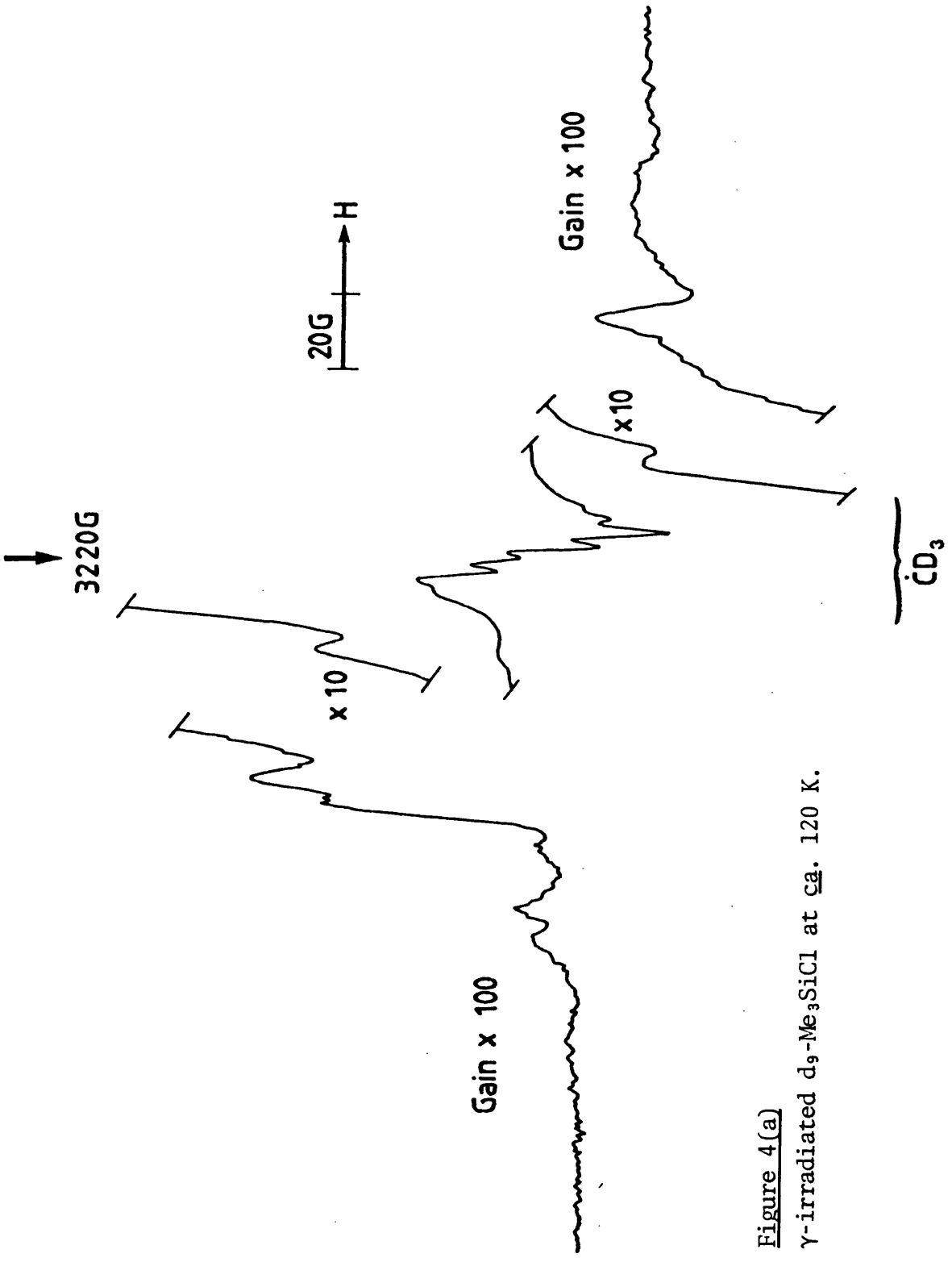


Figure 4(a)
 γ -irradiated d_9 -Me₃SiCl at ca. 120 K.

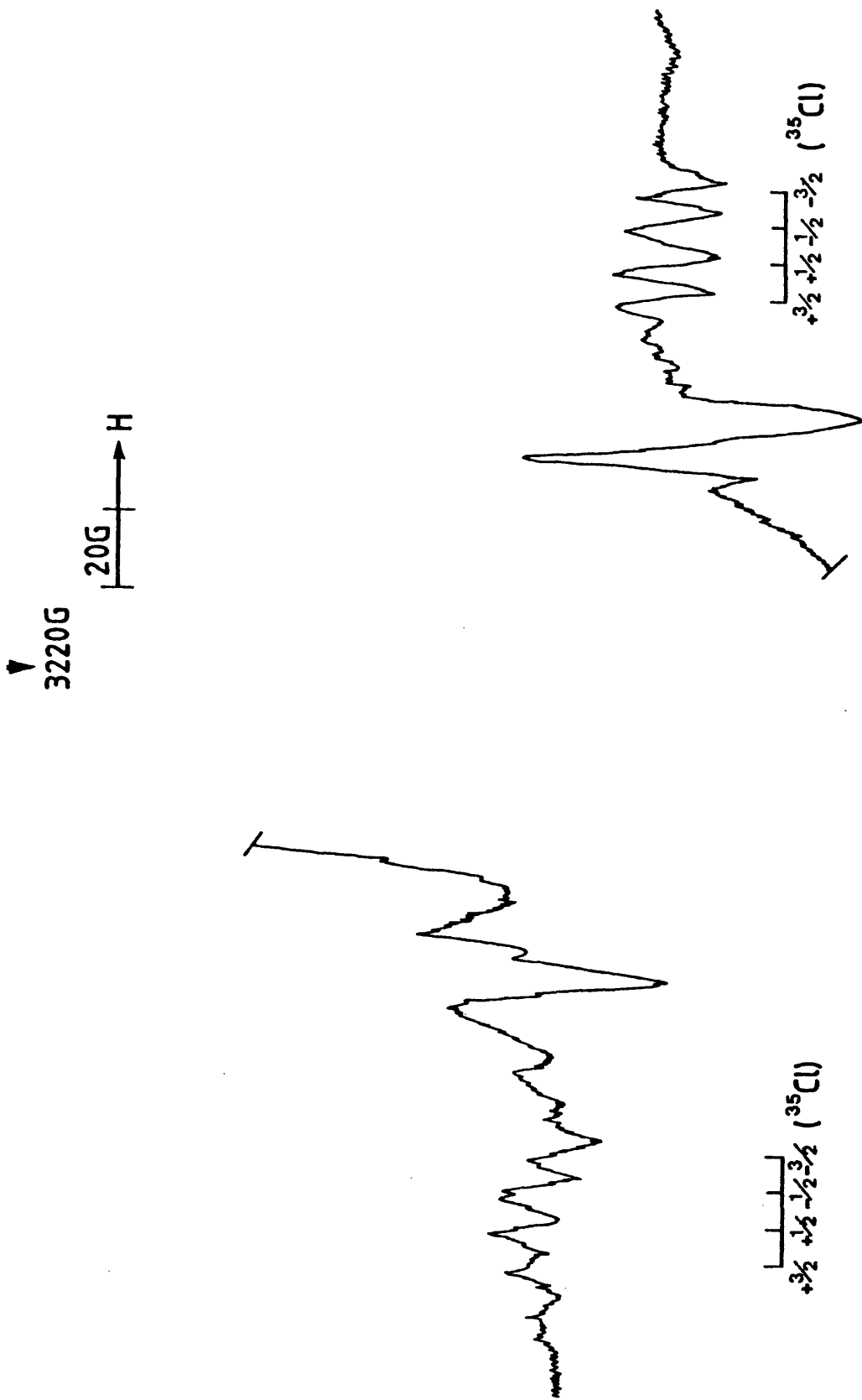


Figure 4(b)
 γ -irradiated $\text{d}_3\text{-Me}_3\text{SiCl}$ at ca. 190 K showing $\text{Me}_2\dot{\text{S}}\text{iCl}$ radical.

While not being able to assign species (A), we feel most definitely it cannot be the $\text{Me}_3^{29}\text{Si}\cdot$ radical due simply to the lack of $\text{Me}_3^{28}\text{Si}\cdot$ radicals whose features should, on comparison of the relative isotopic abundances, make a major contribution to the spectrum obtained.

It does seem that perhaps the major species in the centre of the spectrum is the $\text{H}_2\dot{\text{C}}-^{28}\text{Si}\begin{matrix} \text{Cl} \\ \diagdown \\ \text{Me}_2 \end{matrix}$ radical, exhibiting an $A(^1\text{H})$ coupling of ca. 20 G and an $A(^{35}\text{Cl})$ coupling of ca. 5 G. The analogous $\text{H}_2\dot{\text{C}}-^{29}\text{Si}\begin{matrix} \text{Cl} \\ \diagdown \\ \text{Me}_2 \end{matrix}$ radical would, most probably, be undetectable due to the small value of the $A(^{29}\text{Si})$ hyperfine coupling.

Pure trimethylbromosilane (Me_3SiBr)

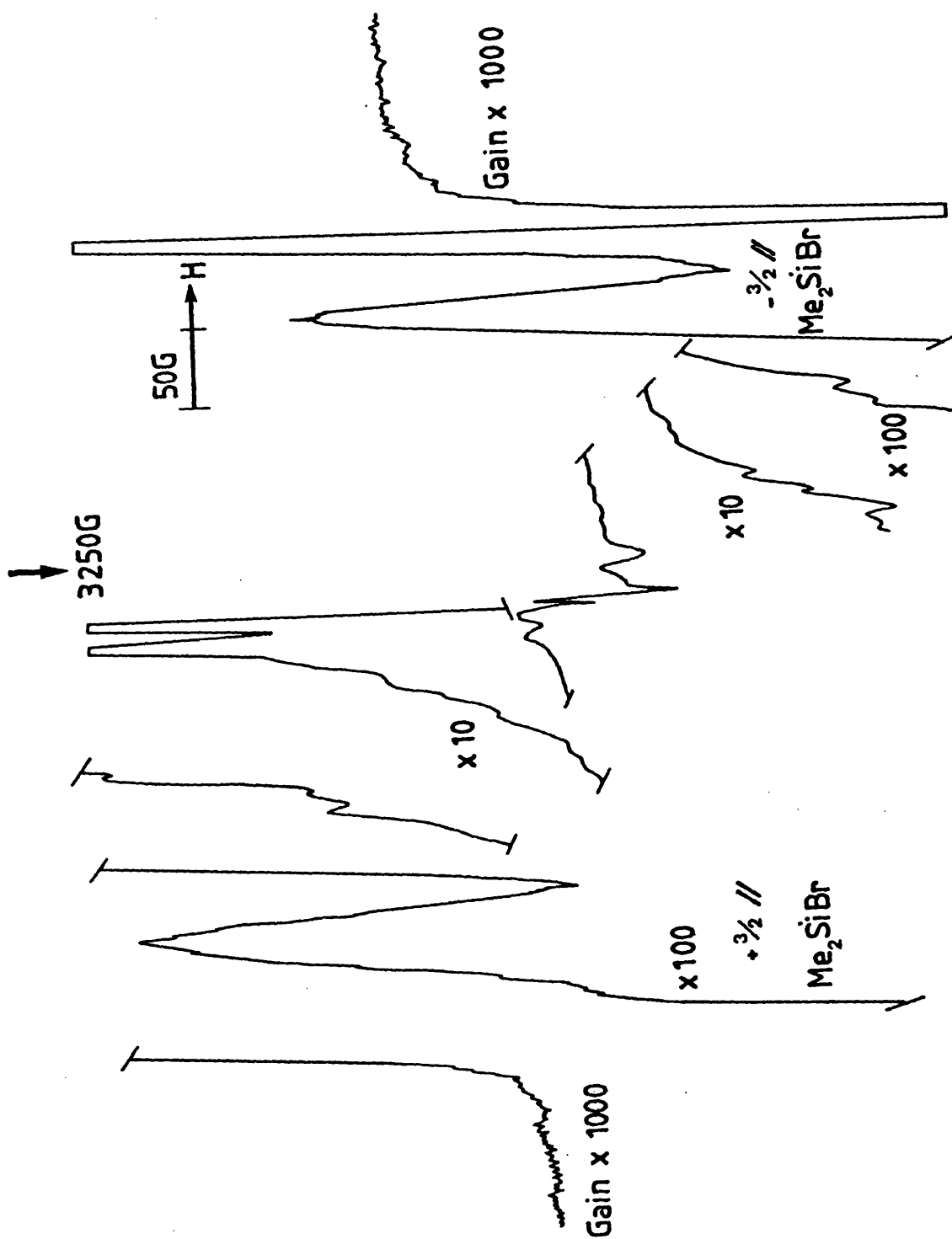
Fig. 5 shows the spectrum recorded at 77 K and generated from the γ -radiolysis at 77 K of pure Me_3SiBr . The outer features are probably due to the rigid $\text{Me}_2^{28}\dot{\text{Si}}\text{Br}$ radical [$A_x(^{81}\text{Br}) = 138$ G] while the inner features are probably due to the $\text{H}_2\dot{\text{C}}-^{28}\text{Si}\begin{matrix} \text{Br} \\ \diagdown \\ \text{Me}_2 \end{matrix}$ radical. Annealing produced the movement inwards, and increased resolution of, the $\text{Me}_2^{28}\dot{\text{Si}}\text{Br}$ radical features, enabling an $A(^1\text{H})$ hyperfine coupling of 6.6 G to be extracted before the species finally disappeared. The multitude of features remaining precluded any further definitive spectral interpretation.

Pure trimethyliodosilane (Me_3SiI)

Figs. 6a and 6b show the spectra generated at 77 K and ca. 140 K respectively after γ -radiolysis of Me_3SiI at 77 K. The $\text{H}_2\dot{\text{C}}-^{28}\text{Si}\begin{matrix} \text{I} \\ \diagdown \\ \text{Me}_2 \end{matrix}$ radical is clearly generated, the features in the wings could be due to perhaps either the $\text{Me}_2^{28}\dot{\text{Si}}\text{I}$ radical or the $(\text{Me}_3^{28}\text{SiI})^-$ anion with an $A(^1\text{H})$ of ca. 22 G. Unfortunately, this $A(^1\text{H})$ coupling constant is in excess of what one would predict for the species suggested. Coupling to an iodine atom is the probable reason for the spectrum spreading over

Figure 5

γ -radiolysis of Me_3SiBr at 77 K.



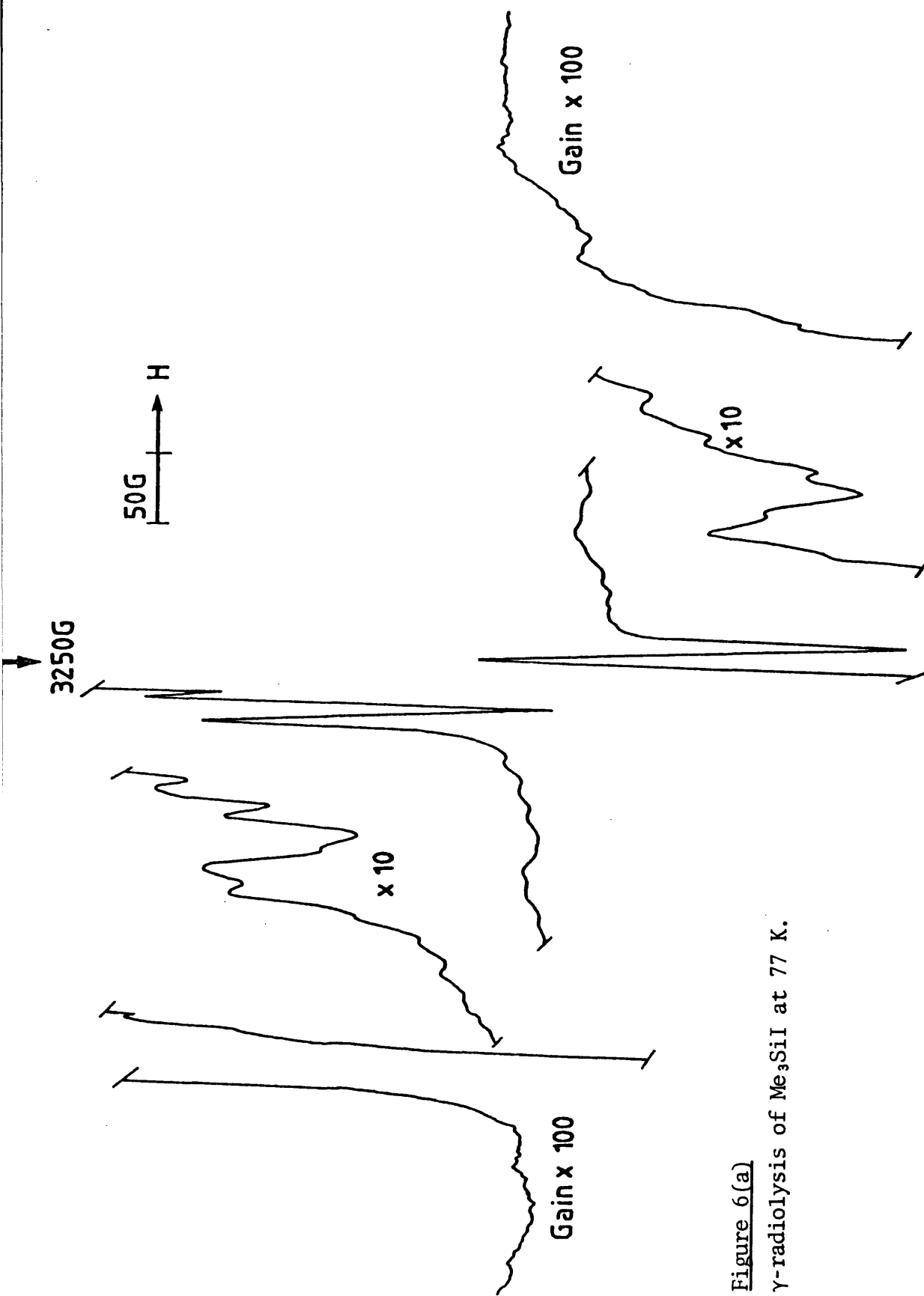


Figure 6(a)
 γ -radiolysis of Me_3SiI at 77 K.

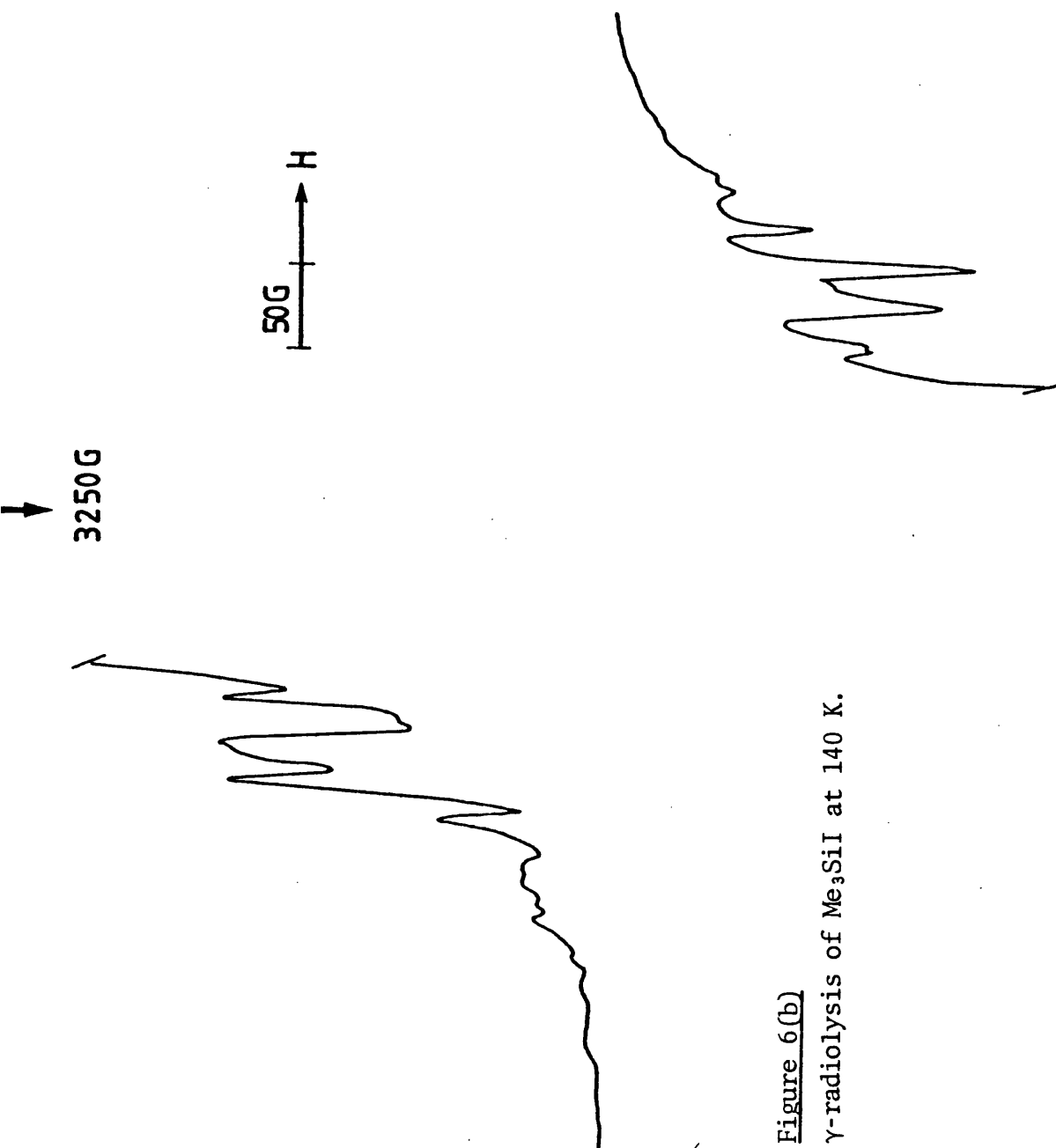


Figure 6(b)
 γ -radiolysis of Me₃SiI at 140 K.

a range of ca. 600 G, however, the spectrum remains, in our view, too complicated for analysis.

TMS in the adamantane-d₁₆ matrix

Although the $\text{H}_2\dot{\text{C}}^{28}\text{SiMe}_3$ radical is the only species apparent immediately after γ -radiolysis at 77 K, (Fig. 7a), annealing did generate unambiguous $\text{Me}_3^{28}\text{Si}\cdot$ and $\text{Me}_3^{29}\text{Si}\cdot$ radicals (Fig. 7b).

What is of real significance is the fact that incorporation of the Me_3SiX (X = Cl, Br, I) substrates into the adamantane-d₁₆ matrix did not result in the generation of $\text{Me}_3^{28}\text{Si}\cdot$ or $\text{Me}_3^{29}\text{Si}\cdot$ radicals, neither did there appear to be any feature likely to be attributable to the $(\text{Me}_3\text{SiX})^-$ anion. In view of the past efficiency at generating electron gain species in the adamantane matrix (e.g. the $\text{R}\cdot/\text{X}^-$ adducts - see chapters 2-4 inclusive), the absence of the $(\text{Me}_3\text{SiX})^-$ anion, or its breakdown product the $\text{Me}_3\text{Si}\cdot$ radical, seems quite remarkable.

Even more remarkable is the lack of any anion formed in the TMS matrix even though Hasegawa et al. have achieved such good results from other anions in this particular medium.

CONCLUSION

The aims of this particular piece of work were to (a) prove the conclusions of Roncin¹ to be incorrect and (b) isolate and detect either the $(\text{Me}_3\text{SiX})^-$ anion (II or III) or the $\text{Me}_3\text{Si}\cdot/\text{X}^-$ adduct (I).

The latter aim was left completely unfulfilled. For reasons which completely elude us, electron addition to the organohalosilanes does

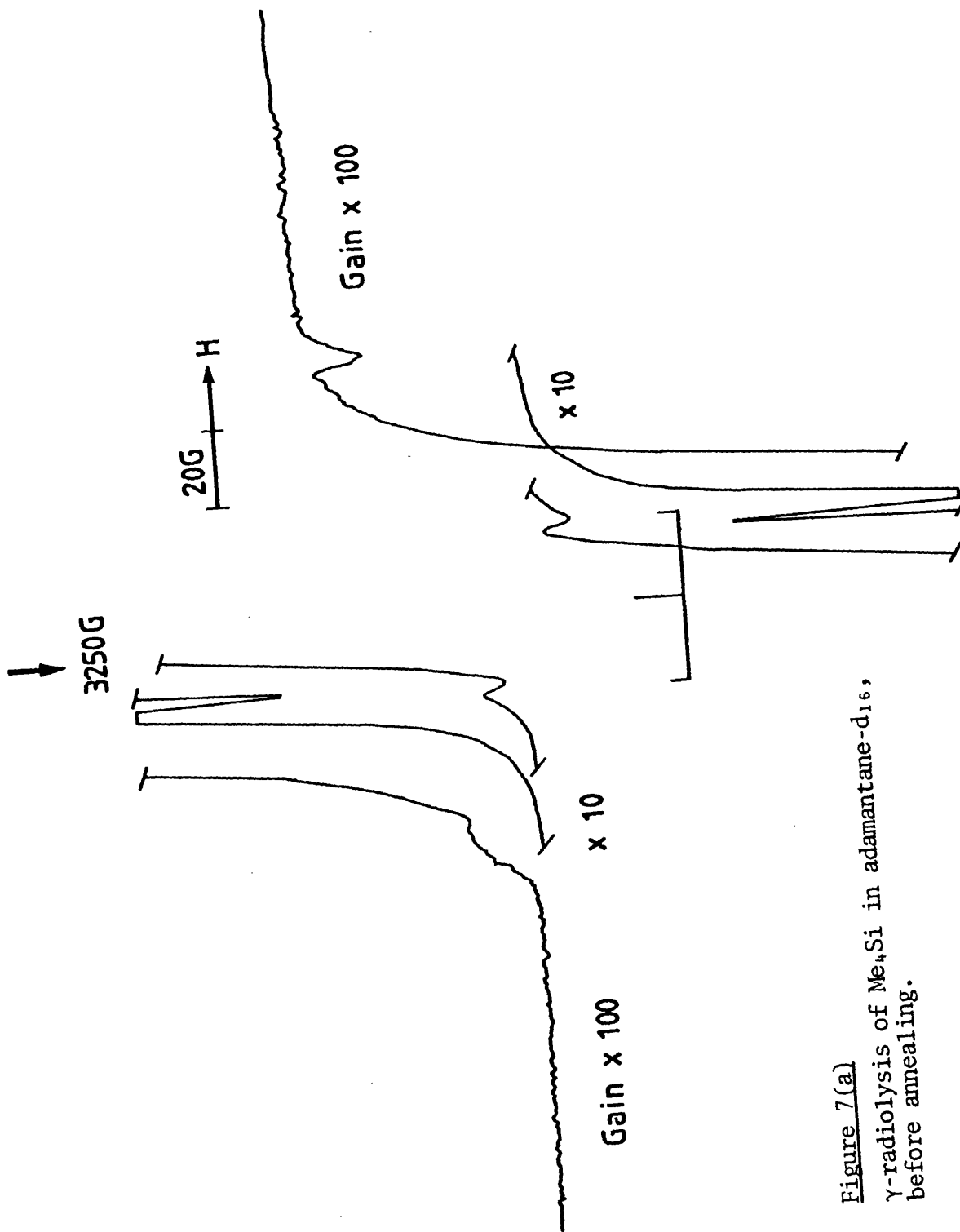


Figure 7(a)
 γ -radiolysis of Me_4Si in adamantane-d_{16} ,
 before annealing.

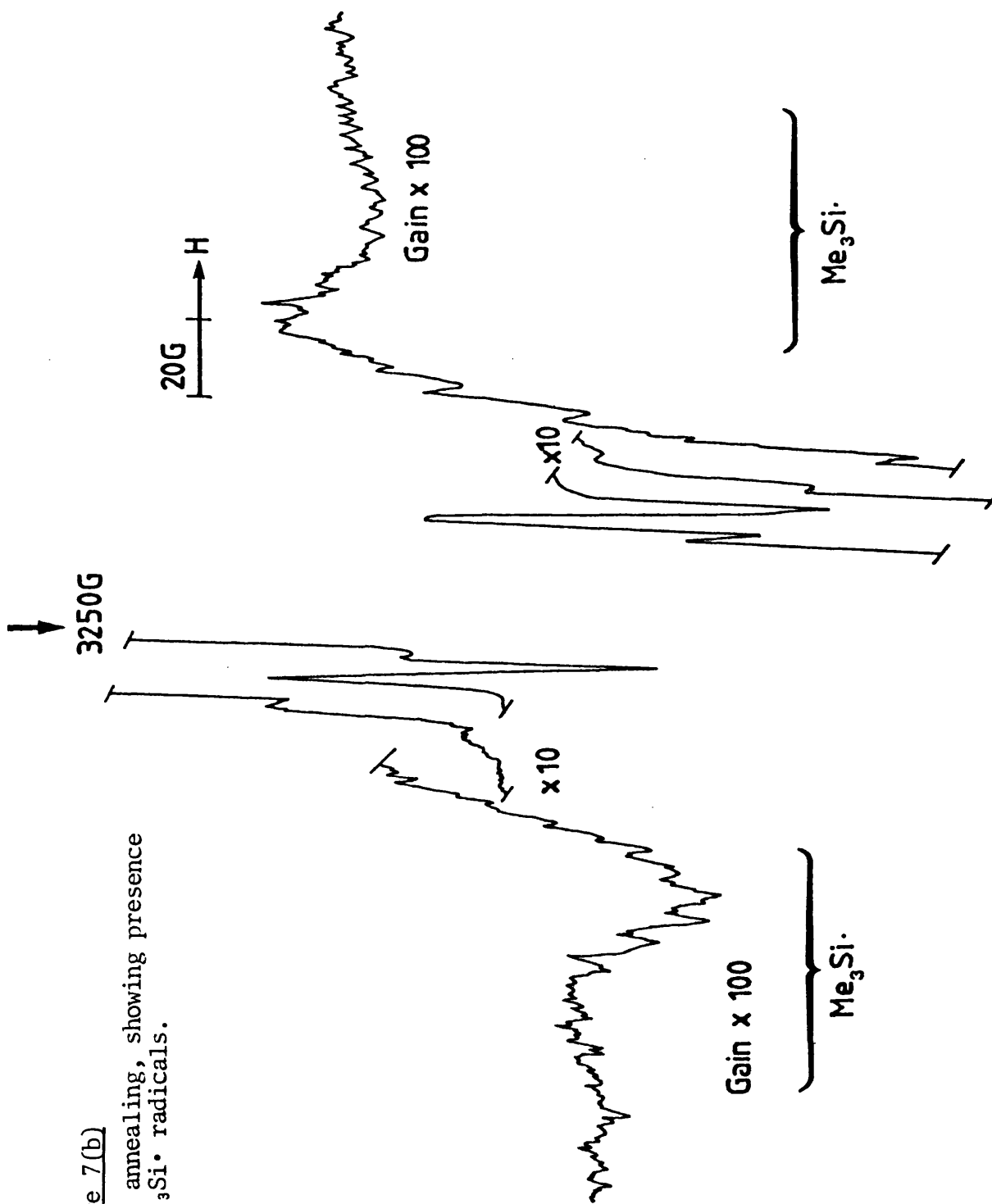


Figure 7(b)
 After annealing, showing presence
 of Me₃Si· radicals.

not appear to be as straightforward as electron addition to organic halides.

With regards to the first aim, while proving his assignment of the spectrum in Fig. 3_b to the $\text{Me}_2\dot{\text{Si}}\text{Cl}$ radical to be correct [species (B)] we have failed to assign species (A). However, there are perhaps five complementary reasons why we believe Roncin has to be wrong.

- (i) In the experiment of Roncin, $\text{Me}_3\text{Si}\cdot$ radicals are needed to decay long before $\text{Me}_2\dot{\text{Si}}\text{Cl}$ radicals. I see no obvious reason why this should be the case.
- (ii) In the experiment of Roncin, if species (A) was indeed the $\text{Me}_3^{29}\text{Si}\cdot$ radical (see Fig. 3_a) then there should have been an overwhelming contribution to the spectrum by $\text{Me}_3^{28}\text{Si}\cdot$ radicals. As can be seen, this is clearly not the case.
- (iii) The γ -radiolysis of pure Me_3SiBr and pure Me_3SiI did not generate $\text{Me}_3^{28}\text{Si}\cdot$ radicals.
- (iv) The γ -radiolysis of Me_3SiCl , Me_3SiBr , and Me_3SiI in the adamantane- d_{16} matrix does not generate $\text{Me}_3\text{Si}\cdot$ radicals, contrary to prediction, even though tetramethylsilane does. This implies $\text{Me}_3\text{Si}\cdot$ radicals need not be generated by the γ -radiolysis of pure Me_3SiCl .
- (v) Experience⁹ in this laboratory and elsewhere over the years is clearly in contradiction to the conclusions of Roncin. While the published parameters for certain species generated by different means and in different environments have varied from time to time, any discrepancies are almost certainly human in character and are due to variations in interpretive techniques and not to true variations in spectral properties.

REFERENCES

1. C. Hesse, N. Leray, J. Roncin, *J. Chem. Phys.*, 1972, 57, 749.
2. J. H. Sharp, M. C. R. Symons, *J. Chem. Soc. (A)*, 1970, 3084;
P. K. Krusic, J. K. Kochi, *J.A.C.S.*, 1969, 91, 3938;
S. M. Bennett, C. Eaborn, A. Hudson, R. A. Jackson, K. D. J. Root,
J. Chem. Soc. (A), 1970, 348.
3. S. Uchimura, A. Hasegawa, M. Hayashi, *Mol. Phys.*, 1979, 38, 413.
4. S. Uchimura, A. Hasegawa, M. Hayashi, *Mol. Phys.*, in print.
5. S. Uchimura, A. Hasegawa, M. Hayashi, *J.C.S. Perkin II*, in print.
6. M. G. Voronkov, B. N. Dolgov, N. A. Dmitrieva, *Doklady Akad. Nauk. SSSR*, 1952, 84, 959.
7. See chapters 2-4 inclusive.
8. P. Schipper, E. H. J. M. Jansen, H. M. Buck, *Topics in Phos. Chem.*, 1977, 9, 407.
9. Landolt-Börnstein, "Magnetic Properties of Free Radicals", eds. H. Fischer, K. H. Hellwege, Springer Verlag, 1977.

CHAPTER 8

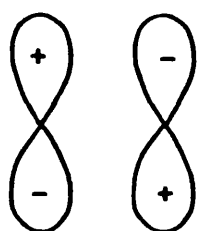
The thermally and photolytically induced
[1,2] hydrogen atom shift

The [1,2] radical shift

The general theory of the principles of orbital symmetry by Woodward and Hoffmann¹ predict that [1,2] hydrogen atom shifts are thermally allowed: the transition state for the sigmatropic rearrangement being considered as the interaction of the H.O.M.O. (Highest Occupied Molecular Orbital) of the rearranging hydrogen atom with the H.O.M.O. of the diradical remaining (see Fig. 1)

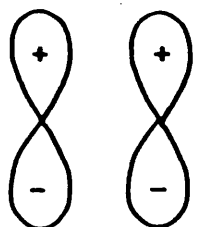
Fig. 1

(a) H.O.M.O. of the $R_2\dot{C}-\dot{C}R_2$ diradical:



Ψ_2

we have two electrons which are fed into the lowest molecular orbital, ψ_1 .



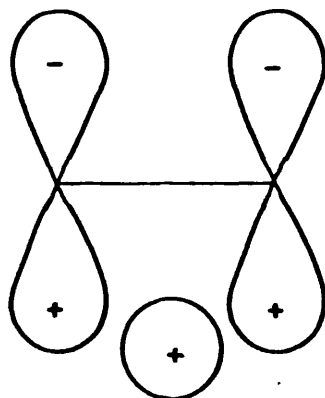
Ψ_1

ψ_1 is, therefore, the H.O.M.O.

(b) H.O.M.O. of the hydrogen atom:

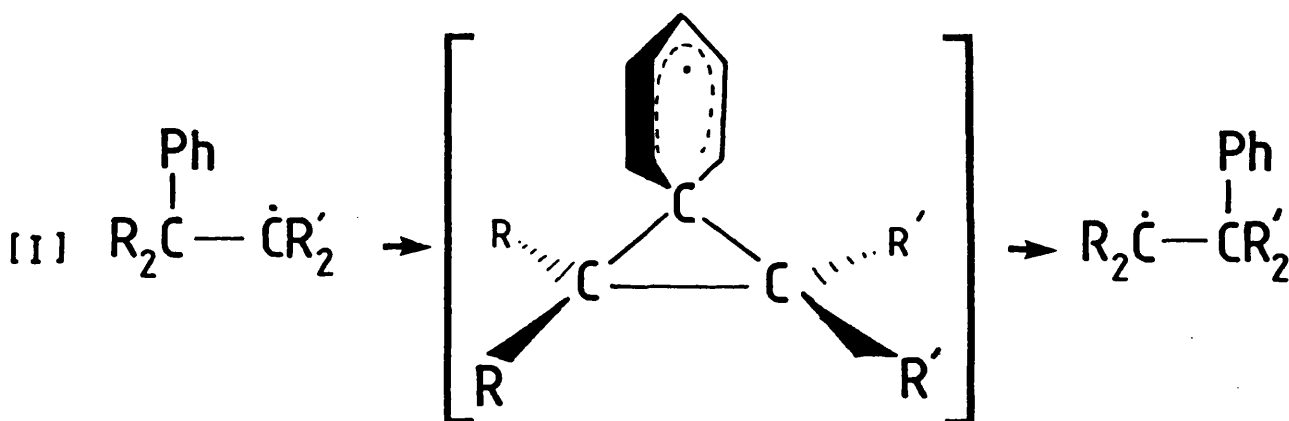


(c) the transition state can be drawn:



The [1,2] hydrogen atom sigmatropic shift, and any [1,2] alkyl radical sigmatropic shift, is therefore permitted suprafacially. However, there is no real, unequivocal evidence that [1,2] hydrogen atom or alkyl group migrations do actually occur in radical reactions. In the few systems where such migrations have been postulated, other, more probable paths could also explain the products.²

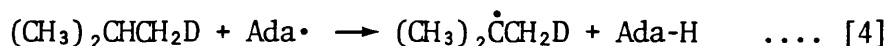
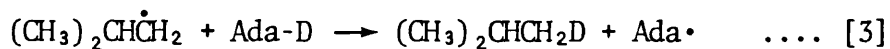
Conversely, [1,2] aryl group migrations are well documented. However, in these cases the reactions are almost certainly not concerted, and there probably exists an intermediate as in reaction [1].



With this background of facts, it was suggested that we had detected a [1,2] intramolecular hydrogen atom shift in our isoBu•/Br⁻ adduct → Bu^t•/Br⁻ adduct rearrangement.³

INTRODUCTION

Chapter 2 documented the rearrangement of the $\text{Me}_2\text{CH}\dot{\text{C}}\text{H}_2/\text{Br}^-$ adduct (Fig. 2a) to the $(\text{CH}_3)_3\text{C}\cdot/\text{Br}^-$ and $(\text{CH}_3)_2\dot{\text{C}}(\text{CH}_2\text{D})/\text{Br}^-$ adducts (Fig. 2b) followed by their dissociation into the $(\text{CH}_3)_3\text{C}\cdot$ and $(\text{CH}_3)_2\dot{\text{C}}(\text{CH}_2\text{D})$ radicals.³ It was suggested that the competing mechanisms involved were an intramolecular rearrangement (reaction [2]) and an intermolecular hydrogen atom exchange process with the adamantane- d_{16} matrix (reactions [3] and [4]).



This intramolecular rearrangement, however, met with some resistance, due to the reasons just rehearsed, and it was suggested that the hydrogen atom pick-up by the $\text{isoBu}\cdot$ radical was not via reaction [2] but via an intermolecular reaction with the ca. 1% of protonated impurities present in the adamantane- d_{16} sample. Subsequent work in this laboratory, documented in chapter 3, then demonstrated the analogous $\text{nPr}\cdot/\text{Br}^-$ adduct \rightarrow $\text{isoPr}\cdot/\text{Br}^-$ adduct rearrangement (Figs. 3a and 3b) to be effectively intramolecular with no detectable contribution from the intermolecular mechanism using precisely the same batch of adamantane- d_{16} . Hence, further evidence in favour of our [1,2] hydrogen atom sigmatropic rearrangement was provided.

We therefore decided to look further into this problem and hopefully produce other results to substantiate our novel and important conclusions. Not only were we interested in the "intra vs inter" story but also in the concept that perhaps the halide ion could contribute to the reaction

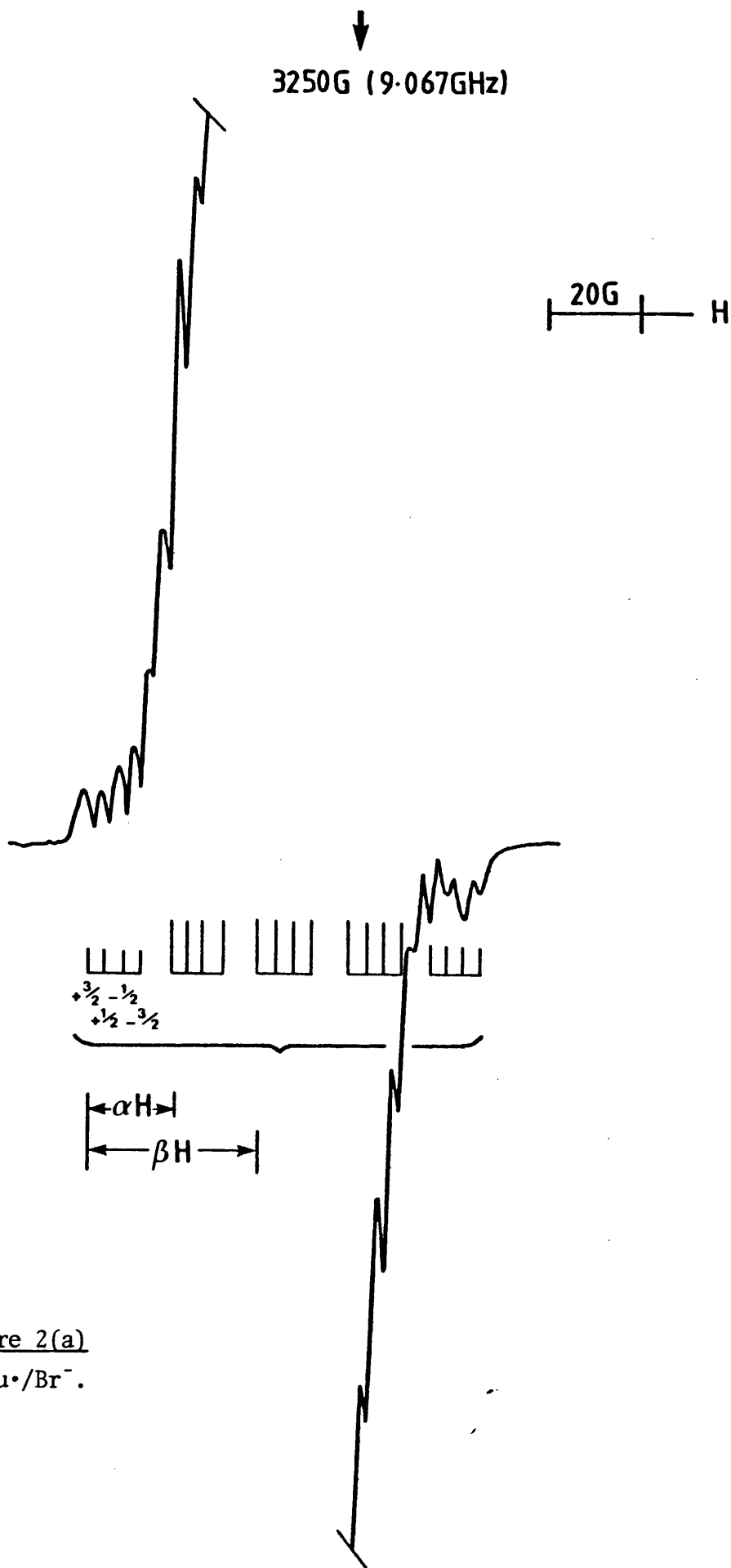


Figure 2(a)
isoBu•/Br⁻.

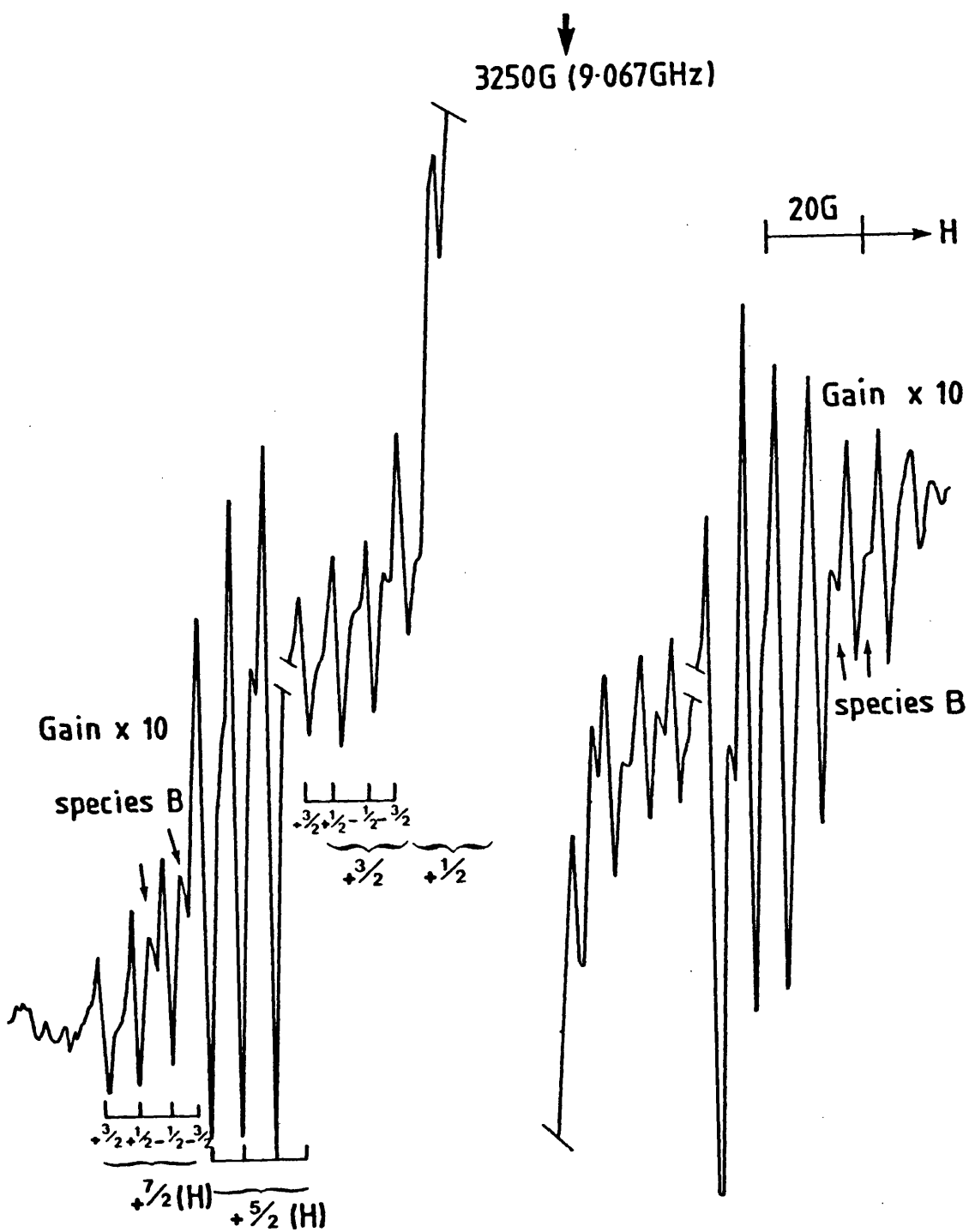


Figure 2(b)

$(\text{CH}_3)_3\text{C}\cdot/\text{Br}^-$ and $(\text{CH}_3)_2\dot{\text{C}}(\text{CH}_2\text{D})/\text{Br}^-$.

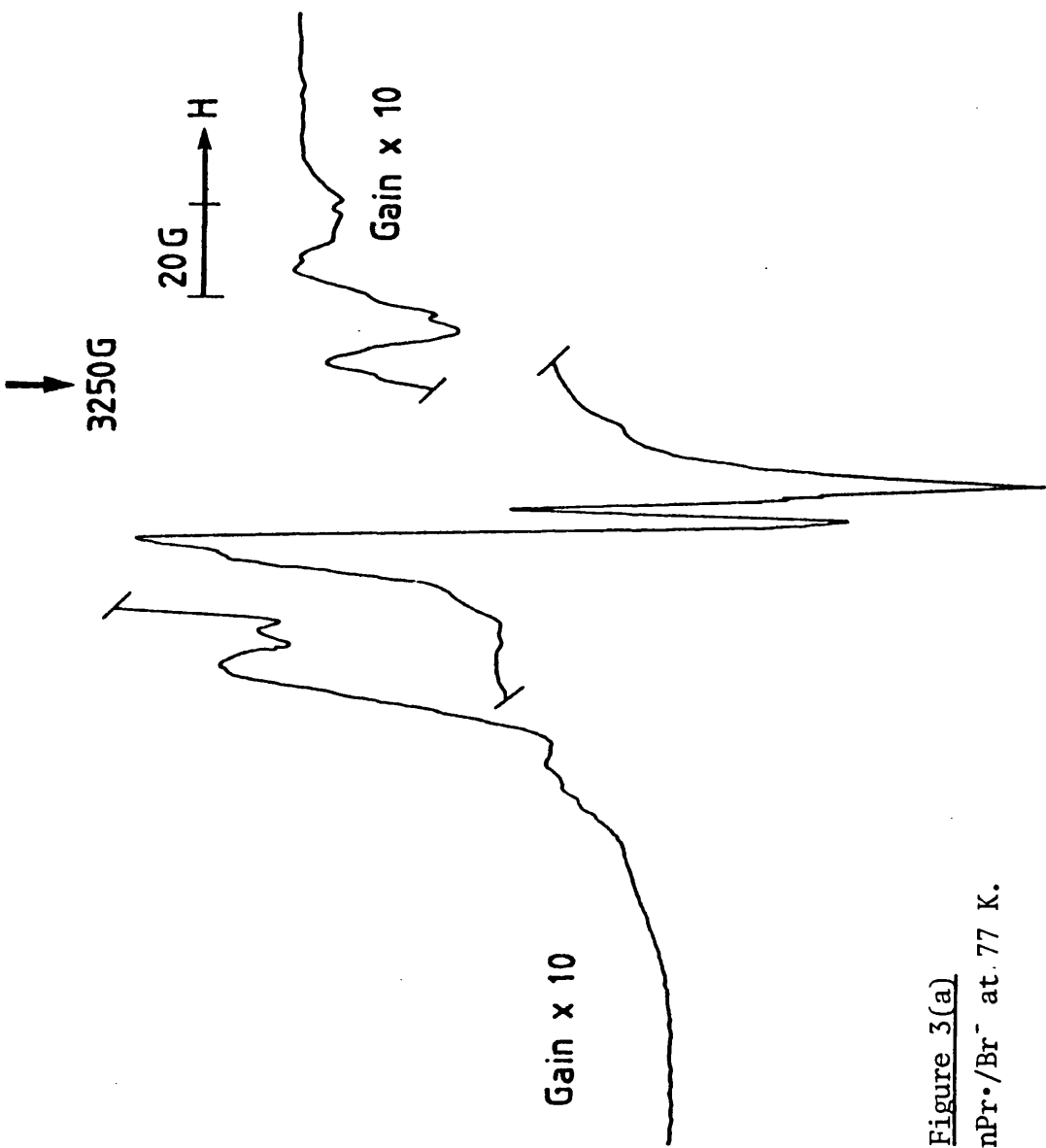
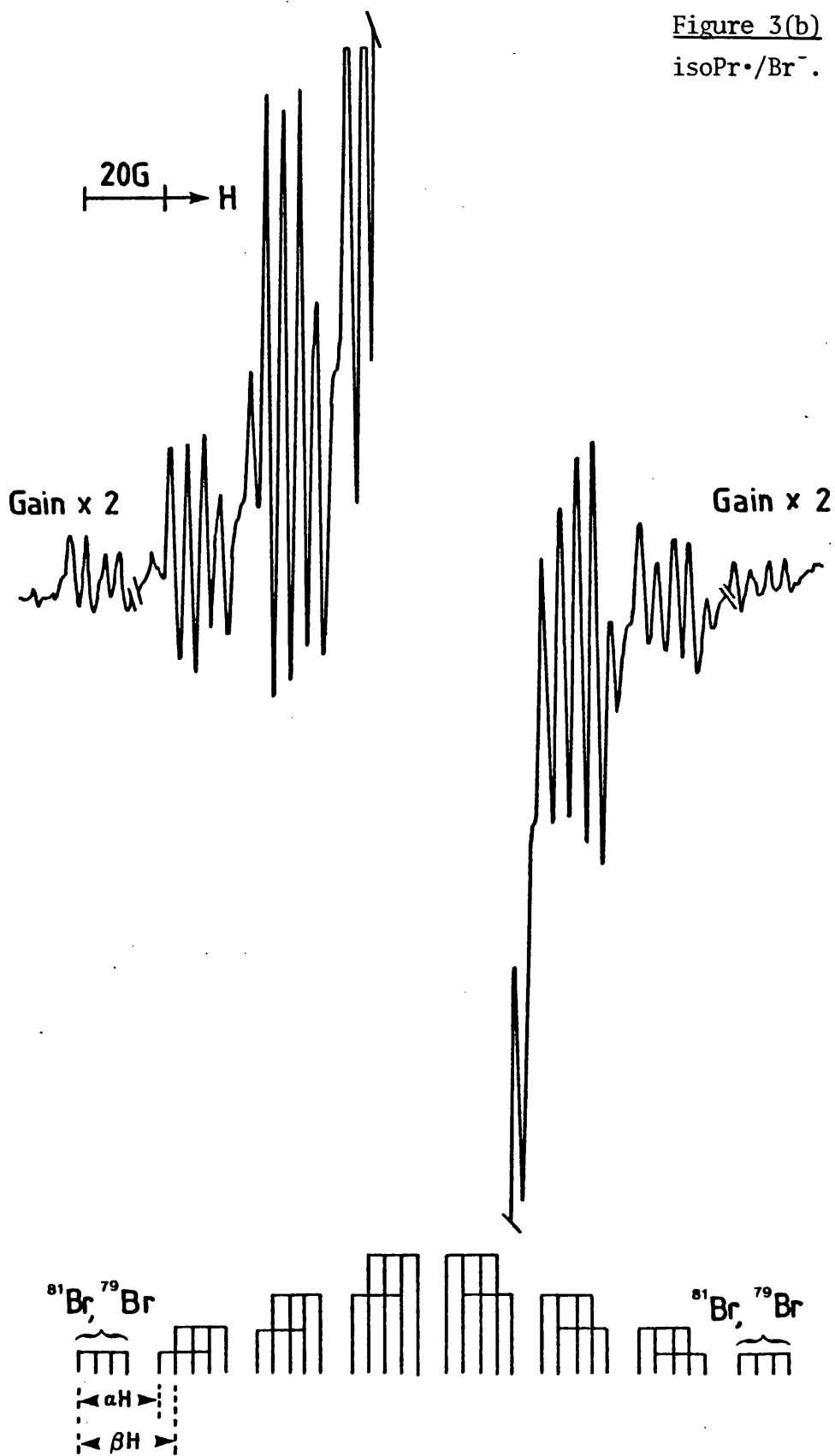


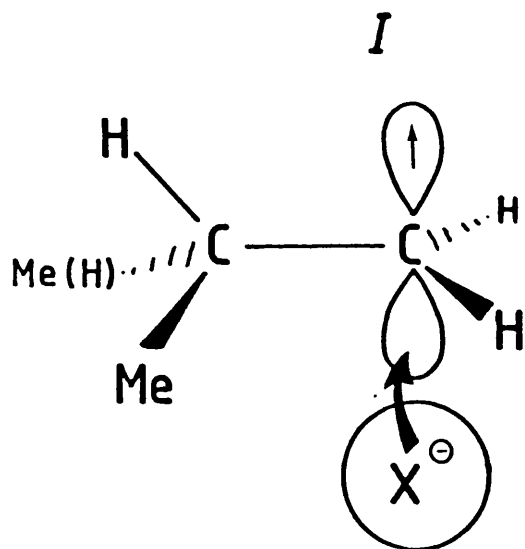
Figure 3(a)
 $nPr\cdot/Br^-$ at 77 K.

↓
3230G

Figure 3(b)
isoPr•/Br⁻.

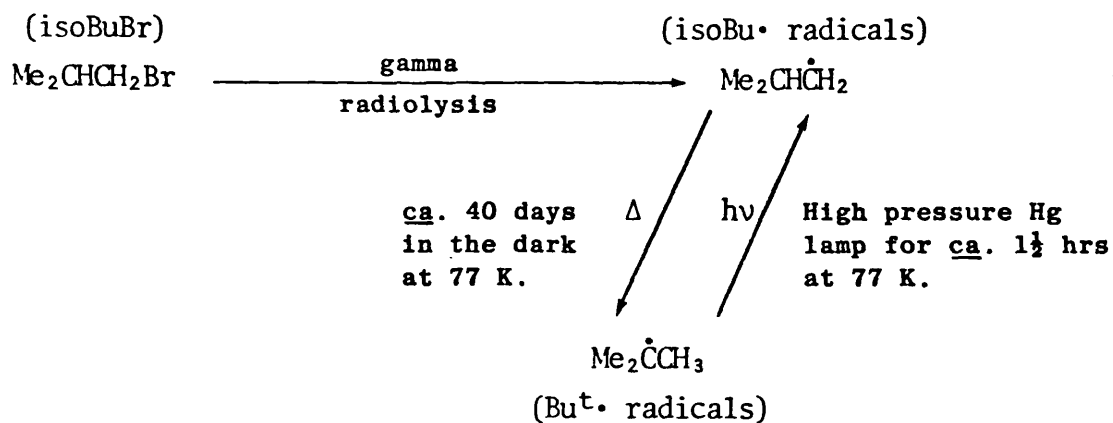


by acting as a catalyst or as an inhibitor. Our solid state results on the adduct show there is considerable charge transfer (ca. 10%) from the halide 'p' orbital into the 'p_z' orbital on carbon, I (see chapter 5), hence, the reactions of the radical may be modified.



Similarly, Iwasaki et al.⁴ have carried out an interesting series of experiments following an observation by Ayscough and Thompson⁵ that the isoBu[•] radical, generated from the γ -radiolysis of isoBuBr, rearranged into the Bu^{t•} radical at 77 K if stored in the dark over a long period of time (ca. 40 days). [Fessenden and Schuler⁶ had found similar results from the irradiation of isobutane in the liquid phase.] It was also found that the Bu^{t•} radical so generated could be rearranged back into the isoBu[•] radical by exposure of the sample to ultra-violet light at 77 K from a high pressure mercury lamp for ca. 1½ hours (Scheme I).

The spectra published by Iwasaki et al. are shown in Fig. 4. Of interest to us was not only the broadness of the spectra attributable supposedly to the free alkyl radicals, but also the A(¹H) hyperfine couplings of 42 G and 21 G for the β - and α - hydrogen atoms respectively



SCHEME I

of the isoBu \cdot radical. The isoBu \cdot radical has exhibited A(^1H) hyperfine couplings of 38.5 G and 21.5 G in other matrices.⁷ It occurred

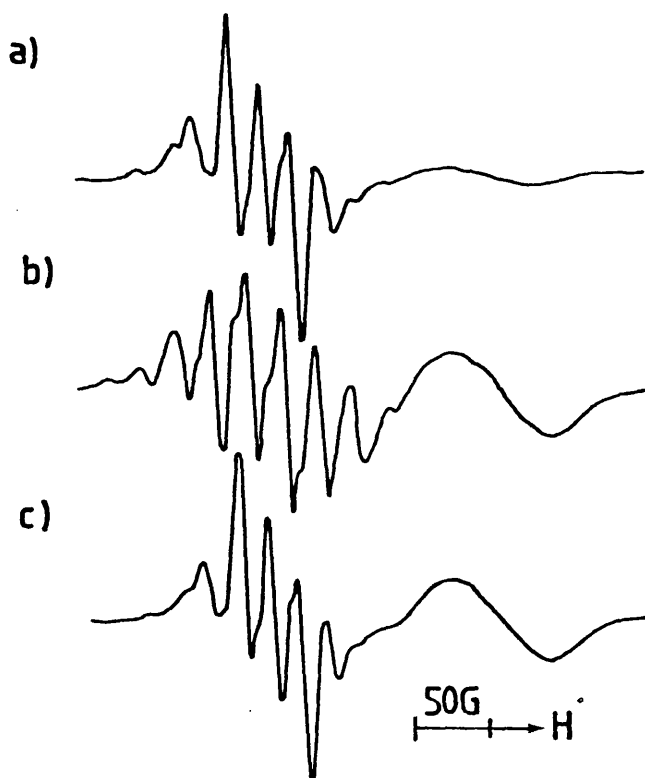
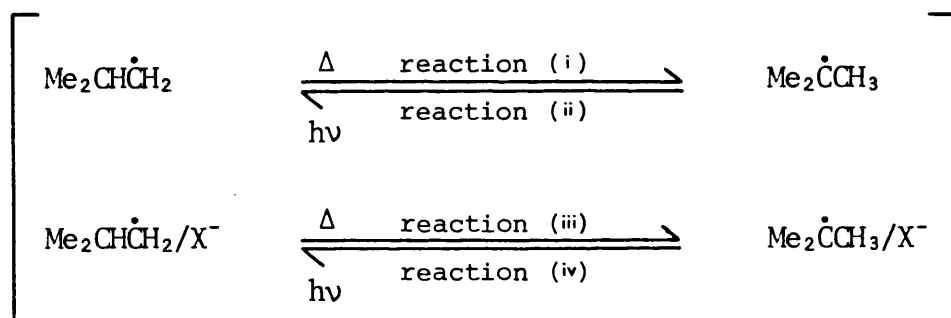


Figure 4

ESR spectra of γ -irradiated isobutyl bromide measured at 77°K: (a) immediately after γ -irradiation at 77°K; (b) after storing in the dark at 77°K; (c) after subsequent exposure to ultraviolet light at 77°K.

to us that perhaps the spectra are attributable not to the free radicals but rather to the $\text{isoBu}\cdot/\text{Br}^-$ and $\text{Bu}^{\cdot}/\text{Br}^-$ adducts. Furthermore, although the authors assumed the rearrangements were intramolecular, there was no evidence to suggest whether either the intermolecular or the intramolecular mechanism was responsible.

Thus, in conjunction with our own results, it was decided to probe similar systems in order to ascertain whether these thermal- and photo-induced rearrangements are intramolecular or intermolecular; and whether the rearrangements are those of the adducts or of the free radicals. These problems can be summarised by the 4 reactions in Scheme II.



SCHEME II

Information known about each reaction

- (i) Ayscough et al. and Iwasaki et al. have studied this reaction.
Could be an adduct rearrangement. Could be inter- or intra-molecular.
- (ii) Iwasaki et al. has shown this can take place. Could be an adduct rearrangement. Could be inter- or intra-molecular.
- (iii) Our results in adamantane- d_{16} have shown this can probably take place via both inter- and intra-molecular pathways.
- (iv) No examples.

The following experiments were carried out:

- (a) The attempted generation of isoBu• radicals in the adamantane-d₁₆ matrix in order to study their thermal rearrangement to Bu^t• radicals and to compare the results with the analogous isoBu•/Br⁻ and isoBu•/I⁻ rearrangements.
- (b) The comparison of the photolysis of the Bu^t• radical and the Bu^t•/Br⁻ adduct in the Bu^tBr matrix.
- (c) The comparison of the photolysis of the Bu^t• radical and the Bu^t•/Cl⁻ adduct in the Bu^tCl matrix.
- (d) The study of the photolysis of the Bu^t• radical in the CD₃OD matrix in order to establish whether the rearrangement is inter- or intra-molecular.
- (e) The comparison of the photolysis of the Bu^t• radical and the Bu^t•/Cl⁻, Bu^t•/Br⁻ and Bu^t•/I⁻ adducts in the TMS matrix.
- (f) The study of the thermal rearrangement of the isoBu• radical in the CD₃OD matrix.

EXPERIMENTAL

Adamantane-d₁₆ (Merck, Sharpe & Dohme), methanol-d₄ (B.D.H.), tertiary butyl chloride (B.D.H.), tertiary butyl bromide (B.D.H.), tertiary butyl iodide (B.D.H.), tetramethylsilane (B.D.H.), n-butyric acid (Aldrich), and 3-methylbutyric acid (Fluka) were all used as supplied.

Incorporation of substrates into the adamantane matrix was carried out by recrystallising the adamantane from the substrate. All samples were placed individually into 4 mm o.d. quartz tubes and degassed via the freeze-thaw method prior to the tube being sealed.

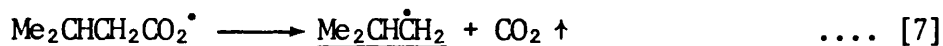
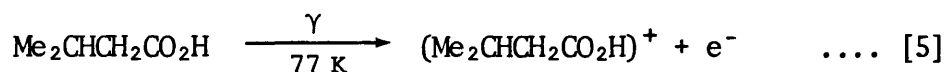
Photolysis of samples was carried out by placing the sample tubes in a quartz 'finger' dewar containing liquid nitrogen and then irradiated using a high-pressure mercury lamp placed external to the dewar.

Gamma radiolysis of samples and recording of spectra were carried out as described in chapter 2.

RESULTS AND DISCUSSION

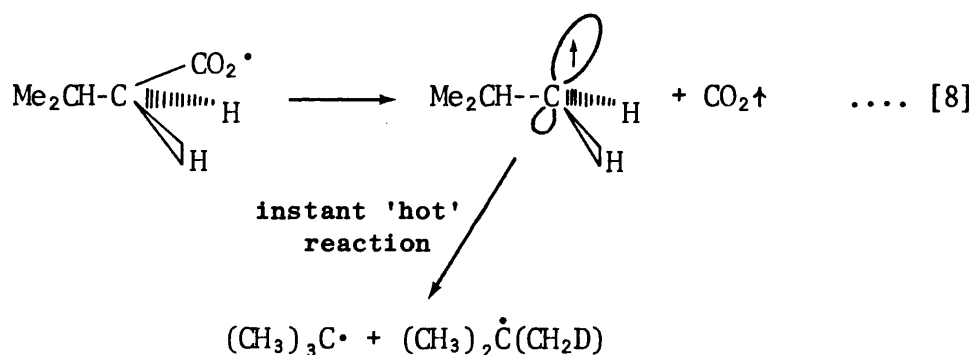
(a) Attempted generation of isoBu• radicals (and nPr• radicals) in the adamantane-d₁₆ matrix

Unfortunately, isoBuBr⁷ and isoBuI⁸ generate their respective adducts on γ -radiolysis in the adamantane matrix, while isoBuCl⁹ generates a high yield of β -chloro radicals with no real sign of the isoBu• radical, adducted or not. 3-methylbutyric acid (Me₂CHCH₂CO₂H) was therefore selected in the high expectation that this compound would generate the required radical via reactions [5] \rightarrow [7]; and that a close, temperature dependent study of its rearrangement into the Bu^t• (and/or Me₂C \dot{C} H₂D) radical would shed some light on our catalysis or inhibition suggestion.



Although a high yield of (CH₃)₃C• radicals and (CH₃)₂ $\dot{\text{C}}$ (CH₂D) radicals began to emerge at ca. 92 K (cf. isoBu•/Br⁻ adduct - chapter 2) and continued to do so up to ca. 220 K, there was unfortunately no sign of the isoBu• radical before or after annealing. Hence, the precursor of the Bu^t• radical was not the expected isoBu• free radical

but possibly a species such as the $\text{Me}_2\text{CHCH}_2\text{C} \begin{smallmatrix} \text{O} \\ \text{=} \end{smallmatrix} \cdot$ radical. Perhaps the rearrangement is a "hot reaction", as portrayed in reaction [8].

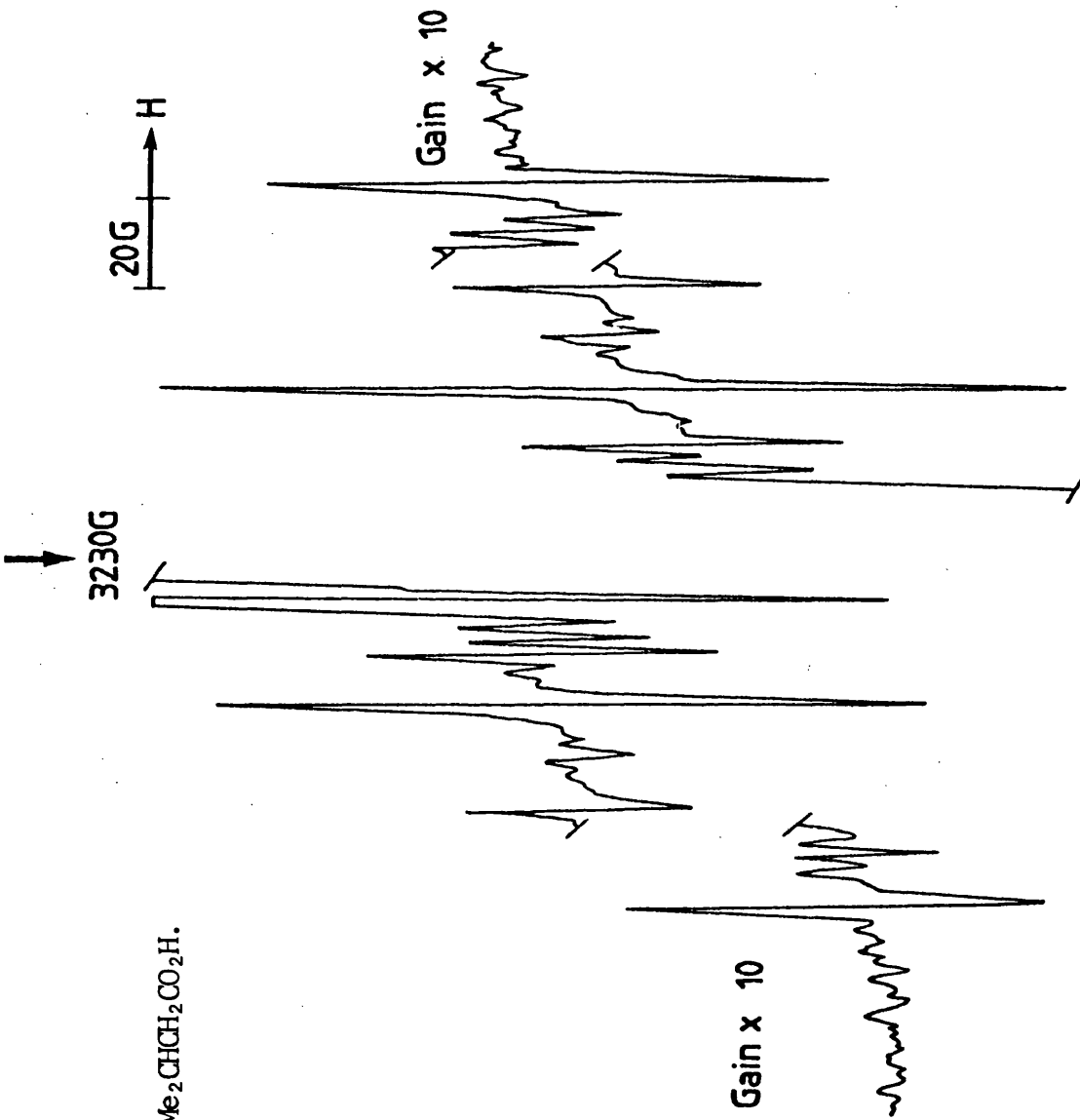


The relative yield of $(\text{CH}_3)_3\text{C} \cdot$ radicals : $(\text{CH}_3)_2\dot{\text{C}}(\text{CH}_2\text{D})$ radicals (Fig. 5a) was very similar to the relative yields from the $\text{isoBu} \cdot / \text{Br}^-$ adduct⁷ and $\text{isoBu} \cdot / \text{I}^-$ adduct⁸ precursors (Figs. 5b and 5c respectively).

Unfortunately, far from supplying us with the answers we required, this particular experiment appeared to pose more questions. Furthermore, when n-butyric acid ($\text{CH}_3\text{CH}_2\text{CH}_2\text{CO}_2\text{H}$) was γ -irradiated in the adamantane- d_{16} matrix, neither $\text{CH}_3\text{CH}_2\text{CH}_2 \cdot$ radicals, $(\text{CH}_3)_2\dot{\text{C}}\text{H}$ radicals, nor $\text{CH}_3\dot{\text{C}}(\text{H})\text{CH}_2\text{D}$ radicals were detected. In view of the results from the previous experiment, this result seemed particularly incongruous. It was then attempted to generate $\text{isoBu} \cdot$ radicals in the adamantane- d_{16} matrix by photolysing $\text{Bu}^t \cdot$ radicals produced from the γ -radiolysis of the $\text{Bu}^t\text{Br}/\text{adamantane}$ system.⁷ This should rearrange the radicals to the desired $\text{isoBu} \cdot$ radicals. Unfortunately, prolonged photolysis (ca. 6 hours with a high pressure mercury lamp) only brought about a conversion of ca. 20%. Furthermore, annealing of the features attributable to the $\text{isoBu} \cdot$ radical did not appear to produce an appreciable growth in $\text{Bu}^t \cdot$ radical concentration.

Figure 5(a)

Precursor: $\text{Me}_2\text{CHCH}_2\text{CO}_2\text{H}$.



↓
3230G (9.088GHz)

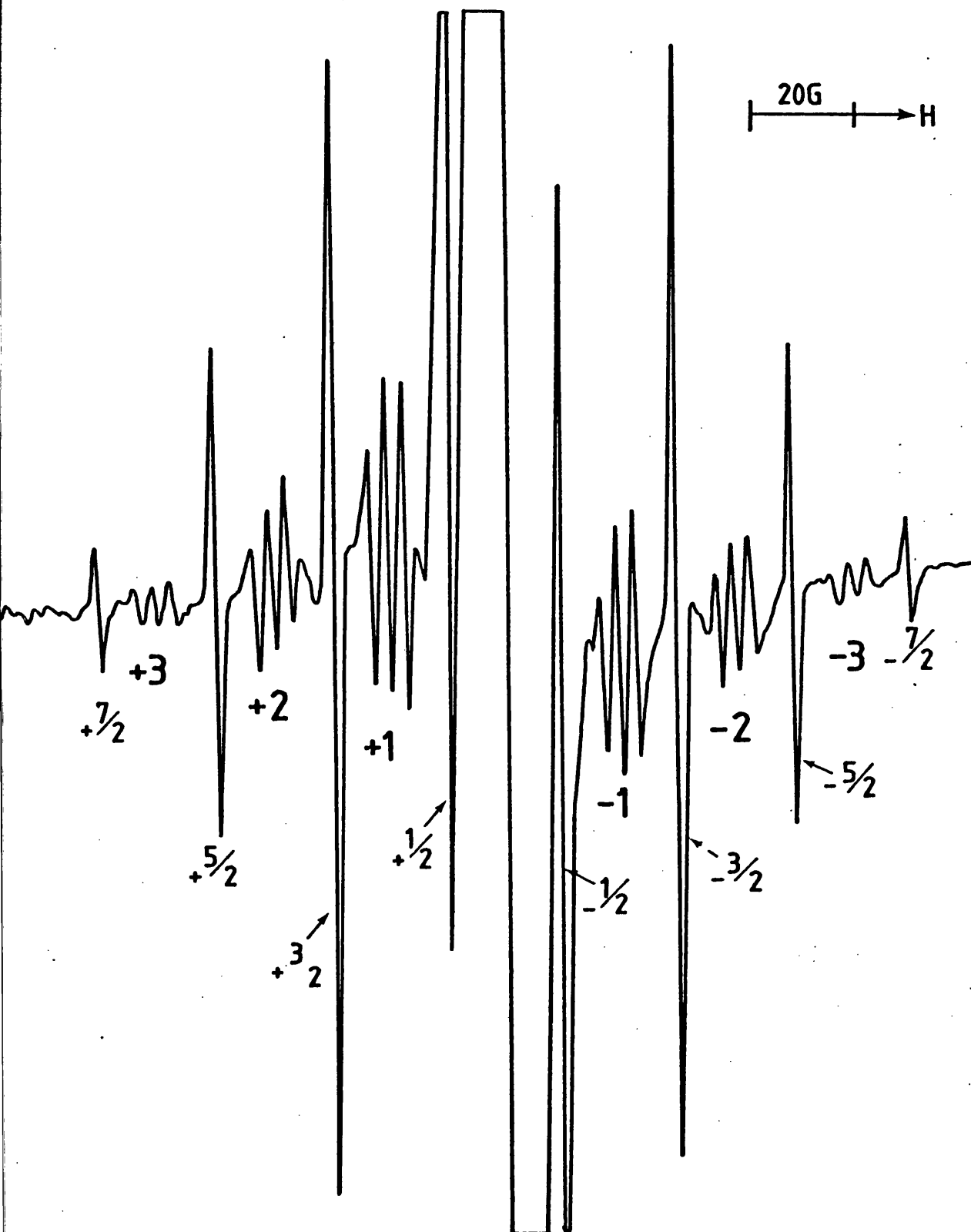


Figure 5(b)

Precursor: isoBu•/Br⁻.

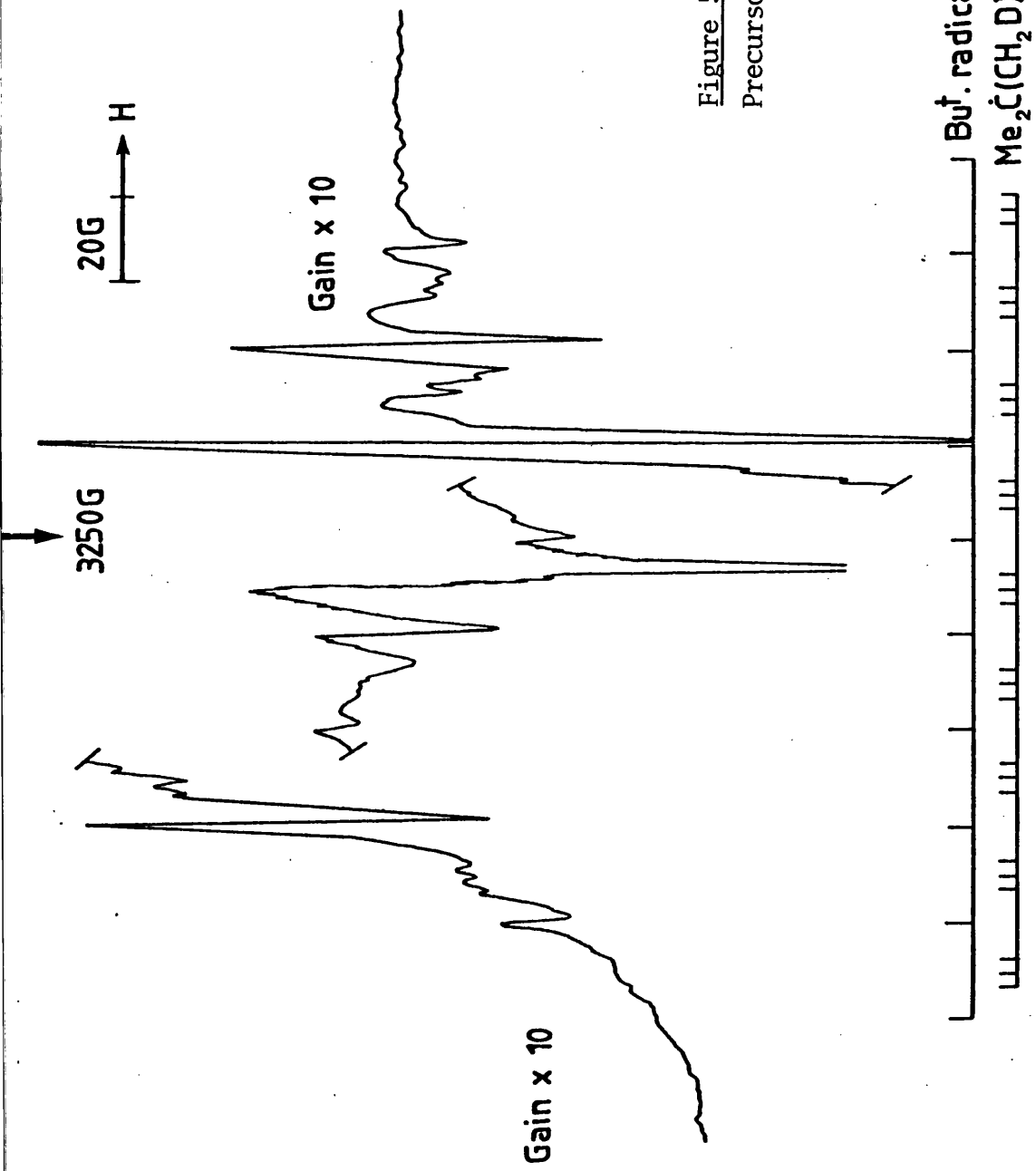


Figure 5(c)

Precursor: isoBu•/I⁻.

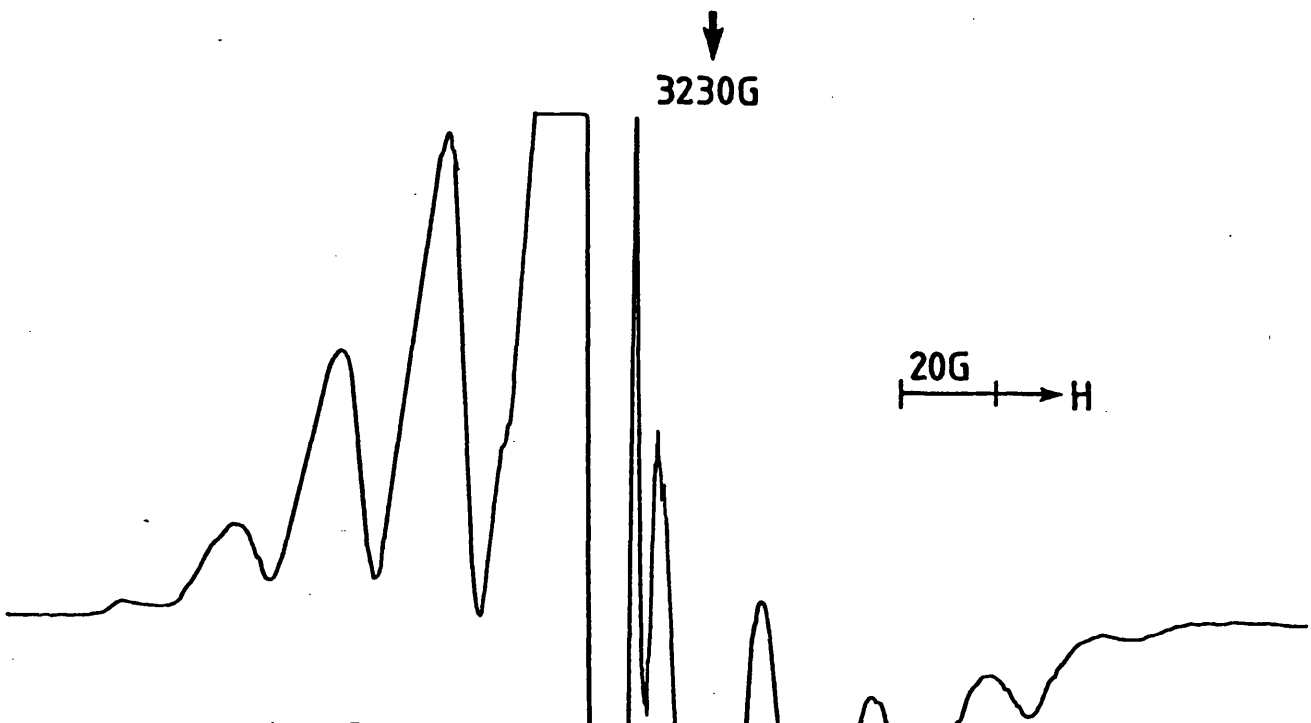
(b) Photolysis in the Bu^tBr matrix

The γ -radiolysis of Bu^tBr generates a broad ten-line spectrum attributable to the Bu^t•/Br⁻ adduct which decays irreversibly into the characteristic, narrow 23 G ten-line spectrum of the Bu^t• radical on annealing.¹⁰ Two samples, one annealed and one not, were therefore photolysed with a high pressure mercury lamp.

(i) Bu^t•/Br⁻ adduct. A quite definite concentration of isoBu• radicals was built up on photolysis. Unfortunately, the Bu^tBr molecule has an ultra-violet absorption in the range required, which results, effectively, in the matrix acting as an internal filter and hence the efficiency of conversion was very low. Figs. 6a and 6b show the spectra of the Bu^t•/Br⁻ adduct, and the products derived from its photolysis after ca. 255 minutes. It is not possible to tell whether the isoBu• radical is adducted or not. Annealing of the sample at this point did not produce a narrowing of the isoBu• radical features (cf. Bu^t•/Br⁻ adduct \rightarrow Bu^t• radical), therefore implying the species is the free radical.

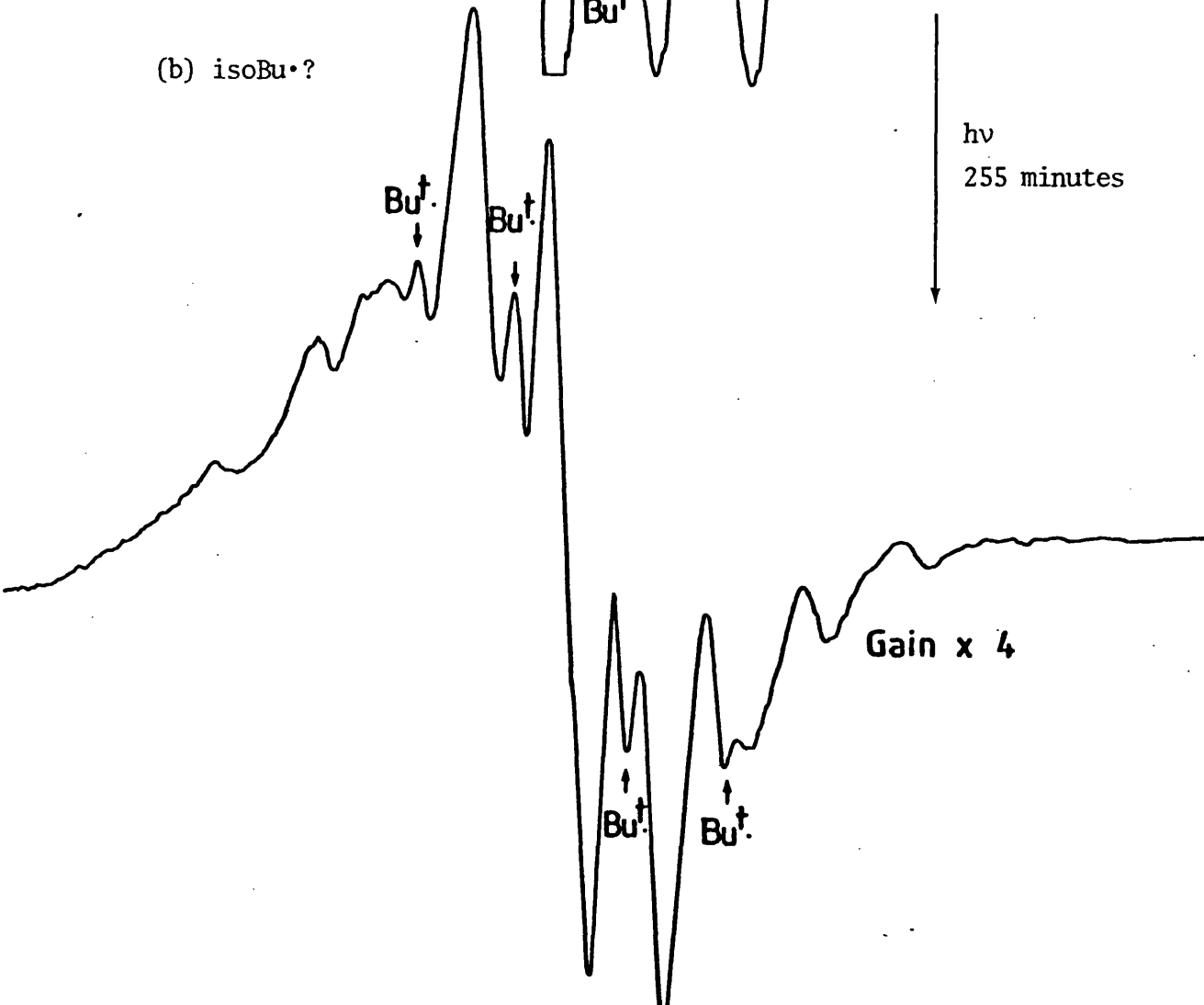
(ii) Bu^t• radical. A higher concentration of isoBu• radicals was generated here than was produced from part (i) of this experiment. The spectrum of the isoBu• radical was identical to that produced from part (i), implying again that the radical is unadducted. Figs. 6c and 6d show the spectra of the Bu^t• radical and of the products derived from its photolysis after ca. 255 minutes

Although by no means as conclusive as the results documented by Iwasaki et al., probably due to the Bu^tBr matrix acting as an internal filter, there is nevertheless a substantial conversion of Bu^t• radicals



(a) $\text{Bu}^\bullet/\text{Br}^-$

Figure 6



(b) $\text{isoBu}^\bullet?$

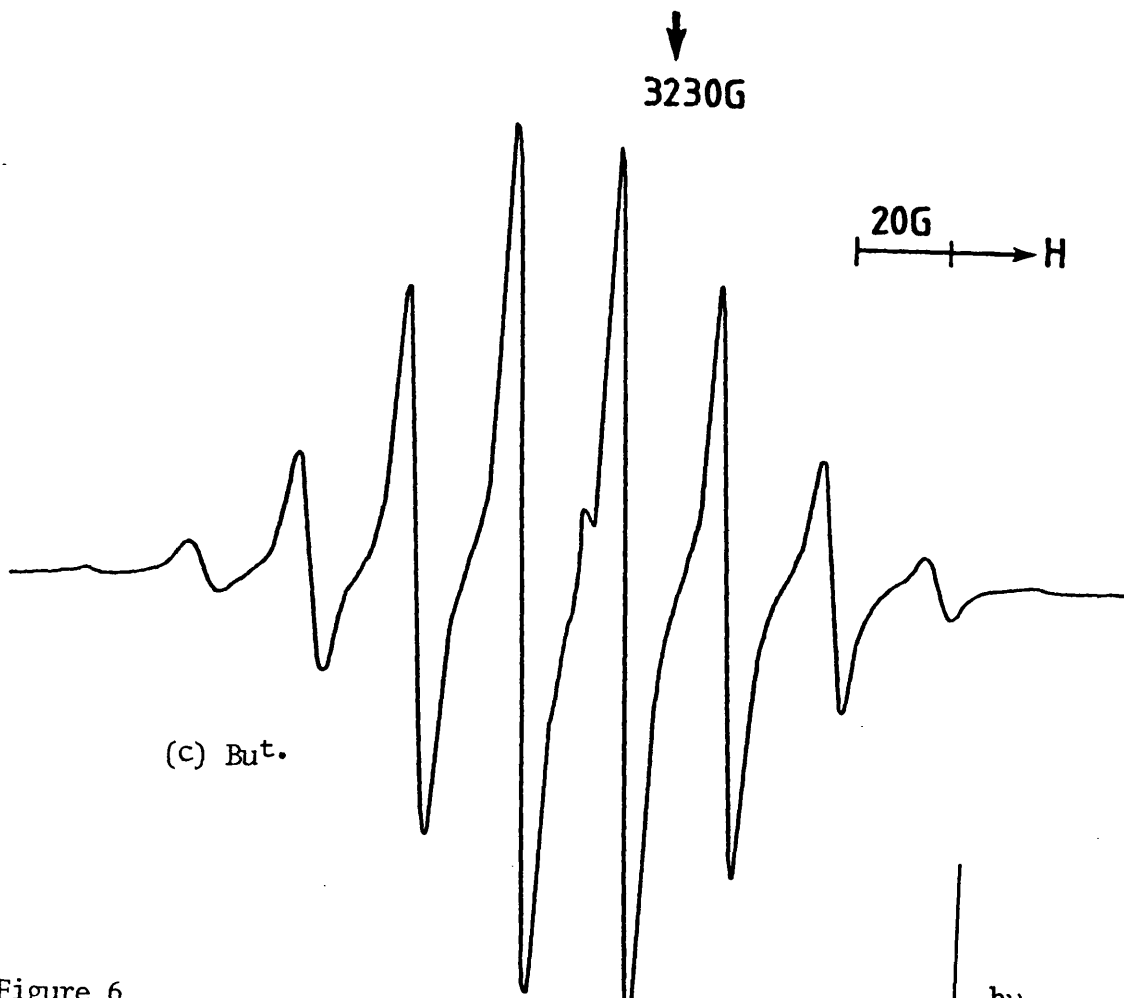
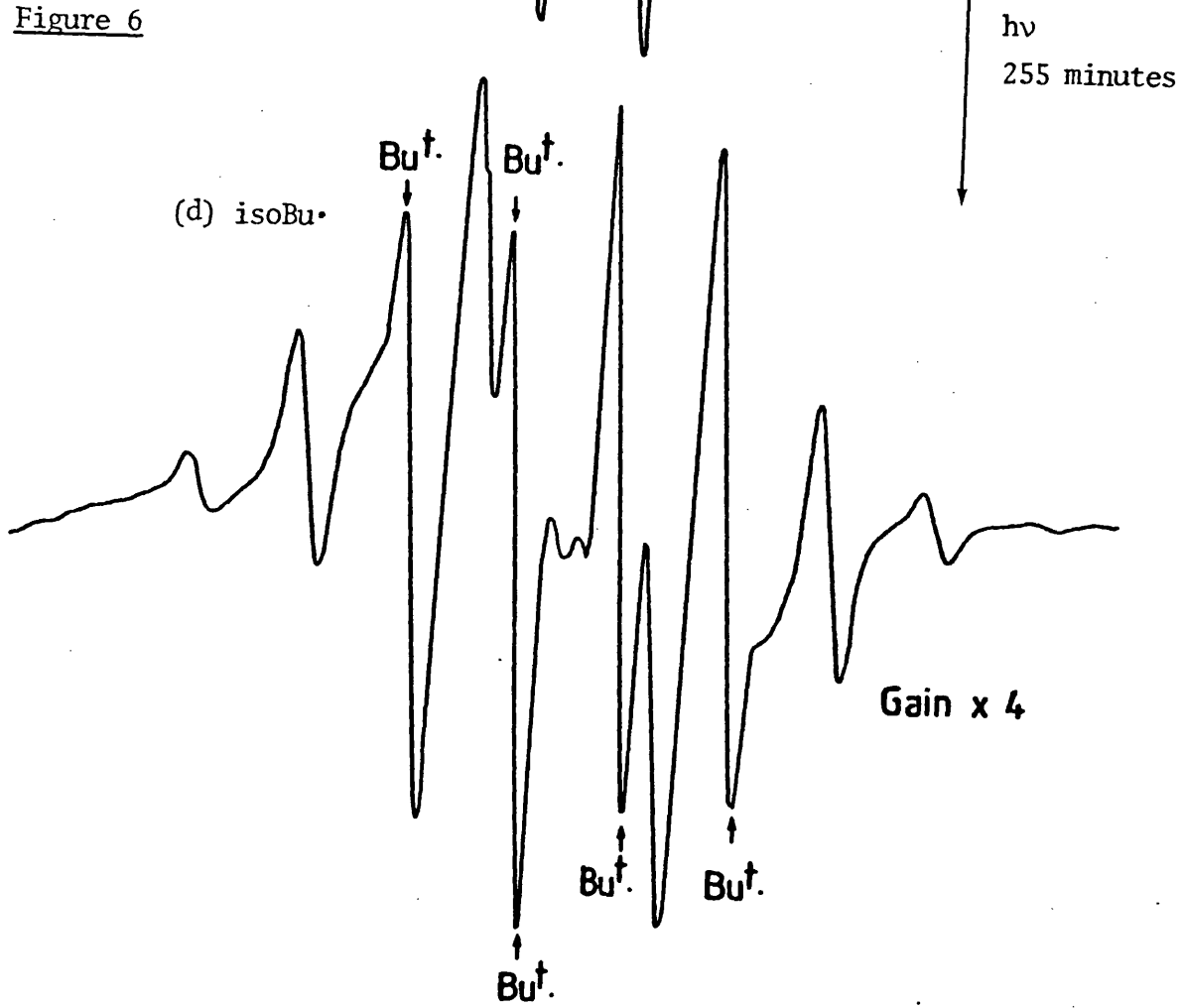


Figure 6



→ isoBu• radicals. This shows, at least, that the photolytically induced conversion is real and is independent of matrix. The relative yields seem to suggest that the presence of the bromide ion interferes with this conversion, and in fact the lack of detection of the isoBu•/Br⁻ adduct does seem to suggest that the Bu^t• radical → isoBu• radical conversion does not take place in the presence of the bromide ion.

(c) Photolysis in the Bu^tCl matrix

Chapter 4 documents the change in form of the spectrum with temperature after γ -radiolysis of Bu^tCl at 77 K. The rigid adduct is generated originally. Marginal annealing produces a less restricted adduct, further annealing produces the free Bu^t• radical. Two samples, one annealed and one not, were therefore photolysed for ca. 45 minutes.

(i) Bu^t•/Cl⁻ adduct (Fig. 7a). Five minutes photolysis resulted in the generation of the same spectrum as that generated from a marginally annealed sample (the less restricted adduct) together with Bu^t• radicals. Photolysis for ca. 45 minutes resulted in a good yield of conversion to isoBu• radicals (Fig. 7b). Annealing did not generate the thermal isomerisation nor the narrowing of the isoBu• radical features.

(ii) Bu^t• radical (Fig. 7c). Photolysis for ca. 45 minutes resulted in a high conversion to isoBu• radicals (Fig. 7d), the concentration being over twice that generated from part (i) of this experiment. Annealing did not generate thermal isomerisation nor the narrowing of the isoBu• radical features.

The results from part (i) seem to suggest that the Bu^t•/Cl⁻ adduct is split into the Bu^t• radical and chloride ion on photolysis prior to rearrangement. This fact, and the lack of detection of the isoBu•/Cl⁻

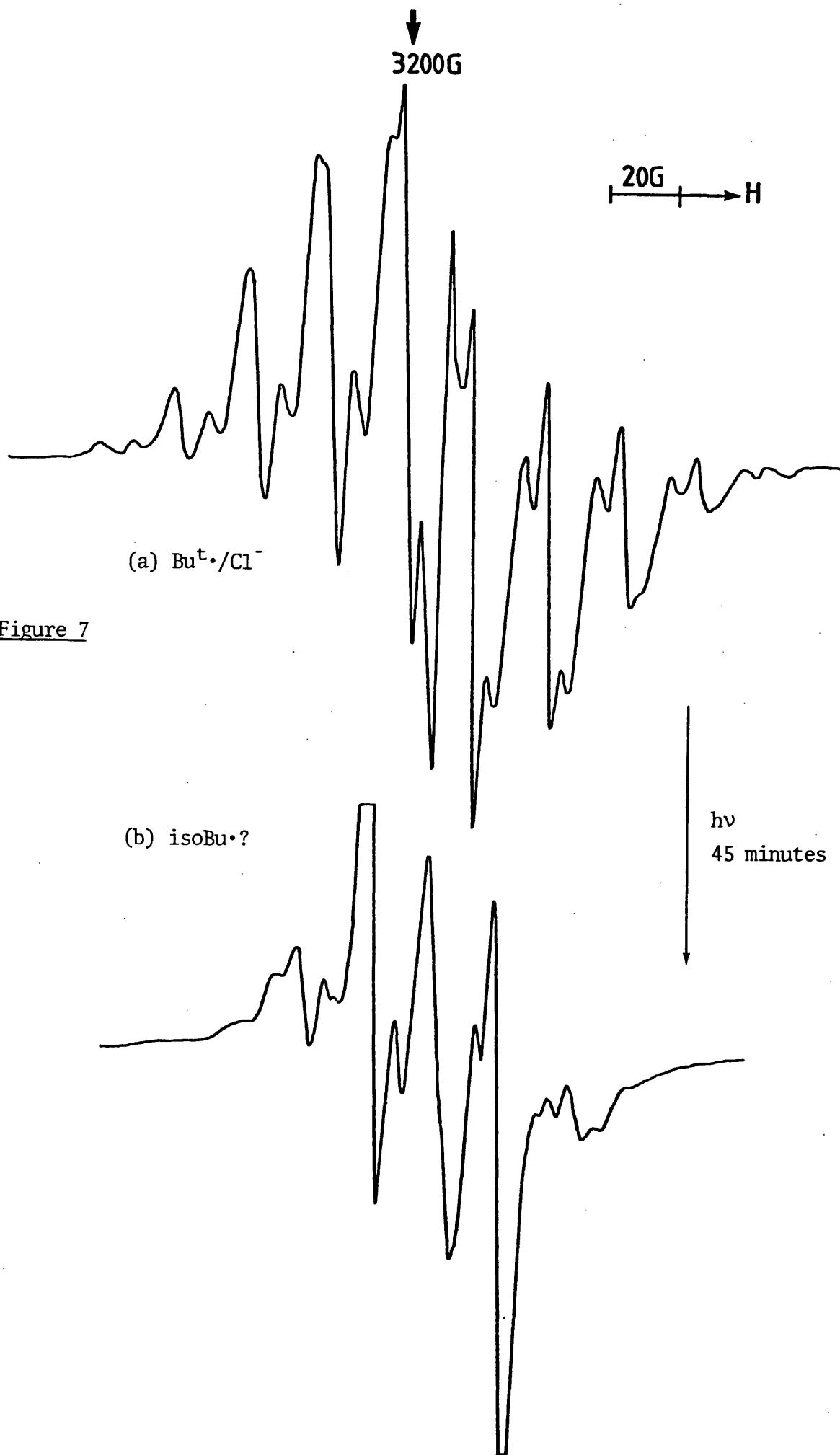
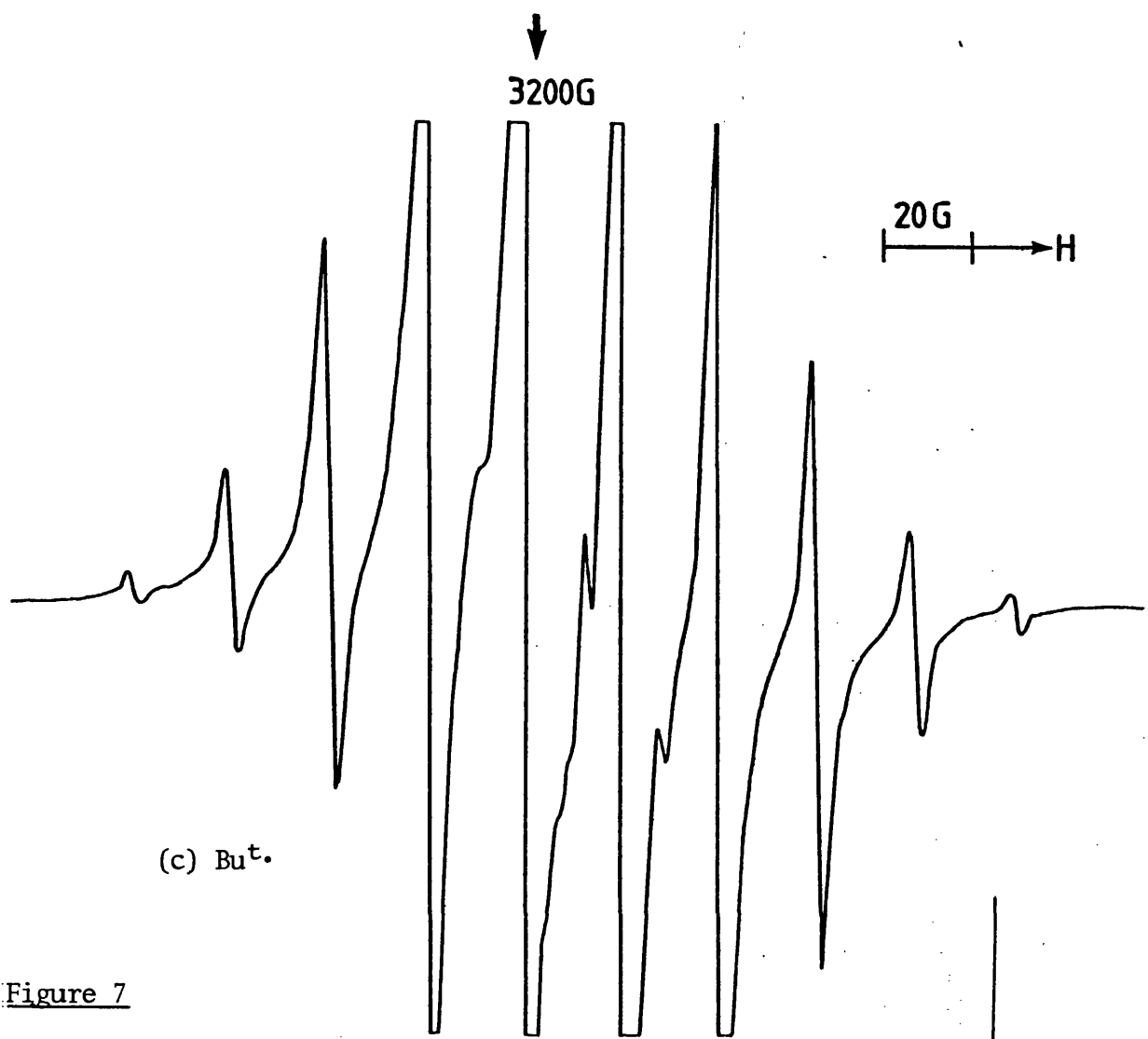
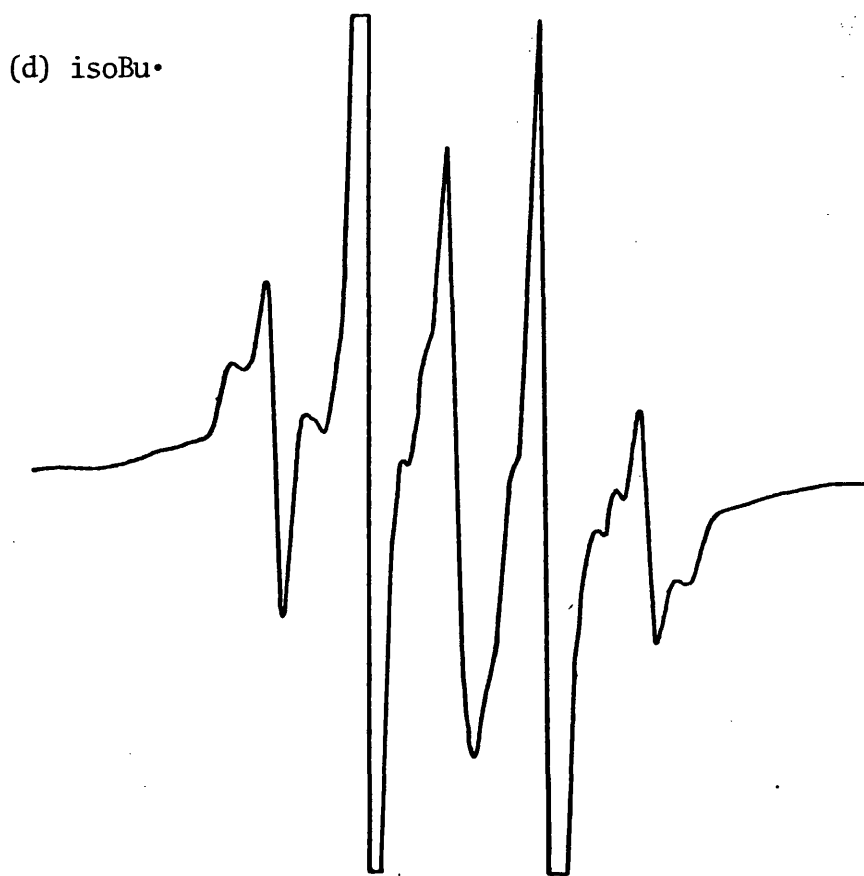


Figure 7



(c) Bu•

Figure 7



(d) isoBu•

↓
hv
45 minutes

adduct, once again implies that it is only the free radical that is photolytically rearranged and not the adduct.

The most prominent observation in this experiment is that the concentration of isoBu• radicals generated from Bu^t• radicals is twice that generated from the Bu^t•/Cl⁻ adduct. Since annealing had to be carried out in order to generate the Bu^t• radical and hence almost certainly resulted in a decrease in the number of radical sites via radical-radical interactions, the presence of the Cl⁻ ion appears to be having a most definite detrimental effect on the photolytically induced isomerisation process.

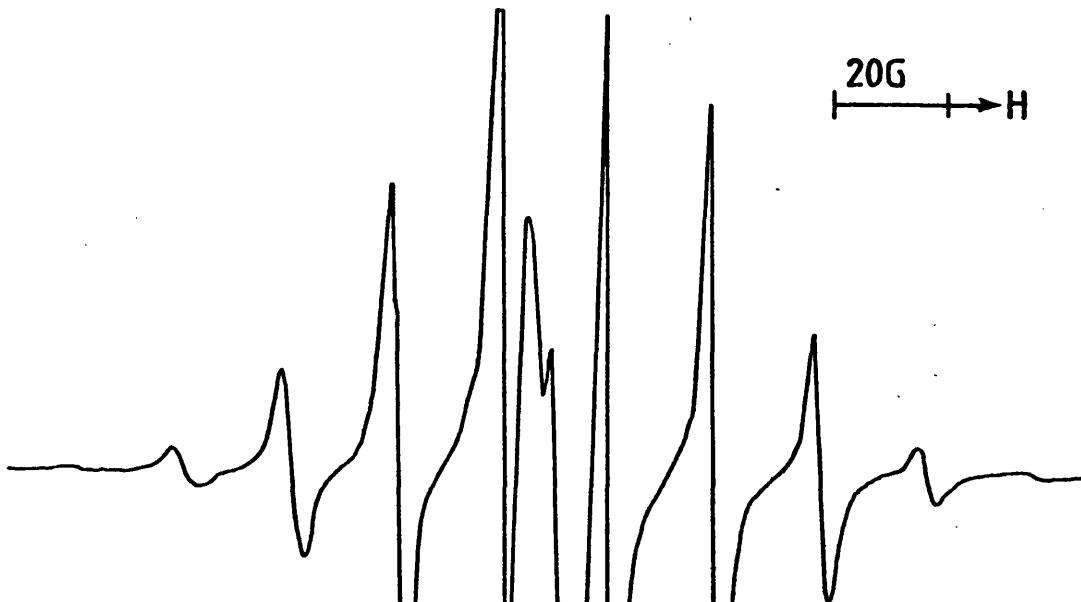
(d) Photolysis in the CD₃OD matrix

A 1 Mol % solution of Bu^tX (X = Cl, Br or I) in CD₃OD was γ-irradiated for ca. 1 hour. Photolysis of the Bu^t• radicals thus formed (Fig. 8a) for ca. 30 minutes generated an efficient yield of isoBu• radicals and CH₃• radicals (Fig. 8b). While not being able, as yet, to define the mechanism responsible for the generation of the CH₃• radicals, the unequivocal conclusion is that the Bu^t• radical → isoBu• radical isomerisation process is intramolecular. Furthermore, by employing the use of filters, it was realised that the active band responsible for this rearrangement resided in the 250 n.m. range.

Analysis of the literature revealed at this point a piece of work by Parkes and Quinn¹¹ where the u.v. absorption spectrum of the Bu^t• radical was reportedly detected. Apparently the Bu^t• radical absorbs over a broad continuum from 220 → 280 n.m. made up from two broad features; the most intense band covering the 220 → 240 n.m. range, the least intense band covering the 240 → 280 n.m. range. The low wavelength band was suggested to be analogous to, though broader than, the spectrum derived from Me• radicals and was essentially a Rydberg transition on

↓
3230G

20G
→ H



(a) Bu^\bullet .

Figure 8

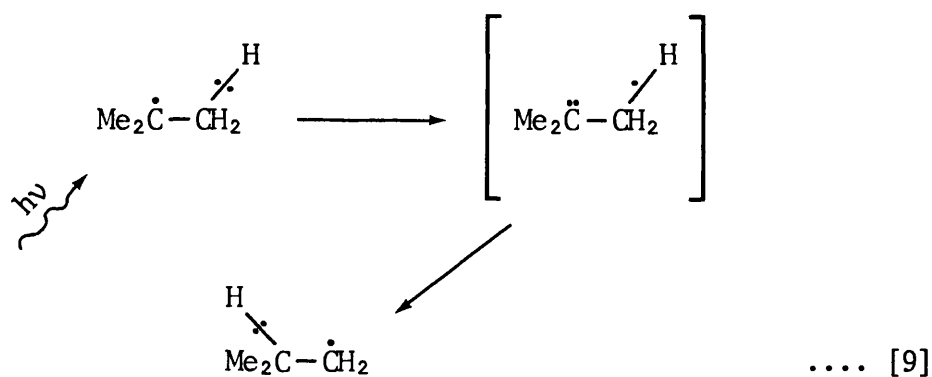
(b) $\text{isoBu}^\bullet + \text{CH}_3^\bullet$.



hv
30 minutes

the carbon atom. The less intense band could not be assigned. We now suggest that this broad, weak 240 → 280 n.m. band is responsible for our photo-induced rearrangement.

Symons has envisaged this rearrangement taking place effectively via an electron movement followed by a proton shift (reaction [9]).



Photolysis in the TMS matrix

By γ -irradiating 1 Mol % solutions of Bu^tCl , Bu^tBr and Bu^tI in TMS, samples of the $\text{Bu}^t\cdot/\text{Cl}^-$ adduct, the $\text{Bu}^t\cdot/\text{Br}^-$ adduct, the $\text{Bu}^t\cdot/\text{I}^-$ adduct and the $\text{Bu}^t\cdot$ radical could be generated. Photolysis of the $\text{Bu}^t\cdot$ radical (Fig. 9a) (produced from the annealing of any of the three $\text{Bu}^t\cdot/\text{X}^-$ adducts) for ca. 75 minutes, brought about a highly efficient conversion to the $\text{isoBu}\cdot$ radical (Fig. 9b). Conversely, the analogous photolysis of the three $\text{Bu}^t\cdot/\text{X}^-$ adducts brought about the disappearance of the adduct features yet did not generate $\text{isoBu}\cdot$ radicals, adducted or not. Neither did annealing produce the $\text{isoBu}\cdot$ free radical.

This system is being studied in greater depth at the moment,¹² nevertheless, the experiments carried out so far do seem to supply unambiguous evidence that the presence of the halide ion greatly

↓
3210G

20G
→ H

Gain x 10

Gain x 10

(a) Bu^t•

Figure 9

hν
75 minutes

(b) isoBu•

Gain x 10

Gain x 10

restricts the efficiency of conversion. In fact, in this system, its presence appears to preclude conversion. It may be reasonably concluded that the inhibition of rearrangement is caused either by the electron transfer process from the halide 'p' orbital into the carbon 'p_z' orbital, or simply by the physical presence of the large halide ion in the same cavity. Unfortunately, it is impossible to say which at this moment. Of great interest would be the implementation of experiments similar to those of Parkes and Quinn¹¹ in the hope of producing the ultra-violet absorption spectra of the Bu^{t•}/X⁻ adducts. If the inhibiting factor is electronic rather than steric in character, then a shift in absorbance bands should be demonstrated.

(f) isoBu• radicals in the CD₃OD matrix

An experiment in progress at the moment¹² is concerned with the fate of isoBu• radicals in the CD₃OD matrix when left for a number of days at 77 K in the dark (cf. Iwasaki et al.). The radicals are generated from the γ -radiolysis of a 1 Mol % solution of isoBuX (X = Cl, Br, I) in CD₃OD. Over a 40 day period, negligible Bu^{t•} radicals were generated and there was no sign of Me₂ \dot{C} H₂D radicals. Further storage (ca. 80 days) has since brought the generation of Bu^{t•} radicals to a relative standstill.

This result is in marked contrast to the results of Iwasaki who had accomplished complete conversion in the isoBuBr matrix over a 40 day period. This, therefore, strongly suggests that their rearrangement is an intermolecular process and the lack of deuterium pick-up in the deuterated matrix in our experiment is probably due to the greater C-D bond strength.

CONCLUSION

Although many of the questions posed in the introduction have been answered, the project is unfinished and more work needs to be, and is being, carried out in this laboratory.¹² Taking reactions (i) → (iv) individually (see Scheme II), I shall now list the conclusions we have come to on the basis of these results.

(i) The lack of rapid rearrangement of the isoBu• radical (over ca. 40 days) in the polydeuterated CD₃OD matrix seems to suggest that the reactions studied by Iwasaki⁴ and Ayscough⁵ probably took place via an intermolecular pathway. The lack of deuterium pick-up in our experiment could be due to the greater C-D bond strength. Analysis of the same system over a 80 day period implies there is a possibility of (CH₃)₃C• radical growth. However, if the intramolecular rearrangement is taking place, then its rate is negligible in this matrix at this temperature.

The most hopeful example of an intramolecular rearrangement is in the adamantane-d₁₆ matrix. Unfortunately, all attempts to generate the isoBu• radical in this matrix have proved inconclusive. This therefore remains, in my opinion, the priority problem.

- (ii) The generation of isoBu• radicals from the photolysis of Bu^t• radicals in the CD₃OD matrix proves conclusively this rearrangement to be intramolecular.
- (iii) Our previous results, recorded in the introduction of this chapter, seem to show that both intramolecular and intermolecular routes are available for this rearrangement. None of the experiments carried out in this chapter have shed any more light on the subject.

(iv) In stark contrast to the free radical, the adduct appears to be particularly defiant in its photolytic rearrangement. For reasons which require further research, the presence of the halide ion appears to cause a most definite inhibition of reaction. The experiments in the Bu^tBr and Bu^tCl matrices do seem to suggest that the ultra-violet light is capable of dividing the adduct into its two independent components prior to rearrangement, while in the TMS matrix, rearrangement does not appear to take place at all.

REFERENCES

1. R. B. Woodward, R. Hoffmann, "The Conservation of Orbital Symmetry", Verlag Chemie, GmbH/Academic Press, Weinheim/Bergstr., 1970.
2. W. A. Pryor, "Introduction to Free Radical Chemistry", Prentice-Hall, Inc., 1966.
3. I. G. Smith, M. C. R. Symons, J.C.S. Perkin II, (1979) 1362.
4. M. Iwasaki, K. Toriyama, J. Chem. Phys., (1967) 46, 2852.
5. P. B. Ayscough, C. Thompson, Trans. Faraday Soc., (1962) 58, 1477.
6. R. W. Fessenden, R. H. Schuler, J. Chem. Phys., (1963) 39, 2147.
7. See chapter 2.
8. See chapter 3.
9. R. V. Lloyd, D. E. Wood, M. T. Rodgers, J.A.C.S., (1974) 96, 7130;
R. V. Lloyd, D. E. Wood, J.A.C.S., (1975) 97, 5986.
10. See chapter 5.
11. D. A. Parkes, C. P. Quinn, Chem. Phys. Letters, (1975) 33, 483.
12. Being carried out by Mr. S. P. Maj.

ABSTRACTElectron Addition to Organic Halides. An Electron Spin Resonance Study

IAN G. SMITH

It had always been assumed that electron addition to organic halides resulted in dissociation as in reaction [1].



In more recent years, intermediate species have been isolated; in particular the $R\cdot/X^-$ adduct (where R is an alkyl group) and the $(R-X)^- \sigma^*$ anion (where R is, for example, the $-CF_3$ group).

Chapters 2-5 document the isolation of a range of alkyl radical/halide ion adducts in a range of matrices. Particularly exemplary results were obtained from the adamantane matrix, Chapter 1 therefore reviews the physical properties of the compound and the chemical methods employed for its purification and for the incorporation of substrates into its lattice. Conversely, Chapters 6 and 7 discuss the theory of formation of σ^* anions and documents a series of attempts at their isolation.

Finally, Chapter 8 probes and compares the thermally and photochemically induced [1,2] hydrogen atom shift isomerisation processes of the $Bu^t\cdot$ and $isoBu\cdot$ radicals and $Bu^t\cdot/X^-$ and $isoBu\cdot/X^-$ adducts ($X = Cl, Br, I$) in a range of matrices (reactions [2] and [3]).

